Using Novel Nanostructured Materials *for* Desulphurisation and Oil Clean-up

A Thesis Submitted to Newcastle University for the Degree of Doctor of Philosophy

by

Ahmed Alibraheemi

School of Engineering, Newcastle University, United Kingdom

September 2020

Disclaimer

This thesis is submitted in fulfilment of the requirements for the degree of Doctor of Philosophy at Newcastle University, Newcastle upon Tyne, United Kingdom. All the studies described within are solely my work otherwise expressly stated and were undertaken at the School of Chemical Engineering and Advanced Materials under the guidance and supervision of Prof Steve Bull and Dr Katarina Novakovic.

I certify that none of the material offered in this thesis has been previously submitted for a degree or any other qualification at the above or any other university or institute.

Neither the author nor the Newcastle University at Newcastle upon Tyne accepts any liability for the contents of this document.

The novelty in this work, is using a modified polyHIPEs as an adsorbent to remove sulphur from prepared model and real fuel oil which is no one has done before. The reason for using this material is its low cost and its improved characteristics, also sulphur adsorption capacity, and the ability to regenerated and reused. This work is paving the way for new modifications and preparing methods for polyHIPE, model fuel oil creation and characterizations also, novel technique and adsorbents in desulfurization.

Conference and Publications

1. Alibraheemi A., S. J. Bull and K. Novakovic, *Using Novel Nanostructured Materials for Desulphurisation and Oil Clean-up*. 4th Iraq Oil & Gas Conference, 13 to 14 December 2017 -Basra, Iraq.
2. Alibraheemi A., S. J. Bull and K. Novakovic, *Using Novel Nanostructured Materials for Desulphurisation and Oil Clean-up*. 23rd International Congress of Chemical and Process Engineering, CHISA 2018 25-29 August 2018 – Prague, Czechia.

Abstract

Fuel specifications for transportation fuels have become increasingly stringent with respect to sulphur content in the past few years. The processing cost and the price of crude oil is influenced by its sulphur content. Consequently, the removal of sulphur from oil remains one of the key issues for all parts of the oil industry, including both upstream and downstream processing. The major challenge is to minimise this cost and sulphur content by using novel methods for deep desulphurisation.

Small and medium-scale Iraqi refineries need a novel, low temperature, and benign desulphurisation method especially in consideration of increasing demand for derivatives due to the decrease in capacity after the war and the lack of hydrodesulphurisation units.

The aim of this work is to develop such a technology based on adsorptive desulphurisation using a nanostructured polymerized high internal phase emulsion polymer due to its high surface area and the sorbent ability that can adsorb many times its own weight in sulphur compounds whilst rejecting hydrocarbons.

A model fuel oil was prepared from n-octane as the solvent and the main organosulphur compounds (butanethiol, di n-propyl sulphide, dimethyl disulphide, benzothiophene and dibenzothiophene) to be used as a feed to the adsorptive desulphorisation process. The basic adsorbent was prepared in different mixing time using a HIPE consisting of an oil phase of 78 wt.% monomer, 8wt. % cross-linking agent and 14 wt.% surfactant mixed with an aqueous phase containing a polymerisation initiator (potassium persulphate), then the product conducted in sulphur removal and characterised in more detail.

The project involved producing further adsorbents by using monoethanolamine and activated carbon that assessing improving the adsorption capacity and regeneration ability. This followed by testing the sulphur removal capacity of the material using real industrial oils. Characterisation and analysis of all materials will be undertaken before and after testing by SEM, then FTIR, BET, mechanical compression, and oil uptake tests to assess material handleability.

Dedication

This thesis is dedicated to my wife Maysoon Alabboodi and my children Ali, Hayder, and Ghadeer whose laughter and smile always brightens up my days.

This thesis is dedicated to my sisters and brothers for giving me the best support I could ever have.

To my teachers who set me on the right path.

The thesis is especially dedicated to the soul of my father that I never forgot and to my mother for opening my eyes to the wonders of the world and for believing in me and all prayers during this journey.

Thank you very much for your love, patience and undivided support which kept me going throughout the years especially during the most difficult times.

Thank you all and may Allah bless you all. I could not have done this without you.

Acknowledgments

This greatly challenging experience would not have been possible without the contribution of my supervisor, Professor Steve Bull to whom I would like to express my sincere appreciation for his supervision, guidance, and the freedom in my scientific research. His encouragement, feedback and patience helped me immensely throughout my study. I am also thankful to Dr Katarina Novakovic for giving me the opportunity to work under her supervision and providing me with constant intellectual motivation and continuous guidance. My supervisors' commitment and endless support over the study years, both academically and personally, have been invaluable and I have been fortunate to have worked with them since giving me the opportunity to start this work.

My special thanks go to the ministry of oil in Iraq, Midland Refineries Company (MRC) and my sponsoring company BP British petroleum company especially Ms Awatif Mumtaz and Unihouse centre, Mr Haider Wazir for allowing me to contribute to the project and provide me with all knowledge and using their facilities when they were needed. Also, I would like to thank Iraqi Cultural Attaché - UK for all their support.

As this journey began, I was happily introduced in Material Group at the School of Chemical Engineering and Advanced Materials (CEAM) at Newcastle University and, in particular, my sincere thanks go Neville Dickman for being supportive, inspirational and, above all, close friends Hassan Izadi, Abbas Al-Gburi, Mohammed Kadhim and Khalil Abbas.

Many thanks to Dr Isabel Acre Garcia /Advanced Chemical and Material Analysis (NACMA) for the microscopy sessions and very special thanks go to Dr Julia Parker for teaching me the GC analytical techniques and finally to the staff people of CEAM I have been dealing with. Finally, yet importantly, I would like to thank the experts Zaid Shareef and Dr Aid Jaber from MRC for their support in the company and its branches in Iraq.

Alhamdulillah, thank you, Allah, for giving me the strength and determination to continue.

Table of Contents

List of Figures

List of Tables

List of abbreviations and symbols

ADS	Adsorptive Desulphurisation	**MEROX**	Mercaptan oxidation
API	American Petroleum Institute	**MTF**	Mechanical test frame
ASTM	American society for testing materials	**MPS**	Roxy propyl trimethoxy silane
ATS	PHP after traditional sulphonation	**MCT**	Mechanical compression testing
ASTM-IP	ASTM-IP petroleum measurement	**OPEC**	Organization of the petroleum exporting countries
AMS	PHP after microwave sulphonation	**ODS**	Oxidative Desulphurisation
BET	Brunauer-Emmett-Teller	**PAC**	Pyrolytic activated carbon
$CACL_2.4H_2O$	Calcium chloride-electrolyte	**PAF**	Porous aromatic frameworks
CB	Chlorobenzene	**PSDBP**	Polystyrene divinyl benzene copolymer
CEB	Chloroethyl benzene	**PolyHIPE**	Polymerised high internal phase emulsion polymers
CF	Final concentration	**PHP**	PolyHIPE before modification
CT	Compression test	**PVC**	Polyvinyl chloride
C30B	Cloisite30b	**R.V. P**	Reid vapour pressure
DVB	Divinylbenzene	**SEM**	Scanning electron microscopy
EFSM	Environmentally friendly sulphonation method	**SNP**	Silica nanoparticles
EDS	Extractive Desulphurisation	**ST**	Styrene
FCC	Fluidized catalytic cracking	**IEC**	The ion exchange capacity
FTIR	Fourier transform infrared spectroscopy	**TNR**	Titania nanorods
GC	Chromatography	**TEA**	Triethylamine
HPCH	Clay heterostructures	**TMA**	Trimethylamine
HIPE	High internal phase emulsion	**TSC**	Total average sulphur removing capacity
HDS	HydroDesulphurisation	**Tw**	Pore wall thickness
HLB	Hydrophile lipophile	**Tv**	Intersecting vertex thickness
IR	Infrared radiation	**UOP**	Universal oil product

1 Introduction

1.1 Overview

Fuel specifications for transportation fuels have become increasingly stringent with respect to sulphur content in the past few years. The maximum acceptable content is that which limits sulphur emissions to 10 ppm (Prajapati and Verma, 2017). Moreover, recent developments in environmental legislation are inexorably moving us to a world of zero-sulphur Consequently, the removal of sulphur from oil remains one of the key issues for all parts of the oil industry, including both upstream and downstream processing.

The processing cost and the price of crude oil is influenced by its sulphur content. Approximately $10–15 billion in the European refinery industry and up to $16 billion in US and Canadian refineries will be invested in direct response to the environmental clean-fuel legislation (Babich and Moulijn 2003). In Iraq the petroleum industry represents 90% of the income of Iraqi economy (Administration, 2016, Donovan et al., 2013). Locally extracted crude oil is essential to this industry, but it has high sulphur content. This industry is facing a major challenge of minimizing this sulphur content by using novel methods for deep Desulphurisation.

Hydrodesulphurisation HDS is the main technology employed industrially for the desulphurisation of heavy oil. Although HDS is quite successful, it is expensive and its carbon footprint is substantial since it involves high-temperature processing, including the production of the hydrogen that is needed for HDS. In addition, another disadvantage in HDS technology is the conversation rate depends on the chemistry of the sulphur species in the oil; the 4,6-dimethyldibenzothiophene (Triantafyllidis and Deliyanni, 2014) present in Iraqi oil derivatives has the lowest conversion rate and needs a novel technique to achieve ultra-deep desulphurisation. Thus, small and medium-scale Iraqi refineries need a novel, cost-effective, low temperature, and benign Desulphurisation method especially in consideration of increasing demand for derivatives, the decrease in capacity after the war and the lack of hydrodesulphurisation units.

A number of alternative desulphurisation techniques have been suggested to overcome the drawbacks of the HDS technology. From comparison of these techniques' adsorptive desulphurisation in the solid or liquid phase appears to be the most promising alternative technology when HDS is inefficient or cost intensive.

1.2 Aims and objectives

The aim of this project is therefore to develop a technology based on adsorptive Desulphurisation using a nanostructured polymerized high internal phase emulsion (polyHIPE) due to its high surface area and sorbent ability that can adsorb many times its own weight in sulphur compounds whilst rejecting hydrocarbons. The main challenge is to find adsorbents able to remove the sulphur compounds with very high selectivity from a complex mixture of paraffins, naphthenes, olefins, and aromatic compounds.

The objectives of the project were to determine if a polyHIPE based sorbent could be processed with a microstructure that could be used to adsorb sulphur compounds from processed crude oil. This involves developing the basic polyHIPE microstructure to maximise the number of adsorption sites and surface area and improve this by surface functionalisation. In addition, it is necessary to make a commercially viable material, so the mechanical strength and regeneration properties of the material need to be assessed and improved.

1.3 Summary of the work carried out

Initial experiments included preparation of the polyHIPE with different stirring times prior to polymerisation have been carried out to assess their ability to act as a sorbent and the key microstructural features necessary for adsorbent behaviour. It was found that increased mixing time reduced aqueous droplet size in the HIPE and increased the number of small pores, and the surface area of the pore walls in the polymerized material. Smaller pores and a narrower distribution of pores are needed for the sulphur adsorption from fuel oil.

A model fuel oil was then prepared from n-octane as solvent and the main organosulphur compounds (butanethiol, di n-propyl sulphide, dimethyl disulphide, benzothiophene and dibenzothiophene) and the sulphur removal was characterised in more detail. This was used as the basis for all adsorption experiments.

A polymerized high internal phase emulsion (polyHIPE) PHP was prepared using a HIPE consisting of an oil phase of 78 wt.% monomer (styrene), 8 wt. % cross-linking agent divinylbenzene (DVB) and 14 wt. % surfactant (Span 80) mixed with an aqueous phase containing a polymerisation initiator (potassium persulphate) to achieve this. The following experiments involved making further polyHIPEs, with potentially better adsorption. Functionalising polyHIPE pellets is essential for optimum sulphur adsorption; different functionalization treatments were assessed for adsorption capacity for the different sulphur compounds. These were chosen from bulk sorbents, namely monoethanol amine and activated carbon, which have been suggested previously.

Batch adsorption experiments were conducted, and the adsorption capacity for each sulphur compound in the model oil was tested by gas chromatography. This was followed by testing the sulphur removal capacity of the best material using a range of crude oil derivatives. In particular, naphtha, kerosene and gas oil produced from an Iraqi oil refinery have been subjected to the optimised adsorbent in a continuous adsorptive desulphurisation process. Characterisation and analysis of all materials was undertaken before and after testing by scanning electron microscopy SEM, then Fourier transform infrared FTIR, Brunauer-Emmet-Teller BET, mechanical compression and oil uptake tests to assess material handleability.

The basic polymer was successfully prepared with varying porosity and activated carbon addition leads to good improvement of the polyHIPE mechanical properties. Also, the modification of polyHIPE by adding monoethanolamine MEA has shown an interesting affinity towards sulphur compounds. This adsorbent is able to remove a significant proportion of all sulphur compounds investigated, even those aromatic compounds that are hard to remove by HDS. Thus, the material is a potential candidate for industrial application. However, the adsorbent needs to have further improved adsorption capacity and the ability to be regenerated if it is to be used industrially. Laboratory-scale regeneration tests have been successfully carried out using the model oil.

1.4 Thesis Structure

The thesis is divided into nine chapters. Chapter 1 provides and introduction to the work and its motivation whilst the literature is summarised in Chapter 2, regarding oil. Chapter 3 discusses desulphurisation approaches. Chapter 4 the sorbent materials including polyHIPEs. Chapter 5 summarises the experimental techniques used in the project whilst results are presented in Chapter 6 for the standard polyHIPE material. Chapter 7 about the developments of the optimised polyHIPE-based sorbent using texting on a model oil. Chapter 8 Testing in Iraqi crude oil derivatives. Chapter 9 summarises the work and suggests areas where more work is required.

2 Crude oil and sulphur removal

2.1 Overview

Crude oil is a naturally occurring mixture consisting predominantly of hydrocarbons and sulphur, nitrogen, and oxygen compounds (Speight, 2014). Densities generally lie in the range 0.79 to 0.95 g/cm^3 under surface conditions and the viscosities vary widely from about 0.7 cp to 42,000 cp. In general, crude oils are flammable under ambient conditions and their odours can vary from an almost pleasant aromatic bouquet to the distinctly unpleasant smell often associated with sulphur derivatives. The main products are liquid petroleum gas, gasoline, jet and diesel fuels, wax, lubricants, bitumen, and petrochemicals (Nelson, 2018). The principal types of hydrocarbon present in crude oils are: normal, branched, or cyclic saturated hydrocarbons; aromatic hydrocarbons, or compounds with structures associating both these basic types. Unsaturated hydrocarbons, such as alkenes (aliphatic olefins) appear to be present only in traces. Sulphur is the third most abundant atomic constituent of crude oils (Gary et al., 2007, Nelson, 2018, Speight, 2014).

One of the most important problems in the oil industry is the presence of sulphur in crude oil since it is usually detrimental to performance and needs to be removed. This affects the price of oil as well as the operating and maintenance costs of equipment in refineries.

In this research, it will first be shown in which forms sulphur exists in oil : elemental or compound, organic or non-organic compounds, how is crude oil classified due to the sulphur content, organic composition and density and the main sulphur-test methods in the industry. Secondly, the effects of this sulphur will be discussed followed by the advantages and disadvantages of the most common methods to reduce its concentration. This is followed by a deeper description of the selected desulphurisation technique which is adsorption (Mantell, 1951) sulphur removal based on chemisorption and physisorption including the definition, principles advantages and disadvantages, challenges, and obstacles.

Adsorption is receiving increasing attention as a result of low energy consumption, deep and ultra-deep desulphurisation, and easy operation conditions (Neubauer et al., 2017). The major element in this technology is the adsorbent; varieties of carbon nanomaterials suitable for adsorptive desulphurisation are discussed. Finally, The selection of an appropriate adsorbent and explanation of activated carbon and reactive-selective adsorption as a new technology that has the potential for a novel desulphurisation method, based on the novel use of functionalized PolyHIPE as a high surface area material for adsorption of sulphur compounds by surface reaction will be justified. (Antos and Aitani, 2004).

2.2 Crude oil compounds

Crude oil, also called petroleum which includes crude oil, natural gas, and heavy oil (Demirbas et al., 2015), is a natural mixture consisting predominantly of gaseous, liquid and solid compounds. These compounds occurring as hydrocarbons and sulphur, nitrogen, and oxygen compounds, are removed from the earth in a liquid state (Speight, 2014). There are two basic theories for the origin of crude oil: biotic and abiotic. The biotic theory predominates. It attributes oil's formation to the decay of animal and plant matter. The less widely accepted even controversial abiotic theory denies the involvement of living organisms in the production of crude oil. (Glasby, 2006).

Crude oils are commonly accompanied by varying quantities of extraneous substances such as water, inorganic matter, compounds of sulphur, nitrogen and oxygen as well as dissolved gases like natural gas, propane and hydrogen sulphide. The removal of such extraneous substances does not change the status of the mixture as crude oil. If such a removal appreciably affects the composition of the oil mixture, then the resulting product is no longer crude oil (Gary et al., 2007).

Crude oil is not a uniform substance; its appearance and characteristics vary from oil field to oil field and even from well to well in the same oil field. Thus, each separate accumulation of crude oil is a unique mixture, not matched exactly in composition by any other sample. The principal types of hydrocarbon present in crude oils are normal, branched or cyclic saturated hydrocarbons, aromatic hydrocarbons, or compounds with structures associating with both these basic types which are illustrated in Appendix-1 (Hydrocarbon Characteristics).

Hydrocarbons are the main components of crude as they represent 97% of the total mass. They occur in three organic groups: paraffinic, naphthenic, or aromatic structures ranging from light gaseous molecules (C_1–C_4 alkanes) to heavy waxes or asphaltene. The rest are organic compounds of sulphur, nitrogen, and oxygen, as well as water, salt, and many metals such as vanadium, nickel, and sodium. (Antos and Aitani, 2004).

Unsaturated hydrocarbons, such as alkenes (aliphatic olefins) appear to be present in only traces. Physically, crude oils can vary from light mobile, straw-coloured liquids containing a large proportion of easily distillable material to highly viscous, semi-solid black substances from which very little material can be removed by distillation before thermal decomposition occurs. Crude oil densities generally lie in the range of 0.77 to 0.95 g/cm^3 (from less than 10 API to over 50 API) under surface conditions (Gary et al., 2007). The viscosities vary widely from about 0.7 cp to 42000 cp; briefly, those which have less than 10,000 cp are either crude oil or

heavy oil while tar asphaltene and vacuum residue (the bottom products of atmospheric and vacuum distillation towers) have a viscosity greater than 10,000 cp (Speight, 2014).

In general, the crude oils are flammable under ambient conditions and their odours can vary from an almost pleasant aromatic bouquet to the distinctly unpleasant smell often associated with sulphur compounds. Despite the wide differences in the physical aspects of different crude oils, their ultimate or elemental composition are remarkably consistent, thus the percentage of the elements present in a crude oil falls within narrow limits as quoted in the following table-2.1 (Speight, 2014, Nelson, 2018).

Element	Composition (wt. %)
Carbon	83.0 – 87.0
Hydrogen	10.0 – 14.0
Sulphur	0.04 – 6.0
Nitrogen	0.10 – 2.0
Oxygen	0.05 – 1.5
Metals (Ni and V)	<1000 ppm

Table 2.1 Elemental composition ranges of crude oils (wt. %). (Speight, 2014, Nelson, 2018).

As indicated by the analytical data, the main compounds of crude oil are hydrocarbons, and compounds involving solely carbon (C) and hydrogen (H) and these can account for over 75% of the material. Of the other elements present, sulphur (S), nitrogen (N) and oxygen (O) appear as heteroatoms in hydrocarbon derivatives some of which involve traces of metals as shown in table 1. Metals may also be present as salts of carboxylic acids.

2.3 Hydrocarbons in crude oil

2.3.1 Alkanes

Originally, and still known as paraffins, these are saturated, aliphatic (open chain), normal (straight – chain) or branched chain hydrocarbons, which constitute a homologous series of general formula C_nH_{2n+2} as shown in Figure 2.1. As one ascends the homologous series of alkanes it is possible, from butane (C_4), onwards for the carbon atoms to be arranged in linear or branched fashion. The branched chain alkanes are termed isomers. At ambient conditions, the hydrocarbons from C_1 to C_4 are gas; from C_5 to C_{16} are liquid and from C_{17} to C_{50} are semi-solids or solids. Usually, the linear alkane amount in crude oils is 15 to 20 per cent of the oil, but their content can be quite low, as in heavy degraded oils or as high as 35 per cent in light crudes (paraffinic crudes). High molecular weight alkanes (>C20) are responsible for high cloud points. (Burrows et al., 2017, Gary et al., 2007, Nelson, 2018, Speight, 2014)

Figure 2.1 Chemical formula of paraffine molecules.

2.3.2 Cycloalkanes

Known formerly as naphthene or cycloparaffins in the petroleum industry, they are saturated compounds that are similar to their aliphatic analogues both physically and chemically. These organic groups belong to those of organic compounds known as alicyclic, possess the general formula $C_nH_{2n+2-2Rn}$, where Rn is the number of naphthenic rings present Figure 2.2. The average crude oils contain about 50% (w/w) of naphthene with concentrations increasing in the heavy distillate fractions. They have higher boiling points and densities than paraffins with the same number of carbon atoms.

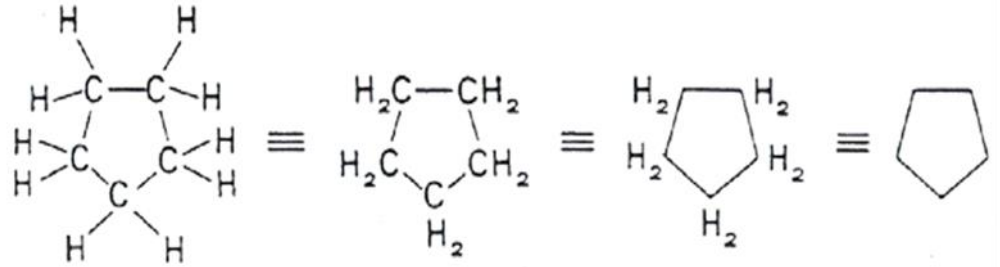

Figure 2.2 Chemical formula of cycloalkanes.

2.3.3 Alkenes and Cycloalkenes

These are olefins such as hydrocarbons including a carbon-carbon double bond (C=C). Reports on the isolation and identification of compounds of this class from crude seem rare as shown in Figure 2.3. They can be arranged as normal or branched chain or as ring chain. The hydrocarbon compounds with one double bond are also called monoolefins and if they have two double bonds they called as diolefins. They are denoted by the endings – ene or diene, preceded by a prefix indicating the number of carbon atoms. Taking in account their chemical reactivity resulting from their double bonds, the olefins regarding oxidation resistance they have poor properties.

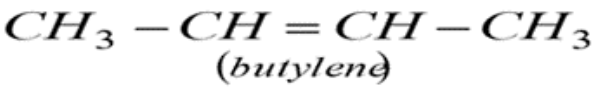

Figure 2.3 Chemical formula of alkenes.

2.3.4 Arenes

These are known as aromatics in the petroleum industry, aromatic compounds or arenes are carbocyclic compounds of the benzenoid class, the archetype of which is the monocyclic compound benzene, C_6H_6. The structure of this compound can be represented by means of a so-called Kekulé formula (Burrows et al., 2017) as shown in Figure 2.4.

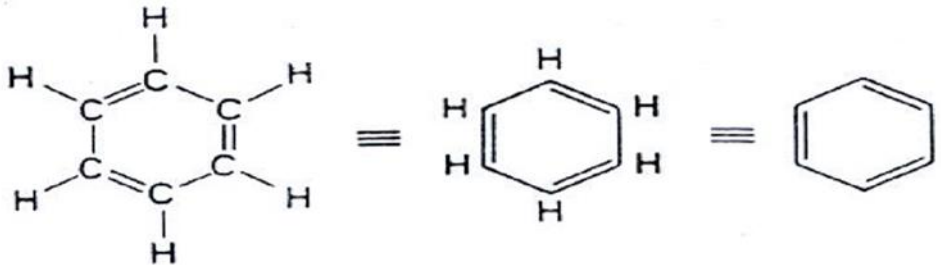

Figure 2.4 Chemical formula of arenes.

In addition to benzene and its homologues (alkyl derivatives, e.g. toluene ethylbenzene, orthoxylene, metaxylene and paraxylene) crude oil contains polynuclear aromatic hydrocarbon of two types: isolated (or non-condensed), e.g. biphenyl, and condensed, e.g. naphthalene, plus their homologues (Gary et al., 2007, Nelson, 2018, Speight, 2014).

Aromatic hydrocarbons do not normally amount to more than 15 w% of a total crude oil; the mononuclear compounds toluene and metaxylene are the most common arenes found, and polynuclear species containing up to at least height condensed rings seem to be possible constituents. Compounds belonging to all the basic types defined above have been found in a crude: benzene (one ring); naphthalene (two rings); anthracene and phenanthrene (three rings) as shown in Figure 2.5 (Bandosz, 2006, Saleh, 2015).

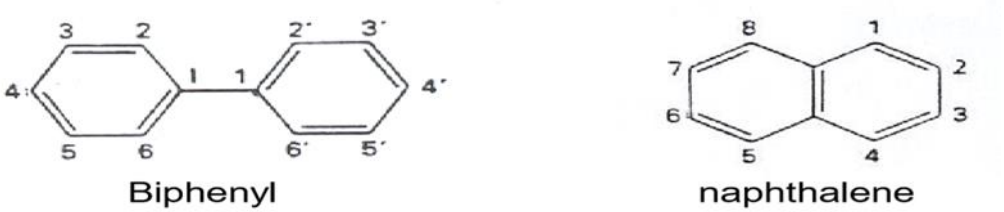

Figure 2.5 Chemical formula of paraffine molecules.

2.4 Non- hydrocarbons in crude oil

Crude oil contains significant amounts of organic compounds with structures combining one or more (the same or different) atoms of sulphur, oxygen or nitrogen, in addition to carbon and hydrogen; some of these are associated with metals such as vanadium and nickel, which are organometallic in nature. The organic non-hydrocarbon components are distributed throughout the whole boiling range of crude oil but appear mainly in the heavier distillation fractions and

the non-volatile residue after distillation. Although concentrations are very small in any one fraction, their influence can be important; for example, acidic components such as thiols and carboxylic acids promote corrosion of metal equipment; reforming and isomerization catalysts are seriously deactivated by sulphur compounds; metal traces (V, Ni) passivate, or poison catalysts used in desulphurisation or cracking. The colour and odour of crude oils stems mainly from NSO compounds which are concentrated in the lubricating oil (C_{26}-C_{40}) and residuum (>C40; asphaltic bitumen) fractions (Antos and Aitani, 2004, Gary et al., 2007, Nelson, 2018, Speight, 2014).

2.5 Crude oil classification

A method of classifying crude oils is necessary to provide a guide to the quality and hence value, of the oil. This helps later in choosing and optimising of the method of formulation, separation technologies and the process economics. There are two main factors taken into consideration in crude oil classification.

Firstly the specific gravity of the crude oil as it provides a rough measure of the amount of the lighter fractions present; hence, the lower the specific gravity (or the higher the API gravity, which is an inverse scale (Awadh and Al-Mimar, 2015)) the greater is the yield of light fractions by simple distillation, and hence the higher is the price of the crude. With the introduction of more sophisticated processes, particularly the introduction of cracking processes, the rough guide provided by specific gravity was insufficient to classify oils.

As a result, crude oils can be divided into four categories according to their specific gravity as indicated below:

— Light crudes	density < 0.825 □
— Medium Crudes	0.825 < density > 8.75
— Heavy crudes	0.875 < density <1.000
— Extra-heavy Crudes	density > 1.000

according to the following definitions:

1— Paraffinic crudes – more than 50% (w/w) of saturated hydrocarbons and more than 40% (w/w) of normal and iso-paraffins; are light crudes with specific gravity around 0.85.

2— Naphthenic/Paraffinic crudes – more than 50% (w/w) of saturated hydrocarbons and less than 40% (w/w) of normal and iso-paraffines. Normally, the amount of sulphur is low.

3— Naphthenic crudes – more than 50% (w/w) of saturated hydrocarbons and more than 40% of naphthenic hydrocarbons. This significant difference between naphthenic and paraffinic hydrocarbons is due to biodegradation of the paraffinic hydrocarbons.

4— Aromatic crudes – more than 50% (w/w) of aromatic hydrocarbons and less than 50% of paraffinic hydrocarbons. Normally, the amount of sulphur is high at more than 1%. They are heavy and viscous crudes.

The last classification is important for this study because it groups crude oils according to the amount of sulphur. The crude oils are classified into two main types: “sweet” crude, if the sulphur content is less than 1% (w/w) and “sour” crude if the sulphur content is higher than 1% (w/w) (Nelson, 2018, Speight, 2014, Gary et al., 2007).

2.6 Crude oil and its derivatives' characterizations

An understanding of the overall physical and chemical characteristics is insufficient to select a crude oil as a feedstock or design a separation process. A detailed of crude oil study of the properties of potential products is of prime technical and economic importance, because it allows the designer to have a choice in selecting feedstocks for the different process units like separation, transformation and conversion and to set their operating conditions, in order to satisfy the customer needs as best as possible. The most essential physical and chemical properties of the fractions of crude oil are the following items: a) Specific Gravity (expressed most often in degrees API) b) pour point c) viscosity d) vapour pressure and flash point e) sulphur content f) salt content g) water and sediment content, and h) total acid number (TAN). A brief explanation of the associated ASTM and API test methods are provided in the appendices (Gary et al., 2007, Nelson, 2018, Speight, 2014).

In this study the identification and presence of sulphur compounds and the methods and techniques for sulphur testing are very important. Crude oil contains organic sulphur compounds, dissolved hydrogen sulphide and sometimes even suspended sulphur. The sulphur comes from decomposition of organic matter and by reduction of sulphates by bacterial action (desulforibrio desulphuricans). The H_2S and SO_2 are mainly formed during refining operations such as catalytic cracking, hydrodesulphurisation, and thermal cracking. The H_2S is corrosive, producing scales of pyrophoric iron sulphides.

Thiols (industrially called mercaptans) are acidic in behaviour; they are corrosive and malodorous. The sulphides are chemically neutral, and they constitute most of the sulphur containing hydrocarbons in the middle distillates. The thiophenes and their derivatives are complex molecules distributed between heavy cuts and residues. Regardless of their presence in very small amounts, on the order of a few dozen ppm, mineral salts cause serious problems during crude treatment.

The selection of the sulphur removal treatment is related to the quantity, types, and distribution of the sulphur compounds in crude oil and its products in all sectors of the oil industry as mentioned before. The oil industry is usually grouped into three main sectors: upstream, midstream, and downstream. The upstream processes are involved in crude oil and gas production, exploration, drilling, digging wells, extraction, and degassing. Meanwhile the midstream categorisation is normally subsumed within the downstream category. It includes oil preparation and transportation, via oil tankers and pipelines, and storage. Also included in downstream activities are marketing functions for crude, natural gas, refined petroleum products and petrochemicals to the consumer. The downstream activities principally comprise the activities that are carried out to produce the final petroleum products (Furman et al., 2017). Petroleum refineries are concerned with the conversion of extracted raw hydrocarbons into useful and saleable products.

Desulphurisation is one of the essential treatments due to the harmful effects of the sulphur in all these products. In the following section this sulphur distribution will be explained for the main final product in most oil refineries.

2.7 Petroleum refineries and the main distillate fractions.

A petroleum refinery is a series of unit operations that are designed to transform crude oil into useful fractions (Demirbas et al., 2015). There are 662 oil refineries throughout the world with a total capacity of 85.1 million barrels per day (BPD) (Gary et al., 2007). The crude oil daily consumption was about 84 million barrels per day in 2005 (Shafiee and Topal, 2008) and is estimated to increase from 99 and 116 million BPD between 2015 and 2030 respectively(Lim and Lee, 2020); about 45 percent of this increase is due to the energy demand relevant to transportation, petrochemicals, and electricity production (Mihaela, 2008, Shahbaz et al., 2017). This indicates two things; firstly, the importance of crude oil to everyday life and the need to update the approaches and technologies to meet the challenges of the demand. Despite crude oil's importance, it is of no value in its natural state unless it is converted into derivatives. Its nature is basically a complex mixture of different hydrocarbons with small quantities of sulphur, nitrogen, oxygen, salt and water (Speight, 2014) while each product should be based on a specific hydrocarbon with a desired composition and properties according to the final consumer requirements. For instance, sulphur is one of the most abundant elements in oil but according to environmental regulations it should be present to <30 ppm or less in gasoline for it to be a saleable product (Babich and Moulijn, 2003) and the sulphur content in this specification is expected to reduce to near –zero levels in future (Farshi and Shiralizadeh, 2015). As a result, several new activities including physical and chemical treatments in petroleum refineries are

required as part of a constant need to meet global demand from one side and the environmental and political legislation from the other.

In general there are four major factors that govern refinery design as shown in Figure 2.6 (Babich and Moulijn, 2003), these are (1) feedstock supply, for instance, there are more than 150 crude grades traded (2) the demand of the product as there are more than 2,000 products made by petroleum industry as shown in figure 2.7 (Gary et al., 2007). (3) environmental and political regulations which are evolving into more stringent regulations in relation to sulphur in gasoline and diesel (4) technology development, for instance, new approaches or catalysts and adsorbents (Speight, 2014).

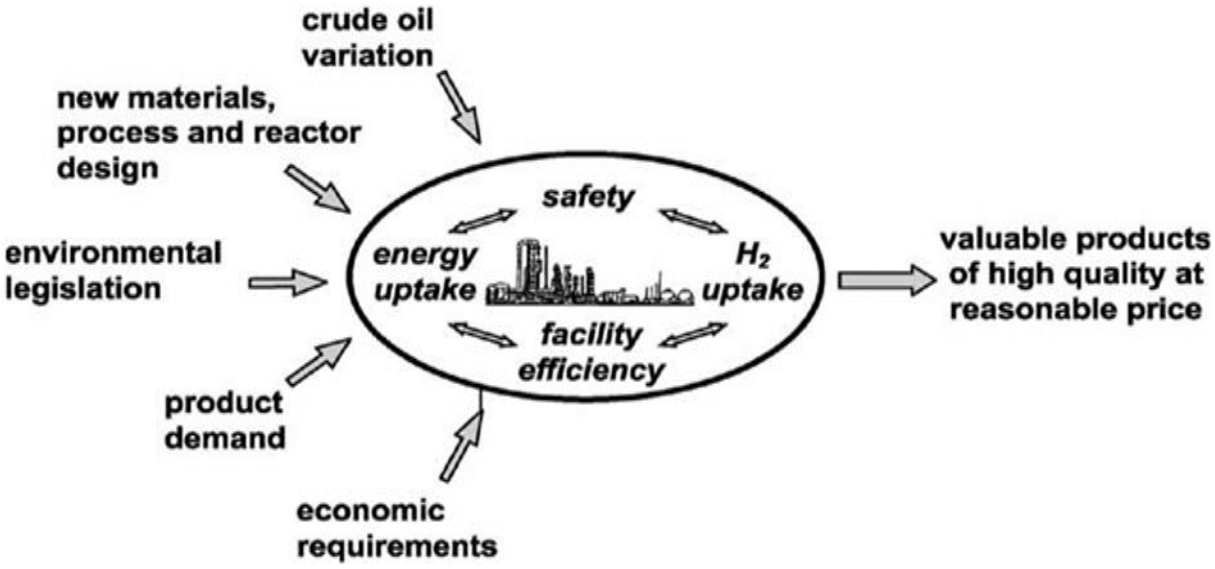

Figure 2.6 The general factors influencing the design and technology of oil refineries (Babich and Moulijn, 2003).

Therefore, not all refineries are designed in the same way to the same pattern. While the earliest refineries were simple low complexity factors, consisting of atmospheric distillation and one or more pre-treatments facilities, today, refineries are very complex and integrate 15-20 unit operations as shown in Figure 2.8 (Gary et al., 2007, Ludwig, 1997) including typical separation processes (atmospheric and vacuum distillation), and more advanced technologies (conversion processes of which coking and catalytic cracking are typical, desulphurisation units like hydrotreatments and adsorptive sulphur removal (Speight, 2014, Antos and Aitani, 2004, Nelson, 2018)).

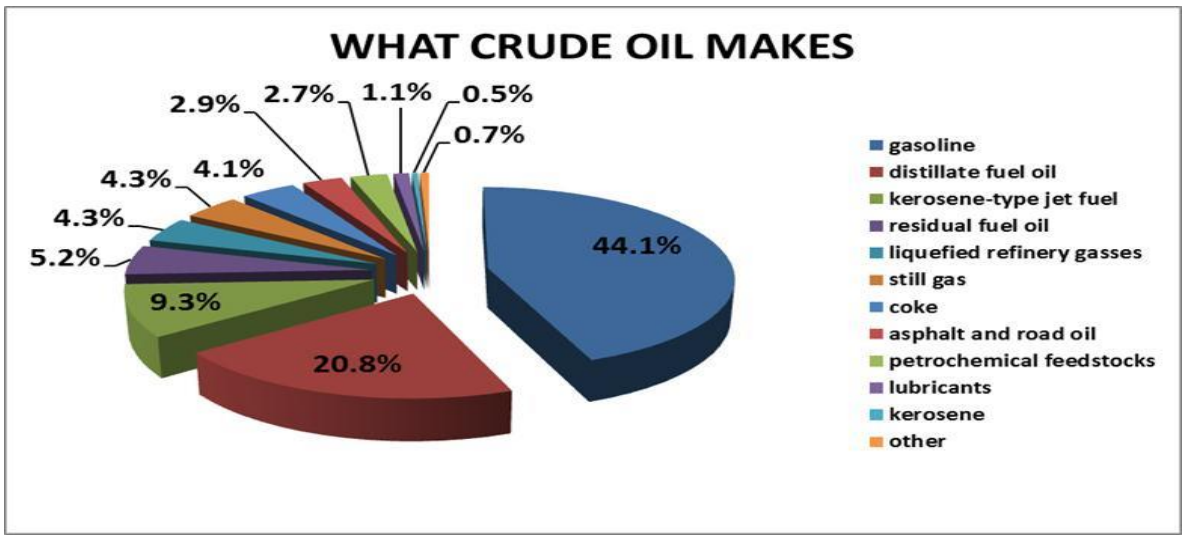

Figure 2.7 Possible demanded petroleum products of typical crude oil. (Speight, 2014)

2.8 The major light distillates and their further treatment

The first major operation unit is the distillation unit, in which crude oil is preheated and converted into the main intermediate fractions (or cuts in) depending on the difference in their boiling point. That is why it is common to express the oil refinery capacity in terms of its distillation unit capacity. The crude oil is preheated to 315-370 ℃ by a serious of heat exchangers and furnaces and then pumped to the distillation tower containing a number of trays 30-42 where it is separated into (from top to bottom) outlet gases (butanes and wet gas), stabilized light naphtha, heavy naphtha, kerosene, atmospheric gas oil and reduced crude (Gary et al., 2007, Speight, 2014, Nelson, 2018), as shown in the Figure 2.8 (Kumar et al., 2017) which represents a typical refinery with the main units and is quite similar to Iraqi refineries.

The overhead fuel gases pass out of the top of the tower and are then sent gas processing units for further separation - part of fuel gas is desulphured by amine treatment that is similar to those used in natural gas desulphurisation (Abedi et al., 2015) to produce sulphur-free refinery fuel, where the side stream is H_2S that is treated in a Claus sulphur plant. At the same time part of these fuel gases are sent to the Merox treatment plant which is a mercaptan oxidation using a proprietary catalytic chemical process developed by Universal Oil Products UOP to produce LPG and butanes in addition to those treated by amine absorption. Amine derivatives are Monoethanolamine (MEA), Diethanolamine (DEA) and Methildiethanolamine (MDEA) as illustrated in table 2.2. They are organic compounds derived from ammonia as a result of the exchange of one hydrogen atom by an alkyl radical (Huertas et al., 2011). Mono ethanol amine (MEA) is specifically used to capture sulphur gases and biogas due to amine high affinity towards them. However, the process is unsustainable due to amine losses, high cost, and

environmental damage associated with amines (Abdulrahman et al., 2015, Huertas et al., 2011, Kussainova and Shah, 2020, Speight, 2014). In this study, the amine will be used to add more activity and selectivity to a synergetic adsorbent in a technique that ensure overcoming the MEA disadvantages.

Olamine	Formula	Derived Name	Molecular Weight	Specific Gravity	Melting point, ℃	Boiling Point, ℃
Monoethanolamine	$HOC_2H_4NH_2$	MEA	61.08	1.01	10	170
Diethanolamine	$(HOC_2H_4)_2NH$	DEA	105.14	1.097	27	217
Triethanolamine	$(HOC_2H4)_3NH$	TEA	148.19	1.124	18	335
Diglycolamine	$H(OC_2H_4)_2NH_2$	DGA	105.14	1.057	-11	223
Diiopropanolamine	$(HOC_3H6)_2NH$	DIPA	133.19	0.99	42	248
Methyldiethanolamine	$(HOC_2H_4)_2NCH_3$	MDEA	119.17	1.03	-21	247

Table 2.2 Olamines used in removal of sulphur and biogases (Speight, 2014).

Naphtha is the precursor of gasoline and many solvents and is also the feedstock of many petrochemical industries. Gasoline, kerosene and diesel oil provide more than half of the world's total supply of energy. The flow chart of typical refinery is shown in Figure 2.8 (Speight, 2014) where it can be seen there are two types of naphtha extracted from the tower at distillation boiling point range of 70-180 ℃. The two streams are light and heavy naphtha. Light naphtha undergoes further hydrotreatment as a result of the sulphur content in its structures as will be explained in the next section. Naphtha is sent to the isomerisation unit to convert the n-butane into isobutane, then alkylate to a hydrocarbon in the gasoline boiling range in which it increases the octane number of paraffins. Finally gasoline is formed by blending treated naphtha which is isomerate, reformate and alkylate. (Speight, 2014, Babich and Moulijn, 2003, Antos and Aitani, 2004).

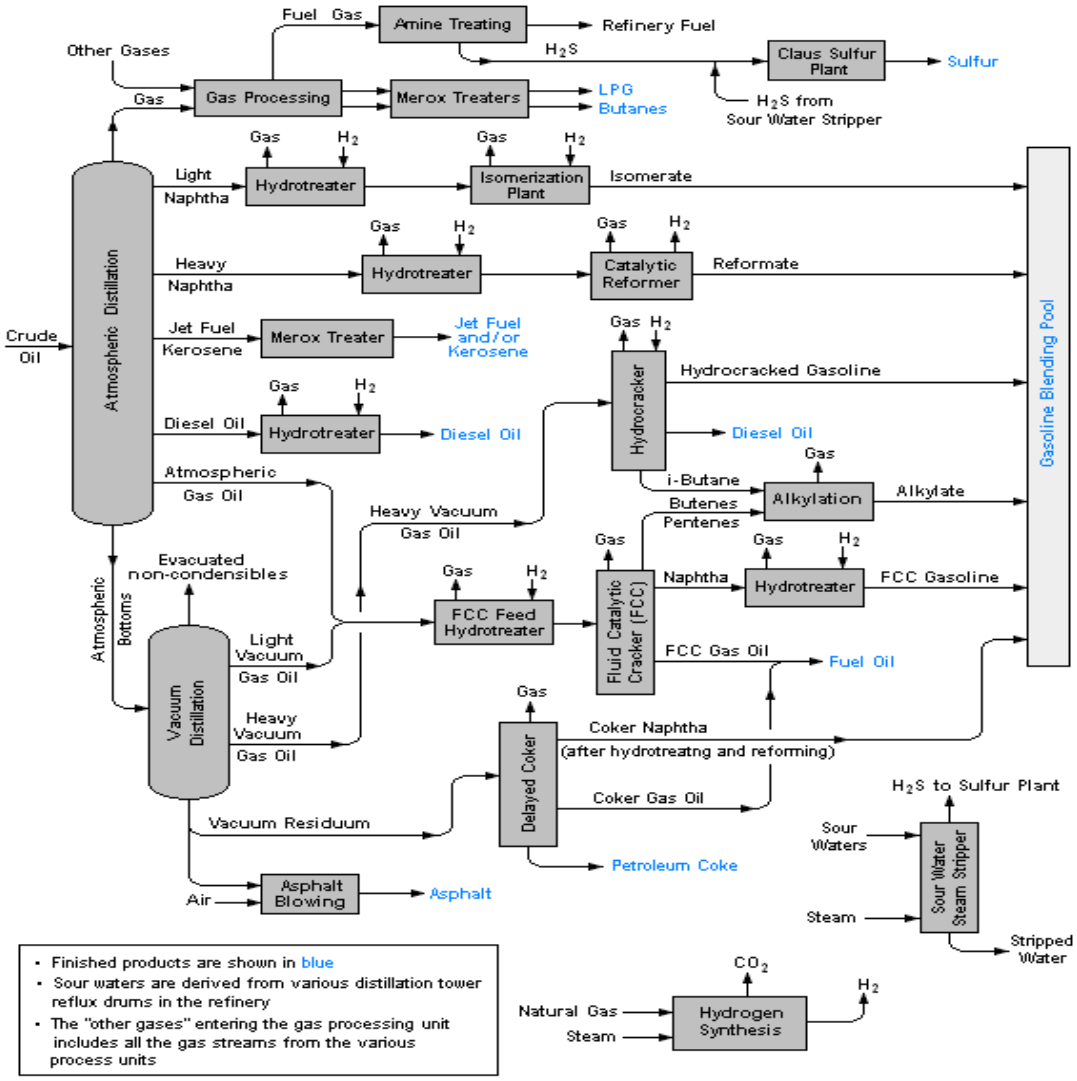

Figure 2.8 Schematic overview of a typical oil refinery process (Speight, 2014).

The following cut is kerosene produced at a distillation range of 160-240 ℃ and due to its sulphur content of 0.02wt %, it is desulphured and in some cases blended with hydrotreated light coker gas oil to produce jet fuel. (Javadli and De Klerk, 2012, Leprince, 2001, Gary et al., 2007). Atmospheric gas oil or Straight run diesel is one of the basic middle distillates produced from the distillation tower at 230-350 ℃ and, due to the sulphur content of about 0.9 wt %, it is pumped out for hydrotreating. As shown in Figure 2.8 diesel fuel is produced from various streams. Vacuum gas oil, light cycle oil from the Fluid Catalytic Cracker (FCC) unit, hydrocracker diesel and coker diesel are desulphuisred individually or blended then used as particular feed stock for the desulphurisation units. Their sulphur content is about 2.5 wt%. It is worth mentioning that in case of atmospheric gas oil, desulphurisation is the only point of

concern in hydrotreating since the cetane number, flash point, density and the other required characteristics are satisfactorily met (Babich and Moulijn, 2003). Finally, the reduced crude is produced from the bottom of the atmospheric gas oil range and either sent to market or fed to the vacuum distillation tower to produce lubricating oils or subjected to a further chemical treatment of delayed coking to produce coker naphtha or gasoil. It should be noted from the previous explanation and figure that sulphur content plays an essential role in the design and the number of units used in the refinery as it exists in all intermediate products with different content and various compound distributions and it is very important to recognize this distribution in order to choose the proper method of desulphurisation.

2.9 Sulphur compounds distribution in distillate fractions.

2.9.1 Inorganic compounds

Inorganic sulphur can be present as elemental sulphur, S, pyrites, hydrogen sulphide (H_2S) sulphur dioxide which is suspended, dissolved or a byproduct in the oil fractions (Nelson, 2018, Samadi and Zarenezhad, 2016). Sulphur is an odourless solid with bright yellow colour, its melting and boiling points are 112.8°C and 444.7°C, respectively. The main elemental sulphur forms (Figure 2.9) are orthorhombic, polymeric and monoclinic (Burrows et al., 2017). The orthorhombic and monoclinic forms contain crown shaped S_8 molecules, which are stacked in a complex array (Bandosz, 2006). It shifts to higher boiling point distillation fraction as a result of its high boiling point and may be it may be produced as a result of H_2S oxidation that occurs in gaseous fractions and gasoline (Farshi and Shiralizadeh, 2015).

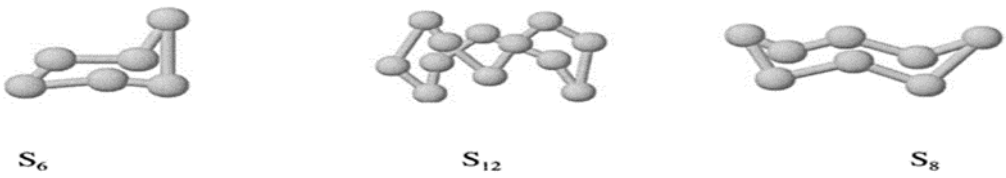

Figure 2. 9 The structure of S6 ,S12 and S8

Sulphur dioxide is a stable, colourless and poisonous gas which can be converted into sulphuric acid. There are over 20 intermediate oxides and acids recognized for instance sulphurous acid and peroxodisulphonic acid (Burrows et al., 2017). Hydrogen sulphide, H_2S is colourless gas ,with a rotten eggs odour and density of 0.00153 g/cm^3 (Meyer, 2013). H_2S and free sulphur occur in dissolved forms in low boiling fractions, where, sulphur reacts with thiols and both produce H_2S (Ahmad, 2016). Most H_2S is flushed off from the top tower with gaseous hydrocarbons like methane, ethane, propane and butane and then sent to further separation units for gas processing followed by amine treatment for desulphurisation e.g. as shown in Figure

2.8. Several studies have demonstrated new adsorption approaches for its more effective removal (Dhage et al., 2011, Samokhvalov and Tatarchuk, 2010) .

2.9.2 Organosulphur compounds

Light distillate fractions are the most important functions as they are responsible for a significant portion of energy supplied and consumed. As a result their percentage in a crude oil controls its price (Gary et al., 2007). Organosulphur compounds present in these light and medium fractions and cause many problems which make Desulphurisation one of the most important treatments effecting costs and prices. In addition, these compounds occur in different distributions which are not uniform in crude oil. In general their concentrations and complexity of structures increase with the increasing the boiling points of the distillate fractions (Leprince, 2001, Ahmad, 2016).They can be divided into three main classes: thiols, sulphides and thiophens as shown in Figure 2.10.

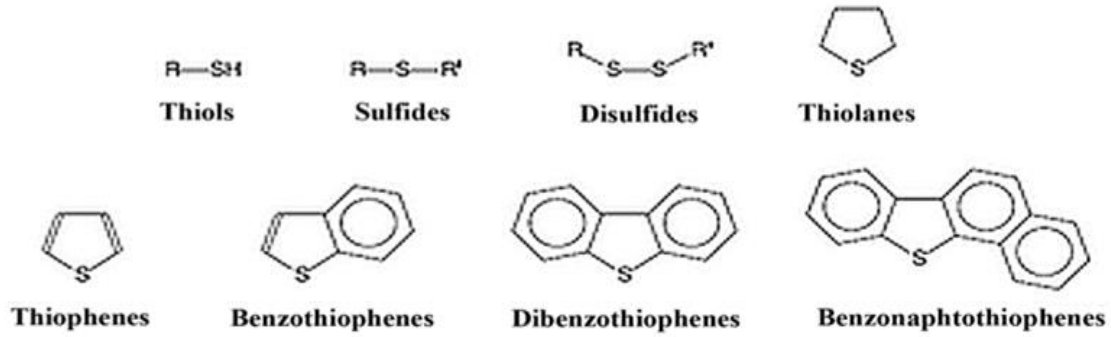

Figure 2.10 Scematic representation of some sulphur compounds in distillate fractions (Javadli and De Klerk, 2012).

Thiols or mercaptans are acidic, reacting stronger than alcohol due to their high reactivity towards metals (Bandosz, 2006). They can be characterised by the presence of the sulphur-hydryl group (Sentorun-Shalaby et al.), which takes the place of a hydrogen atom in an alkane or cycloalkane molecule (RH→ RSH) as shown in Figure 2.11. They also can be mono-alkyl or mono-cycloalkyl derivatives of the hydrogen sulphides. Thiols (C1-C8) are the principal organosulphur components of low-boiling petroleum fractions (below 200 ºC).

$$\underset{(methyl\ mercaptan)}{CH_3SH} \quad ; \quad \underset{(ethyl\ mercaptan)}{CH_3CH_2SH}$$

Figure 2.11 Methyl and ethyl thiols or mercaptans formulae.

Sulphides Figure 2.12 (or thioethers as they represent the sulphur version of ethers) are compounds formally derived by the replacement of both hydrogens of hydrogen sulphide by hydrocarbon groups, appear in very low abundance in crudes, of low molecular weight.

Disulphides Figure 2.12 have also been shown to be present in crude such as dimethyl sulphide, ethyl methyl sulphide, dimethyl disulphide and methyl n-propyl sulphide, as shown in the examples in Table 2.3.

Figure 2.12 Examples of sulphides and disulphides :ethyl methyl sulphide and diethyl disulphide.

The third class of organosulphur components in crude oil is characterised by the presence of a thiophene heterocyclic ring as; examples shown in Figure 2.13. These may carry one or more alkyl substituents or be fused to one or more other ring systems (aromatic or naphthenic) which can also carry alkyl groups. The major sulphur compounds existing in current liquid hydrocarbon fuels are thiophene compounds and their alkyl-substituted derivatives.

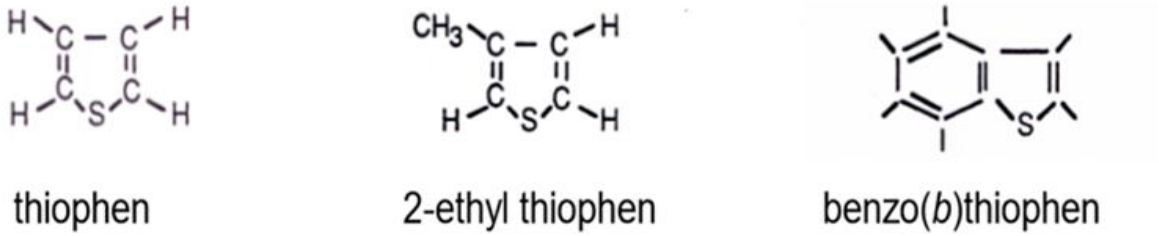

Figure 2.13 Examples of thiophenes.

Benzothiophens, dibenzothiophens and higher policylics) are important components of all high sulphur crudes, examples shown in Appendix 2 a and b.

The distribution of various classes of sulphur compounds among different light distillates has been studied often and it has been shown that the proportion of sulphur increases with boiling point during distillation as shown in Table 2.3 (Javadli and De Klerk, 2012, Velu et al., 2002, Speight, 2014).

The naphtha fraction obtained at 70 to 180 ℃ contains 0.02wt% sulphur compounds, of this 50% are thiols and 50% sulphides while thiophenes usualy do not occur in straight run gasoline. However, in some cases of gasoline that are produced in Fluid catalytic cracking (FCC) and

Residue Fluid Catalic Cracker (RFCC), the concentration is quite different with relatively amounts of thiophene (Martin and Grant, 1965, Yin and Xia, 2004).

Distillate fractions	B.P Range ℃	Carbon Limit	Thiols	Sulphides	Thiophenes	Higher Thiophene	Total Sulphur Content wt%
Naphtha	70-180	C_5-C_{17}	50	50	Rare	----	0.02
Kerosene	160-240	C_8-C_{18}	25	25	35	15	0.2
Diesel	230-350	C_8-C_{18}	15	15	35	35	0.9
Vacuum gasoil	350-550	>20	5	5	30	60	1.8
Vacuum residue	>550	>20	Rare	Rare	10	90	2.9

Table 2.3 Distribution of sulphur compounds during the distillation of crude oil.

Kerosene oil produced with boiling point ranging from 160-240 ℃ contains about 0.2 wt% sulphur compounds with equal proportion of thiols and sulphides but more thiophens and dibenzothiophenes.

Sulphur compounds in diesel oil contain less thiol and sulphides than those in kerosene 15 wt % for each. While same amount of thiophenes 35 wt % as kerosene is seen there is increasing concentration of heavier compounds such as Benzothiophene, dibenzothiophenes, and alkylated thiophene as shown in Table 2.4.

Some of these compounds have been considered to be the refractory sulphur compounds in the fuels due to the steric hindrance of the alkyl groups in hydroDesulphurisation HDS (Babich and Moulijn, 2003, Ma et al., 1996). Consequently, it is difficult or very costly to use the existing HDS technology to reduce the sulphur in the fuels to less than 10 ppmw. Thiophene itself, a well-known heterocyclic aromatic compound, and its alkyl derivatives are normally relatively scarce constituents of crudes, but condensed systems (benzothiophene, dibenzothiophene and higher polycyclic chemicals) are important components of all high sulphur crudes. These thiophenes contain compounds are more difficult than mercaptans and sulphides to convert via hydrotreatment.

Using adsorbents to selectively remove the sulphur compounds in liquid hydrocarbon fuels is promising approach, as the process can be conducted at ambient conditions without using costly

hydrogen (Babich and Moulijn). As is well known, the liquid hydrocarbon fuels contain not only sulphur compounds but also a large number of aromatic compounds that have aromatic structure similar to the coexisting sulphur compounds, this inherent problem provokes a significant challenge in the development of an effective adsorbent with high adsorptive selectivity for the sulphur compounds.

2.10 The consequences of sulphur content in crude oil

Removing or reducing sulphur in oil is one of the most essential processing requirements in both upstream and downstream processing of crude oil. The necessity of Desulphurisation is to avoid many issues governed by two main factors, firstly governmental legislation related to human health and environmental pollution because of its contribution to atmospheric pollution and acid rain effects on soil and plants, and secondly economic factors starting from the effect of the sulphur on crude oil prices due to corrosion problems, deactivation or poisoning of catalysts and its influence on octane numbers in gasoline (Saleh, 2015).

2.10.1 Health and Pollution

Reducing the risk of sulphur contamination when emitted from internal combustion into the atmosphere is a primary goal of the recently introduced regulations (by the Directive of the European Parliament and the Environmental Protection Agency (EPA) Clean Air Act (Babich and Moulijn, 2003). Consequently, the environmental legislation has imposed conditions for the maximum acceptable content that limits the release from engine exhausts to 15 ppm (Hosseini, 2012). New sulphur limits of 30–50 ppm for gasoline and diesel marketed in the European community and the USA were introduced starting from January 1, 2005 (Babich and Moulijn, 2003). Germany even passed legislation limiting the sulphur in diesel and gasoline to 10 ppm as of November 2001. In fact, zero-emission and, as a consequence, zero levels of S were called for worldwide in next 5–10 years (Danmaliki et al., 2017). Such environmental drivers are thus very important to address, as well as very costly to meet. According to various estimation models, $10–15 billion in the European refinery industry and up to $16 billion in US and Canadian refineries will be invested in direct response to the new environmental clean-fuel legislation. In order to minimize this cost, it is essential to find a novel method for deep desulphurisation. (i.e. to remove sulphur to less than 0.1% by weight) (Babich and Moulijn, 2003, Danmaliki et al., 2017, Brunet et al., 2005).

2.10.2 Operation and maintenance cost

Sulphur and its compounds are very corrosive materials and corrosion can occur in oil fields in three areas, which are oil and natural gas production, transportation and downstream processing in refineries. Corrosion increases the operation and maintenance costs. Many expensive materials and additives are used to reduce corrosion but the presence of toxic gases such as $H_2S/SO_2/NO_x$ still represent a serious threat to both people and equipment integrity, which will lead to high maintenance costs. Such gas mixtures can damage the catalysts used in the refineries, which are usually very expensive and essential for desulphurisation reactions at high temperature (Javadli and De Klerk, 2012, Gary et al., 2007, Salem, 1994).

2.11 The conventional and modern Desulphurisation technologies

Iraqi oil is characterised by the high content of sulphur (EIA 2016) (Administration, 2016) and so desulphurisation is essential in many refineries. The most commonly used technology in Iraq is hydrodesulphurisation (HDS). However, the disadvantages of HDS technologies in terms of cost, safety and environmental impact are driving the development of alternative methods for the desulphurisation of heavy fuel. In the past few years, many researchers (Al Zubaidi et al., 2015, Breysse et al., 2003, Gerber et al., 1999, Abid, 2015, Ahmad et al., 2017, Gary et al., 2007, Saleh, 2015, Speight, 2014) have studied alternative technologies, among which oxidation, absorption, extraction, desulphurisation by polymer Membranes (PV Process), Bio-desulphurisation (BDS), ultrasound-assisted technologies and desulphurisation using nanomaterials have found wide attention. A comparison of the major desulphurisation methods is shown in Table 3.2.

2.11.1 Hydrodesulphurisation (HDS)

HDS is the most commonly used desulphurisation technology. The removal of sulphur achieved by co-feeding oil and H_2 to a fixed bed reactor packed with an appropriate cayalyst; standard HDS catalysts are NiMo/ Al_2O_3 and CoMo/Al_2O_3. It needs severe conditions with a high temperature range of 280-400°C for 0-90 min under a total pressure of 2.9 MPa (Administration, 2016, Ma et al., 1995, Ma et al., 1996, Ma et al., 2002, Ma et al., 2003, Ma et al., 2005).

The main disadvantages are the high cost due to the temperature and pressure conditions, the need for a large reactor, and the use of a metal catalyst. The need for a large size reactor is because these operations are generally carried out in multiphase con-current trickle-bed reactors in which the liquid hydrocarbon and the gaseous hydrogen pass in a downward way through a fixed bed of solid catalyst. However, these reactors have their own limitations (Breysse et al., 2003, Brunet et al., 2005, Gerber et al., 1999, Ma et al., 1995, Ma et al., 1996, Abid et al., 2019,

Ahmad, 2016). For example, for the case of HDS, the concentration of hydrogen sulfide, an inhibitor for the HDS of the refractory sulphur compounds, increases along the downward axial length of the reactor. As a result, the concentration of H_2S becomes higher at the bottom zone of the reactor where the desulphurisation of the most refractory sulphur compounds takes place. In addition, the concentration of hydrogen becomes lower in this zone of the reactor thereby slowing down the rate of desirable hydrogenation reactions. The temperature of the catalyst bed at the lower part of the reactor also becomes higher which is not desirable for several reactions (Gerber et al., 1999, Babich and Moulijn, 2003).

H_2S is produced from the reactors as a waste stream. the hydrogen sulfide gas is then subsequently converted into the byproduct elemental sulphur or sulphuric acid, H_2SO_4. A large amount of hydrogen is required from a stream of hydrogen rich recycle gas or made up from an H_2 plant or by-products from the refinery units.

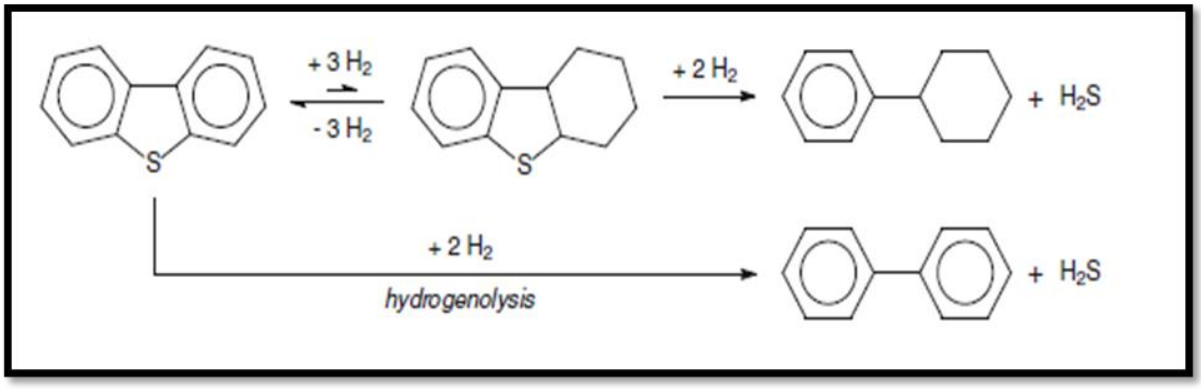

Figure 2.14 Hydrogenation and hydrogenolysis pathways of hydroDesulphurisation as illustrated by the Desulphurisation of dibenzothiophene (Babich and Moulijn 2003; Hosseini, 2012).

In addition, studies indicate that HDS is efficient only for specific hydrocarbon groups - mercaptans, thioethers, sulphides disulphides and thiophenes - and there is limited treatment of alkylated aromatic organosulphur as shown in schemes in Appendix 3 (Song, 2003) which represents the reactivity of various organic sulphur compounds in HDS versus their ring sizes and alkyl position which is a sufficient reason for finding alternative methods for desulphurisation (Farshi and Shiralizadeh, 2015). Two pathways of desulphurisation are distinguished as shown in Figure 2.14 (Babich and Moulijn, 2003, Hosseini, 2012).

The least hydrogen intensive pathway is by hydrogenolysis. For the reasons mentioned above, resonance stabilization of the sulphur in the thiophene ring makes direct hydrogenolysis difficult and the main HDS pathway requires saturation of the aromatic ring before HDS can take place. However, the equilibrium concentration of the hydrogenated product is low, because there is a significant driving force for aromatization by dehydrogenation. Hydrotreating

conditions typically range from 200 to 425 ℃ and 1 to 18 MPa, the specific conditions depending on the degree of desulphurisation required and the nature of the sulphur compounds in the feed.

There are many small capacity refineries in Iraq (10,000 - 30,000 b/d) (Administration, 2016), that cannot afford to install HDS and need to identify other suitable methods according to requirements and disadvantages of HDS (Song, 2003).

2.11.2 Oxidative Desulphurization (ODS)

The first research into oxidative desulphurisation was started in the 1960s. By 1990 some significant industrial processes had been developed for desulphurisation of petroleum blends including oxidation with peroxides and liquid-liquid extraction. The ODS process includes the steps as shown in Figure 2.15 below : 1-Reaction (ODS oxidative reactors (blue block) mixing and heating can be done in a mixing vessel) 2-Separation (can be done in a separator (green block) 3-Extraction (can be done in both mixing and separation vessels) (Farshi and Shiralizadeh, Fleming and Williams, Hosseini, Liu et al., Ma et al.)

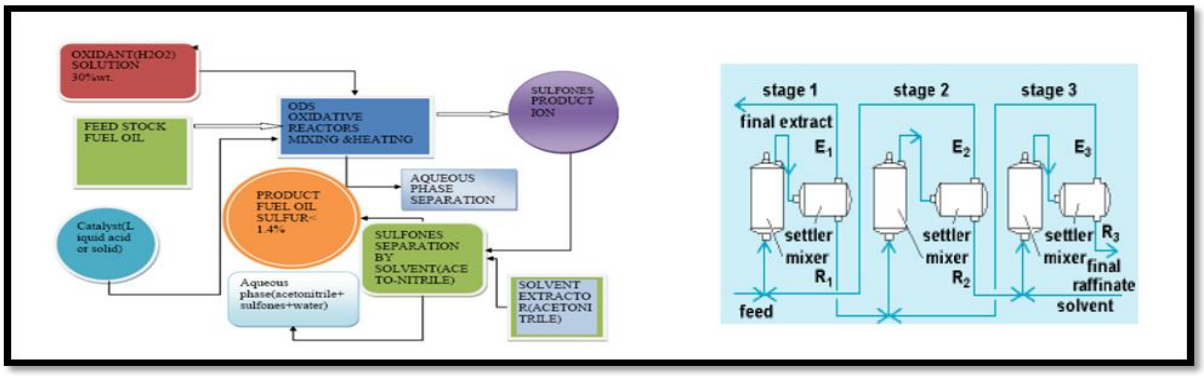

Figure 2.15 Oxidative desulphurisation Process steps (Farashi and Shiralizadeh 2015).

2.11.3 Extractive Desulphurisation (EDS)

Solvent extractive Desulphurisation is a simple and more desirable method because of its straightforward industrial application, with no requirement for H_2, and moderate, near-ambient conditions (Babich and Moulijn, 2003). Different types of solvents have been tried which resulted in 50–90% Desulphurisation depending on the number of extraction cycles in the process (Funakoshi and Aida, 1998, Forte, 1996, Kumar et al., 2017, Shakirullah et al., 2010). Solubility can be enhanced by choosing an appropriate solvent considering the nature of the sulphur compounds to be removed. This is usually achieved by preparing a ‘solvent cocktail’ such as acetone–ethanol or a tetraethylene glycol–methoxy triglycol mixture and mixtures of polyethylene glycols. In a mixing tank, the sulphur compounds are transferred from the fuel oil

into the solvent due to their higher solubility in the solvent. Subsequently, the solvent–fuel mixture is fed into a separator in which hydrocarbons are separated from the solvent by gravity. The desulphured hydrocarbon stream is used either as a component to be blended into the final product or as a feed for further transformations. The organosulphur compounds are separated by distillation and the solvent is recycled in Figure 2.16 (Babich and Moulijn, 2003).

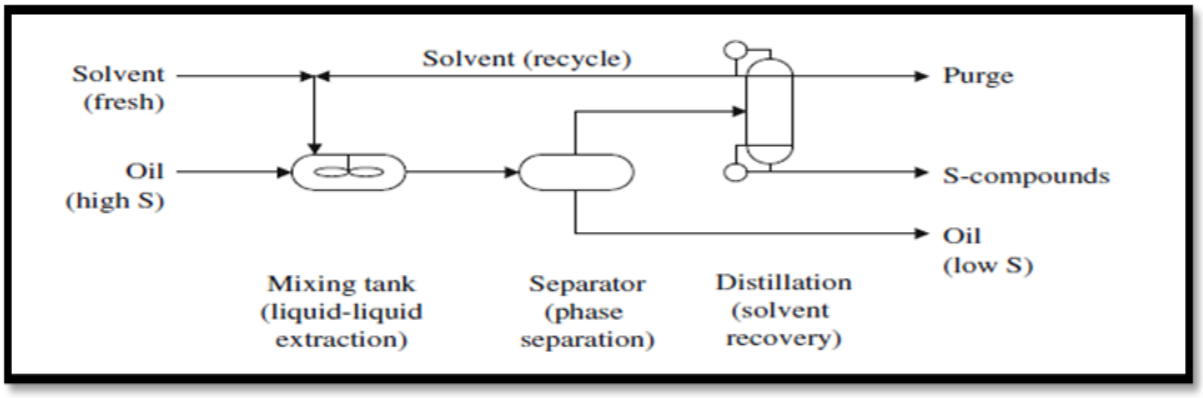

Figure 2.16 General process for extractive Desulphurisation as illustrated by extraction with a low boiling solvent (Babich and Moulijn 2003).

However, there are a few pitfalls:

(a) The solubility of the organosulphur compounds in the solvent and the number of process cycles influences the efficiency of the process. Different types of solvent have been used such as acetone, ethanol, and polyethylene glycols (Javadli and De Klerk, 2012) which resulted in 50–90% desulphurisation depending on the number of extraction cycles of the process (Forte, 1996, Funakoshi and Aida, 1998, Kumar et al., 2017, Shakirullah et al., 2010) .

(b) In order to allow proper physical separation between the solvent and the oil, the two phases must be immiscible. The solvent should also have low equilibrium solubility in the oil to limit solvent loss during the process. In addition, interfacial surface tension is an important property to consider in the design of liquid-liquid extraction processes. Ideally, it would be desirable that the immiscible mixture had a moderate interfacial tension, thus balancing the ease of dispersion (of non-equilibrated phases) and the promotion of phase separation (once the phases are equilibrated)(Burrows et al., 2017, Perry, 1954).

(c) The viscosity of the oil and solvent should be as low as possible to improve mixing and extraction. While it requires a boiling point difference to separate the solvent-oil mixture later. Due to these conditions, this method is heavily reliant on solvent properties.

The most difficult part of the process is separating the solvent/oil mixture. Since the solvent needs to be immiscible the need to make use of a light solvent and the potential loss of solvent by dissolution in such a complex matrix as heavy oil erodes the cost effectiveness of extractive

processes for desulphurisation of heavy oil. This might be achieved by using a high surface area material for sulphur removal as a solid sorbent in the adsorption process instead.

2.11.4 Adsorptive Desulphurisation

One easy and fast method to remove sulphur from oil is the adsorption desulphurisation process since it operates under normal atmospheric conditions. Adsorptive desulphurisation depends on a solid sorbent to selectively remove undesired sulphur from the oil. The effectiveness and selectivity of this depends on the hydrocarbons present and the materials adsorption capacity, durability, and regeneration ability (Ahmad et al., 2017, Chitanda et al., 2016, Mataji and Khoshandam, 2014, Prajapati and Verma, 2017, Saleh and Danmaliki, 2016).

Depending on feed properties and operation conditions several sorbent materials have been suggested. Among others, activated carbon, zeolites, amorphous silica-alumina, and metal organic framework (MOF) sorbents have been evaluated for desulphurisation of model oils, fluid catalytic cracking feedstock, coker naphtha, and distillates (Cychosz et al., 2009, Danmaliki and Saleh, 2017, Ma et al., 2003, Song and Ma, 2004) and the feasibility of the technology has been demonstrated. However, so far nothing is suitable for commercial use and, in order to improve this method, the target should be to develop the sorbent performance to be sufficient for industrial applications.

Thiophenes play an important role in desulphurisation, giving prominence to the adsorption process over the hydrotreating process as it is easier to be remove them by adsorption. Indeed, removal of thiophenes by hydrodesulphurisation is based on the reactivity while it depends on selectivity in adsorptive desulphurisation.

In the HDS process, the order of reactivity of various organosulphur compounds is as: Thiophene > R-Thiophene > Benzothiophene > R- Benzothiophene > Dibenzothiophene > R-Dibenzothiophene > 4-R-DBT > 4, 6-R2- Dibenzothiophene (Gates and Topsøe, 1997, Shafi and Hutchings, 2000). Ma and Song have recorded how the interaction between the S atom and the adsorption sites plays an important role in the competitive adsorption between DBTs and the adsorbent. From a comparison of DBT, 4-MDBT and 4,6-DMDBT, the adsorption selectivity increases in the order of 4,6-DMDBT < 4-MDBT < DBT, implying that the methyl groups at the 4 and 6-positions inhibit the interaction between the S atom and the adsorptive sites on the adsorbent, which leads to a decrease in the adsorption capacities of 4,6-DMDBT and 4-MDBT (Ma et al., 2003). However, the extent of removal of thiophenes in adsorption is higher than in hydrodesulphurisation.

Despite higher sulphur content in heavy oil, this method is impractical, due to the poor accessibility of large molecules in the narrow pores and steric hindrance that reduces adsorption effectiveness in the materials tried so far. This could probably be solved by using more open polyHIPE materials with better oil uptake; these will be developed to assess if this is practical in this project. General Comparison of the major desulphuration methods is shown in Table 2.4

Method	Operation Conditions	Conversion Factor	Advantages	Disadvantages
HydroDesulphurisation HDS	280-400 °C 2.9 MPa	90-95 %	-Efficient process has a high conversion factor. -Most common current use. -More appropriate for middle and large refineries. -The hydroDesulphurisation and hydrotreating units have a high operating and capital costs but are still economically successful for large refineries because of high sulphur recovery about 20 ton /day which is difficult to achieve in medium and small refineries.	-High Cost -High pressure and temperature -This process is efficient for mercaptans, thioethers, sulfides, disulfides and thiophene removal, but it has shown limitations regarding the treatment of alkylated aromatic sulphur compounds. - Need for catalyst, large reactor.
Oxidative Desulphurisation ODS	Low temperatures 30-60 °C Normal atmospheric pressure	45-50 %	- Easy deletion of sulphur species that were resistant to hydroDesulphurisation. - Availability of air in refineries. - Reduction of the sulphur in fuels to new levels of ultra-low sulphur approximately 10 ppm. - Good size for small and medium refineries. - Has potential for ultimate Desulphurisation. - Fuel oil Desulphurisation to low amount.	- ODS process is not commercial till now and HDS process is an industrial process that many technologists support. - A large volume of chemicals are used in ODS processes and have environmental impact not solved till now.

Extractive Desulphurisation EDS	0-60 °C atmospheric pressure	50–90%	-Extractive Desulphurisation is an attractive method because of its straightforward industrial application. - No requirement for H_2 - Moderate process conditions; the mixing tank can be operated at near-ambient conditions - The feedstock is not chemically converted and the process is a purely physical extraction.	-The solubility of the organosulphur compounds in the solvent influences the efficiency of the process. The process requires immiscibility for the two phases of solvent and oil to allow proper physical separation between them. - The viscosity of the oil and solvent should be as low as possible to improve mixing and extraction, while it requires a boiling point difference to separate the solvent –oil mixture later this will consume more energy leads to increase operation costs . - Due to these conditions, this method is heavily reliant on solvent properties.
Adsorptive Desulphurisation ADS	0-80 °C atmospheric pressure	65-100%	-Acceptable Desulphurisation degree that was achieved under mild reaction conditions. -The efficiency of this method depends on the properties of the sorbent material: selectivity to organosulphur compounds relative to hydrocarbons, adsorption capacity, durability, and regenerability.	-The performance of even the most efficient of the adsorbents is still insufficient for industrial applications. -Regeneration costs of the sorbent, regeneration is usually done by flushing the spent sorbent with a desorbent, resulting in a high organosulphur compound concentration flow.

Table 2.4 Comparison of the major desulphuration methods.

3 Adsorption

3.1 Definition, concepts, principles, and theory

The earliest and most widely read studies that described adsorption were established by Freundlich in 1906, Langmuir in 1918 and Brunauer et al., in 1938, in which adsorption theories and the governing equations were developed based on firstly empirical observations that describe the adsorption characteristics on a heterogeneous surface then monolayer adsorption processes on energetically homogeneous surfaces. They were further extended based on the adsorption of gases in multimolecular layers and finally the Brunauer-Emmett-Teller (BET) equation which is mostly used in gas phase adsorption and is itself based on statistical analysis of adsorption sites occupied during a multi-layer adsorption of gases (Brunauer et al., 1938, Suzuki, 1990, Langmuir, 1918, Gary et al., 2007).

Adsorption is defined as a physical-chemical phenomenon in which a certain substance in a liquid or gas (called an adsorbate) tends to adhere to the unoccupied spaces on the surface of solid material (called the adsorbent) due to the presence of unsaturated molecular forces within them (Mantell, 1951). The principle of adsorption is based on the selectivity of the solid surface that relates to the substance capability to adhere via either physical bonding, in terms of Van der Waals forces describing the intermolecular forces that cause the interactions between two different molecules or chemical bonding. Physical adsorption includes dispersive, polarization and dipole forces. Chemical adsorption includes the formation of chemical bonds between the adsorbate molecules and the surface of the adsorbent as a result of the interaction of electrons between the solid and the fluid atoms. (Ruthven, 1984, Burrows et al., 2017).

There are some major differences between adsorption and absorption which can modify these theories. First of all, adsorption occurs only where atoms, ions or molecules from a substance which could be gas, liquid or dissolved solid adhere to a surface of adsorbent creating a film of adsorbate. However, in absorption the entire volume of the fluid is dissolved by a liquid or a solid absorbent as shown in Figure 3.1. Adsorption is an exothermic process, in which surface phenomenon could be affected by temperature and the material concentration is different in the surface and the bulk. Absorption is an endothermic process, a bulk phenomenon not appreciably affected by temperature with uniform concentration throughout the material. Finally, the reaction rate is constant and uniform in absorption while adsorption steadily decreases as

surface sites are used up until an equilibrium is reached and the material needs regeneration if further adsorption is to occur.

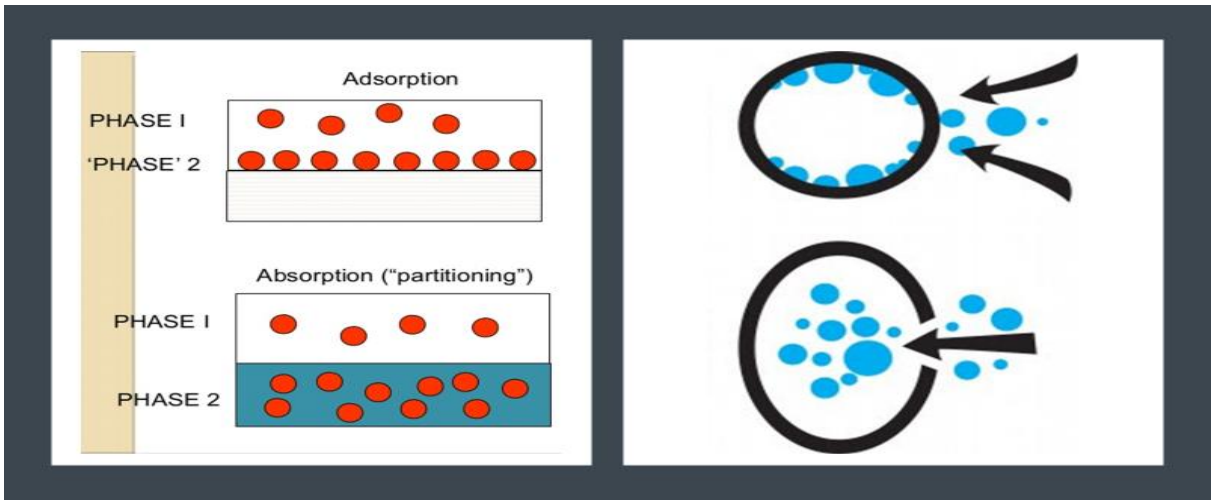

Figure 3 1 The differences between adsorption and absorption.

Regeneration is the reuse of adsorbent after being saturated with the selected molecules and is essential in the petroleum industry for economic reasons. It may take place by washing the adsorbent with a proper solvent to recover adsorbates that cover the surface or by heating in air to displace the adsorbates depending on the adsorbent nature and the adsorbate characteristics. Moreover, for the physical adsorption it is generally possible, as physisorption is reversible, unlike chemisorption which may be irreversible or very difficult to regenerating the adsorbent because of the strength of the chemical bonds formed. However, the selectivity of chemical adsorption is higher than physical adsorption. (Babich and Moulijn, 2003, Hernández-Maldonado and Yang, 2004, Zaki et al., 2013).

3.2 Adsorption types in desulphurisation.

During recent years sulphur adsorption has attracted extensive research interest. Researchers have been motivated by increasing concerns for safety and environmental limitations of current approaches that govern legislation. As a result, several models of sulphur absorption have been demonstrated. Some of these models will be covered in this section as shown in Figure 3.2

Figure 3.2 Types of adsorptive desulphorisation. (Song and Ma, 2003)

3.2.1 Selective adsorption

This adsorption model is suggested and named SARS (Selective Adsorption for Removal of Sulphur Compounds) by Pennsylvania State University (Ma et al., 2002, Song, 2003) in which the feedstock contains less than 1wt % sulphur compounds. The aim of SARS is to formulate suitable adsorbents which are appropriate, effective, and selective for surfaces that have high attraction to sulphur compounds.

The surface is activated from nickel on an alumina support and an air regenerable metal oxide is produced that creates a site-specific interaction actively uniting with thiophene compounds in terms of coordination geometrics. The theory of the SARS technique depends on the site-specific interaction between sulphur and metal species which is possible with selected organometallic complexes. The likely adsorption configurations of thiophenic compounds on adsorbents used in SARS process can be explained from the known coordination geometries that thiophene exerted upon contact with organometallic complexes. An example of coordination geometries is given in Figure 3.3. This coordination geometrics explain the tendency of the sulphur atom in the thiophene molecules to interact with metal species by p-electrons; in other words, the sulphur atom of thiophenes interacts with one or two metal atoms in the adsorbent.

Figure 3.3 Coordination geometrics of thiophene in organometallic complexes.

3.2.2 Reactive adsorption

This model is based on the possible chemical attraction between the sulphur compounds in the fuel and sorbent material, the result is sulphur free fuel and total or partial removal (or transfer) of sulphur compounds that deposit on the surface of the adsorbent. The adsorbent could be regenerated by disposing of the adsorbates on the surface converting them to SO_2, H_2S, or elemental sulphur depending on the techniques used.

Two main factors affect the efficiency of this model, firstly the operational conditions, as it could be carried out at standard conditions or elevated temperature, high pressure and with /without the presence of hydrogen. Secondly, the adsorption capacity that depends on 1) the adsorbent surface activity and affinity to the sulphur compounds 2) its thermal and mechanical stability and 3) the ability to be regenerated (regenerability). The adsorption mechanism is shown in Figure 3.4. The sulphur atom removed from the molecule and adhering on the surface of the adsorbent, bound by the sorbent while hydrocarbon part is returned to the final product without any structural changes (Gupta and Turk, 2007, Turk and Gupta, 2001, Babich and Moulijn, 2003).

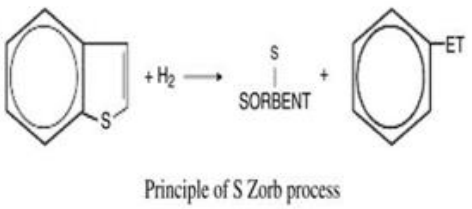

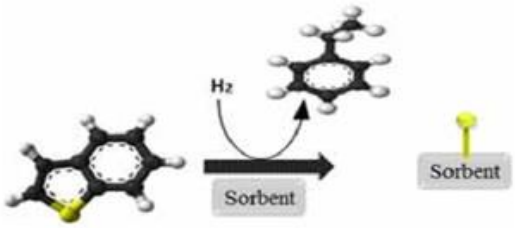

Figure 3.4 Reactive adsorption model of benzothiphene on metal oxides adsorbent in presence of hydrogen.

The widely used S Zorb process designed by Philips Petroleum in the US developing an efficient Desulphurisation at higher temperatures of between 340 -410°C and lower pressure of H_2 between 2-20 Atm (Song and Ma, 2004).

3.2.3 Polar adsorption

The IRVAD process is an example of adsorption-based Desulphurisation based on the polarity of sulphur compounds in various light fractions including FCC gasoline. This technology called IRVAD is a combination of the inventor's name 'IRVine' and 'ADsorption' and was developed by the Black and Veatch Pritchard Engineering Company. The elemental material in adsorption manufacture is activated alumina which has an affinity for polar compounds (Irvine, 1998). The process technique is operated over an alumina adsorbent based on a counter-current moving bed in contact with liquid hydrocarbon in a multistage adsorber as shown in Figure 3.5. It is conducted at over 240 ℃ and at low pressure with a sulphur/adsorbent weight ratio of around 1.4. The adsorbents are regenerated in the reactivator with slightly higher temperature exposure. The adsorption capacity depends on many factors including the adsorbent characterstics such as particle size, or the technique's parameters such as the number of adsorption–reactivation steps, the weight ratio of the hydrocarbon feed to the adsorbent and could reduce sulphur from various feedstocks to about 0.5 ppmw. (Babich and Moulijn, 2003).

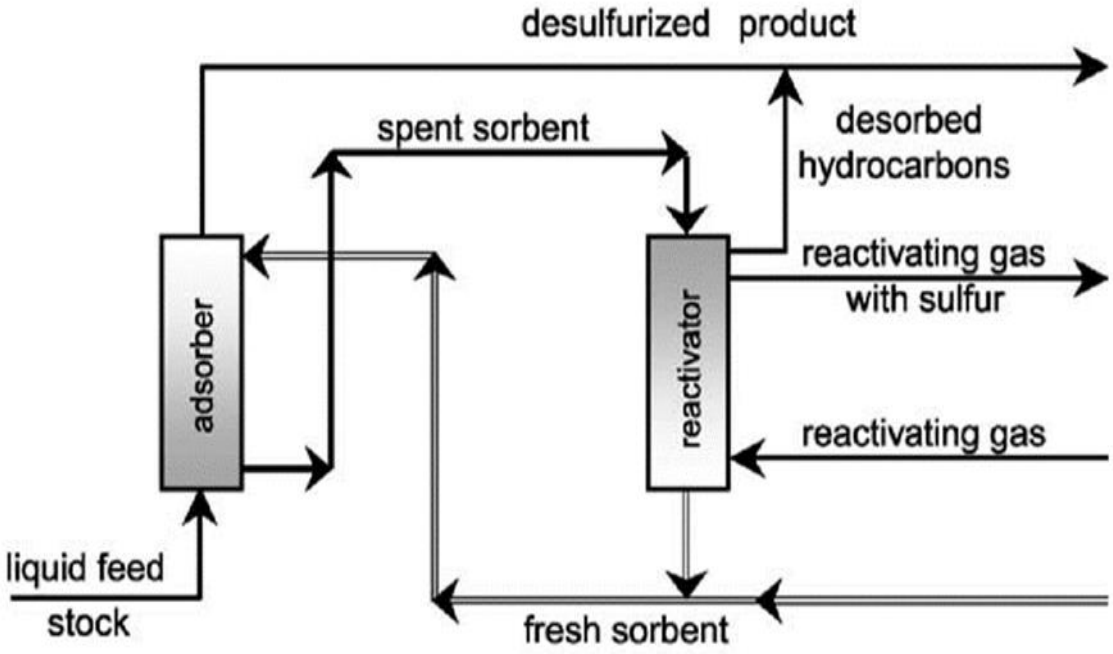

Figure 3.5 IRVAD adsorptive adsorptive Desulphurisation process flow diagram. (Irvine, 1998)

3.2.4 π-Complexation

This technique, based on the forming of π-Complexation between cations metals such as Na^{+}, Zn^{2+}, Ni^{2+} ,Cu^{+}, Ag^{+}, Fe^{2+}, Ce^{4+} , sulphur compounds such as thiophene, BT and DBT from light distillates, has been studied by a group of researchers including (Hernández-Maldonado and Yang, 2004, Yang et al., 2006, Shen et al., 2012). Deep-desulphurisation levels have been achieved as a result of a π-complexation between the Cu+ ions ($1s^2 2s^2 2p^6 3s 23p^6 3d^{10} 4s^0$) and the thiophene rings as seen in Figure 3.6. These cations form the usual σ bonds with their empty s-orbitals and other bonds when their d-orbitals can back-donate electron density to the antibonding π-orbitals (π*) of the sulphur rings.

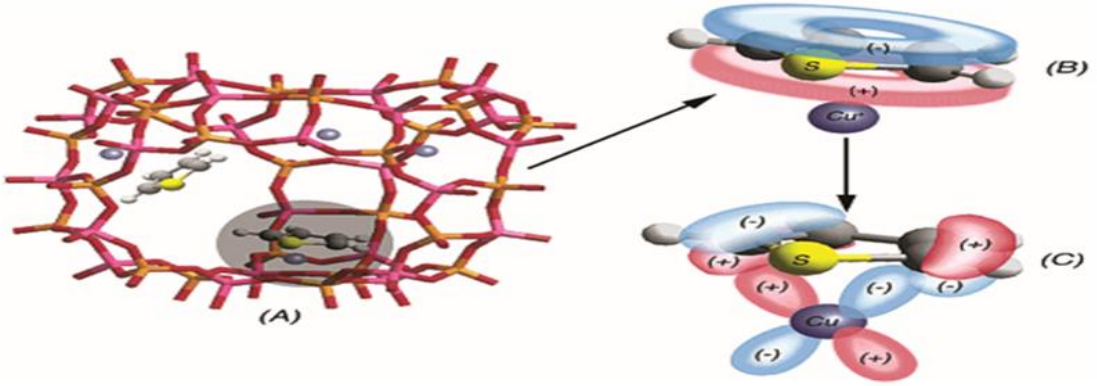

Figure 3.6 Faujasite supercage with copper ions occupying 6-ring windows sites (A); σ-donation of π-electrons of thiophene to the 4s orbital of copper(I) (B); d-π* back-donation of electrons from 3d orbitals of copper(I) to π* orbitals of thiophene (Hernández-Maldonado and Yang, 2004).

Different adsorbents have been developed based on this mechanism for aliphatic, olefin and aromatic separation (Takahashi et al., 2001) .

3.2.5 Integrated adsorption technique

This novel technique combines selective adsorption with HDS technology using deep and active catalysts for effective removal of sulphur compounds from light distillates. It improves the process features by reducing cost, maximizing efficiency, accelerating Desulphurisation rates, and reducing reactor volumes rather than using a single process alone. The schematic diagram (Figure 3.7) for the technology is discussed in detail elsewhere by (Song and Ma, 2003, Song, 2003).

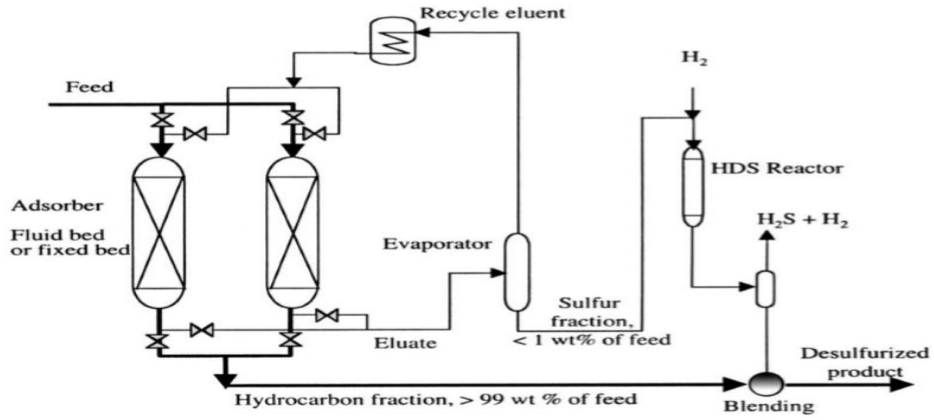

Figure 3.7 The proposed adsorption process for deep Desulphurisation.

All adsorptive desulphurisation processes require suitable adsorbent materials. This is discussed in the next section.

3.3 Nanomaterials and hybrid adsorbents.

In the literature, there are reports of several different types of materials being used as adsorbents for adsorptive desulphurisation of various distillate fractions like model oil and gasoline, naphtha, diesel, and jet fuel oil. These are activated carbon (AC), alumina, zirconia, silica, and various kinds of nanomaterials, hybrid or porous materials such as metal−organic framework materials (MOFs) (Peralta et al., 2012, Wu et al., 2012). They are applied in most industrial applications to improve performance because of their surface properties far exceeding their bulk properties.

Nanomaterials are all types of materials with nanoscale dimensions; a material that has a unit size between the ranges of 1-100 nm such as alumina, zirconia, silica, and AC. These have been the subject of research recently due to their promise in adsorption desulphurisation (Triantafyllidis and Deliyanni, 2014).

Adsorbents are generally classified into organic sources and inorganic sources. Adsorption on commercial and industrial scale depends solely on the type, quantity, economic cost, and effectiveness of the adsorbent material. Therefore, studies on adsorption currently focus on the development of better adsorbent materials for large-scale industrial applications. Most materials used as adsorbents are relatively porous and have a large surface area with pore diameters of the order of nanometers (Saleh et al.,2017).

The most widely used adsorbents are: AC, silica gel, zeolites, molecular sieve carbon, activated alumina, polymers and nanocomposites. Each of these materials has distinct physical and chemical characteristics such as pore sizes and structure, porosity and nature of the adsorbing surface that are different from other materials. The materials that can be used as adsorbent

should be thermally and mechanically stable, highly porous with a balance between micro and macro-pores with high surface area, high affinity for the adsorbate and should be cheap and easily regenerated. Table 3.1 outlines the classes and the applications of the major adsorbents. In the previous section the known adsorbent materials in use were explained, namely: nickel/alumina, zeolites, silica, based adsorbents as well as activated carbon (AC), metal oxides, metal sulphides and reduced metal-based sorbents (Hernández-Maldonado and Yang, 2004, Hernandez et al., 2010, Fukunaga et al., 2003, Ma et al., 2003, Dhage et al., 2011, Samokhvalov and Tatarchuk, 2010, Samadi and Zarenezhad, 2016). The target beyond studying each individual adsorbent is to focus on the development of the adsorbent synthesis and process efficiency to meet parameters such as cost effectiveness, efficiency and reliability as adsorbent materials. Consequently, high adsorption capacity and selectivity to reduce the sulphur compounds directly lead to minimization of the sulphur concentrations and to easier regeneration, which result in minimal environmental disposal impact.

3.3.1 Silica

Silica has been used as an adsorbent in wide research applications in desulphurisation. It is also used in ODS due to the simplicity of modifications desired to improve the process. Moreover, several reports demonstrate the suitability of using silica in desulphurisation as a consequence of the fact that mesoporous silica is effective in ODS. Silica has a high affinity for sulphur compounds, and high regeneration potential (De Filippis and Scarsella, 2008). In addition, mesoporous silica of high and low surface area combined with zirconia has been demonstrated in ADS and denitrogenating of light distillates. SEM images of the synthesized sample show a particle diameter between 2-4 µm. In addition, Mesoporous silica nanoparticles are also effective in desulphurisation of DMDBT and can perform better than other adsorbents (Palomino et al., 2014). Lead loaded on mesoporous silica reduces 1000 ppm sulphur containing gasoline to 50 ppm in three rounds of adsorption/desorption cycle (Rodrigues et al., 2014). Silica is used as a reinforcing agent for polyHIPE due to its good mechanical properties (Haibach et al., 2006) and silica particles can be easily stabilized in high internal phase emulsions (Ikem et al., 2008) synthesizing highly interconnected microporous polymers. (Zheng et al., 2014) . This suggests it is a good potential material for developing a polyHIPE based material for Desulphurisation in this project.

3.3.2 Zeolite

Zeolites have been reported by many workers as both adsorbent and polyHIPE reinforcement. It has been used in three types of adsorption processes; reactive, selective and π-Complexation (Takahashi et al., 2001, Velu et al., 2002, Dehghan and Anbia, 2017). Zeolite was employed for Desulphurisation of various model fuels containing about 500 ppm. At normal conditions, the adsorption capacity of TH, THT and 4,6-DMDBT is indicated to be about 7.0, 17.4 and 14.5 mg of sulphur/g of adsorbent, respectively (Tang et al., 2008). The removal of dibenzothiophene from model fuel was investigated by adsorption on commercially available adsorbents including aluminum oxide, 13X and Y zeolite. Adsorption of benzothiophene (Abdulrahman et al., Ganiyu et al., Jimat, Ma et al., Menner et al., Triantafyllidis and Deliyanni) as a model heterocyclic and aromatic sulphur compound present in road fuels, over agglomerated zeolites with modified structure was clearly demonstrated. it should high removal capacity and good adsorbent features as shown in Table 3.1. (Yang and Kaneko, 2002, Yang et al., 2006, Sotelo et al., 2007).

3.3.3 Zirconia

Zirconia has shown suitable properties for adsorption, in terms of structure, morphology, surface area, good thermal stability, etc. and possesses both oxidizing and reducing features as it shows bi-functional acid/base properties. In general, it can be synthesized by the sol-gel process in a crystallite size ranging from 2 to 10nm with particle size of around 50-80nm. All these properties suggest it to be a good adsorbent for adsorption and ADS and oxidation Desulphurisation (ODS) of thiophene from n-octane and n-heptane has been demonstrated (Kumar et al., 2011, Wang et al., 2009).

3.3.4 Alumina

Adsorptive desulphurisation theory is in principle based on the contact between a solid material that has high porosity and surface area in contact with fuel to selectively adsorb the aromatic sulphur. Alumina has attracted much attention from researchers due to its good adsorptive characteristics and chemical stability. In addition, it has high thermal conductivity compared to most ceramics and is highly insoluble in water; aluminum oxide can be converted to boehmite ($Al(OH)_3$) in hot water but reaction rates are slow. Moreover activated alumina has been tested in adsorption studies but the result was not good due to large steric effects, however, this work revealed how the adsorption selectivity could depend heavily on the acid-basic interaction and the molecular electrostatic potential with the adsorbate (Kumar et al., 2011, Zaki et al., 2013, Srivastav and Srivastava, 2009, Jeevanandam et al., 2005).

3.3.5 Activated Carbon

The use of carbonaceous materials to eliminate liquid or gaseous contaminants has been practiced since the late 18th century. Wood charcoal, one form of activated carbon, was applied in refining raw sugars, while the carbons used in air purification were developed for gas masks during World War 1 (Gray, 1993). There is a much greater need to use the material for contamination reduction nowadays due to increasing concerns about environmental pollution from industrial gaseous emissions (Ali and Khan, 2017). For instance, the annual emissions of CO_2 , SO_2 and NO_2 are around 100 million tons to the atmosphere. However, the high cost and limitation of the traditional technologies (Shang et al., 2013), have meant that novel and modern techniques have received significant attention and modifying active carbons has been a critical part of this. In particular specific carbon adsorbents have gained prominence in numerous studies or applications over the last decades (Bandosz, 2006) due to the deep removing of sulphur which is supposed to deliver the acceptable sulphur content in gasoline as an example, being reduced to 10 ppm in most developed countries (Shang et al., 2013).

In the crude oil industry the problem was more complicated with the shortage in production of low sulphur level crude oil during the last decades (Song, 2003). Modern activated carbons are one of the most important adsorbents used. This is based on their physical properties; namely, very high surface area and adsorption capacity, high mechanical and thermal stability. Recent developments are based on the emergence of nanoscience concepts and nanotechnology techniques and have led to the development of nanocarbons with great potential as shown later. Activated carbon represents a high efficiently adsorbent towards different pollutants including inorganics, namely: CO_2, (Deng et al., 2017, Liu et al., 2018). SO_2 (Bashkova et al., 2001), H_2S (Shen et al., 2018), NO_x (Pietrzak and Bandosz, 2007) and organics such as organosulphur compounds, thiols (Dalai et al., 1997, Chiang et al., 2000, Bashkova et al., 2002) and thiophenes compounds (thiophene, benzothiophene and dibenzothiophene (Li et al., 2016, Saleh et al., 2017, Anisuzzaman et al., 2017) and 5-methyl-1-benzothiophene (MBT), 4,6-dimethyldibenzothiophene (DMDBT) and 4-methyldibenzothiophene (MDBT). (Saleh et al., 2018).

Activated carbon has an internal area higher than its outer surface area as a result it can adsorb large quantities of the adsorbate. In addition, activated carbon surface chemistry can be easily modified by oxidation or adding metals and other techniques as reported in previous studies (Jiang et al., 2003, Chiang et al., 1999, Deng et al., 2017, Yu et al., 2013) to obtain an

active surface of high surface area and the maximum variety in pore sizes classes (Triantafyllidis and Deliyanni, 2014):

1) Macro porous adsorbents (>50nm),
2) Meso porous adsorbents (between 2 and 50nm) and
3) Micro porous adsorbents (between 0.2 and 2nm)

Ania and Bandosz (2005) illustrated in their study the importance of the pore sizes and surface chemistry of AC and linked them with the sulphur removal capacity. They suggested that the higher capacity depends on large volumes of narrow micropores. The dependency of sulphur removal capacity on AC porosity and sulphur compounds particle and molecular size were also mentioned by (Bandosz, 2006, Triantafyllidis and Deliyanni, 2014, Bandosz and Ren, 2017). For instance, the SO_2 adsorption capacity depends on the volume of pores with widths between 0.679 and 0.858 nm is significant for the sulphur compounds since they are similar in size to molecules as estimated by molecular orbital calculations to be 0.59×0.89 nm, and thus enhance the adsorption potential.(Bandosz, 2006)

Besides surface chemistry and porosity, mechanical and thermal properties play sufficient roles to consider the adsorbent industrially and commercially. In general, AC is nanocomposite and hybrid material could be used as directly as an adsorbent or as a filler to polymer composites to enhance their thermal, mechanical, electrical properties. It is useful as a result of its low weight, ability to readily spread, whether it is powder or granules and availability in various structural forms and ease of fabrication of these composites through compression moulding. (Abdul Khalil et al., 2013, Haibach et al., 2006, Luo et al., 2012b, Saeidi and Lotfollahi, 2015, Yang et al., 2018).

3.4 Applications of adsorbent materials and potential for crude oil Desulphurisation

Numerous published results indicate all of these five adsorbents, (zeolite, zirconia, silica, alumina and activated carbon (AC) have potential for industrial application illustrated in Table 3.1. Some of the most relevant literature regarding their use for desulphurisation of oils is summarized in Table 3.2. In these studies, different adsorbents, models of fuel oil (or distillates) and various testing methods have been used.

Activated carbon will be used in this study for the following reasons; firstly due to it being a raw material resource; usually agricultural waste such as oil palm, coconut, and bamboo are used to produce it at low cost compared to the other adsorbents. The cost factor represents an essential factor in process design (Abdul Khalil et al., 2013). In addition, according to the study by (Miao et al., 2015), it was found that sulphur removing capacity of the activated carbon is about 3.3 times higher than that of Ni/SiO_2-Al_2O_3 and about 4.6 times higher than that of the activated alumina. Secondly, it is a highly efficient adsorbent for those feedstocks that have high sulphur content compared to other adsorbents but generally attains low levels of total desulphurisation when treated by adding MEA. In contrast, zeolite is efficient only with deep desulphurisation of low sulphur feeds. As a result, AC is more appropriate in this study as the model fuel oil and the real distillate of high sulphur feedstock. Applications of the main different adsorbents are shown in Table 3.1 (Saleh, 2015).

Adsorbent	Applications
Carbons	Widely used in the removal of hydrogen, nitrogen, odors, vinyl chloride, desulfurization of SOx and denitrogenation of NOx from gasses, in water treatment, and in the treatment of nuclear waste.
Alumina	It is mostly used in drying of gasses (as a desiccant) and adsorption of fluoride, chromium, arsenic and selenium in water treatment. It is also used in desulfurization.
Silica	It is used as a desiccant in drying of gasses, maintenance of relative humidity, and in desulfurization.
Zeolites Zirconia	• Helps in drying of gasses, water treatment, sweetening of gasses and liquids, aids in pollution control of SOx and NOx through desulfurization and denitrogenation, recovery of CO_2, and in the separation of aromatics from paraffins etc. • Desulfurization, adsorption of gasses such as: CO, CO_2, NH_3, dentistry, biomedical, ceramics, and sometimes used as an alloying agent.

Table 3.1 Applications of the main different adsorbents (Saleh, 2015).

no	Investigator	Feedstock Solvent	S-compounds	Adsorbent ADS Capacity	Analytical method
1	**(Miao et al., 2015)**	1—toluene; solvent 2—40 wt.% toluene in 60 wt.% dodecane; and solvent 3—dodecane	naphthalene (Nap, 99%), benzothiophene (BT, 99%), dibenzothiophene (DBT, 98%), 4-methyldibenzothiophene (4-MDBT, 96%), 4,6-dimethyldibenzothiophene (4,6-DMDBT, 97%), and dibenzothiophene sulfone ($DBTO_2$, 97%), respectively	TiO_2/SiO_2 85%	Antek 9000 series total sulphur analyser
2	**(Ma et al., 2005)**	*gasoline* *iso*-octane	190 ppmw sulphur in the form of thiophene(3-methylthiophene (2-MT), 2,4-dimethylthiophene (2,4-DMDBT) and BT	nickel-based adsorbent Cu(I)Y-zeolite 60%	Antek 9000S total sulphur analyser
3	**(Kim et al., 2006)**	n-Decane 44.01 nHexadecane 44.02 nTetradecane	dibenzothiophene (DBT), 4,6-dimethyl-dibenzothiophene (4,6-DMDBT),	activated carbon, activated alumina and nickel-based adsorbent) 90%	Antek 9000 series total sulphur/nitrogen analyser
4	**(Ma et al., 2007)**	Real jet fuel (JP-8)	benzothiophene (BT), 2-methylbenzothiophene (2-MBT), 5-methlybenzothiophene (5-MBT) and dibenzothiophene (DBT)	Group of Fe supported on an activated carbon 82%	ANTEK 9000 series sulphur analyser
5	**(Xiao et al., 2008)**	n-octane	benzothiophene (BT) and dibenzothiophene (DBT)A126	The activated carbon (40-60 mesh) Zeolite 85%	high-performance liquid chromatography (HPLC).
6	**(Zhou et al., 2009)**	model diesel fuel 400 ppmw of sulphur	benzothiophene (BT), dibenzothiophene (DBT), 4-methyldibenzothiophene (4-MDBT) and 4,6-dimethyldibenzothiophene (4,6-DMDBT)	Activated carbon treated with HNO_3 77%	ANTEK 9000 series sulphur analyser ≤50%
7	**(Seredych et al., 2009)**	mixture of decane and hexadecane	same molar concentrations of dibenzothiophene (DBT), 4,6-dimethyldibenzothiophene (4,6-DMDBT), naphthalene (Nap) and 1-methylnaphthalene (1-MNap)	Activated carbon of specific pore volume and particle size . 90%	Waters 2690 liquid chromatograph equipped with a Waters 996 photodiode array detector Sulphur content was estimated using Perkin Elmer total sulphur analyser.
8	**(Wang et al., 2012)**	n-octane	Thiophene Benzothiophene (BT), dibenzothiophene (DBT),	Polymer-Supported Metal Chlorides Ionic Liquid Moieties 87%	GC-flame photometric detector (GC-FPD) with SE-54 capillary column (30 m × 0.32 mm inner diameter × 1.0 μm film thickness).

9	**(Khan et al., 2013)**	n-octane (75 vol.%) and toluene (25 vol.%)	Benzothiophene	Cu+/activated carbon 86%	Langmuir and Freundlich equations
10	**(Triantafyllidis and Deliyanni, 2014)**	hexadecane	4,6-DMDBT	different origin and surface chemistry nanoporous activated carbons 95%	UV spectrophotometer
11	**(Fallah et al., 2014)**	heptane (> 99%)	thiophene, Benzothiophene (BT), dibenzothiophene (DBT) and 4,6-dimethyldibenzothiophene (DMDBT)	activated carbon cloth 87%	Thermo Trace GC Ultra, equipped with a flame ionization detector (FID)
12	**(Xia et al., 2016)**	n-octane	thiophene, BT or DBT	hierarchical porous organic polymer of poly-methylbenzene with metal impregnation 83%	GC-950, Haixin Chromatography
13	**(Neubauer et al., 2017)**	jet-A1 fuel	Benzothiophene (BT), dibenzothiophene (DBT), and 4,6-dimethyldibenzothiophene (4,6-DMDBT)	Ag-Al_2O_3 80%	Shimadzu TQ 8040 triple quadrupole system equipped with a Shimadzu AOC autosampler
14	**(Danmaliki and Saleh, 2017)**	solvent of 85% hexane and 15% toluene.	thiophene, benzothiophene (BT), and dibenzothiophene (DBT)	Activated carbon modified with Ce/Fe nanoparticles 91%	Gas chromatography equipped with sulphur chemiluminescence detector (GC-SCD)
15	**(Ahmad et al., 2017)**	Cyclohexane Kerosene 0.0542 wt% Diesel 1.041 wt%	DBT 1000 ppm	Montmorillonite Clay +metals 90%	CHNS analyser +UV-visible spectrometer
19	**(Saleh et al., 2017)**	mixture of hexane (85 vol%) and toluene (15 vol%)	thiophene, benzothiophene and dibenzothiophene	activated carbon manganese oxide nanocomposite 90%	gas chromatography employing sulphur chemiluminescence detection (GC-SCD).
20	**(Prajapati and Verma, 2017)**	n-octane commercial diesel	TH/DBT	nickel nanoparticle-doped activated carbon beads with/without carbon nanofibers 85%	X-ray fluorescence spectrometer (XRF-Rigaku) with an X-ray generator (4 kW, 60 kV, 150 mA)

Table 3.2 Studies about adsorbents, model fuel oil, test methods and adsorbate .

3.5 Summary and outlook of Chapter 2 and Chapter 3 on adsorbents synthesis methods linked to PolyHIPE in the next chapter.

In chapter 2, the importance of crude oil in both the exporting sector and in local petroleum consumption to the Iraqi petroleum economy has been discussed and the main industrial obstacles to improving the oil industry, particularly those issues relevant to crude oil, sulphur content and desulphurisation technologies, has been identified. The three essential fundamentals: crude oil, sulphur content and desulphurisation methods have been discussed to provide the foundation for the research to be undertaken in this project; the polyHIPE polymer preparation, adsorbent syntheses, and model fuel oil creation in the next chapters.

The chapter starts with a discussion of crude oil composition with a description of the main elements and compounds that form this complex mixture. This demonstrates how organic materials (hydrocarbons) and inorganic compounds characterize crude oil. Their appearance is different in different crude types which makes them an important criterion for crude oil classification beside the sulphur content. At the same time, these hydrocarbons create bonds with sulphur forming organosulphur compounds which, adding to inorganic sulphurs, have numerous effects in the petroleum industry in terms of crude oil price, crude oil classification, governmental and environmental legislation and the complexity of the petroleum refinery.

The refining process of the crude oil is also significant; the main distillate stream compositions and operation conditions generate different sulphur contents. The distribution, and consequences of sulphur compounds in these distillates and finally the main desulphurisation techniques and units have been discussed. Unlike the hydrodesulphurisation unit it has been shown that adsorptive desulphurisation is a promising technology due to cost-effectiveness, viability, and suitability to Iraqi small and medium size refineries and the sulphur removal capacity towards the complicated sulphur compounds. However, hydrodesulphurisation is still the most efficient and commonly used desulphurisation technology. This is because adsorptive desulphurisation needs more modification and optimisation as it depends heavily on its core factor which is the adsorbent.

Chapter 3 started with reviewing the adsorption theory. Then it has been discussed the difference in adsorbents types have been explained. In order to develop new adsorbents with high selectivity and high capacity, it is necessary to modify the commercially available adsorbents, or to design a layered adsorbent bed for a practical application. In ultra-deep desulphurisation, it is critical to fundamentally understand the adsorptive mechanism and selectivity for various species over different adsorbents. Consequently, more work has been

done on activated carbon as it represents a major solid adsorbent with potential similar to the liquid sorbent monoethanolamine (MEA) which is used for gas treatment. Both of these materials could be used to generate a novel solid adsorbent based on a porous polymer support. Thus, this study will focus on the preparation and modification of the basic PolyHIPE material. Also, the factors affecting the adsorption process should be investigated including

1) contact (agitation or shaking) time,
2) agitation speed,
3) feedstock type and initial concentration
4) adsorbent mass and
5) treatment temperature.

These will be explained in detail in the later results chapters.

In conclusion, adsorption capacity of adsorbents usually depends on 1) surface chemistry and their active sites on surface 2) availability of appropriate pore volume and size to the adsorbate and 3) the inclusion of high surface area to ensure the maximum contact (Miao et al., 2015).

In this study a novel combination of polyHIPE, MEA and activated carbon is used to create a adsorbent with synergetic properties. It is expected that adsorbent synthesis can ensure the major requirements for a successful adsorbent. These are adsorption capacity, thermal and mechanical stability, and the ability to be regenerated (regenerability).

PolyHIPE preparation and morphology will be defined according to these requirements. Moreover, in order to add more activity to the polyHIPE adsorption MEA and activated carbon will be added to the polyHIPE preparation process. It will be shown that the role of activated carbon in improving the density and mechanical properties of the polyHIPE is crucial. The next chapter will overview the preparation, properties, applications, and morphology of polyHIPE.

4 Literature Review on Porous Materials and PolyHIPE

4.1 Overview

This chapter introduces the background and usage and a critical comparison of the basic adsorbents, porous polymers and polyHIPEs.

Adsorption was reviewed in the last chapter and described as one of the most promising desulphurisation technologies now available due to its lower operational cost, specific targeting, high selectivity and capacity in removing pollutants from a wide variety of feedstocks. Both the selectivity and capacity of various adsorbents are the most important factors in adsorption as shown by the comparison of the major desulphurisation methods in Table 2.4. The most common types of adsorption and commonly used adsorbents were also reviewed and compared in Section 3.2 and 3.3. To summarise these are bulk ceramics (such as activated carbon, alumina, zirconia, silica, and various kinds of nanomaterials), hybrid materials (such as metal−organic framework materials MOFs), and porous polymers (such as hierarchical porous carbons (HPCs) porous coordination polymers (PCPs), and porous organic polymers (POPs)) (Tan and Tan, 2017, Xia et al., 2016, Ma et al., 2003, Hernandez et al., 2010, Hernández-Maldonado and Yang, 2004, Fukunaga et al., 2003, Wu et al., 2012, Peralta et al., 2012, Dhage et al., 2011, Samokhvalov and Tatarchuk, 2010, Samadi and Zarenezhad, 2016).

Porous polymers Figure 4.1 have attracted an increasing level of research interest in their usefulness such as the availability of various synthetic techniques, easy preparation and functionalization, high surface area, low-cost reagents and mild operating conditions (Misra et al., 2017, Tan and Tan, 2017). Peralta and collaborators studied various sulphur- adsorbents and mentioned that activated carbons showed great adsorption capacities in model fuels, but the performances of these adsorbents decreased by a factor of 10 in real diesel fuel as a result of insufficient selectivity for the adsorption of sulphur-containing aromatic compounds compared to polyaromatics. The authors showed that some MOFs have a sufficient ability to adsorb thiophenic molecules in large quantity, even in the presence of aromatics**.** (Peralta et al., 2012).

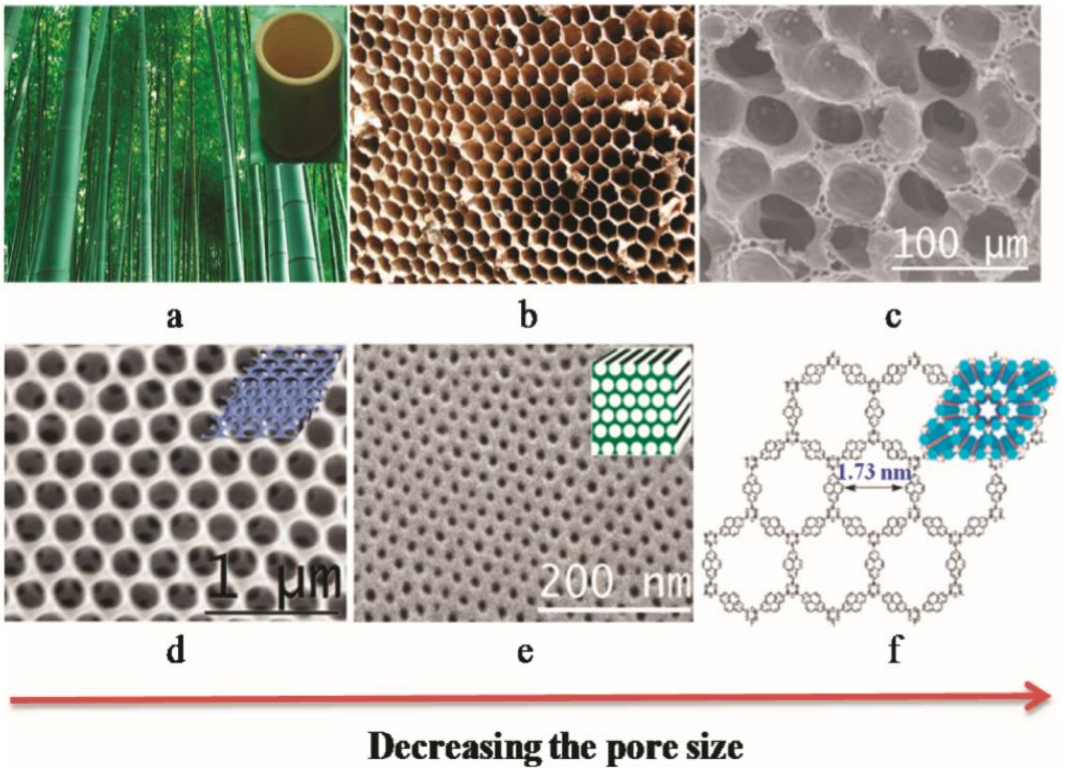

Figure 4.1 Illustration of porosity existing in nature and synthesized materials with a decreasing pore size: (a) bamboo; (b) honeycomb; (c) SEM image of alveolar tissue in mouse lung (d) SEM image of an ordered macroporous polymer from direct templating (e) SEM image of an ordered mesoporous polymer from self-assembly of block copolymers (f) structural representation of an ordered microporous polymer (Tan and Tan, 2017).

In addition, as they have variety in the scale of their porosity, in terms of possessing meso, macro, and micro porous, porous polymers provide further opportunities for pollutant removal by the surface as there are abundant narrow micropores each connected with each other by channels so the adsorbate molecules or micropollutants can transfer from the adsorbent outside surface into the inner micropores through these channels, thus explaining their high capacity (Tan and Tan, 2017). While the larger macropores, support diffusion through the adsorbent with lower resistance expected to mass transfer of the adsorbate molecules into the particle (Koparkar and Gaikar, 2011) .For example, it has been found that the effective diffusivity of benzothiophene, in a mesoporous polymeric structure is of the order of to$10^{-10}m^2/s$ compared to ~$10^{-13}m^2/s$ for a zeolite matrix (Haji and Erkey, 2003, Jayne et al., 2005, Schuring, 2004). Moreover, porous polymers can potentially combine both selectivity and adsorbent capacity if they are designed to take advantage of both well-defined porosity and high surface area. (Jiang et al., 2009, Jiang et al., 2008).

The other advantage of porous polymers is easy processability as will be shown below in the sections on preparation, functionalization and moulding 4.5.5, and 5.5. They are easily molded whether produced in a molded monolithic form (Beiler et al., 2007), in thin films (Olson et al., 2008) cylindrical shape (Thumbarathy, 2018) or flat plate in plastic tubes or glass containers (Greco, 2014), and can be manufactured with controlled micropores such as in hollow capsules, quasi zero-dimensional nanoparticles, and two or three dimensional (2D, 3D) membranes and monolithic blocks (Tan and Tan, 2017). Easy functionalization improves selectivity and capacity in many practical applications. During functionalization, incorporating additives, fillers, and multiple chemical functionalities to the polymer bulk body is possible. A surface can be produced has specific properties without affecting the main polymer properties (Noor, 2006). Moreover, some of polymer adsorbents can even be dissolved in a substance and then processed directly using solvent-based techniques without destroying the porosity (Weber et al., 2007). In this way, polymer functionalization can be designed to demonstrate stimuli-responsive characteristics capable or switching from the general properties.

On the other hand, to maintain inner cavities, rigid polymer networks must be constructed to avoid the collapse of polymer chains to a nonporous dense state. The key factor to achieve this purpose is to use rigid building units fixed with strong covalent bonds (Tan and Tan, 2017). This provides a strategic advantage over the other types of porous materials such as activated carbon, zeolite, or porous silica, which is almost impossible to produce in different shapes and structures. (Wu et al., 2012, Im et al., 2005).

In addition, due to both polymer functionalization and their organic nature, the polymeric frameworks consist of light materials providing a weight advantage or disadvantage in some circumstances where lack of buoyancy is critical depending on the application (Im et al., 2005, Greco, 2014, Cote et al., 2005).

Moreover, the above stated advantages of using the functionalized polymers, there are other factors mentioned by Abdi and collaborators. They investigated the removal of sulphur and nitrogen from gas oil by using a functionalized polymer and noted other advantages such as (1) the easiness of separation and handling, (2) insignificant contaminants in the gas oil, and (3) the ability for regeneration and reuse (Abedi et al., 2015). Last but not least, these polymers are also less toxic, and therefore more environmentally friendly. (Abedi et al., 2015).

On the other hand, a wide range of preparation methods are available to generate porous organic polymer networks with different structures such as: conjugated microporous polymers (CMPs) (Jiang et al., 2007), covalent organic frameworks (COFs) (Ding and Wang, 2013), covalent triazine frameworks (CTFs)(Ren et al., 2012), hyper crosslinked polymers (HCPs) (Xu et al.,

2013), polymers of intrinsic microporosity (PIMs) (McKeown and Budd, 2006), porous aromatic frameworks (PAFs) (Ben and Qiu, 2013) and polyHIPEs (PHPs) (Wu et al., 2012, Abedi et al., 2015, Noor, 2006).

Among the previously mentioned polymer materials, PHPs, strictly speaking, are not so much a novel porous polymer but the novelty of this study is in using PHP as an adsorbent towards petroleum sulphur. However, the material has still undergone rapid development in recent years which has led to the production of various pore architectures, which boost the high surface area and internal mass transfer features at low cost which are superior to adsorptive desulphurisation by other materials.

The literature on adsorptive desulphurisation reveals a substantial range of adsorbents but very few studies discuss polyHIPEs. These can have several microporous structures and surface functionalities, particularly at a commercial scale. The present work will develop a polyHIPE to be used as a sulphur adsorbent functionalized by an amine and reinforced by activated carbon.

4.2 PolyHIPE Polymer

PolyHIPE Polymer is (PHP) is a highly porous polymeric foam, which is easily produced by polymerisation of the oil phase of a High Internal Phase Emulsion (HIPE) as a monomeric continuous phase. HIPEs are defined as emulsions in which the droplet phase occupies greater than 74% of the emulsion volume, this number represents the maximum volume that can be occupied by packing uniform spheres (Greco, 2014). The maxing of an oil phase containing oil phase monomers such as styrene (ST), a cross-linker agent such as Divinyl benzene (DVB) and a surfactant such as Sorbitan Monooleate (SMO) with deionized water containing a polymerisation initiator such as potassium persulphate enables the formation of a stable emulsion which can then be polymerized at 60^{o}C. The foam like morphology produced is shown in Figure 4-2, can be clearly seen in scanning electron microscopy images (Bokhari, 2003).

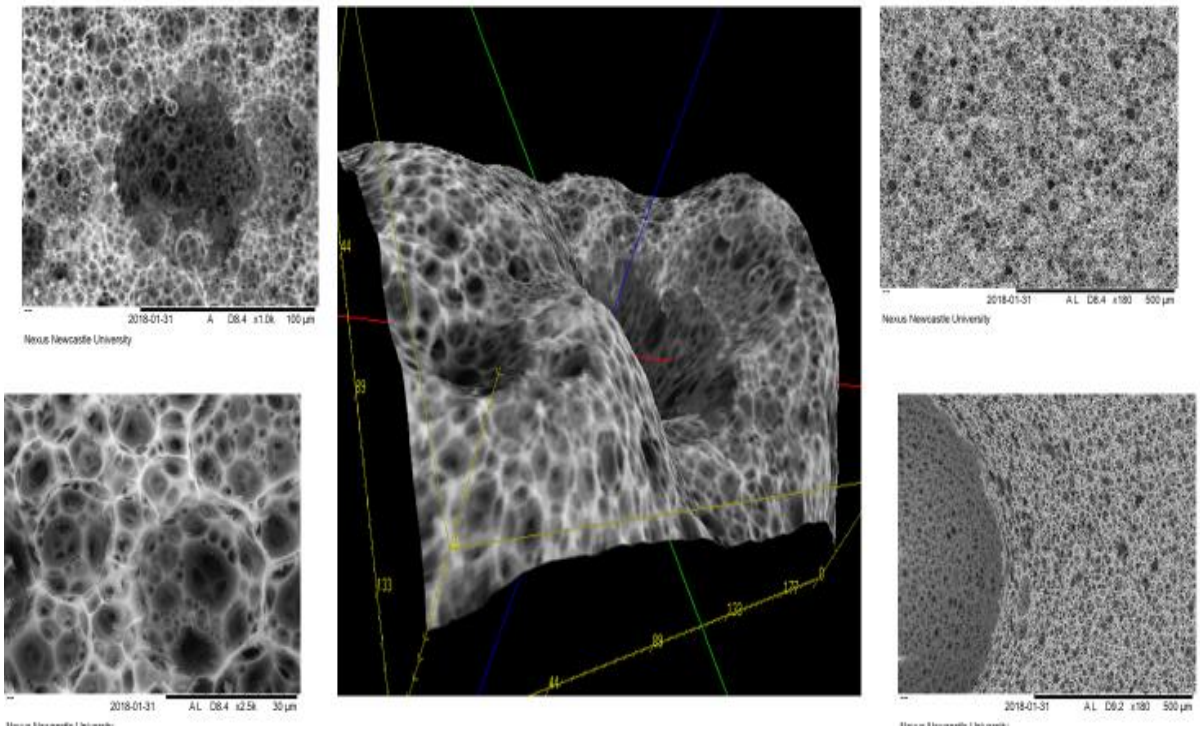

Figure 4. 2 Different magnifications of low-density polystyrene foam of very high porosity.

PolyHIPE polymers have gained significant attention recently because of their 1) good porosity, 2) structural and chemical diversity, 3) specific functionality, and 4) good physicochemical properties. Different PHPs that have high adsorption capacity have been synthesized by different polymerisation reactions (Cooper, 2009, Mahadik et al., 2018, Cote et al., 2005, Luo et al., 2012a). Moreover, the aromatic networks on the surface of PHPs could display an active interaction towards some types of S-compounds, however, their applications as the adsorptive Desulphurisation are minimally developed.

4.3 Polymerisation Reaction and Chemistry

To produce PHP when using styrene as a monomer a cross linking agent should be added. The role of the cross linker is to join polymer chains, to prevent styrene from dissolving and to limit the swelling when it is exposed to solvents that would dissolve a linear non cross-linked polymer (Bokhari, 2003). The monomer based HIPE can be polymerized to obtain micro-porous polyHIPE polymers (PHP). Barby and Haq (1982) discovered that an open-cell HIPE based polymer can be polymerised by using relatively simple low HLB (Hydrophile-Lipophile Balance) surfactant and HIPEs composed of styrene-divinylbenzene (DVB) were initially developed (Barby and Haq, 1985). Figure 4.3 illustrates the polymerisation of styrene in the presence of divinylbenzene as a crosslinker.

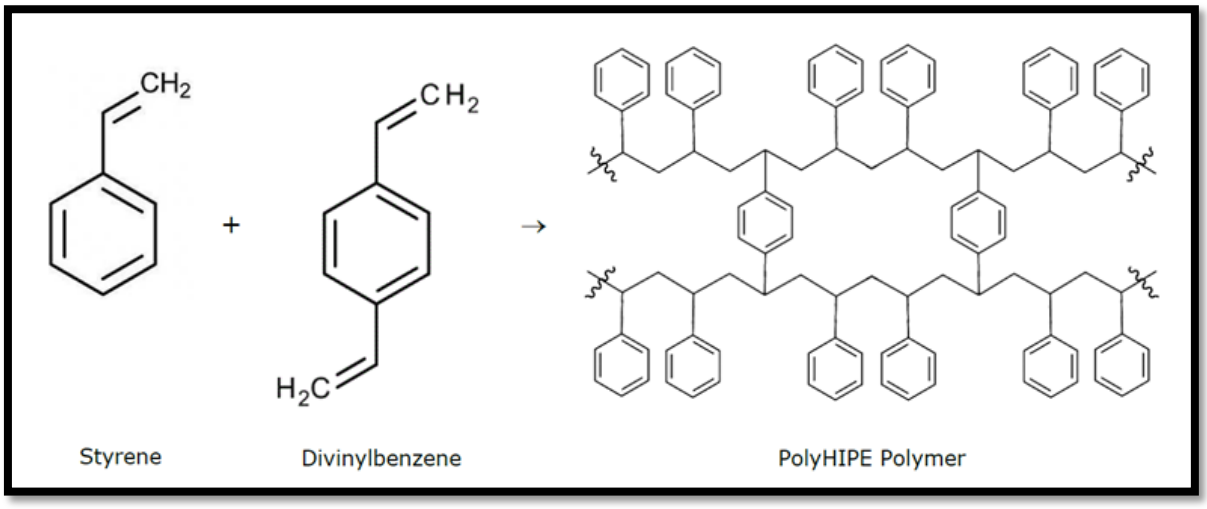

Figure 4.3 The polymerisation reaction between styrene and Divinylbenzene producing PHP in the rigid form (Barby and Haq, 1985).

4.4 The PolyHIPE Morphology

In general, morophology of PHP relies heaviely on controlling the structure controllability of the internal architecture (pore size and voidage) and the formation and chemical modifications of the interconnected pore walls. The monomer-based HIPE can be polymerised to obtain micro-porous polyHIPE polymers. The first main compostion in preparing the HIPE is the oil phase which creates an emulsion with the second componenet which is the aqueous or internal phase. This will be easily and quickly separated from PHP to produce a highly porous material with very low density approximately 0.1 g/cm^3, in with a range of pores sizes. These range can be grouped into four types:

1. Coalescence pore D, (0.5 μm<D< 5000 μm), depending on the conditions of the starting emulsions. These are formed from the coalencece of smaller pores created the HIPE processing

2. Primary pores which produced by the aqueous droplets created by mixing during HIPE processing

3. interconnect pore size. This type of pore architecture is obtained through the control of the type 1 pores during polymerisation.

4. nano-scale pore size – the walls of microporous PHP can be made nano-porous by using suitable fillers and additives (Mohamed, 2011).

The relationship between these is shown in Figure 4.4. In some references, pores are named voids or cells and the interconnecting pores between each void and its neighbours are referred to as windows (Cameron, 2005). In addition to type of pores there are other factors

characterising polyHIPE porosity. These are the pore wall thickness (Ali and Khan, Awadh and Al-Mimar, Bettermann and Staudt, Dağ et al., Dicks et al., Hua et al., Jiang et al., Jiang et al., Jiang et al., Mahadik et al., Normatov and Silverstein, Tai et al.) and intersecting vertex thickness (Lindberg et al.) (as shown in Figure 4-4). The importance of these parameters is, firstly they indicate how the solid content is distributed besides the pore size and interconnect parameters (Greco, 2014) which furtherly helps in understanding the structure of the adsorbent. Secondly, these parameters are manipulated to reach a higher elastic stiffness or Young's Modulus of polyHIPEs, as it was reported by (Williams and Wrobleski, 1989) that, at a given density, thicker walls provide maximum mechanical properties. These factors are very important in understanding the mechanical response of polyHIPE granules in this study.

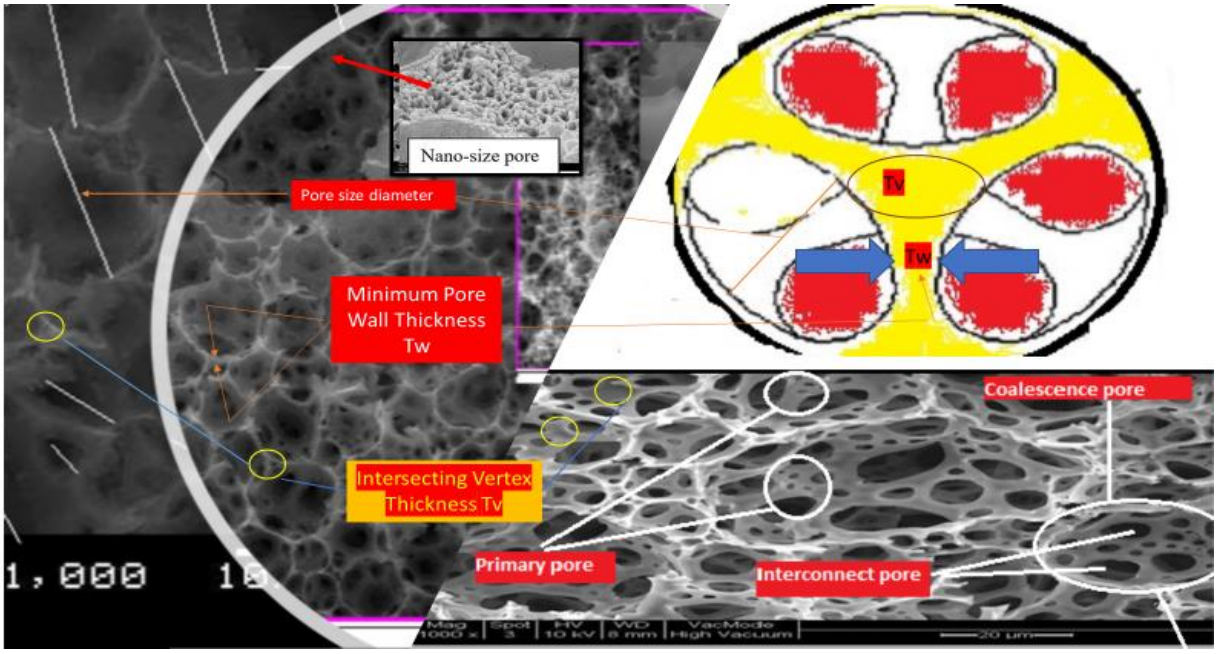

Figure 4.4 Detailed view of primary, interconnecting, coalescence and nano pores also pore size (diameter), intersecting vertex thicknesses and minimum pore thickness.

The effect of porosity on the polyHIPE morphology and how it can is be changed will be described in the Section on Polymer Preparation. In summary, the structure of polyHIPEs is characterised the following typical features, as displayed in Figure 4.4

1. The presence of open and/or closed cells/pores.
2. The presence of interconnect pores.
3. The presence of much larger/smaller pores.
4. The diameter of the pores (D), its distribution and average value (d).
5. The pore wall thickness (Tw) and intersecting vertexes thickness (Lindberg et al.) and their distribution.

These factors are very important to form a polyHIPE that can be used as adsorbent because they are relevent to the polyHIPE ability to adsorb the target substance and also its mechanical properties. The polyHIPE could be easily modified by changing some factors; adding materials or by chemical surface modification. The role of porosity is also related to its volume ratio of free space to the bulk body of the polyHIPE as it represnts the media of mass transfer between soild and liquid materials. In general polyHIPEs possess a porosity value around 90% and a non-modified polyHIPEs has a relatively small surface area of between 3 – 20 m^2/g (Thumbarathy, 2018). The density, porosity and surface area are the major properties that characterize a PHP for use as and adsorbent. These properties depend on several factors as explained in the next section. Another important property of PHP is that it can be tailormade depending on its application, for example, it can be synthesised with a specific interconnecting size of open-cell structure which can be produced by using a relatively simple low hydrophile-lipophile balance (HLB) surfactant and HIPEs containing styrene-divinylbenzene (DVB) (Barbetta et al., 2000, Cameron and Barbetta, 2000, Barby and Haq, 1985). As shown in Figure 4.5 (Mohamed, 2011) these high volume fractions, in term of droplets, shape the internal growth phase to be overcrowded and it cannot retain its spherical shape but forms deformed polyhedral droplets with relatively large contact areas, dammed by the continuous phase and stabilized by a thin surfactant film. After polymerisation, the configration of the PolyHIPE consists of a highly porous material with a pore volume fraction in some cases exceeding 0.99. Morever, it possesses an obvious open cellular structure where each cavity has connected to its neighbours (Thumbarathy, 2018, Hasan, 2013, Calkan, 2007).

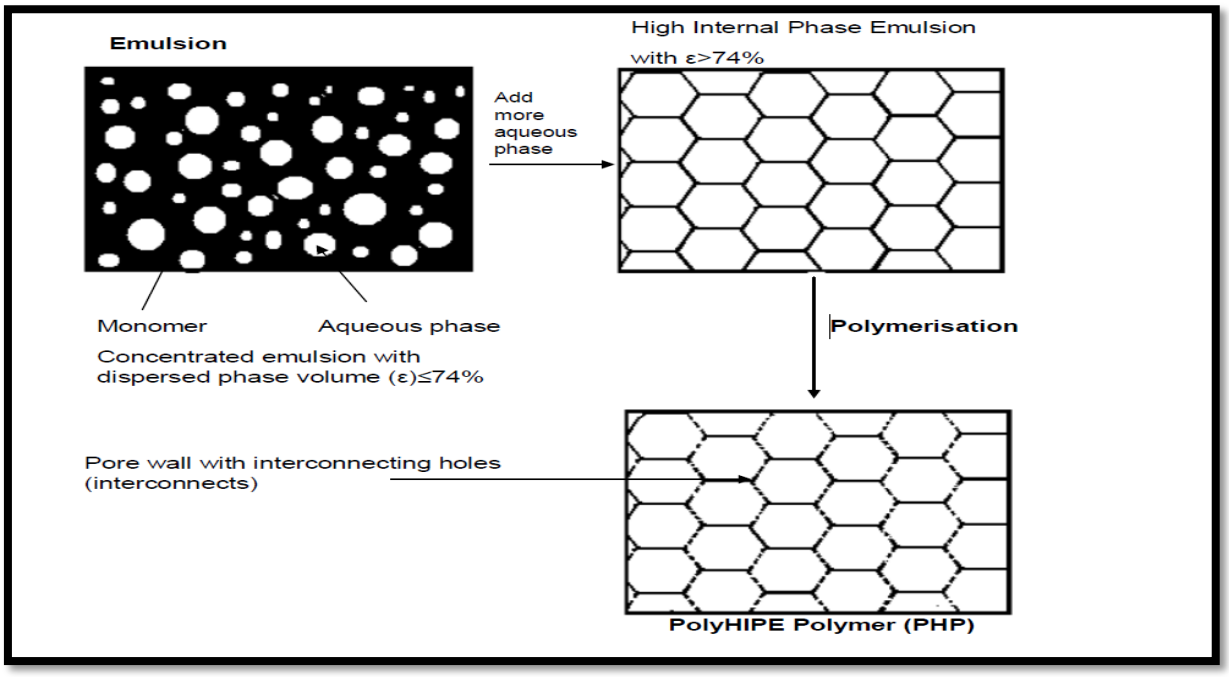

Figure 4.5 Schematic representation of PHP formation. (Mohamed, 2011).

The term monomer in the figure above refers to the oil phase, which aqueous phase droplets are dispersed in, under initial conditions that change with time. When water is added gradually into the oil phase, these droplets reach the undistorted maximum packing around ε =74 %. Additional aqueous phase entering the system, results in the droplets distorting and arranging themselves into the typical polyhedral (tri-dimensional) layout of HIPEs. This configuration is retained during the polymerisation and forms the walls and interconnecting holes as shown in the bottom right of Figure 4-5. The result is a nanostructured micro-porous polymeric material in which the water droplets serve as a structural template.

4.5 Factors Affecting PolyHIPE Polymer Morphology

Porosity, surface area, surface chemistry and mechanical properties are the major properties that characterize polyHIPEs (Zhou et al., 2007) which have been developed to be a good adsorbent (Saleh, 2015). An earlier study reviewed the factors affecting these properties in which Williams and Wrobleski (1988) included that favorable properties can be achieved by the control of various factors, such as the internal phase DVB/ Styrene ratio and the surfactant and co-surfactant concentration and type (Williams and Wrobleski, 1988). Other studies discussed the nature of organic phase, its density and its ratio to the liquid phase, and the use of porogenic solvent and electrolytes (Abbasian and Moghbeli, 2010, Busby et al., 2001). These factors are discussed in the next sections.

4.5.1 Internal phase DVB/ Styrene ratio

Divinylbenzene (DVB) plays its role as a cross linker creating a network through the polymer that prevents the collapse of the PolyHIPE structure by linking polymer chains (Barbetta et al., 2000). Williams and Wrobleski (1990) found that the DVB/Styrene ratio plays a significant role in the determination of the polyHIPE morphology and properties (Williams et al., 1990). They prepared several polyHIPEs with different ratios starting with zero DVB to 100% and concluded that emulsions with DVB can be mixed more easily and produced more uniform emulsions than those prepared with only styrene, which leads to increase in emulsion stability as a result of decreasing the average pore size in diameter from 15 to 5 μm. Moreover, Calkan and coworkers (2010) studied a phase composition consisting of DVB/styrene with various ranges of DVB changed in the range $2 < X < 10$ wt % to the total oil phase consisting of styrene (86 - X wt %), Span 80 (14 wt %), and DVB (X wt %). It was observed that the DVB concentrations cause significant changes on the maximum surface area, rigidity and adsorption capacity, for example, the maximum surface area was reached at 8% wt DVB of the total oil phase (Burke et al., 2010). Abbasian and Moghabeli (2010) have shown a similar effect of the internal phase ratio 1-10 DVB/ Styrene on microstructure and properties of the polyHIPE, particularly its density and Young Modulus (Abbasian and Moghbeli, 2010).

4.5.2 Surfactant concentration

An earlier study by Rosen in 1972 defined the surfactant as **surf**ace-**act**ive age**nt** that has the ability to be adsorbed onto the interfaces of various boundaries between any two immiscible phases in a two phase system (Rosen, 1972). When present at low concentration in a system it causes a significant modification the surface or interfacial free energies of those interfaces**.** The reason behind this ability is the existence of two groups in the surfactant chemical structure. These are polar and non-polar groups which interact at the boundaries of the oil and aqueous phases creating an interfacial film which improves increasingly the stability of the emulsion (Hauthal, 1990). Cameron mentioned that the level of the surfactant should be at least 4% volume due to the total oil phase that is needed for polyHIPE preparation (Cameron et al., 1996). Moreover, it has been found that levels between 4-5% produced closed structure materials, whereas an open cell structure is produced at levels between 7-50 % volume.

Furthermore Hasan (2013) illustrated that an increase in the amount of surfactant could lead to decrease in pore size (around 50%) and more surfactant caused a crumbled or weak polymer (Hasan, 2013). This crucial role was found to be more important than that of internal phase volume as it relates to the fact that when increasing the level of surfactant the film between two boundaries in the monomer becomes thin and at a particular thicknesses it can create new pores

inside the polymer. (Williams and Wrobleski, 1988, Williams, 1988). In addition, when the surfactant is removed through the washing process of the polyHIPE new pores are formed (Hasan, 2013, Mohamed, 2011). Sorbitan monooleate, also known as 'Span 80' structure shown in Figure 4-6 is commonly used as a non-ionic surfactant for stabilization of polyHIPEs and was used in this study.

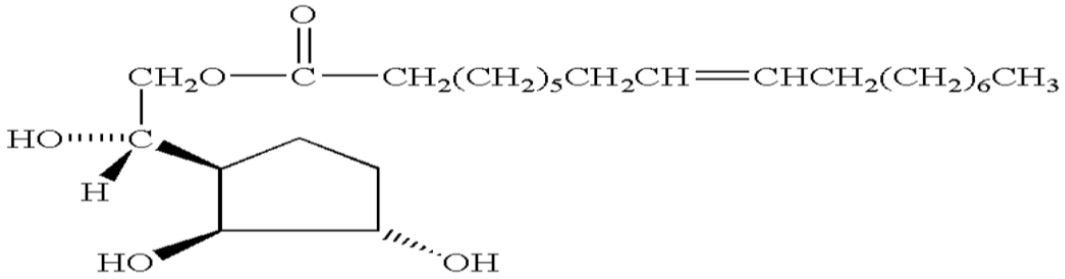

Figure 4.6 Sorbitan Monooleate (Span 80) (Thumbarathy, 2018).

Among various surfactant Span80 has unique characteristics, low cost, high density, and viscosity (Hasan, 2013). Surfactants used to form a polyHIPE should have a low HLB value (between 2 and 6) (Barby and Haq, 1982). The optimum surfactant was found to be Sorbitan Monooleate (Span 80), which has an HLB value of 4.3. This have been used for many years in many applications such as food preparation, cosmetics, oil recovery and many others (Mohamed, 2011).

4.5.3 Mixing Time/Dosing Time

The stability of HIPE varies greatly over time because of high interfacial tension. At the beginning during the dosing process where water us added to the oil, the emulsion droplets start to accumulate and coalesce, producing large pores if polymerised without further mixing. During mixing, these droplets easily undergo uniform break down into small emulsion droplets which produce more stable emulsion. The emulsion stability and polymer porosity are controlled by putting a certain energy into the system dependent upon the speed of mixing (Jimat, 2011). Walsh et al.'s 1996 study demonstrated that besides a high mixing speed, prolonged mixing time causes a reduction in aqueous cavity size that leads to an increase in the number of windows and the formation of a more micro-size open structure polymer (Walsh et al., 1996) . However, at very long mixing times pore coalescence may occur again that creates occasional larger pores and reduces the good properties introduced by mixing for shorter periods.

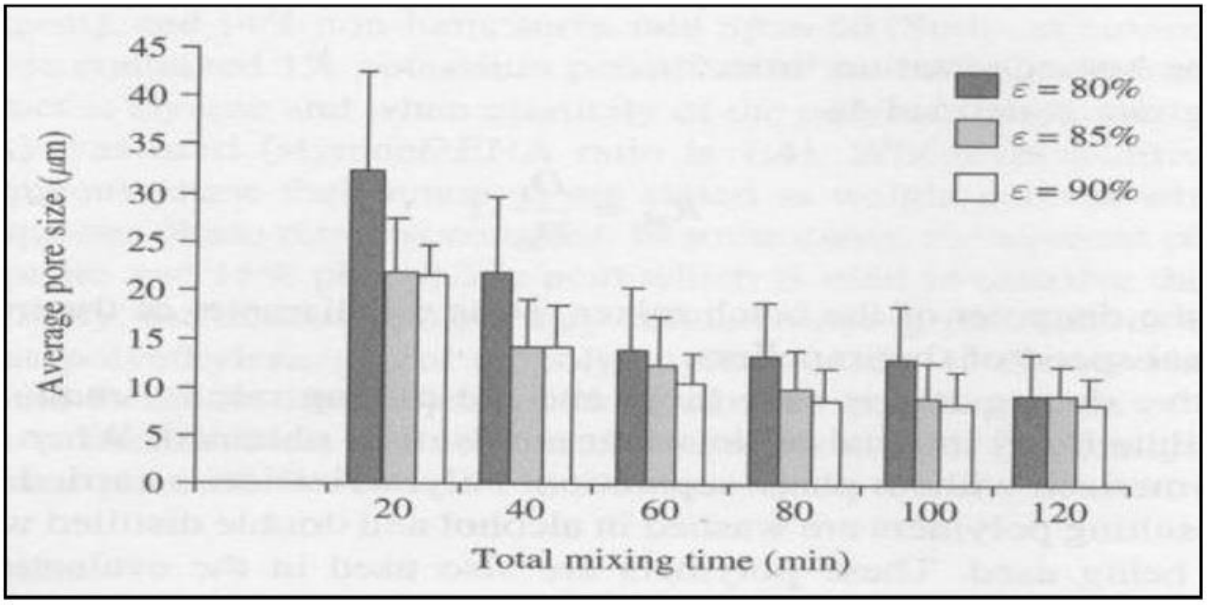

Figure 4.7 Variation of average pore size (D) with total mixing time (Bokhari, 2003).

Significant studies were conducted by Bokhari in 2003 to specify the effect of mixing and dosing time in the morphology of polyHIPE. It was established that increasing parameters for mixing and dosing time from 20 to 120 minutes respectively with the variation of average pore size of three different HIPEs as shown in Figure 4-7. It has been reported that the average pore size decreased with increasing mixing time for all HIPEs (Bokhari, 2003). In chapter 6 of this study a novel search is performed starting from 5 minutes instead of 20 minutes to identify the changes in average pore size over a wider time period.

4.5.4 Electrolyte Content

The addition of electrolyte affects the emulsion stability as it causes reductions in the interfacial tension improving the final structure of the polyHIPEs (Aronson and Petko, 1993). Another study carried out by Cameron in 2005 reported that there are significant influences of the electrolyte content in the aqueous phase on the average pore size. When the electrolyte content increases, the pore diameter is reduced, and pore growth (Ostwald ripening) is reduced; limiting Ostwald Ripening leads to a more stable emulsion with a smaller average droplet diameter (Cameron, 2005). It has been reported that when the K_2SO_4 salt concentration increased from 10^{-6} to 10 g/100 ml, within the initiator, the pore size decreased from about 50 to 5 μm. This is because of reducing the propensity for Ostwald ripening, a process whereby bigger pores grow occurs at the expense of smaller ones, as a result of the migration of droplet phase molecules within the continuous phase. In general, when the salt is mixed with the aqueous phase, a significant impact appears on the stability as a result of increasing the interaction of surfactant molecules in the presence of salt. (Kunieda et al., 1989).

4.5.5 Moulding Type

The moulding step is an integral one after the emulsification stage when the HIPE is transferred to suitable containers in the oven under a specific polymerisation temperature, usually 60 ℃. The polyHIPE takes the shape of the container whether these containers are plastic cones, cylindrical, spherical, flat plate or square. It has been reported that moulding type and shape have significant effects on the polyHIPE structure, morphology and degree of adhesion to the mould (Cameron, 2005, Akay et al., 1995). The difference in mould material was reported by Cameron (2005) first, when a glass mould is conducted, a surface bonding with PolyHIPE occurs in the form of a film between the outer surface of the material and its contact surface with the glass which is relatively easy to separate after polymerisation. However, with a polyvinyl chloride (PVC) mould, the PolyHIPE sticks to the mould as a result of the reaction between the HIPE and the container. This affects the structure and properties of the polymerised HIPE.

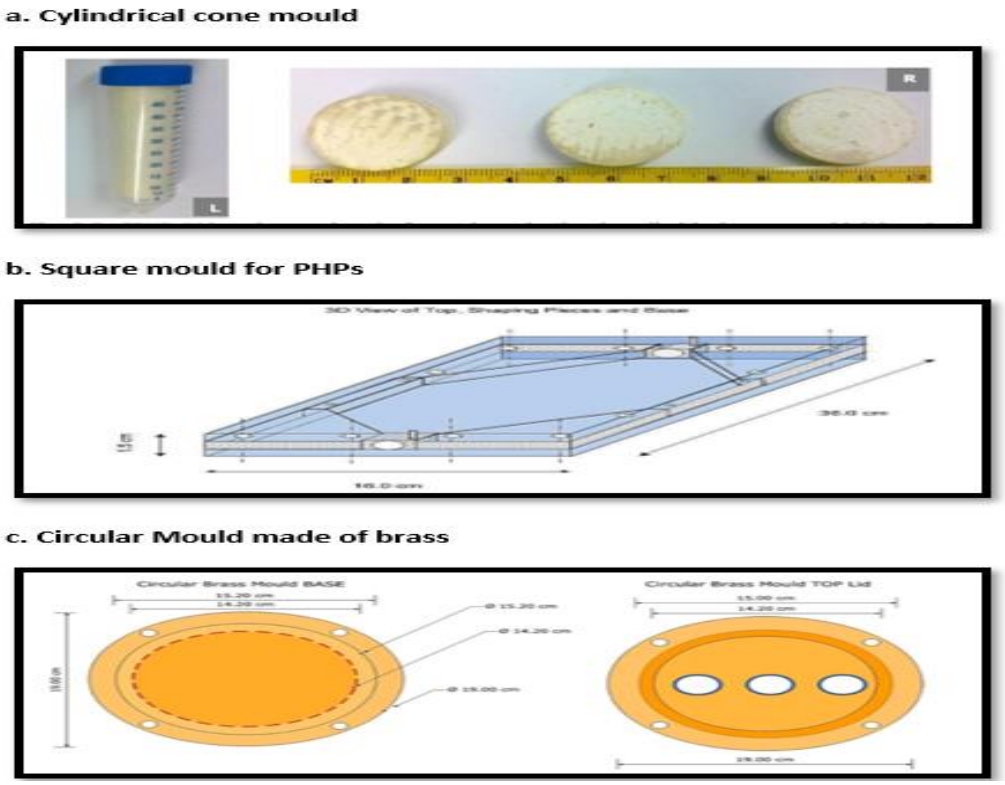

Figure 4.8 Different type of moulding: a. cylindrical cone mould, b. square mould, c. circular mould (Greco, 2014).

Greco in 2014 reported three types of moulding and studied their effects on the structure and morphology of polyHIPEs (Greco, 2014). These are 1) monolithic tubes of cylindrical shape: 2) square moulds and 3) circular mould as shown in Figure 4.8 Larger moulds with corners and non-optimised flow patterns during filling lead to non-uniform structure and large coalescence

pores in the polyHIPE. The rate at which the HIPE is pumped into the mould is very important and care should be taken to limit pumping pressure to minimize instability. In this study two types of cylindrical moulds, filled by gravity from the mixing chamber, to produce samples as shown in Figure 4-9 have been investigated to reduce the weight losses in adsorbents mass.

Figure 4.9 Two different dimensions in moulding types used to improve the adsorbent.

4.6 PolyHIPE Properties

The polyHIPE is to be used as an adsorbent in this study and its most important properties will be discussed in the following sections. The main factors were mentioned in the previous section and the challenge is to find the optimum version of polyHIPE that meets the significant process-structure-properties requirement of an adsorbent and to reach the maximum adsorption capacity, at reduced cost and with the ability for regeneration (regenerability). (Babich and Moulijn, 2003, Javadli and De Klerk, 2012) .

It is worth mentioning that these properties and the factors controlling them may counteract each other which suggests caution is required in manufacturing. As a result of trial-and-error studies there is a tendency to select the optimal material based on its mix of properties and not the best in a particular property. Adsorbent manufacture, characterization and optimisation are discussed in the next chapter.

Adsorption capacity is related directly, to the mass transfer of adsorbate through the adsorbent which further depends heavily on the distribution and size of available pores. The second adsorbent feature is the selectivity which is driven by both the micro-porosity and the surface chemistry of the adsorbent surface. The mechanical stability us also important; mechanical properties are expressed in terms of stress-strain curves and Young's Modulus, which is very important to understand regenerability.

4.6.1 Surface Area

The surface area of a polyHIPE prepared in the manner described in previous sections is low (3-20 m^2/g) although it has numerous pores and highly interconnected walls (Noor, 2006). This is because the surface area is driven by the pore size. A study by Krajnc et al., in 2005 mentioned that when the range of pore size is (3-7 µm) the surface area tends to be about 10 m^2/g (Krajnc et al., 2005). However, an efficient adsorbent should have a higher surface area and specific mesoporous structure. (Srivastav and Srivastava, 2009, Xia et al., 2016). Since the surface area is driven by the pore size and distribution (Zheng et al., 2014), therefore, this requires significant enhancement to the morphology by either using new modification parameters or by adding new materials with high impact on the surface area.

The first approach to increase the surface area is by adding additives such as the porogenic compounds like (chlorobenzene (CB) and/or chloroethylbenzene (CEB) and toluene to the oil phase. These additives have the ability to create additional micro pores in the contacting film of the droplets which leads to higher surface area of 350 m^2/g (Williams, 1991, Cameron and Barbetta, 2000). Essentially these porogens introduce micropores and nanopores into the walls of existing meso- and macroporous material. However, it has been found that adding toluene causes severe degradation in the mechanical properties of the material (Greco, 2014). In other studies, it has been reported that an optimal concentration of additives could increase the surface area to 554-550 m^2/g and improve the mechanical properties at the same time (Pakeyangkoon et al., 2008, Barbetta and Cameron, 2004, Cameron, 2005). Moreover, some additives negatively impact the surface area, for example, adding 2-Vinyl Pyridine to the emulsion led to a reduction in surface area. On the other hand some chemical modifications such as thermal sulphonation decreased the surface area of polyHIPE drastically to 3 m^2/g while microwave sulphonation increased it from 3.52 m^2/g to 243 m^2/g (Mohamed, 2011).

It should be stressed that in this study, for the first time, activated carbon has been added to the polyHIPE to make an improvement in both surface area and mechanical properties.

4.6.2 Mechanical Properties

Wakeman et al reported that the combination of high surface area and penetrability of the high internal phase emulsion makes polyHIPE attractive as a potential adsorbent (Wakeman et al., 1998)**.** However, in order to produce a commercially attractive adsorbent it is crucial to have superior strength towards external forces because the adsorbent particles will be exposed to a compression whether they are used in a packed bed column, a plate column or molecular sieve reactor in both adsorption and regeneration stages (Speight, 2014). Adsorbent size and shape affects the design of the column (Sinnott, 2014). The mechanical properties of the PolyHIPE are inversely related to its density and surface area (Menner et al., 2006b). Consequently, a technique that improves the overall mix of properties by combining conflicting factors should be used. These techniques can be classified as, those that depend on the internal composition only and those that add an external filler material, thereby making a composite. Both need to be followed by polyHIPE functionalisation for optimum performance.

4.6.2.1 Compositions Technique

Many approaches have been used to enhance the toughness and modify the properties of the polyHIPE through a combination of different factors. Early studies by Williams and co-workers (1988) demonstrated how to improve the mechanical properties. The first in 1988, investigated the mechanical properties as a function of the surfactant ratio and content. As expected, the authors found that a higher content of surfactant has the effect of creating thinner oil layers in the HIPE until reaching oil layer retraction where the aqueous droplets started to touch. The effect is that foams with no walls but only struts are formed, thus possessing a very low modulus. As shown in Figure 4-10a the Young's Moduli are generally maximised at around 10% surfactant then largely decreased with increasing surfactant presence. The aim is to reach the highest modulus against specific amount of surfactant SMO as in the figure 4-10a (Williams and Wrobleski, 1988).

A further study by the same investigators discussed the influence of crosslinker content**,** salt content, degree of crosslinking, polymerisation initiators and oil-water solubility, regarding compressive properties of polyHIPEs in terms of Young's Modulus. The most interesting results were that only a few percent DVB cross-linking was necessary to obtain near optimum stiffness. In addition, Williams and co-workers were the first to use the Gibson and Ashby model ($E/E_S = (\rho/\rho_S)^2$) to explain behaviour, as shown in Figure. 4-10b. From 0-10% DVB, the polyHIPE produced was not chalky but increasing to 20% DVB, it became slightly chalky, and was very chalky at 100% DVB. The Young's Modulus was denoted as a function of the PolyHIPE density and showed an increasing value, as expected, with increasing density (Williams et al., 1990) .

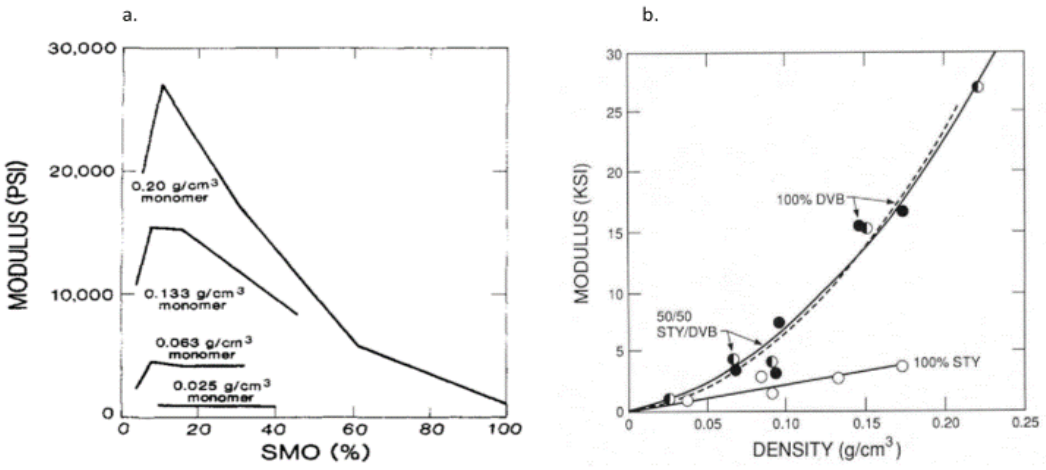

Figure 4.10 a. Young's modulus dependence on emulsion surfactant level (Williams and Wrobleski, 1988), b. Compressive modulus dependence on foam density. The modulus data are those at 10% Surfactant (Williams et al., 1990).

In 1991 Williams studied the influence of several surfactants and co-surfactants on the general behaviour of polyHIPE. The polyHIPEs were prepared with different concentrations of 8 surfactants and 22 co-surfactants and they showed different densities and structures which generate different mechanical properties (Williams, 1991). In other studies by Cameron it was reported that the selection of the monomer and crosslinker have a significant influence on the mechanical properties; for instance, polyHIPEs prepared with styrene and divinylbenzene are usually brittle and chalky while those prepared with bisphenol-A-polycarbonate have outstanding mechanical properties (Cameron, 2005, Cameron and Sherrington, 1997). Burke and co-workers prepared two type of polyHIPE morphologies termed spongy and rigid (Burke et al., 2010) by changing the styrene /DVB ratio; improving the properties of each was observed by increasing the crosslinker. However, cross-linking can cause embrittlement in styrene-divinylbenzene systems if a large amount >20% of DVB is used (Hainey et al., 1991).

4.6.2.2 Filler Technique

It is notable that all previous studies used a specific category of treatment that depends on the type or/and composition of the original ingredients such as monomer, co-monomer, crosslinker, surfactant, salt and initiator. However, there have been some novel studies which used another approach by adding filler materials to improve the mechanical properties. In general, adding a stronger, stiffer filler not only provides reinforcement that enhances the mechanical properties and improves morphology and surface area of the polyHIPE but also adds new properties without majorly affecting the pore structure of the material. This provides new opportunities for new applications.

In Menner's (2006b) study polyHIPE was synthesised using a series of carbon black filled HIPEs in a new preparation protocol; 1 wt% carbon black was dispersed in the monomer mixture and enhanced the stability and mechanical properties of the polyHIPE. It also acted to reinforce the polymer matrix with nanosized particles leading to a drastic improvement in morphology, porosity, pore size, pore throat size and density along with related properties such as permeability and mechanical performance (Menner et al., 2006b). Haibach et al in their 2006 research enhanced the mechanical properties of polyHIPE foams by incorporation of another filler. Nano-sized silica particles are added along with a silane coupling agent, methacryloxypropyl trimethoxy silane (MPS), to reinforce the polymer. They demonstrated that both Young's Modulus and the crush strength of PHP was increased by 280% and 218% respectively in comparison to those without reinforcement (Haibach et al., 2006). Menner et al. (2009) studied reinforcing PolyHIPEs to improve the mechanical properties without the need to increase the density by using titania nanorods (TNR) in the organic phase or oxidized carbon nanotubes in the aqueous internal phase.

This technique enables a wide range of polyHIPE applications especially those in which low density and high mechanical properties are required, such as, scaffolds for tissue engineering or filters (Menner et al., 2008). Despite the increase in density and improvement in mechanical properties, the filler titania nanorods (TNR) do not affect other properties such as mass transport in the material. This contributes to making the filler technique better/more flexible than the changing the material compositions.

As mentioned above the introduction of the fillers enhanced the modulus from 200% MPa. In fact, the probable good dispersion of high modulus fillers platelets in the cells wall leads to a good stress transfer from the polymer matrix to the platelets and improves the mechanical properties in the reinforced foams when compared with the standard polyHIPE without any additives.

Nevertheless, the incorporation of higher level of additives or fillers showed an inverse effect on the modulus and crush strength of the foam. This decrease in compressive properties can be connected to the probable existence of agglomerate of additives platelets inside the polymer matrix, which may result in stress concentration and build-up around the agglomerates. As a result, this study aims to produce more elastic and improve Young Modulus.

Mechanical properties are usually inversely related to the bulk or envelope density and surface area (Menner et al., 2006b). However, the successful improving of mechanical properties of the foams using fillers also increases the surface area achieved, e.g. by incorporating hybrid organic–inorganic porous clay heterostructures (HPCH) derived from Na-Bentonite as an inorganic filler (Pakeyangkoon et al., 2009). Wu and co-workers (2010) reinforced polyHIPE by adding silica particles and achieved Young's Modulus up to 600% greater when compared with non-reinforced polymer without affecting the open and interconnected pores. Despite these significant results, the extra process steps which are about 10 sequential steps in the methodology and silica filler costing 60% more than the material it replaces is the major drawback (Wu et al., 2010). Furthermore, increasing the filler up to the optimum concentration levels could lead to negative effects on other properties. Alikhani and Moghbeli's, 2014 research synthsised novel porous polymer from a vinyl benzyl chloride/divinylbenzene polyHIPE and functionalized the foam by using Trimethylamine (TMA) and triethylamine (TEA). In order to improve the ion exchange capacity of the membrane, the emulsion was reinforced by adding various amounts of an organically modified montmorillonite, Cloisite30B (C30B). It was reported that an amount of 1 wt% C30B decreased the mean cell diameter and intercellular pore size, consequentially improving the mechanical properties and increasing the ion exchange capacity (IEC) value to 1.78 mequiv./g of the copolymer foam. However, a further increase to 3 wt% decreased the IEC value to even lower than that of the pure membrane as shown in Figure 4.11a (Alikhani and Moghbeli, 2014).

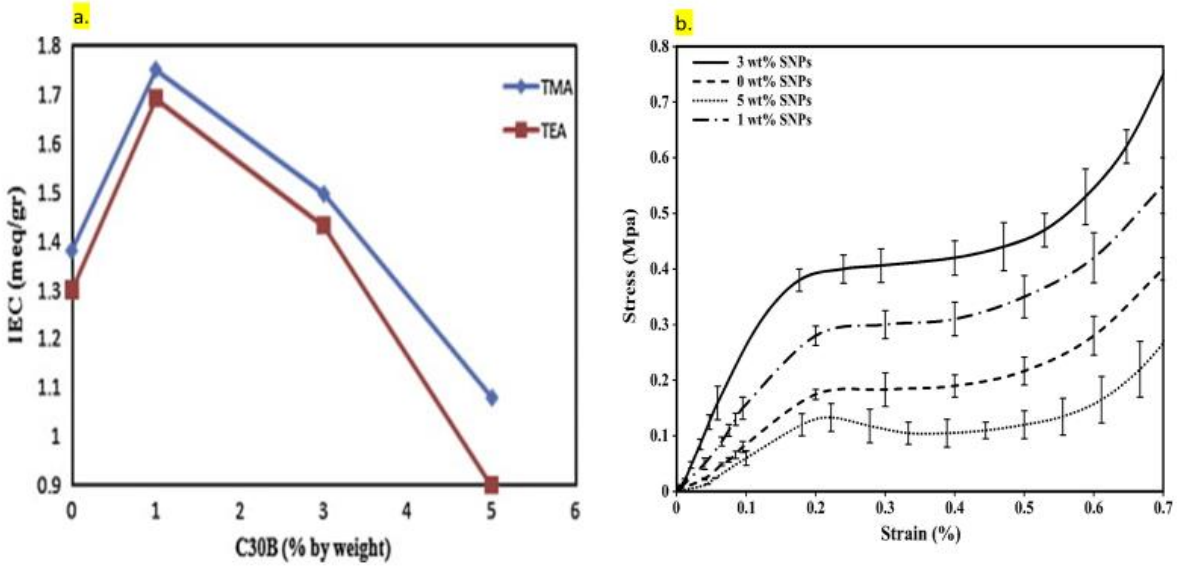

Figure 4.11 (a). Effect of organoclay (C30B) content on the IEC value of the TMA- and TEA-functionalized polyHIPE membranes (Alikhani and Moghbeli, 2014). (b). Compressive stress-strain curves of the polyHIPE foams reinforced with different SNPs content (Moghbeli et al., 2017).

In another work, Moghbeli et al (2017), showed the necessity of optimisation of the incorporation of a limited amount of an expensive filer, silica nanoparticles (SNP). PolyHIPE containing the highest SNP level (5% wt) did not exhibit any significant increase in the compression properties as shown in Figure 4.11(b) (Moghbeli et al., 2017).

4.7 Chemical Modification of PolyHIPE

PolyHIPE properties can be improved by changing the factors previously mentioned, changing monomer or by adding fillers to add new properties to the foam without affecting the pore structure. Other types of modification can be conducted by using different types of monomers in the oil phase to produce hydrophobic or hydrophilic substances (Çalkan, 2007) or adding a new production route by chemical reaction (Alikhani and Moghbeli, 2014). These chemical modifications increase the polyHIPEs usefulness in many applications like adsorption, filtration and the tissue scaffold industry. (Ergenekon et al., 2011). Cameron et al. (1996) established that HIPEs prepared from styrene/divinylbenzene (STY/DVB) can be functionalised by bromination, sulphonation and nitration (Cameron et al., 1996).The phenyl rings in polystyrene is contribute significantly in the chemical modification of polyHIPEs, representing the reactive sites in the HIPE that have the ability to substitute, add or subtract functional groups producing polyHIPEs with enhanced surface properties. This has encouraged many studies to investigate using the usual HIPE preparation conditions with an adjustment of electrophilic aromatic substitution in order to yield sulpho-, nitro, phospho- and bromo- substituted materials (Noor, 2006).

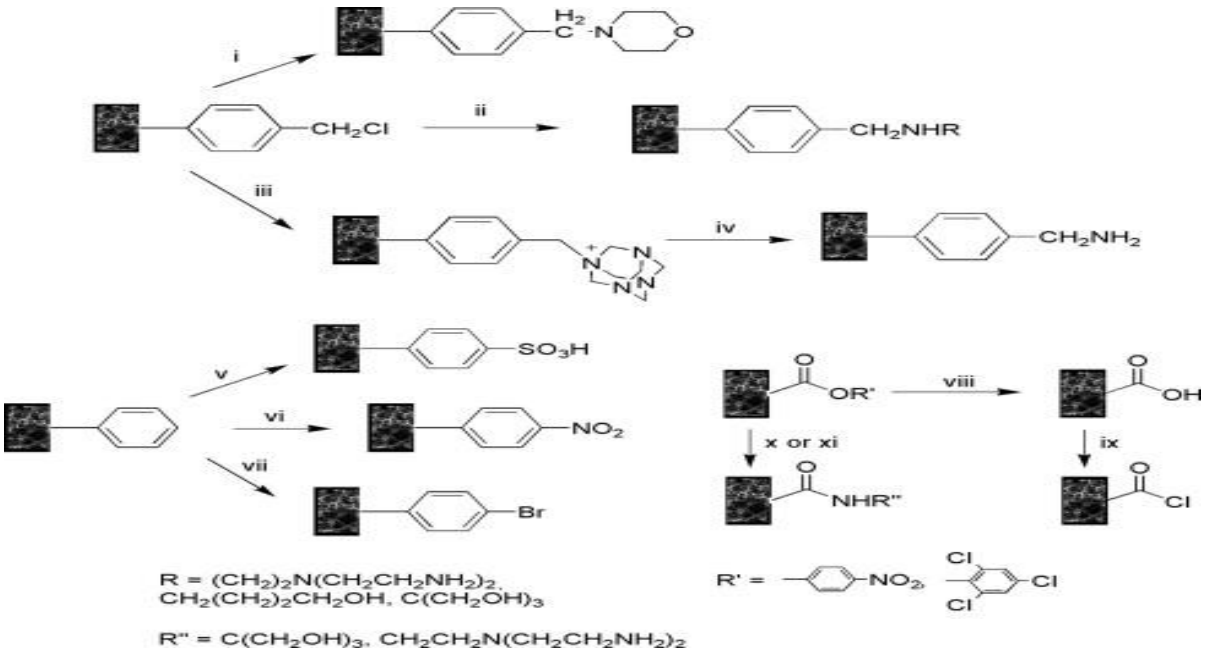

Figure 4.12 Scheme of functionalisation of PolyHIPE materials. Reagents and conditions: (i) morpholine (Braginskii) amine(iii)hexamethylenetetramine (Cameron, 2005).

A study by Cameron in 2005 concluded that the HIPE preparation conditions were identical to those conducted to prepare simple polystyrene PolyHIPEs. The resulting materials were functionalized porous polyHIPEs with a range of nucleophilic amines, including hexamethylenetetramine (as a means of introducing primary amine residues), morpholine and tris (2-aminoethyl) amine (trisamine) as illustrated in the scheme drawn in Figure 4.12 (Cameron, 2005).These studies inspired the recent work to modify a typical polyHIPE by MEA to increase its affinity towards sulphur capture. Below the most important modification approaches are briefly discussed.

4.7.1 Sulphonation

Sulphonation is simply an interchange reaction between phenyl rings of styrene and an electrophilic group such as the sulfonic acid group (SO_3H^+) (Noor, 2006, Çalkan, 2007). Sulphonation can be achieved using different sulphonation reagents for aromatic compounds such as sulphuric acid, oleum, free sulphur trioxide and halogen derivatives of sulphuric acid which all are derived from sulphur trioxide as discussed by (Kučera and Jančář, 1998). Recently, a plethora of studies have discussed the fabrication of porous materials by sulphonation and its to applicability in various applications such as in adhesion promotion in epoxy polymers (Muraoka et al., 2002), intensification and gasification processes (Noor, 2006, Çalkan, 2007), active solid acid catalysts (Xing et al., 2007), catalyst supports (Ordomsky et al., 2012), sulphur compound capture (Ergenekon et al., 2011), ion adsorption (Barlik and Keskinler, 2014) and agro- and bio-processes (Thumbarathy, 2018). The sulphonation reaction factors depend on the desired final product used in each application. These factors are contact time, sulphonation reagent type and concentration, temperature and degree of sulphonation (Çalkan, 2007). The degree of sulphonation is an expression of the number of attached $SO^-_3H^+$ bond with the benzene ring (Noor, 2006).

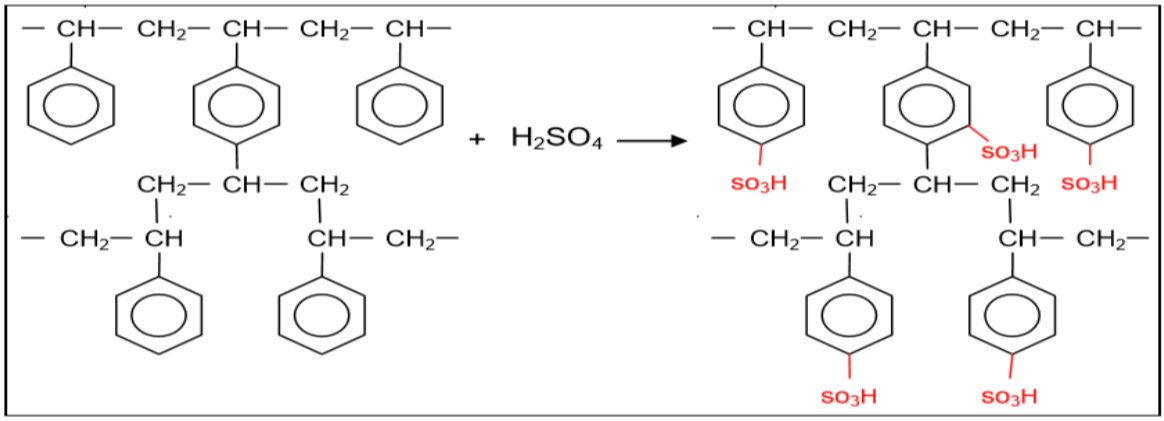

Figure 4. 13 Chemical structure of 100 % sulphonated polyHIPE(Çalkan, 2007).

Aromatic sulphonation reaction is an organic substitution reaction occurring in the polyHIPE in which a hydrogen atom of an arene organic compound is replaced by an SO_3H^+ functional group which as a result, transfers the polyHIPE hydrophobicity from hydrophobic to hydrophilic as shown in Figure 4-13 below and described by Calkan for 100 % sulphonated polyHIPE (Çalkan, 2007). Nevertheless, a sulphonation degree of 100% is lamost impossible to reach because of the internal stresses in the polymer matrix. Moreover, in previous studies it had been reported that degree of sulphonation is up to 68 % to 80 % and it depends directly on the contact time usually reaching a plateau value of about 60% (Mohamed, 2011).

Despite tailored properties of polyHIPEs, high porosity, interconnected macropores with surface chemistry for separation applications and ease of modification, there are only very rare studies that applied polyHIPE in the oil industry and particularly in adsorptive Desulphurisation (Ordomsky et al., 2012, Ergenekon et al., 2011, Barlik and Keskinler, 2014). A study by Ergenekon et al., in 2011 demonstrated a combination of polyHIPE sulphonation and adsorptive desulphurisation in a single compact method. (Ergenekon et al., 2011). In the proposed method, a novel sulphonation for microporous polystyrene divinyl benzene copolymer (PSDBP) was achieved. PSDBP reacts as a solid adsorbent to capture the gaseous SO_2 from waste gas streams; SO_2 is used as the sulphonation agent.

This method could overcome the disadvantage of the conventional desulphurisation method that uses excess amounts of the reagent needed for the process. Also, this method is considered to be an environmentally friendly sulphonation method (EFSM) because gaseous SO_2 is passed through solid polyHIPE in the presence of H_2O_2 solution and heterogenous sulphonation is achieved. This compares to typical SO_2 removal catalysts promote either SO_2 oxidation to SO_3 or SO_2 reduction to sulphur with a reducing gas (Kim et al., 1998, Wang et al., 2006). This method is a non-regenerative desulphurisation technology because it creates a high amount of

solid waste. However, there is an advantage of converting the disposed adsorbent material to an economically valuable finale product if a suitable process can be identified. The main drawback of this method is the low adsorption capacity of about 13% and a low degree of sulphonation at about 10%. This can be explained as follows; as discussed before the adsorption capacity and adsorbent selectivity depend heavily on the system porosity, internal surface area and contact area of the adsorbent (Xia et al., 2016) while the sulphonated polyHIPE beads or discs have a diameter about 0.3-1.0 mm (Hart et al., 2002). Therefore, the adsorbent has a relatively small fluid /surface contact area on the adsorbent bed (Barlik and Keskinler, 2014). This should be taken into consideration in the manufacturing process of the adsorbent.

Several methods have been reported in attempting to sulphonate the polyHIPEs to use in applications requiring hydrophilic material (Cameron et al., 1996, Williams and Wrobleski, 1988, Bokhari, 2003, Çalkan, 2007, Calkan, 2007). Conventional and microwave sulphonation are the two main methods discussed in detail in Chapters 5 and 6. Most of these studies reported that the major disadvantage of the conventional methods was in producing excessive waste acid after the sulphonation. In this study, a comparison between these methods has been demonstrated and it will be shown how to overcome this obstacle by introducing the sulphonation agent as a feedstock during polyHIPE preparation.

4.7.2 Silanation

One other type of chemical modifications of the interactive polymer surface is silanation**.** This is a good example of chemical surface modification in which silane coupling agents promote a polymer that strongly adheres to metals. This reagent could work as an adhesion promoter between a template and a metal because it possesses two reactive groups of different types bonded to the silicon atom in its molecule. The first group (like an epoxy, amino, vinyl, or methacryl group) can react with synthetic resins and organic materials to form a chemical bond. However, the second group is reactive towards inorganic materials such as metals, glass and silica sand. These groups are silanolic hydroxyl, ethoxy and methoxy groups (Goyal, 2006). Silane coupling agents are a type of organosilane compound R'- Si $-(OR)_3$ having a short hydrocarbon chain, R', which is a hydrolysable alkoxy group such as $-OC_2H_5$-OCH_3 alkoxysilane-terminated organic monomers or macromonomers (Lindberg et al., 1998).

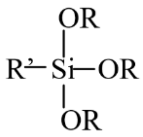

More recently, investigations have reported that alkoxysilane-terminated organic monomers or macromonomers $R'Si(OR)_3$ can be utilised in three basic methods for different applications .These are 1) as surface treatment (Witucki, 1993) ; 2) as an additive (Plueddemann, 1983) and ; 3) as a crosslinker. (Tai et al., 2001).

Haibach et al. (2006) demonstrated the improvement of the mechanical properties of PolyHIPE by ensuring that silica reinforcement particles were covalently bonded into the inorganic polymer network created by the hydrolytic condensation of the organic silane groups (Haibach et al., 2006). This was similar to work done by Menner ((Menner et al., 2008) and (Menner et al., 2006a)). On the other hand, Normatov and Silverstein reported a synthesis of nano porous polymer nanocomposites with high mechanical properties by the addition of TEOS, a tetra alkoxysilane, to the EHA 2-ethylhexyl acrylate and DVB in the organic phase within HIPEs by utilizing a silane with a vinyl group combined with the oil phase.(Normatov and Silverstein, 2007) .

In addition to sulphonation and silanation, Tebboth et al (2014) discussed various studies that produce high porosity, very interconnected macroporous polymers with tailored properties and surface chemistry for separation applications such as filtration, membrane, chromatography applications and chemical scavenging and sorption applications (Tebboth et al., 2014)**.** For instance, Lucchesi *et al* (2008) prepared amine scavenging polyHIPEs, by post functionalization of polyHIPEs with 4-vinyl-2,2-dimethylazlactone to produce a suitable polyHIPE for the chemical scavenging and sorption applications. (Lucchesi et al., 2008). Alikhani and Moghabeli prepared and functionalized polyHIPE to be used for removing nitrate ions by Ion-exchange adsorptive membrane. Trimethylamine (TMA) and triethylamine (TEA) were used to functionalize the foam in a process called amination. This process is the reason for the modification of polyHIPEs by amines in this study and is described in the Sections 4.3 and 6.2 (Alikhani and Moghbeli, 2014).

4.8 Summary and outlook on adsorbents synthesis methods linked to PolyHIPE

This chapter has discussed the most important results relevant to the use of porous polymers and polyHIPE as adsorbent materials. When added to the previous chapter it discusses the foundations of the adsorption process on porous polymers and adsorbent synthesis and identities the existing knowledge, gaps, and current trends that justify the need for this study and its novelty.

This literature survey is aimed at supporting the choices behind the materials investigated and the experimental results in the next chapters by investigating similar areas of research and interpreting the factors that cause the importance and preference of these substances over the rest of the adsorbents.

General applications, morphology and, characteristics, and preparation methods for polyHIPE are introduced and discussed. These are important for the adsorbent synthesis and sulphur removal from model fuel later, which will be discussed in the next chapters.

It has also been demonstrated that the morphology of polyHIPEs and is affected by many factors such as mixing time, DVB/styrene ratio and surfactant. Moreover, the most important properties that characterize the polyHIPE and play a significant role in adsorbent manufacture were discussed. These sections covered the polyHIPE surface area and mechanical properties, knowing that porosity was included in the polyHIPE morphology. These properties are very important for the adsorbent synthesis as they identify the adsorption capacity, selectivity, and mechanical properties of the adsorbent. Finally, chemical modification of polyHIPE has been explained and sulphonation, silanation and other methods mentioned to help in studying the chemical modification of the adsorbent synthsised in this study.

In the present work, novel combination of functionalized adsorbents will be developed by preparation of polyHIPE linked with another industrially tested absorbent MEA and reinforcement material that is usually used as an adsorbent and absorbent. A macroporous polyHIPE support was selected because its lower diffusion resistance is expected to facilitate mass transfer of the sulphur components into the adsorbent particles.

The next chapter details the experimental methods and approaches that are used in this study.

5 Methodology

5.1 Introduction

The methods that have been used in this project can be grouped in four main areas as shown in Figure 5.1 The first step involves the evaluation of Iraqi crude oil and creation of a model fuel oil for the adsorptive desulphurisation process. This model oil should have its major physical and chemical properties as similar as possible to those of the original parent feedstock. This is beneficial in two ways, firstly it allows a detailed study of the adsorbents behaviour towards both the main solvent and each individual sulphur substance individually, and secondly the subsequent steps in regeneration and solvent recovery are simplified paving the way to the later field study and the feasibility study in Iraq.

In order to ensure this similarity, several experiments were conducted to determine the specification of the crude oil and then those of its derivatives including their physical and chemical properties especially the sulphur content and the kinds of sulphur groups present within them. Finally, octane containing five sulphur substances was chosen and carefully mixed homogeneously by using a stirrer to produce the model fuel oil.

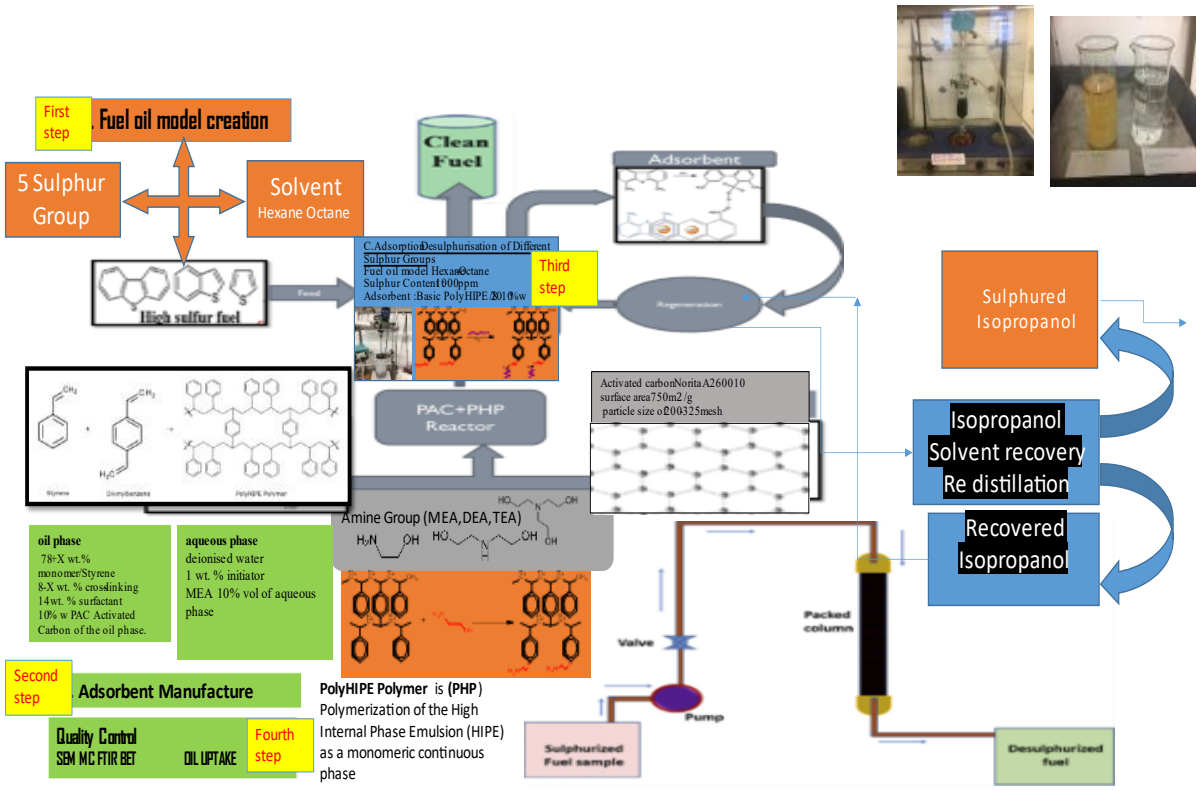

Figure 5.1 Methodology Procedure Scheme.

The second step concerns the production of polyHIPE and the manufacture of the adsorbent which is the central element of the adsorption desulphurisation process. The first part of this step is the preparation of the porous polymer as a template for the whole process.

Firstly, a standard porous polymer is made via the polymerisation of a high internal phase emulsion HIPE. A common material used in many previous studies was used as a starting point based on styrene as a monomer, divinylbenzene as a cross linker and span 80 as a surfactant (Akay, 1995, Çalkan, 2007, Bokhari, 2003, Akay et al., 2004, Akay and Calkan, 2015, Akay et al., 2002, Hasan, 2013, Mohamed, 2011). These substances form an oil phase which represents 10% of the total solution volume while the aqueous phase representing 90% of the volume consists of deionised water and an initiator, in some cases electrolytes can be added if needed. (Greco, 2014, Akay and Calkan, 2015, Alikhani and Moghbeli, 2014) .

There are many features of polyHIPE that have led researchers to use it in various applications. The economics of manufacture is very important also; the preparation and functionalisation of this material is inexpensive as the raw materials are cheap and the manufacturing technique used are simple and straightforward as mentioned in chapter 3. The structure of this basic polyHIPE was manipulated and optimized in this study in order to use it as a sulphur adsorbent.

It is known that the critical factors for a successful adsorbent are its: selectivity, capacity, durability, and regenerability (the ability to be regenerated). (Babich and Moulijn, 2003, Javadli and De Klerk, 2012). Selectivity refers to the ability of the solid material to attract a desired substance in specific liquid without the other components and it depends mainly on the chemistry of the solid surface and its physical properties. Capacity means the general permeability of the adsorbent to allow to the fluid to flow through the pores of the solid to encounter unused adsorption sites. Therefore, the macro- and mesopores will ensure mass transfer and increase the capacity while the micro- and nanopore structures will control the selectivity of the adsorbent towards the desired material and the extent of adsorption. In order to satisfy all these conditions, the basic standard PolyHIPE, needs to be evaluated in batch adsorptive desulphurisation tests which is the third step of method. This involves batch and continuous adsorption, regeneration, and solvent recovery. Last but not least, it is necessary to evaluate the steps of quality control which are very important to produce reliable PolyHIPE. This step includes the material characterization which takes place throughout the project in order to determine the next needed modification to satisfy the previous step in a cycle as shown in Figure 5.2. PolyHIPE characteristics were adjusted so as to produce the most suitable adsorbent.

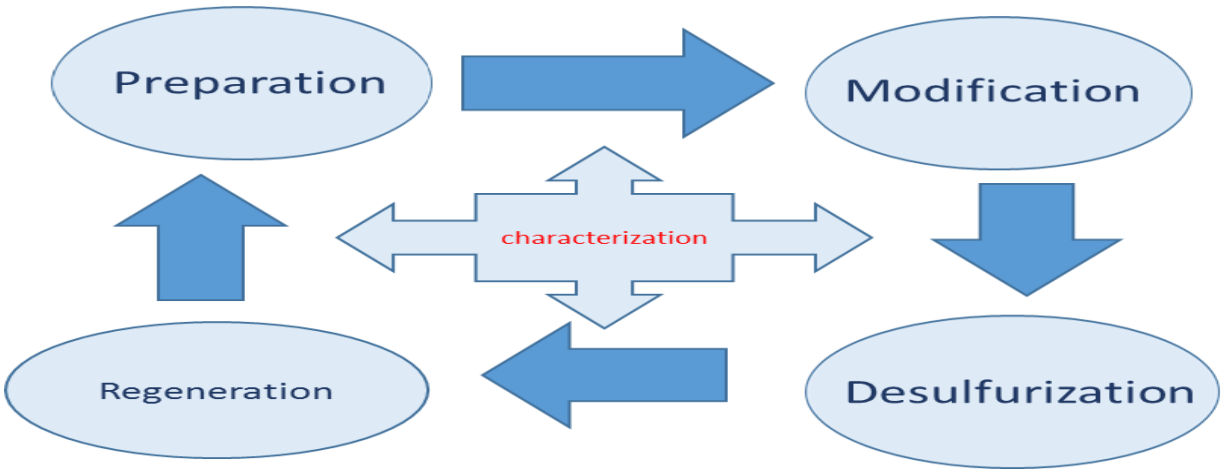

Figure 5.2 Adsorbent manufacture and characterization optimisation.

According to the scheme in Figure 5.2, once the first production cycle had been completed and depending on the adsorption results obtained, further modification may be required to increase the adsorption capacity.

Sulphonation is a technique has been applied to polyHIPEs for many applications. Previous studies (Çalkan, 2007, Calkan, 2007, Noor, 2006) have shown that sulphonation can increase the surface area of the polymer and convert it from being hydrophobic to hydrophilic and increase its chemical surface activity. However, it may also diminish very important features such as the mechanical properties (Noor, 2006, Çalkan, 2007, Thumbarathy, 2018). Two sulphonation methods have been used in this study; traditional thermal sulphonation and microwave sulphonation. Characterisation of the polymer showed these produce different polyHIPE surfaces, but both improved the extent of sulphur capture compared to the unsulphonated material. Nevertheless, the adsorption rate was relatively low which leads to the need for further modification.

Sulphur removal by absorption Desulphurisation using amines is one of the common techniques in the oil industry although the process has many drawbacks that make it imperfect to use (Abdulrahman et al., 2015) namely expensive investment, heat required for regeneration, corrosion, decomposition and poisoning of the amines by O_2 or other chemicals precipitation of salts, possible foaming (Huertas et al., 2011) In this study, mono ethanol amine was used as a promising candidate for adding to the polymer to increase its chances of sulphur removal.

Since it will be part of the solid polyHIPE-Adsorbent material many of its problems might be overcome as a result of no need severe operation condition for both adsorption and regeneration and less expensive investment because its small amount of MEA is will be used. PHP/MEA was therefore the third type of polymer produced for evaluation.

The polyHIPEs was functionalized by adding the amine in three different ways inspired by previous studies of sulphonation and amination (Alikhani and Moghbeli, 2014, Hasan, 2013). Unfortunately, despite its relatively good results as an absorbent material, PHP/MEA cannot be used as an adsorbent because of the degradation of its mechanical properties compared to the original polyHIPE, which results in an inability to regenerate it.

This means that a new technique is requited such as adding other materials that make the PolyHIPE possible to use as an adsorbent and be regenerated. Therefore, the active carbon powder material was selected a good candidate to reinforce the polyHIPE while affecting the other properties as little as possible and potentially adding to its adsorbent capability. A challenge was to know the correct amount and proper way to add activated carbon to the PolyHIPE. The use of ultrasound to disperse the activated carbon was investigated here.

Finally, the last PolyHIPE produced both activated carbon and the amine treatment in a single material.

Once trial materials had been produced and their structure optimised for adsorption further tests were carried out to measure details of their adsorption ability using gas chromatography whether in a batch or continuous process as shown in Figure 5.3 (Danmaliki and Saleh, 2017) .

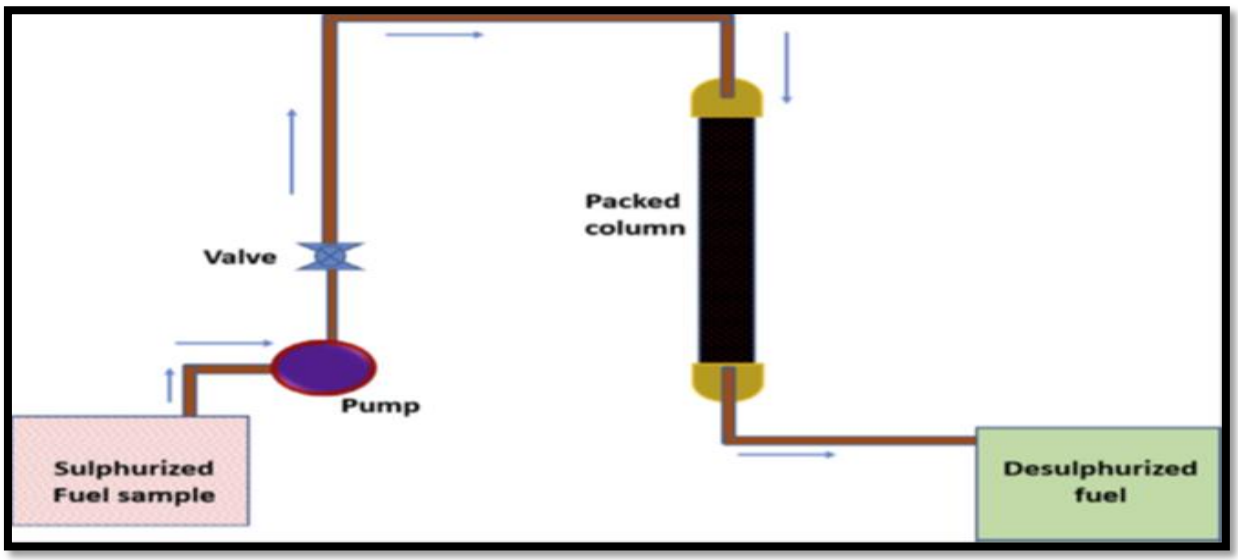

Figure 5.3 Continuous adsorptive Desulphurisation.

This paved the way for the best polyHIPE to be tested as adsorbent to reduce the sulphur from real feeds of Iraqi oil products. These methods and procedures were performed according the procedures used in oil refineries philosophy which is that they should be integrated with each other to provide the maximum profit at the lowest cost. So, additional steps have been done to test the continuous adsorption and then regeneration after more than one cycle of operation. Furthermore, solvent recovery testing has been conducted on solvent used in the regeneration process to ensure its possibility to reuse as shown in Figure 5.4.

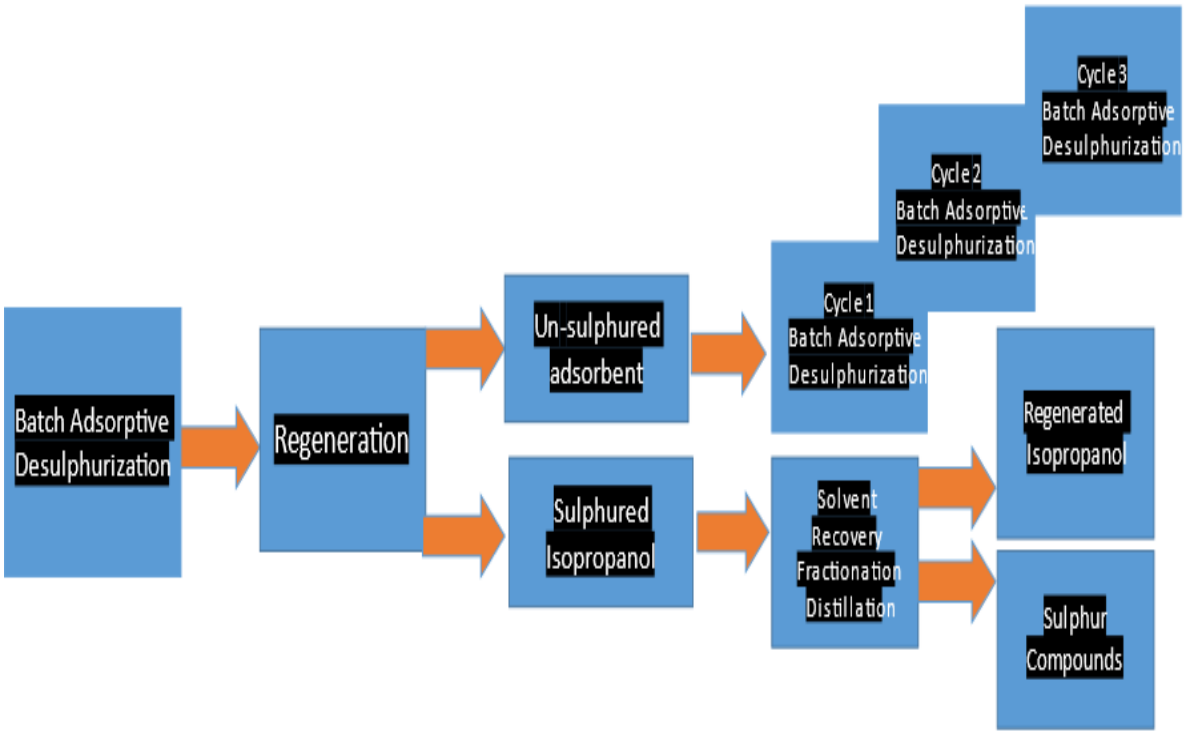

Figure 5.4 Schematic of the integrated process.

The last study took the Iraqi oil light products as a feedstock for adsorptive Desulphurisation using the best performing polyHIPE as an adsorbent.

Since the adsorbent is the main factor in adsorptive desulphurisation, the target for this material is to have special features that allow it to be productive, active, applicable and economic. The polyHIPE was functionalized and its characteristics was modified to achieve this target. A number of physical and chemical analytical methods were used in the analysis of the polyHIPEs produced in order to direct the previous steps of adsorbent manufacturing and the sulphur adsorptive Desulphurisation process as shown in Figure 5.5:

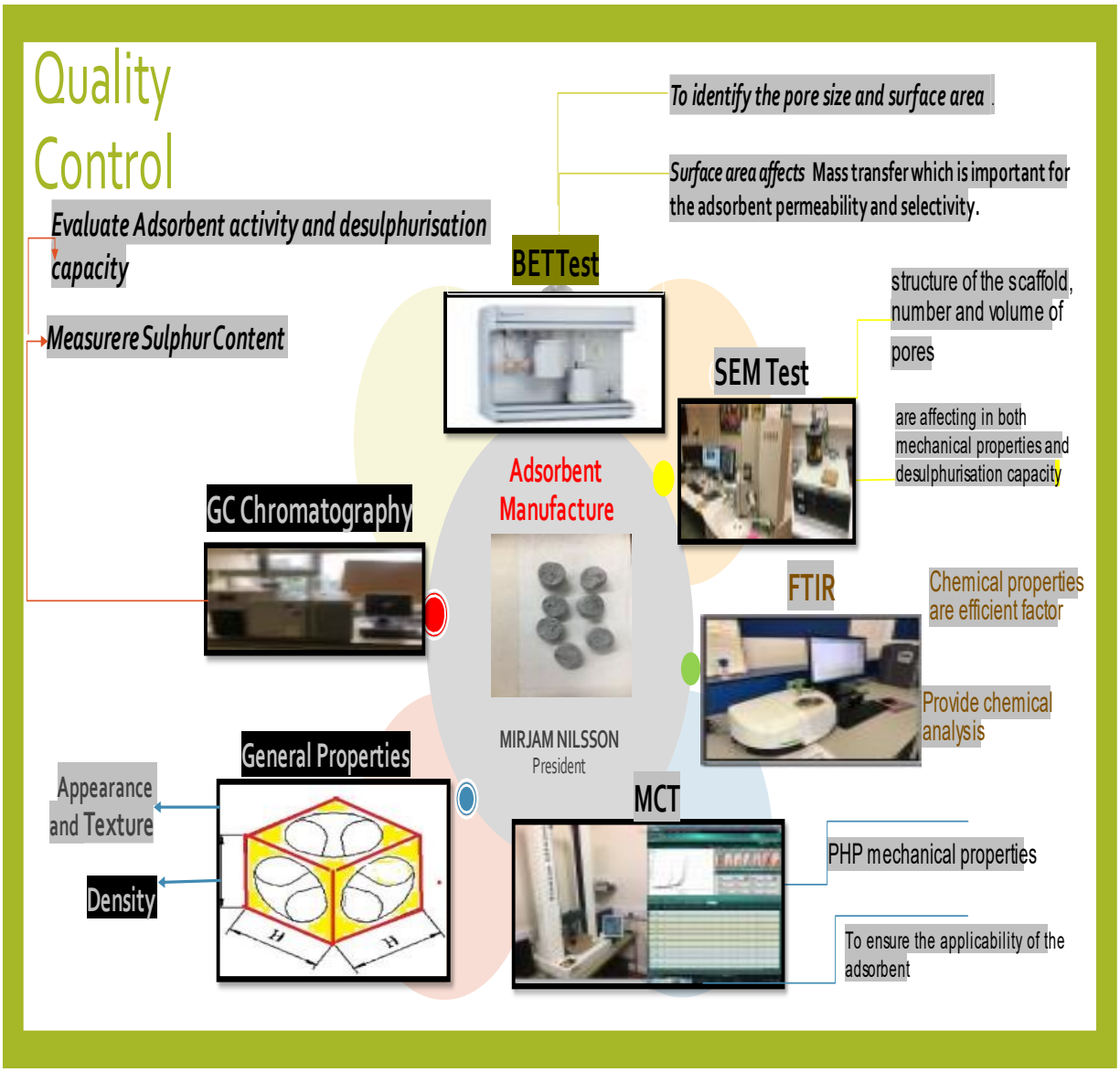

Figure 5.5 Quality control scheme.

1. The architectural properties were determined by using a Brunauer-Emmet-Teller (BET) test to identify the pore size and surface area of the adsorbent. Mass transfer is important for the adsorbent permeability and selectivity. The adsorption capacity and the adsorption rate of an adsorbent is directly related to the specific surface area and the pore size distribution of the adsorbent (Chiang et al., 1999). Pore interconnectivity at a larger scale is also critical. Scanning electron microscopy SEM with image analysis (ImageJ software) was also conducted since the structure of the scaffold, the number and volume of large pores affect both mechanical properties and Desulphurisation capacity.
2. To ensure the applicability of the adsorbent, it should have sufficient mechanical properties – the strength of the polymer was tested by a compression test (CT).

3. Since the surface chemistry is an important factor playing controlling the polyHIPE's ability to adsorb sulphur and which chemical compounds that the polymer (and solvents) can adsorb bulk and surface analysis techniques such as Fourier Transfer Infra-Red (FTIR) spectroscopy have been used in this study to characterise materials before and after use.
4. Certain physical properties of crude oil and the adsorbent in combination with crude oil have been investigated including, density, colour and oil uptake.
5. Finally, Gas Chromatography has been used to evaluate the desulphurisation capacity of the adsorbent and the stability of model fuel oil. This technique has previously been used in many studies including (Ma et al., 2005, Hua et al., 2003, Catalan et al., 2006, Gough and Simpson, 1970).

Given thus, the chapter is divided into four parts:

- Crude oil evaluation and fuel oil creation
    - Crude oil evaluation by sulphur content from different Iraqi oilfields.
    - Fuel oil creation, solvent and chemical mixing, GC test.
    - Oil Uptake.
- PolyHIPE production and Adsorbent manufacture
    - Standard PolyHIPE Preparation.
    - Adsorbent Manufacture.
- Adsorption Desulphurisation.
    - Batch Desulphurisation
    - Continuous Desulphurisation
    - Regeneration
    - Solvent Recovery.
- Quality Control

5.2 Crude oil evaluation and sulphur content testing

As previously stated, crude oil is very complex mixture with a non-uniform composition. This may consist of up to 200 or more different hydrocarbon compounds. The quality of crude oil is based on two main factors. The first is the American Petroleum Institute (API) gravity, which is obtained from the specific gravity i.e., the density of substance divided by that of water. Equation 1 shows that the specific gravity of crude oil is inversely related to its API value. (Nelson, 2018)

$$API = (141.5 / SG) - 131.5 \qquad \text{Equation (1)}$$

where API = degrees API gravity SG = specific gravity at 60^{o}F or 15.5^{o}C

The value of API gravity was designed to include a wide range of crude oils. It indicates the quality of crude oil and its price. As it is an inverse relationship (equation 1), higher API gravity means a lighter specific gravity and that means lighter crude because it contains more light compounds which are more valuable and generate a higher sale price.

The second factor that plays a crucial role in the evaluation of crude oil is its sulphur content. Iraqi crude oil samples were analysed in order to understand the relationship between these two factors, study the impact of the sulphur content on oil classification and therefore its price. Typical examples of the main sulphur contaminants as discussed earlier were identified and their concentrations in crude oil obtained from refinery data and the literature. This enables the manufacture of standard contaminated oil solutions for adsorption testing each containing a single component. Different crude from different oil fields, as shown in table 4.1, have been tested in the Midland Refineries Company –Iraq (see Appendix -4 a, b, c, d Typical Refinery analysis log sheet for crude oil and light products (Aldaura refinery –Iraq).

SAMPLE	SAMPLE
Basra crude oil (BSH)	Mushraf shamia gas station .(MSGS)
Kirkuk crude oil. (KKO).	Qurainat gas station .(QGS)
Rumaila South crude oil. (RSC)	. Alnasiriya crude oil .(NSCO)
Alahdab oil field. (AOF)	. Algaraf crude oil. (GRCO)
Ashamia degassing station. (ADSH).	. Neft khana crude oil.(NKCO)
Almarkazia degassing station. (AKDS)	. Crude oil mix and fed to Midland refineries
Mushraf qurainat degassing station (MQDS)	Company. (MRCF)

Table 5.1 The Iraqi crude oil from different oil fields.

The methods were used to evaluate these crude oils are illustrated in Table 5.2 referenced to their ASTM standard. These standard methods are commonly used in both crude oil production and refineries as explained in Appendix 5.

NO	TEST	METHOD	NO	TEST	METHOD
1	API Gravity @15.6 C°	ASTM-D1298	9	Ram. Carbon Residue wt.%	ASTM-D524
2	SP. Gravity @ 15.6 C°/ C°	ASTM-IP	10	Asphaltenes Content wt.%	JPI-5S-45-95
3	Sulphur Content wt.%	ASTM-4294	11	Ash Content Wt.%	ASTM-D482
4	Kinetic Viscosity Cst.	ASTM-D445	12	Vanadium PPM	ASTM-D6728
5	Pour Point Co	ASTM-D97	13	Nickel PPM	ASTM-D6728
6	R.V.P Kg/cm2	ASTM-D323	14	KUOP Characterization Factor	UOP Method 375
7	water and sediment Vol.%	IP-75	15	Water Content Vol.%	IP-74
8	Salt Content wt.%	IP-77 & ASTM-D3230	16	Distillation	IP-24

Table 5.2 Characterization and Standard Tests Methods of crude oil (Appendix 4).

It is very important to study the nature of the crude oil and its derivatives, as their features and characteristics will dramatically affect the design of the equipment and the kind of desulphurisation process used.

5.3 Fuel oil creation, solvent, and chemical mixing, GC Test

A model fuel oil was created according to the previous specifications by adding different organic sulphur groups available in a typical Iraqi oil to a base fluid. The model oil was prepared by dissolving butanethiol, dipropylsulfide, dimethylsulfide, benzothiophene and dibenzothiophene in n-octane. Other factors taken into consideration were explained in chapter 2. According to the wide of research investigated in many studies of different solvents and sulphur groups test fluids usually contain of one (or more) solvent and also one or more sulphur group or substances (Brunet et al., 2005, Ma et al., 2007, Ma et al., 2005, Kim et al., 2006, Xiao et al., 2008, Zhou et al., 2009, Seredych et al., 2009, Wang et al., 2012, Triantafyllidis and Deliyanni, 2014, Khan et al., 2013, Fallah et al., 2014, Xia et al., 2016, Neubauer et al., 2017, Danmaliki and Saleh, 2017, Ahmad et al., 2017, Saleh et al., 2017, Prajapati and Verma, 2017).

The main factors in these studies are solvent; sulphur compounds; desulphurisation capacity; analysis method, and regeneration approach. These factors represent the basic principles which should be considered in the creation of model fuel oil.

Different solvents were considered and then changed to find the most suitable solvents. So, toluene has an adverse effect on the adsorbents in that it changes their mechanical properties.

Hexane cannot be used due to its low boiling point and its volatility. Finally, normal octane (boiling point 125℃ and molecular weight 114 g/mol) was chosen based on literature data.

NO	S-group	S-compound	Code	Boiling Point BP / ℃	Molecular weight g/mol	Structure Formula
1.	Thiols RSH	Butanethiol 99%	C4	98	90	$C_4H_{10}S$ 
2.	Sulphides RSR	Di n-Propyl sulphide 98%	DPS	142	118	$C_6H_{14}S$ 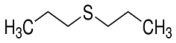
3.	Disulphides RSSR	Dimethyl disulphide 99%	DMDS	109	94	$C_2H_6S_2$ 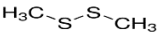
4.	Cyclic S group	Benzothiophene 97%	BT	220	134	C_8H_6S 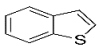
5.	Cyclic S group	Dibenzothiophenee 98%	DBT	332	184	$C_{12}H_8S$ 

Table 5.3 Sulphur-containing compounds in octane to form model fuel oil.

As mentioned in the previous chapter sulphur compounds have been used to represent the main groups in crude oil and its derivatives as shown in Table 5.3. Organic sulphur compounds were added to the solvent prepared with a total sulphur concentration ranging from 0 to 1000-4000 ppmw for each one.

5.3.1 Mixing Unit

The mixing of the solvent and the five materials was carried out in a 1000 ml stirred reactor (Duran GLS80 as shown in Figure 5.6 a-c). The cap has four connections as shown in figure 5b which permits media to be added or removed during mixing. Also, the variable stirrer shaft can be driven by using a standard magnetic stirrer fixed at 300 rpm (figure 5.6 c). The fuel oil model samples were tested after one hour of mixing and readings were taken each hour for 8 hours to evaluate the stability of its chemical composition using FTIR. A final sample was taken the next day for comparison to recheck the stability of the mixture again using FTIR and also GC.

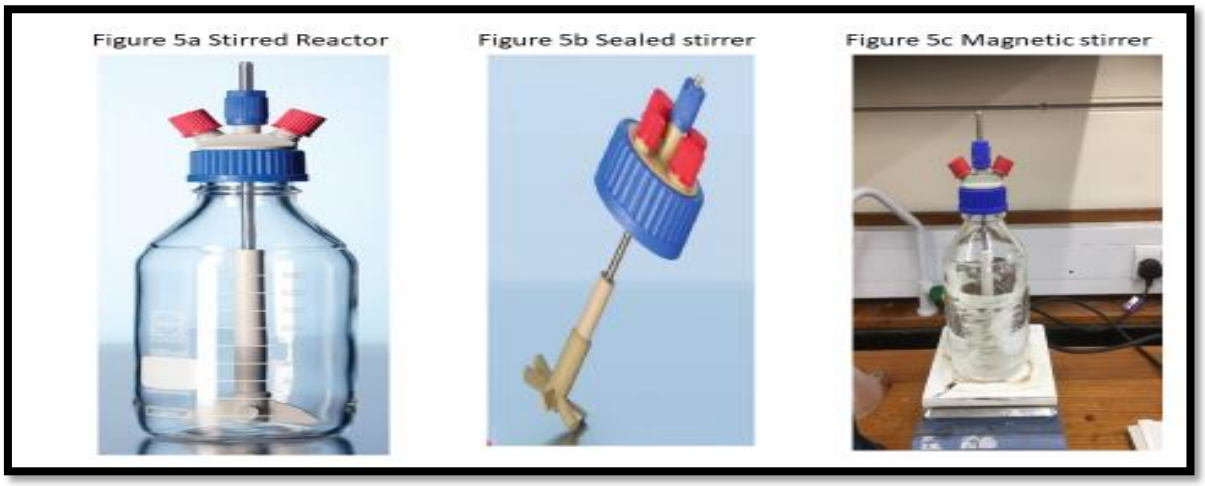

Figure 5.6 Duran GLS80 mixing unit a. stirred reactor, b. sealed stirrer, c.magnetic stirrer.

5.3.2 Prepare Calibration Standards at Several Concentrations

The next step of the analysis was to build the calibration curves by diluting the fuel model with octane and then carrying out the test for total sulphur content using GC mass chromatography of each individual sulphur compound. Each single compound had the same concentration range as in table 5.4.

Octane Concentration%	Sulphur content Concentration%
100	0
80	20
60	40
40	60
20	80
10	90
5	95
3	97

Table 5.4 Composition of calibration standard samples.

5.3.3 PolyHIPE oil uptake and adsorbent preliminary solvent test.

The oil uptake test was used to study the behavior of PolyHIPE as an adsorbent for oil (Saleem et al 2014; Hasani 2013). For the determination of oil uptake simple immersion test was used. The standard polyHIPE samples were completely immersed in octane and hydraulic liquid (ISO-10 Revol-Voler density 0.82 gm/cm^3) separately for 24h - 48h. The weights of the

PHP samples before and after immersion were measured twice and the percentage of oil uptake was calculated using the following formula in equation 2.

$$\left(\frac{(Wf-Wi)}{Wf}\right) \times 100\% \text{ ----------Equation (2)}$$

Where W_f = final weight of the PHPs and W_i = initial weight of the PHPs. Three measurements were carried out from independent samples of the same Batch of PHP. Three different types of PHP were investigated: PHP ST= Standard PolyHIPE before sulphonation, AMS= PolyHIPE after microwave sulphonation, AST = PolyHIPE after traditional thermal sulphonation.

5.4 PolyHIPE production and adsorbent manufacture

A range of PolyHIPEs with different surface functionalisation have been produced as candidate adsorbent materials in this project:

- **i.** Standard PolyHIPE Preparation with different mixing time (Xia et al., 2016).
- **ii.** Sulphonated PolyHIPE by thermal and microwave.
- **iii.** Aminated PolyHIPE by adding mono-ethanol amine MEA in three concentrations.
- **iv.** Carbonated PolyHIPE by adding activated carbon in different concentrations.
- **v.** Adding both mono ethanolamine and activated carbon to optimize PolyHIPE as an adsorbent.

All chemicals were purchased from Aldrich Chemicals and used as received except in the case of activated carbon when further processing and filtration was required. Table 5.5.

Component	Phase	Function
Styrene (ST) 99%	Oil	Monomer
Divinylbenzene (DVB) 80%	Oil	Cross-linker
Span 80 Sorbiton Monooleate (SMO)	Oil	Surfactant
Potassium persulphate (KPS) 99%	Aqueous	Initiator
Water	Aqueous	Emulsion Template
Sulphuric acid (H_2SO_4) 98%	Aqueous	Sulphonation Agent
Calcium Chloride ($CaCl_2.4H_2O$) 93%	Aqueous	Electrolyte
Mono-Ethanol Amine (MEA) 99%	Both	Additive
Activated Carbon (PAC)	Oil	Additive
Isopropanol C_3H_8O 99.5 %	---	Washing Agent
Acetone 99.8%	---	Swelling Agent

Table 5.5 Materials used in PHP preparation and adsorbent manufacture.

For these experiments, the composition for PHP is made up as shown in Table 5.6. Numerous studies have described the preparation of basic polyHIPE (Bokhari et al., 2005, Akay et al., 2002, Akay et al., 2004, Burke et al., 2010, Cameron and Barbetta, 2000, Akay and Calkan, 2015, Woodward et al., 2017, Yuan and Su, 2006). A well-researched basic polyHIPE been chosen as a starting point and modified according the purpose of the present study.

Within each material group different processing conditions were investigated to optimise material structure (pore size and surface area) for absorbency as described in the following sections.

Type of Polymer	Oil phase	Aqueous phase	Function	Target
Standard polyHIPE	Styrene (ST) 78 wt % Divinylbenzene (DVB)8wt % (Span 80) 14 wt.%	Distilled water 225 ml Potassium persulphate (KPS) 1 wt.%	Emulsion prepared at different mixing time	To prepare the best morphology
Microwave sulphonated polyHIPE AMS	Styrene (ST) 78 wt % Divinylbenzene (DVB)8wt % (Span 80) 14 wt.%	Distilled water 225 ml Potassium persulphate (KPS) 1 wt.% +5% wt H_2SO_4	Microwave sulphonation 230 v -50 Hz -1305 W)	To: Increase the surface activity.
Thermal sulphonated polyHIPE	Styrene (ST) 78 wt % Divinylbenzene (DVB)8wt % (Span 80)14 wt.%	Distilled water 225 ml Potassium persulphate (KPS) 1 wt.%	Traditional thermal sulphonation Set temp. 80 oC 5 oC/hr to 100 oC	To: Increase the surface activity
Aminated polyHIPE	Styrene (ST) 78 wt % Divinylbenzene (DVB)8wt % (Span 80)14 wt.% Plus 10 wt.% MEA of the total oil phase weight.	Distilled water 200 ml Potassium persulphate (KPS) and calcium chloride $CaCl_2$ 1 wt.% 10 wt.% MEA of the total liquid phase weight.	Adding MEA to the emulsion. Adding Electrolyte to the liquid phase Acetone stage MEA aging	To: Increase the surface activity To help MEA absorbent PHP Swelling Extra Amination
Carbonated polyHIPE	Styrene (ST) 78 wt % Divinylbenzene (DVB)8wt % (Span 80) 14 wt.% Plus 10 wt.% PAC of the total oil phase weight.	Distilled water Potassium persulphate (KPS) 1 wt.%	Adding PAC to the emulsion. Overnight oil phase mixing and sonification	Reinforced Increase surface activity Equal PAC diffusion
Modified Adsorbent	Styrene (ST) 78 wt % Divinylbenzene (DVB)8wt % (Span 80) 14 wt.% Plus 10 wt.% MEA of the total oil phase weight. 10 wt.% PAC of the total oil phase weight.	Distilled water 200 ml Potassium persulphate (KPS) and calcium chloride $CaCl_2$ 1 wt.% 10 wt.% MEA of the total liquid phase weight.	Adding MEA to the emulsion. Adding Electrolyte to the liquid phase Acetone stage MEA aging	To: Increase the surface activity To help MEA absorbent by PHP emulsion. PHP Swelling Extra Amination

Adding PAC to the emulsion.	Reinforce the adsorbent
Overnights oil phase mixing and sonification	Increase surface activity
	Equal PAC diffusion

Table 5.6 Compostion of oil and aqueous phase of PHPs.

.

5.4.1 Standard PolyHIPE preparation with different mixing time

Oil phase (The DVB concentration has been set at 8% as result of several experiments, where this level gave the highest surface area *(Burke et al., 2010)*

78 wt. % styrene (monomer) cross linked with

8 wt. % Divinyl benzene (cross linking agent) and to this add

14 wt. % volume Span 80 (surfactant)

Aqueous phase

1 wt. % potassium persulphate (polymerisation initiator) *was made up* with deionised water

Experimental procedure

PolyHIPE was prepared in several steps as shown in Figure 5.7 (Noor, 2006). Firstly, the continuous oil phase was prepared, which consists of 78 wt. % styrene monomer, 8 wt. % divinyl benzene crosslinker and 14 wt % Span 80 surfactants and placed in a jacketed stainless-steel reactor 12 cm in diameter. The reactor is equipped with stirring shaft consisting of two 2 flat impellers where each set has two flat paddles of 9 cm in diameter stacked at right-angles to each other. The bottom end of the impeller is placed 1 cm from the bottom of the vessel to obtain homogeneous mixing. The impeller was set to a mixing speed of 300rpm. Secondly, a mixture of 225 ml of aqueous phase 1 wt. % of potassium persulphate as a polymerisation initiator was slowly dosed through a funnel inlet into the mixing vessel using a peristaltic pump at a constant rate 25 cm^3/min for the duration of the dosing time. The aqueous phase was pumped into the reactor under continuous mixing. Then, to obtain a small pore volume, after addition of the aqueous phase, mixing was continued with adjustment of the time and stirrer speed. Once all of the aqueous phase had been added, stirring was continued for a further period called the mixing time. Mixing times used were 5 10 15 20 25 30 60 90 and 120 minutes for each test. After emulsification, the emulsion was transferred to cylindrical containers with an internal diameter of 26 mm and polymerised at 60°C for at least 8 hours. After polymerisation, PHP samples were cut into disks 26mm in diameter and 4 mm thick. The samples were then

dried in a fume hood for 24 hours, to be ready for washing. An example of the sample coding is PBS-5, where PBS refers the polymer prepared before sulphonation, the number 5 represents the mixing time.

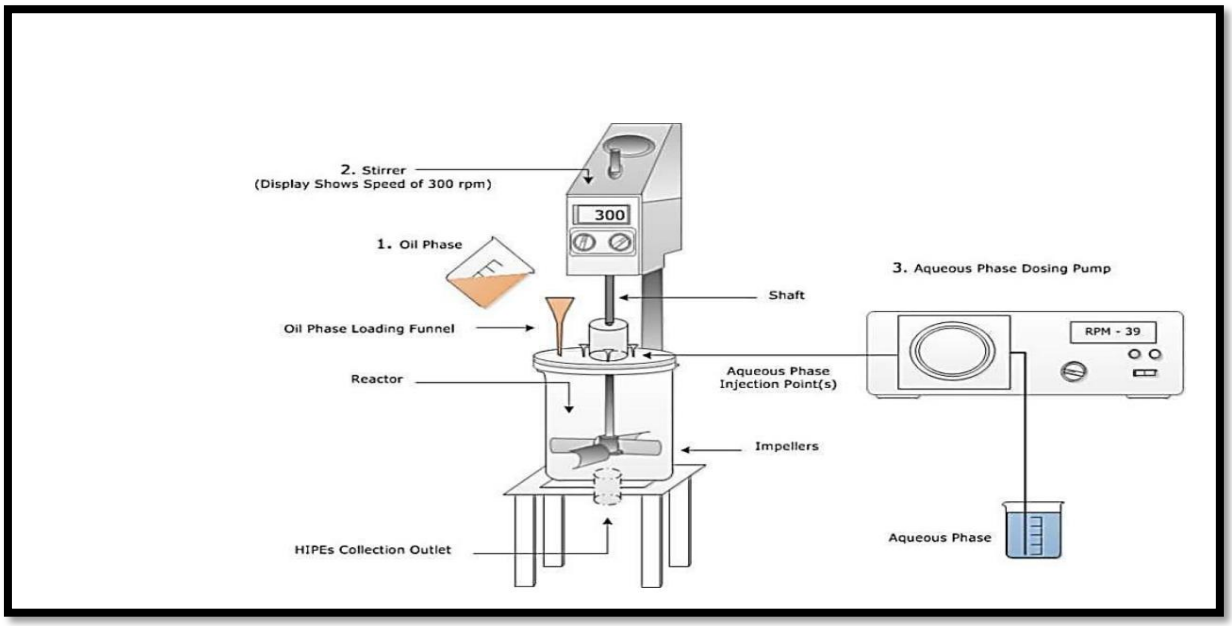

Figure 5.7 Schematic diagram of PHP production (Noor, 2006).

5.4.1.1 Washing PolyHIPE Polymers

To remove surfactants from the PHP samples they were washed in a soxhlet set-up as shown in Figure 5.8 (Hasan, 2013). The washing was conducted with two solvents firstly using iso-propanol for 3-4 hours at 70 C° and then with deionized water twice for 6 hours to remove any remaining residue in the PHP pores. The hydrophobic polyHIPE can be used for adsorption trials at this point but the hydrophilic material may need further sulphonation.

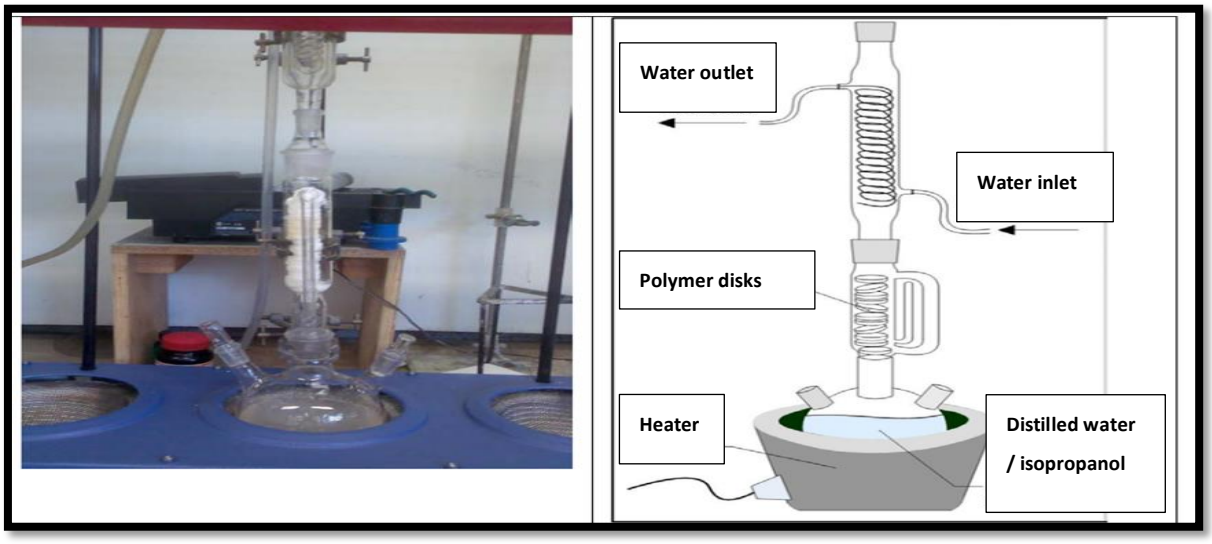

Figure 5. 8 Schematic diagram of the soxhlet apparatus used for polymer washing (Hasan, 2013).

5.4.2 Sulphonated PolyHIPE and sulphonation methods (thermal and microwave).

The PHP was saturated in concentrated sulphuric acid by immersion and then either thermally treated or microwaved to functionalize the surface. During the reaction of concentrated sulphuric acid with the surface, an atom of hydrogen in the monomer could be replace by the ($SO_3^-H^+$) group, as shown in Figure 5.9 (Çalkan, 2007).

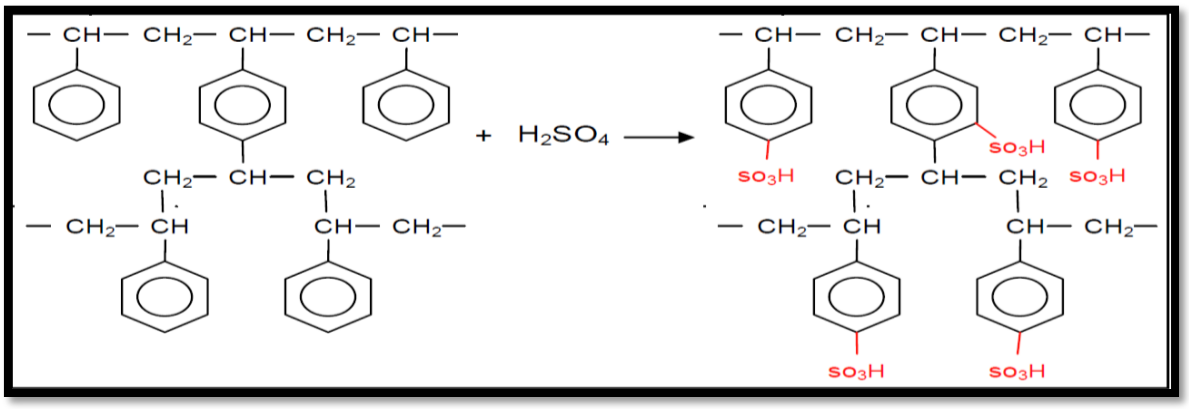

Figure 5.9 Chemical structure of ions substitution to produce sulphonated polyHIPE (Çalkan, 2007).

The technique for driving chemical reactions and concentration of the sulphuric acid used play a significant role in obtaining the sufficient functionalisation of the polyHIPE structure. Two techniques have been used:

In microwave sulphonation (Figure 5.10) the PHP discs were soaked in concentrated (99.98 % concentration) sulphuric acid for three hours and then microwaved (230 v -50 Hz -1305 W) for a total of 40 seconds in which the PHP discs were inverted four times (every 10 seconds) at room temperature (Noor, 2006).

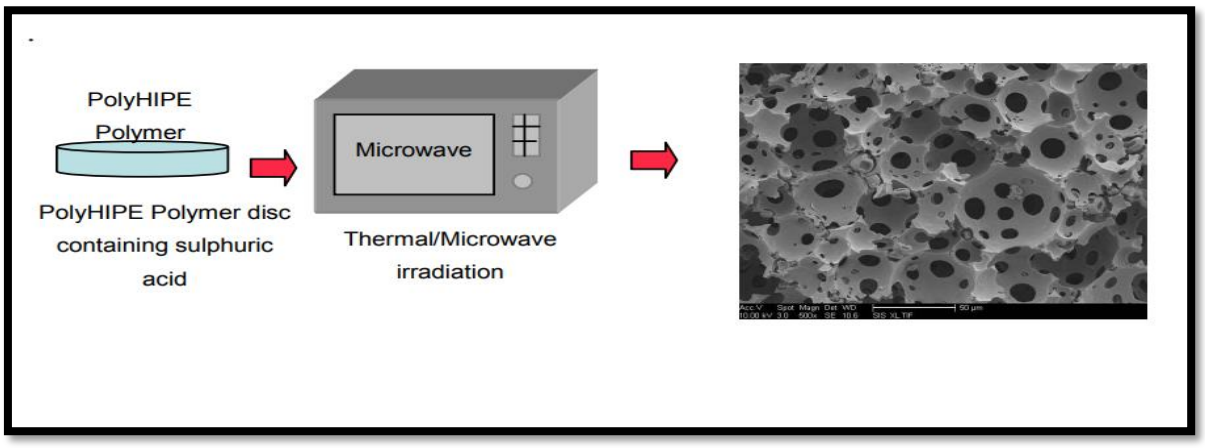

Figure 5.10 Picture and schematic diagram of microwave Sulphonation (Noor, 2006).

In conventional thermal heating sulphonation (Hasan, 2013) PolyHIPE discs were soaked in concentrated sulphuric acid for three hours then placed with 250 g caustic soda powder in a ceramic vessel in an oven to absorb humidity and acid gases as shown in (Figure 5.11) (Calkan, 2007)(Burke et al., 2006). The temperature was set to 80 ^{o}C and then increased gradually by 5 ^{o}C/hr to 100 ^{o}C.

The coding used for these samples is AMS for those after microwave sulphonation and ATS after thermal sulphonation followed by a number representing mixing time used.

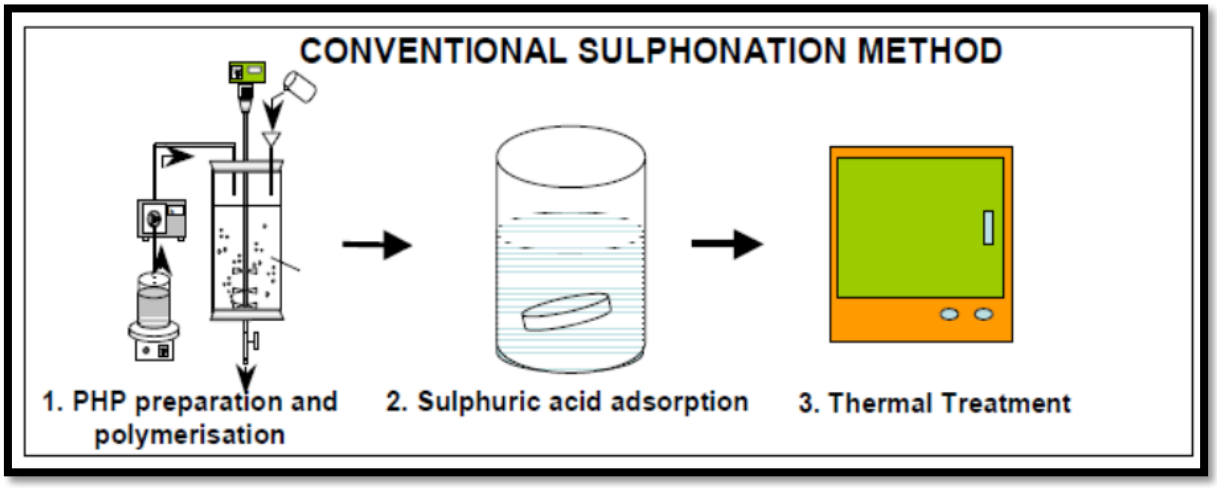

Figure 5.11 The Conventional PolyHIPE Sulphonation method. Adapted from (Calkan, 2007).

5.4.3 Aminated PolyHIPE by adding mono-ethanol amine (MEA) in three categories.

PHP/MEA was prepared using the same technique as above, but with incorporation of MEA in different trials until the optimum material was achieved. MEA addition was conducted to improve the surface chemical activity of polyHIPE towards the sulphur compounds.

PHP/MEA Procedures

Materials

Oil phase 10%

78 wt. % styrene (monomer) cross linked with

8 wt. % Divinyl benzene (cross linking agent) and to this add

14 wt. % volume Span 80 (surfactant)

Plus **1**0% wt MEA of the total oil phase

Aqueous phase 90%

1 wt. % of both potassium persulphate (polymerisation initiator) and calcium chloride $CaCl_2$ of the aqueous phase

Made-up with deionised water

Preparation

The liquid aqueous phase was prepared solution by adding 1% wt of equal amounts of potassium persulfate ($K_2S_2O_8$) as initiator and calcium chloride ($CaCl_2.4H_2O$) as electrolyte to 225 ml distilled deionised water. The solution was mixed in a magnetic stirrer for 20 minutes until a homogeneous transparent solution, due to total solubility of the salts in water, was obtained. The oil phase was prepared by mixing 78 wt. % styrene (monomer), 8 wt.% Divinyl benzene crosslinking agent, 14 wt. % Span 80 (surfactant) plus **1**0% wt MEA of the oil phase weight. The oil phase was transferred to the 12 cm reactor the same way as shown in Figure 5.7. Then the HIPE was formed when the aqueous phase was dosed into the reactor using a peristaltic pump with a flowrate of 25 ml/min while mixing. Mixing took place in the reactor equipped with the same stirring shaft. The dosing time with continuous mixing for 25 min was followed by a further 30 min of mixing with the impeller set to 300 rpm to form the emulsion with a similar time that used in the preparation of the optimum standard polyHIPE. The polymerisation step started once the HIPEs were placed into 50 ml plastic containers and closed carefully before heating in the oven for 60 $^{\circ}$C overnight. The presence MEA in both oil and aqueous phase during polymerisation, contributed the adhesion of amine droplets on the polyHIPE surface. This resulted in the formation of very large pores several hundreds of micrometers in diameter dispersed in the normal polyHIPE pore structure. The resulting deterioration of mechanical properties makes the material inappropriate for industrial application despite the drastic increase in sulphur adsorption due to the amines ability to attract sulphur compounds.

After polymerisation, solid PHP cylinders were cut into 0.4-1 cm thickness slices with a diameter of 2.6 cm (Figure 5.12), filtered and separated to eliminate waste pieces and then subjected to flowing air in the fume cabinet to be dried ready to swell. As a result, approximately 80% of their weight was usually lost due to the evapouration of water (Burke et al., 2010). The discs were then immersed in acetone for three hours at room temperature and then washed dropwise with MEA before heating This involved swelling of the crosslinked polymer discs by acetone (acetone stage) to allow the maximum amount of excess MEA to be absorbed by the solid discs in the ageing step, which can ensure continued access of the reagents to the reactive sites (Cameron et al., 1996). The polyHIPE totally absorbed the MEA and adhere to its surface.

Figure 5.12 PolyHIPE solid cylinder, filter wash and cutting into discs.

The surface functional group of the discs was then permitted to adhere or react with the amine agent at 80 ˚C for 4 hours. Then the ageing stage was completed by submerging the polyHIPE discs in excess MEA at room temperature overnight to enrich the polyHIPE with extra amine as shown in Figure 5.13. After that, the amine-treated polyHIPE discs were washed in a beaker with deionized water at 60˚C for three hours. The water was changed each hour. They were dried at 60˚C in a vacuum oven until they had reached a constant volume and were ready for characterization and adsorption testing (Alikhani and Moghbeli, 2014).

Figure 5.13 PHP/MEA discs submerged in acetone then ageing in MEA.

5.4.4 Carbonated PolyHIPE (adding Activated carbon to create PHP/PAC).

From the characterization and adsorption data for the PHP/MEA material, it was found that although the material could be successfully manufactured its mechanical properties need to be enhanced in order for it to be reused and regenerated with minimum losses. To achieve this goal research has been conducted to find a material with superior mechanical properties, thermal stability, high surface area, high permeability and porosity. The mechanical properties of the polymer can be improved by reinforcing the cell walls with a stiffer adsorbent material. The reinforcement should, on its own, can have in an increase in sulphur adsorption in addition to what is achieved by the polyHIPE alone (Leboda et al., 2003).

For these reasons, activated carbon has been chosen to increase the oil phase density thereby improve the mechanical properties as explained in section 2.4. It has been recorded that activated carbon having the largest surface area and highest surface polarity shows the highest total capacity for adsorption of sulphur (Yu et al., 2013). Consequently, activated carbon was treated with concentrated H_2SO_4 to maximise surface area before being mixed with the oil phase in polyHIPE manufacture. The biggest challenge was to add activated carbon powder to the oil phase whilst ensuring its stability in the emulsion. Furthermore, the powder should be distributed evenly through the emulsion in all formation stages, i.e. in the oil phase preparation, in the emulsion stage and in the final polymer product.

Because of the physical differences, density and chemical nature this material is hard to be insoluble in both liquid and oil phases. The first PHP/PAC modified experiments recorded a degradation in stability, as the PAC tends to settle to the bottom as a sediment in each of the three stages of polyHIPE formation (mixing, emulsification and polymerisation). Moreover, it can cause breakage, deformation or degradation of the cell walls if added in excessive quantities above those required to reinforce the polymer. Moreover, an uneven distribution occurred if it was added in insufficient quantities due to its tendency to agglomerate.Therefore, a highly specific amount must be added. Many tests were performed to achieve the optimum distribution and the characterisation results are presented in chapters 6 and 7. A reinforced PAC/PHP was prepared by adding different amount of PAC, 1-20 % wt into the oil phase. The monomer/PAC dispersions were mixed for three days at 400 rpm as shown in Figure 5.14a and then homogenized by using sonication (Mesroghli et al., 2016). This is a technique in which sound waves are conducted to agitate particles in solution. Where ultrasound is a cyclic sound pressure

with a frequency that over the upper limit of human level of hearing starting from the frequency of 20 kHz. Homogenization took place in ultrasonic bath for 20 min Figure 5.14 b before pumping the oil phase into the reactor. 7-10% wt of the total weight of the oil phase was the optimum activated carbon content; the liquid-solid system was exposed to microjet impact and shock waves of 43 kHz frequency at around 225 W power in this process. The rest of the method is exactly the same of those of standard polymer preparation.

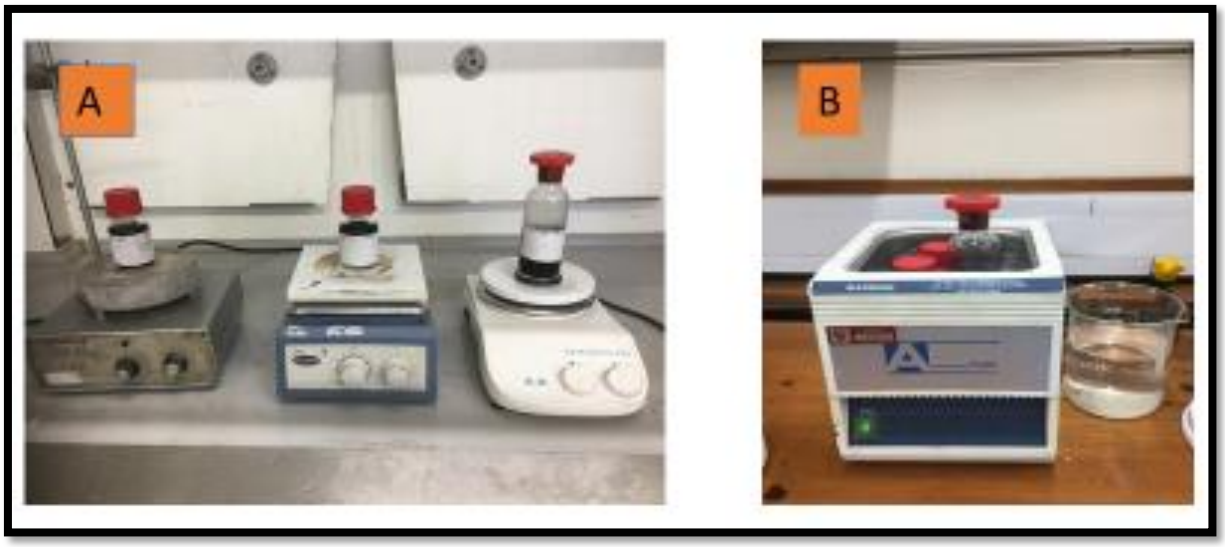

Figure 5.14 a. Mixing unit, b.Ultrasonic unit.

5.4.5 Adding both mono ethanolamine and activated carbon to optimize PolyHIPE as an adsorbent.

PHP/MEA/PAC was finally produced using a combination of the PHP/MEA and PHP/PAC methods. It is an integrated way by adding both monoethanolamine and activated carbon to optimize PolyHIPE to manufacture the adsorbent. Furthermore, using a new moulding type was necessary for this as discussed in the next section.

5.5 Moulding Type

After the emulsion stage, the emulsion was placed in cylindrical tubes with an internal diameter of either 26 mm or 10 mm and polymerized at 60 ° C overnight. After polymerisation, the PHP samples were cut into discs 26 mm or 10 in diameter and 4-1 mm thick Figure 5.15. The samples were dried in a fume hood for 2-3 days .The diameter was decreased from 26 mm to 10 mm in the PHP/MEA/PAC system to reduce losses in the total weight of the polymer used during drying.

Figure 5.15 Two different dimensions in moulding types used to improve the adsorbent.

Although there were no huge differences in structure and properties between the two sizes as the results in Chapter 7 showed that the two sizes possess identical or approximate characteristics as they are made of the same material. However, the small size has more uniform particles shape, less deformation that reduced losses and smaller discs provide an increasing in contact surface area.

It is worth mentioning that when the sample is transferred from the reactor to the sample tube care should be taken not to disturb the emulsion by the transfer process as follows: the tube should be placed in an inclined position during filling to minimise the fall height and pour the viscous emulsion smoothly and homogeneously avoiding the bubbles or air currents inside the material. Otherwise, bubbles produce a weak point when the liquid solidifies leading to fracture. In addition, avoid filling the sample to the top of the tube as this will provide a space for volume expansion caused by the heat of polymerisation.

5.6 Adsorption Desulphurisation.

5.6.1 Batch Desulphurisation

Batch adsorption experiments were performed in a closed, stirred, cylindrical tank 30 cm in height and 10 cm in diameter as shown in Figure 5.16 equipped with an agitator with crossed double stainless steel stirrer isolated with a stainless steel mesh at 3 cm above the bottom to avoid adsorbent-agitator contact which might lead to crush or fracture the adsorbent .

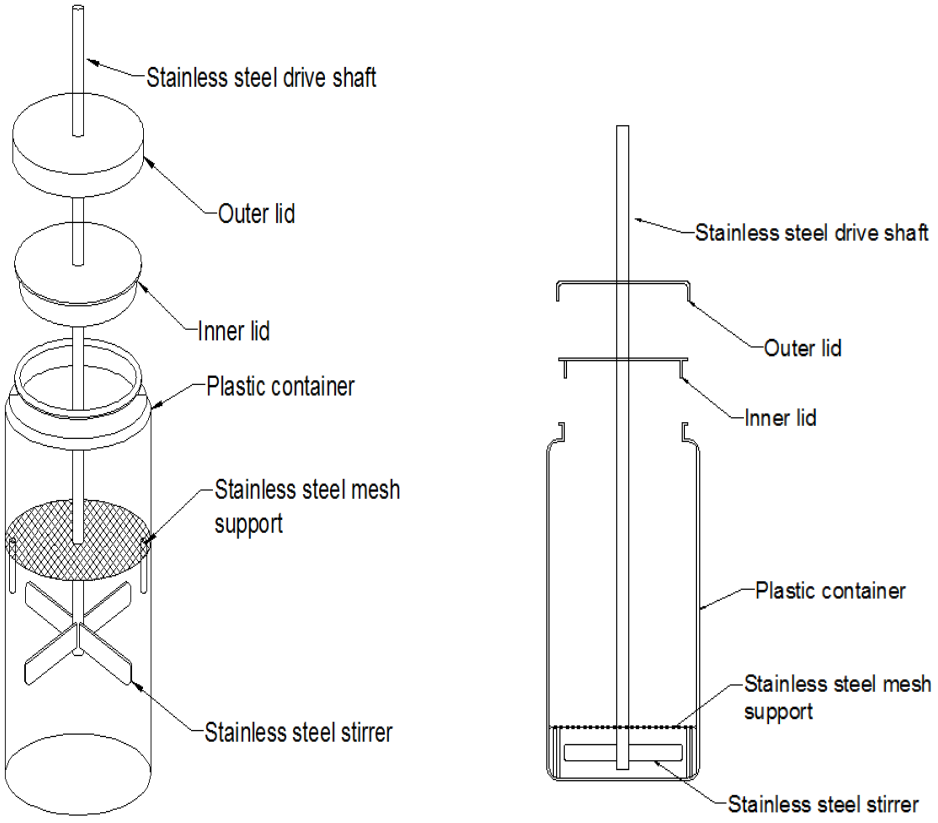

Figure 5.16 Adsorber mixer.

The experiments were performed by adding 10% weight of the adsorbent to the oil feed 1000 ml. The reactor flask was agitated with the velocity of the stirrer set at 300-rpm (Figure 5.17). The model fuel oil was added, and mixing started at normal pressure and room temperature for a fixed contact time of 72 hours.

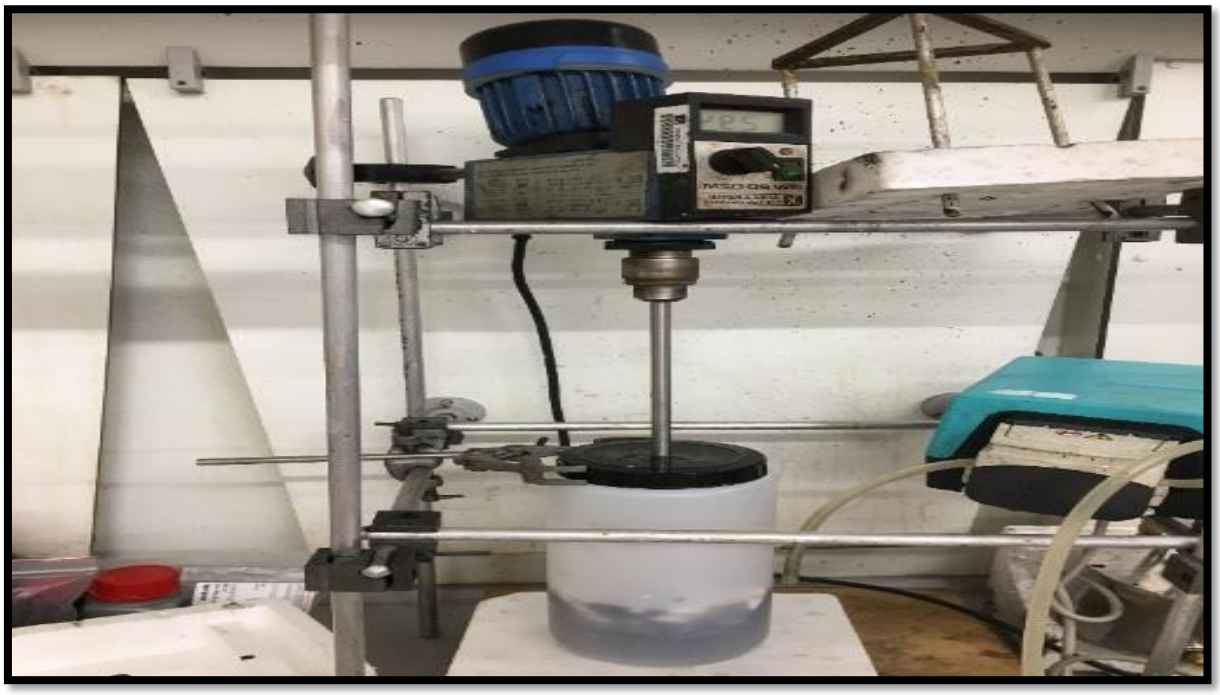

Figure 5.17 Batch Process the motor and the Mixer.

After adsorption, the solution sample was filtered from the adsorbents using BD Plastipak 20 ml syringe filter connected with VWR sterile filter 0.2-µm Figure 5.18.

Figure 5.18 Syringe filter connected with VWR sterile filter.

The sulphur content of the model oil was measured every 30 min of the first 8-12 hours of the test depending on the saturation level of the adsorbent (when the adsorption capacity curves reached the plateau and achieved the equilibrium) when it was decided to stop the process. For

the first group of experiments 5000-ppm sulphur concentration was used. This amount of sulphur contains 1000-ppm of each organo-sulphur compound used. The sulphur concentration was monitored by gas chromatography as mentioned before. The adsorption capacity at each time was determined by

$$X = \frac{Ce - Cf}{Ce} * 100\% \quad \ldots\ldots\ldots\ldots\ldots \textit{equation (3)}$$

Where X is the sulphur adsorption percentage for instance, X1 and X2 are the sulphur adsorption percentages at the first and second hours for instance), C_e is the initial concentration in ppm (parts of solute per million parts of solvent) and C_f is the final concentration in ppm. To take into consideration the different sulphur compounds an average removal capacity was defined by

$$TSC = \frac{\sum X}{5} \quad \ldots\ldots\ldots\ldots\ldots\ldots \textit{equation (4)}$$

Where TSC is the total average sulphur removing capacity of each adsorbent.

5.6.2 Continuous adsorptive Desulphurisation

This technique was used to simulate the industrial units in oil refineries. This was done with the best potential adsorbent following the evaluation of each adsorbent in a batch process after its optimisation and characterization. The feedstock of the process is a real light oil product, Naphtha, Kerosene and gas oil produced in Midland Refineries Company in Iraq. This is fed into a unit shown in Figure 5.19 and flowed up through the four columns with 30 cm in height each one connected by outlet and inlet valves. The adsorption bed is packed by filling with the adsorbent of PHP/MEA/PAC equal to 10-15% of the total weight of the feed.

The flowrate was controlled to be 2 ml/min using a peristaltic pump. Liquid is fed into the first column from its bottom with help of flexible tubes to avoid bubble creation and ensure a fully developed flow. In the same manner liquid from the top of the first column is transferred to the second column entering at the bottom side; this principle is applied for all columns.

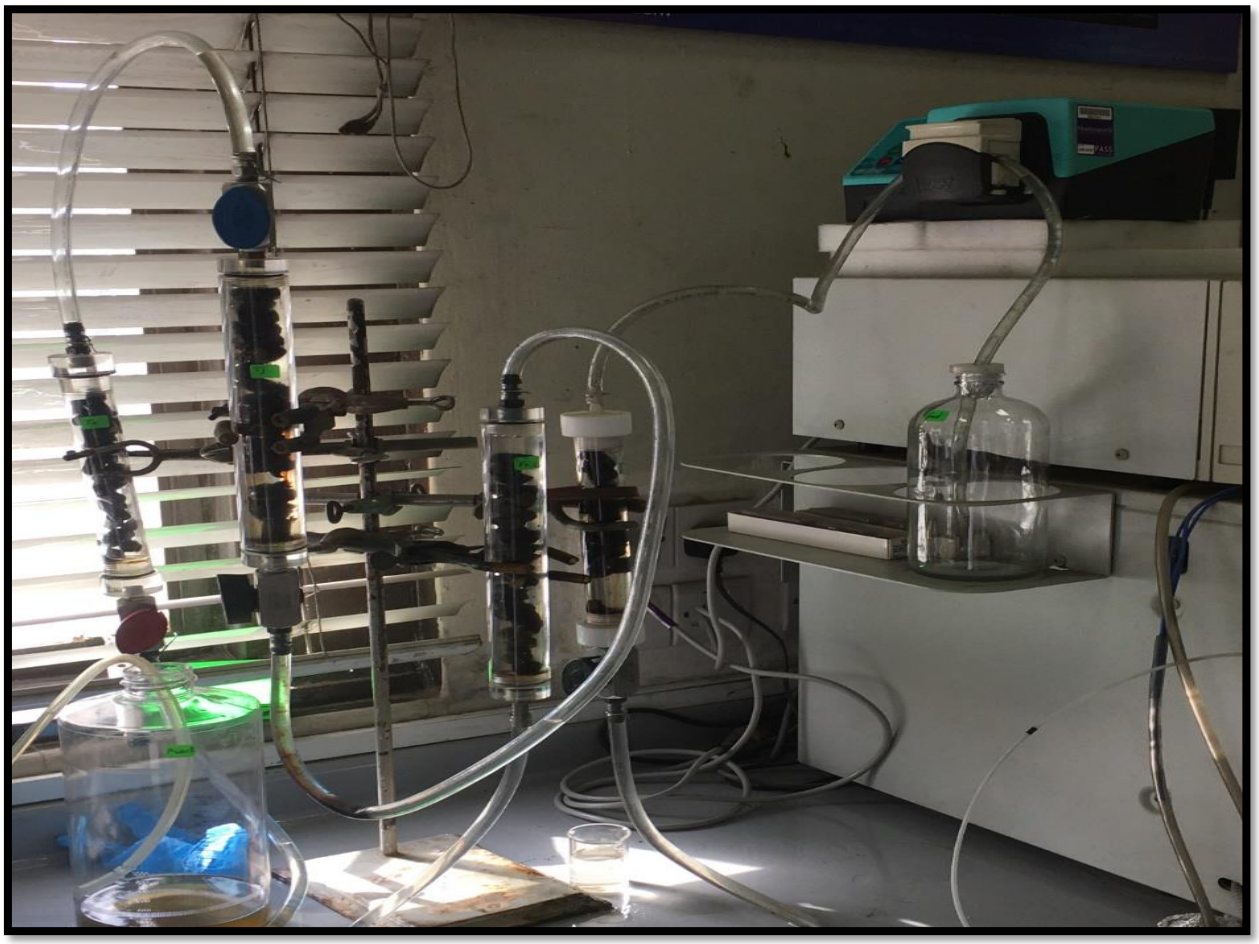

Figure 5.19 Continuous adsorptive Desulphurisation apparatus.

The test methods used are as follows:

1. D 5453 which is the standard test method for the determination of total sulphur in light hydrocarbons, spark ignition engine fuel, diesel engine fuel, and engine oil by using ultraviolet fluorescence1) (Appendix 5).

2. D 4294 which is the standard test method for sulphur in petroleum and petroleum products by energy dispersive x-ray fluorescence spectrometry (Appendix 5).

5.7 Regeneration

One of the most important factors in manufacturing a successful adsorbent is the ability to regenerate and reuse it with minimal weight loss compared to the total fresh adsorbent and with the same or similar activity levels and adsorbent capacity:

Weight loss $W = (g_0 - g_{i+1})/g_0 * 100\%$ ……. *equation (5)*

Where g_0 is the initial weight and g_{i+1} is the weight of dry adsorbent after regeneration. The first three optimized adsorbents could not be regenerated, while the spent PHP/PAC and PHP/MEA/PAC was regenerated and reused. After adsorption, the spent adsorbent was

separated from the desulphured oil and collected after adsorption process. The first filtration was carried out to separate the damaged and fractured solid discs from the uniform saturated adsorbent. The adsorbent discs separated and cleaned by sedimentation to remove the liquid impurities then filtrate by using sieves with a primary cold wash and remove the solid sediments and fractured and smashed discs then dry to prepare them for regeneration by isopropanol as shown in the Figure 5.20

Figure 5.20 Sepration of desulphured oil from the adsorbent discs.

The regeneration process of the rest of the spent samples was accomplished by washing them with isopropanol for 3 hours using the Soxhlet apparatus, at 70 C° which is close to the isopropanol boiling point at normal pressure as shown in Figure 5.21. The adsorbent samples were transferred to dry using an oven and heated to 60C°. Their weight was measured until it was constant used in Equation 5. In addition, compression testing was used in order to determine the mechanical strength of the adsorbents. The regenerated adsorbent was also subjected to the same characterisation tests as the virgin material to determine if any changes had occurred. The regeneration process was repeated five times for each of the adsorbents used. The isopropanol solvent used to remove sulphur was characterised by performing FTIR and GC in order to evaluate the regeneration activity due to the amount of sulphur present in it. Finally, the solvent was recovered as explained in the next section.

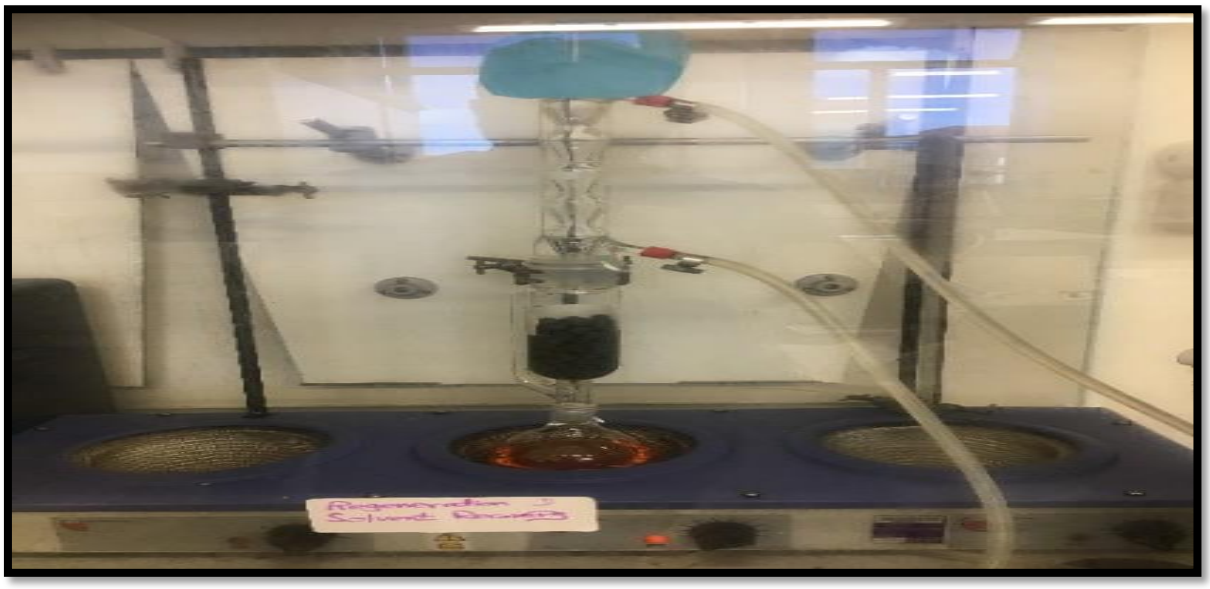

Figure 5.21 Soxhlet System - apparatus used in the regeneration of the adsorbent.

5.8 Solvent recovery.

The next step is to recover the solvent used in the adsorbent regeneration. This experiment was carried out by using a fractional distillation apparatus as shown in Figure 5.22. The solution was heated to the boiling point of the isopropanol (80 ˚C). The isopropanol evapourates and the vapour enters the top of a long condenser, where it cools, and liquid is collected dropwise into a beaker. This produced high sulphur content waste in the flask and desulphurised solvent which was used for further FTIR and GC tests.

Figure 5.22 Fractional distillation apparatus used for solvent recovery.

5.9 Quality Control

5.9.1 Scanning Electron Microscopy SEM

In order to investigate the cross-sections of the PHP structure, scanning electron microscopy (Dağ et al., 2019) has been used. The analysis investigates important information relevant to the processing, properties and behavior of materials that involves their microstructure at a higher depth of field and magnification compared to conventional light microscopy, making it more suitable for nanostructured materials. It also provides information relating to topographical features, morphology, differences in phase distribution, crystal structure and orientation, and the presence and location of defects (Greco, 2014).

SEM tests were performed in the NACMA laboratories at Newcastle University using an environmental SEM (model Hitachi S2400) supplied with an Oxford Instrument Isis200 Ultra-Thin Window X-ray detector as shown in Figure 5.23.

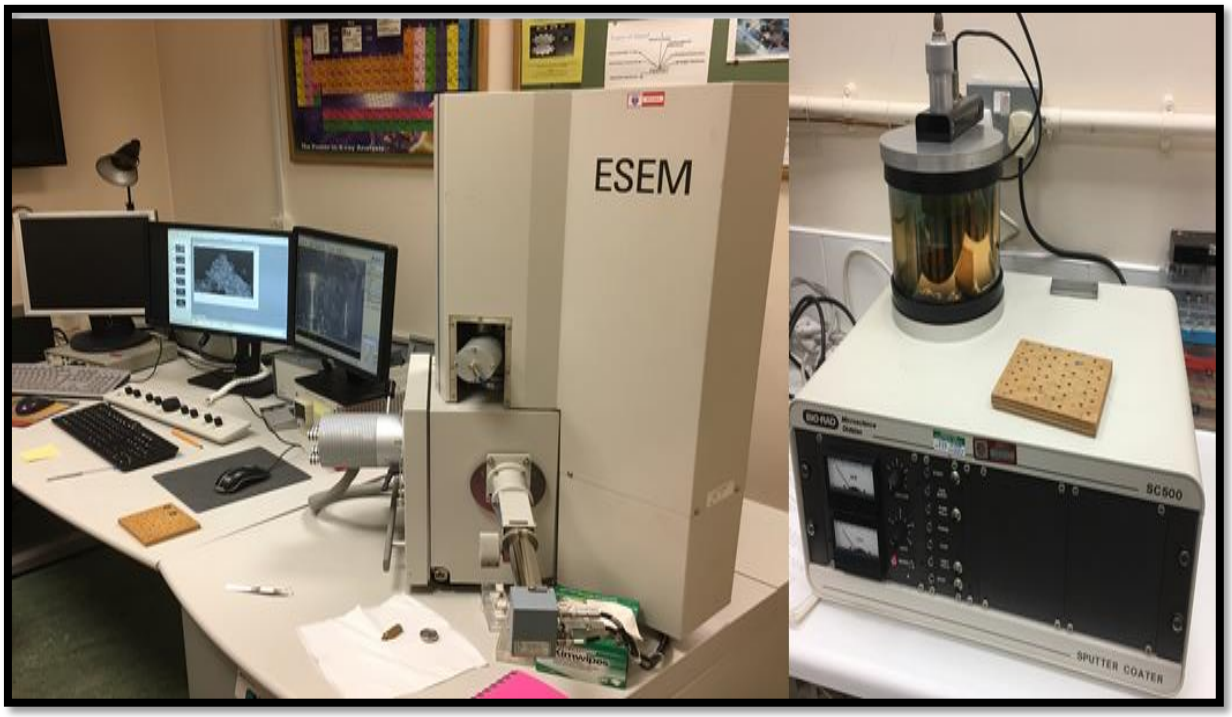

Figure 5.23 Scanning electron microscope and gold coater.

Samples were fractured rather than cut or sawed to avoid any damage to the cellular structure then cut with a sharp knife from the other edges and gold coated by using a Polaron e1500 Sputter Coater prior to imaging using a Philips Field Emission Gun (FEG) electron microscope to prevent charging affecting the image quality (Kadhim, 2017, Greco, 2014). A schematic diagram of the device is shown in Figure 5.24 (Thumbarathy, 2018). The theory of SEM involves scanning an electron beam of high energy over a specimen. Then by using a magnetic lens focusing the beam on the surface and electrostatic scan coils are used to deflect the raster

scan which controls the magnification of the sample image produced. The interaction between the primary electrons and the specimen surface produce a variety of probable signals which can be used for topographic imaging. The leading imaging mode is based on detectors collecting the secondary electrons emitted from the specimen surface after the bombardment by the primary electrons. The image formed when the electron beam hits the sample and various signals from the sample can be collected creating the images. For a more detailed description of SEM and ESEM working principles and characteristics reference books by (Zhou et al., 2006) are particularly useful.

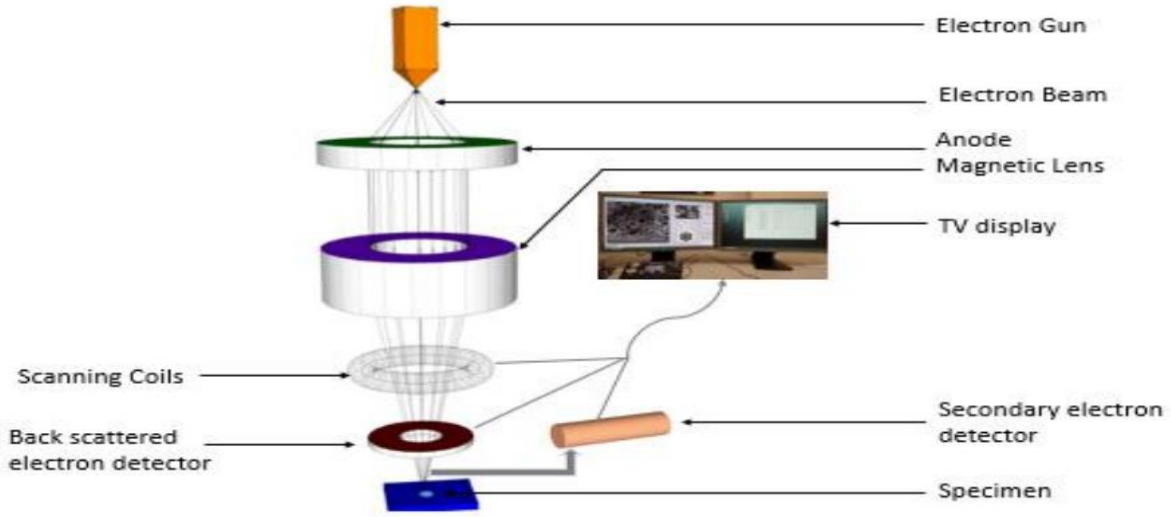

Figure 5.24 Schematic of a scanning electron microscope (Thumbarathy, 2018).

The analysis was conducted to identify the differences in structure with different mixing times for the standard PHP formed (PHP-ST 30-120 min), then to compare between PHPs before and after both microwave sulphonation and thermal sulphonation to identify the sulphonation effect on the PHPs structure. Moreover, it was also used to study the effect of the PHP modification by adding novel materials which are mono ethanolamine (MEA) and activated carbon (PAC). Finally, to analyse the changes in adsorbent structure after adsorptive Desulphurisation. The diameter of the pores, distribution and average value pore wall thickness and intersecting vertices thickness were measured by the program ImageJ (Figure 5.25).

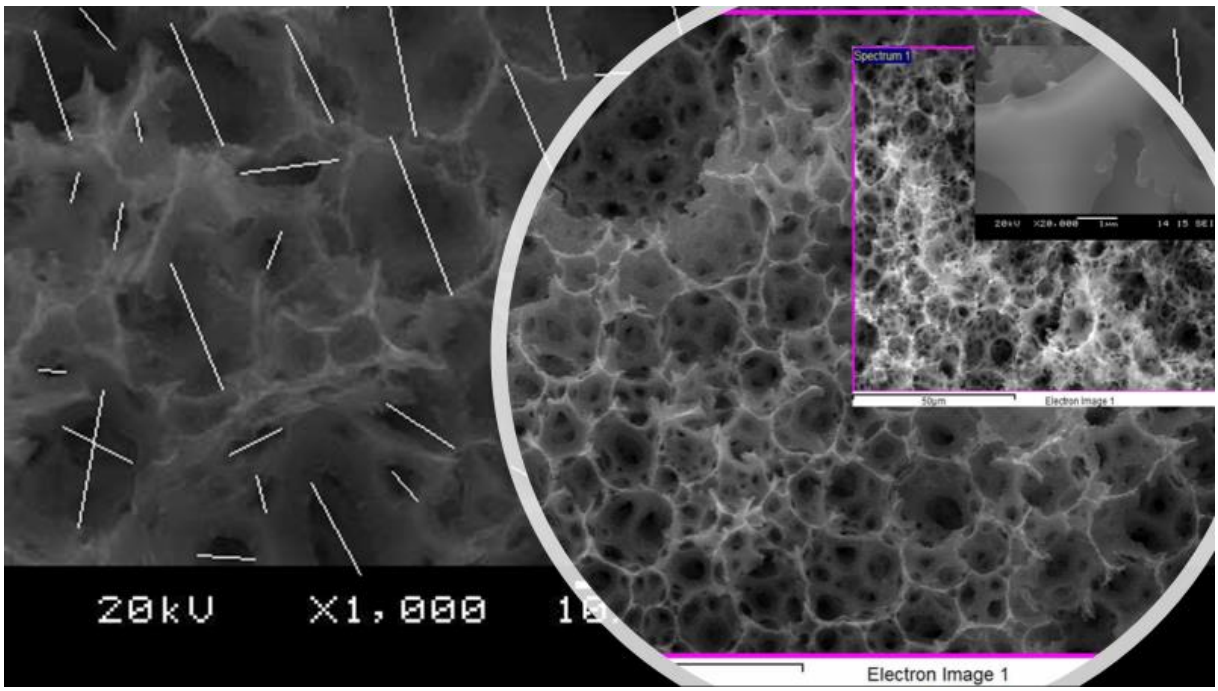

Figure 5.25 SEM image of PHP shows a wide mignification used for the computation of average pore size /diameter using ImageJ.

5.9.2 Fourier Transform Infrared Spectroscopy (FTIR)

The polyHIPEs were characterised spectroscopically and compared before and after sulphonation and other modification using Fourier transform infrared spectroscopic analysis FTIR. A Varian 800 FT-IR spectrometer system was used to analyse the solid samples. The machine produced spectra between 4000 cm^{-1} and 400 cm^{-1} from solid, liquid and oil samples using a Pike Technologies diamond crystal plate ATR (attenuated total reflection) immersion probe. as shown in Figure 5.26 Also, this was used to evaluate the model fuel oil before and after both adsorptive Desulphurisation, adsorbent regeneration and the solvent before and after recovery (Mercier et al., 2001).

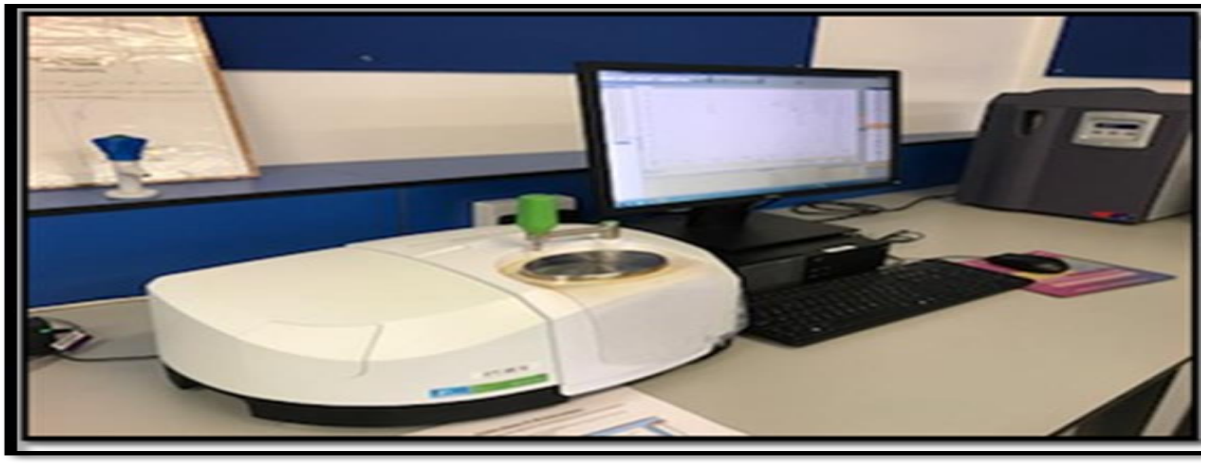

Figure 5.26 Fourier Transform infrared spectroscopy (FTIR) (Perkin Elmer spectrum 2 with ATR) with typical polystyrene spectrum.

In general, FTIR can be used to identify unknown materials, determine the quality or consistency of a sample, and measure the amounts of components in a mixture with characterize functionalities e.g., to measure the vinyl group content of polyHIPE (Hasan 2013)). In this technique, a monochromatic radiation penetrates the sample disks were infrared (IR) radiation was passed through a slit which collects and focuses the light towards them. Some amount of the radiation is absorbed by the sample and some is passed through or transmitted. The results are translated into a spectrum of molecular absorption and transmission, creating a molecular fingerprint for the sample. Each fingerprint belongs to a unique molecular structure. Working principles are shown in schematic diagram illustrated in Figure 5.27

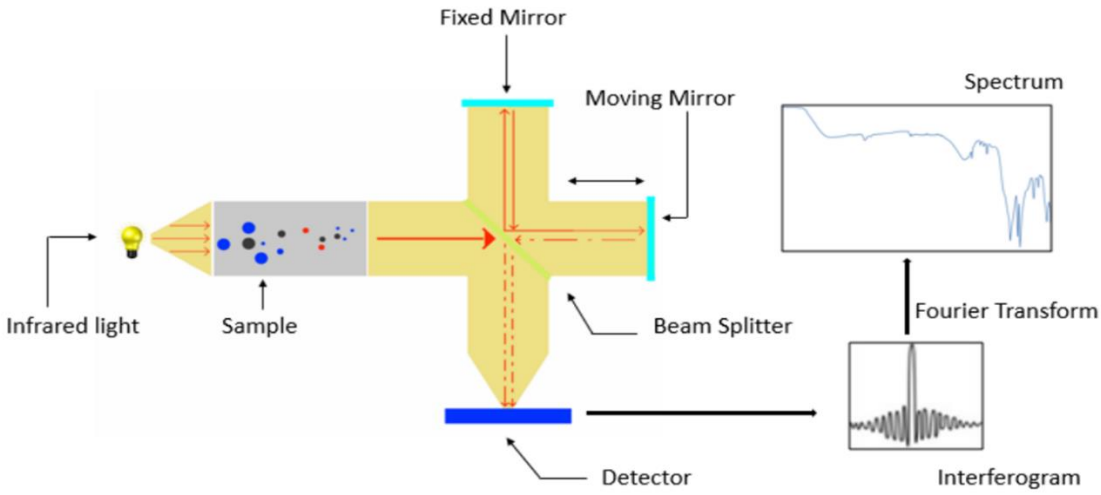

Figure 5.27 Schematic of Fourier Transform Infrared Spectroscopy (FTIR) (Thumbarathy, 2018).

Infrared energy emission in term of beam send from a source passes through a hole to manage the amount of energy applied to the sample. Afterwards the beams enter the specimen compartment while IR is transmitted or absorbed at particular energy depending on the type of analysis. The energy at which any peak appears in the spectrum match a frequency of vibration of the sample. The beam enters the interferometer where the spectral encoding conducted. Then the beam passes through the detector, which is used to measure the special interferogram signal. The measured signals are then digitized and passed to computer where the Fourier transformation takes place. Finally, the infrared spectrum is available for interpretation (Thumbarathy, 2018)

5.9.3 Surface area and pore volume measurement (BET)

Surface area and pore volume are the most important physical features of PHPs because their importance in providing sufficient sites for adsorption and controlling the mass transfer through the adsorbent. Whereas the SEM can measure large pores and surface topography at the micron scale gas adsorption techniques using the BET approach are needed for assessment at the nanometre scale. The equipment used to measure surface area was using the Micromeritics ASAP 2020 accelerated surface area and porosimetry system and the SURFER analytical unit manufactured by Thermo Fischer Scientific as shown in Figure 5.28 a and b. The equations used in this analysis are described by Hasan,2013 (Hasan, 2013). The theory describes physical adsorption of gas molecules, usually nitrogen, on the surface of the solid powder sample. Adsorption of the gas molecules occurs on the surface of the sample and as a result the micropores are filled up forming a monolayer. The amount of adsorbate gas corresponding to the monolayer formation on the sample surface is used to identify the specific surface area. On the other hand, capillary condensation processes, in which multilayer adsorption from the vapour phase into porous medium continues to a point where the condensed liquid from the vapour phase fills up the pores spaces within the sample. The samples were placed in a sample tube with a volume of 9 cm^3. Next, the samples were degassed for at least 6 hours at constant temperature of 50 ^oC. The tube containing the degassed polymer was connected to the analytical port of the ASAP 2020 and immersed in liquid nitrogen while the instrument calculated the Brunauer, Emmet and Teller (BET) surface area. A typical analysis takes between 30 min and two hours.

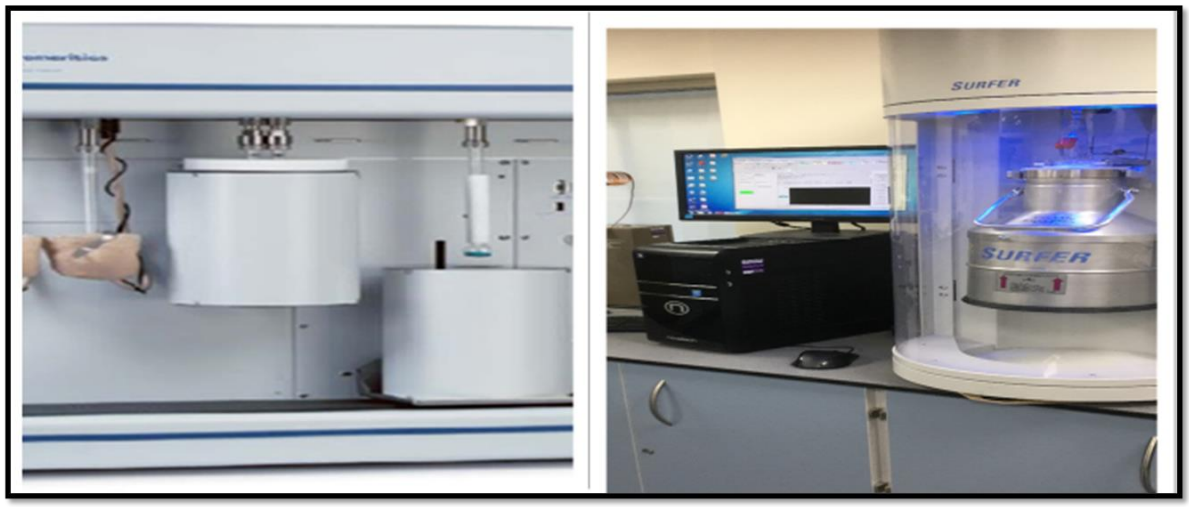

Figure 5.28 BET surface Area and porosimetry System (a) ASAP 2020 (Chitanda et al., 2016) and (b) ThermoFisher Scientific Surfer.

5.9.4 Mechanical compression testing (MCT) of PHPs

Mechanical compression tests (MCT) were performed in order to assess the effects of structural changes in the PHPs due to differences in mixing time and the various HIPE processing treatments before and after modification. The strength and stability of the PHPs and how these properties are affected by processing are important aspects of the handleability of the adsorbent. Hence, process-structure-property relationships are obtained from the test results. In general, good mechanical properties are essential for any solid adsorbent, catalyst, catalyst supports, conductive composite foam, and separation membrane, because they all require a porous structure with high specific surface area that remains stable in service (Hermant et al,2009; Zouboulis et al, 2002; Pulko,et al 2007) .

MCT tests with of the adsorbent samples were performed using a mechanical test frame (MTF) manufactured by Tinius Olsen. The machine was fitted with a 5 kN load cell and equipped with the Horizon testing software, a screenshot of which is depicted in Figure 5.29.

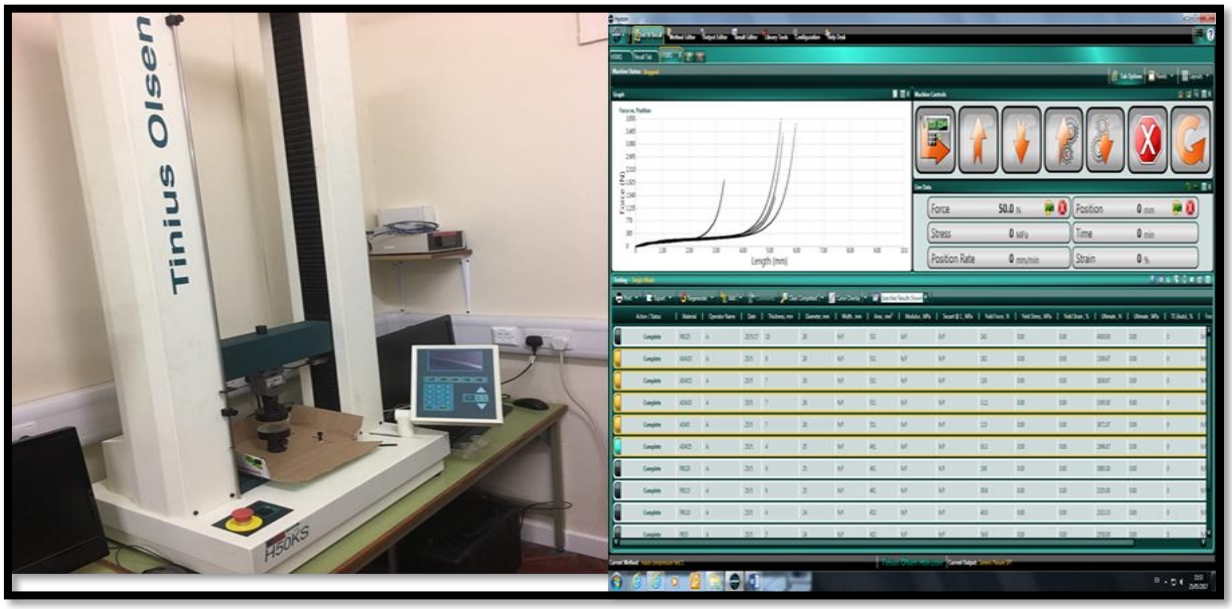

Figure 5.29 Mechanical test frame (L) manufactured by Tinius Olsen, dual column model HK-S. Screenshot of the testing software "Horizon" (R) used to set up test conditions.

This software program enables the plotting of force-extension diagrams from which stress-strain curves can be determined and the Young's Modulus for each sample extracted. The Young's modulus of the various PHPs series is calculated by using the stress vs. strain curves generated by the MCT equipment at room temperature. While the elastic modulus (Figure 5.30) represents the initial region of the curve where proportionality between stress and strain exists, the whole stress vs strain curves are shown for each sample to highlight the effects of increased

mixing time and the structural changes discussed earlier.The load-unload behavior at 1mm/minute loading speed was almost completely reversible show that viscoelastic effects were not significant in the basic PHP and this was expected to be reduced in the modified adsorbents. The polyHIPE is moulded in two different volume cylindrical tubes which were cut into two kinds of disks. The MCT were performed for each of these discs to identify the mechanical properties and determine any effects of sample size. (Greco, 2014)

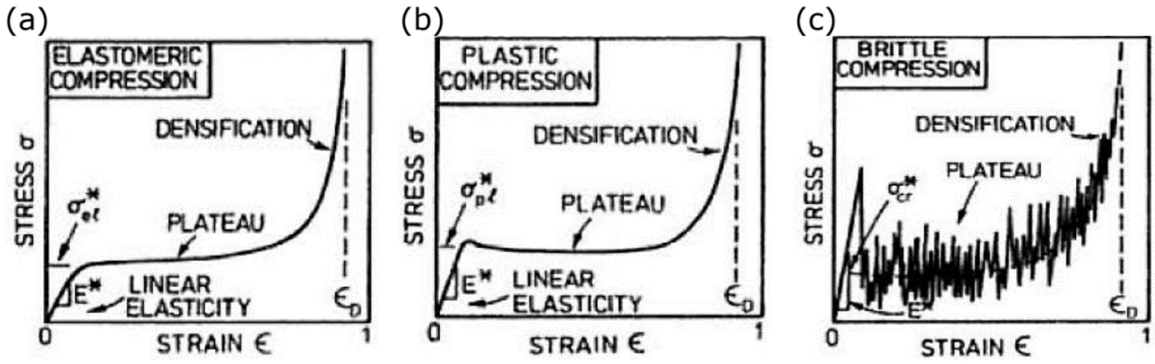

Figure 5.30 Schematic representation of stress-strain curve for a honeycomb loaded in in-plane compression (Greco, 2014).

5.9.5 Gas chromatography (GC)

The analysis of total sulphur content and sulphur group identification is an integral part of quality control in the petroleum, petrochemicals and power utilities industries. This is because inorganic or organic sulphur compounds are found in most crude oils and in light and heavy products in both upstream and downstream processing at a wide range of concentrations (Speight, 2014, Gary et al., 2007). Many different test methods can be used to determine sulphur content, including : atomic absorption; X-ray fluorescence; microcoulemetric analysis; UV fluorescence, and GC methods, each having benefits and difficulties depending concentrations used or the nature of feedstocks. The main methods used in Iraqi oil refineries are D 4294 (Standard Test Method for sulphur in Petroleum and Petroleum Products by Energy Dispersive X-ray Fluorescence Spectrometry) and D 5453 (Standard Test Method for Determination of Total Sulphur in Light Hydrocarbons, Spark Ignition Engine Fuel, Diesel Engine Fuel, and Engine Oil by Ultraviolet Fluorescence1) which are explained briefly in Appendix 5.

In previous research, gas chromatography has been used in studies of adsorption and model fuel oil creation. (Dantas et al., 2014, Xia et al., 2016, Khan et al., 2013, Baeza et al., 2012, Hua et al., 2003, Çalkan, 2007) so was adopted as the main analysis technique here. This has the

advantage that it can be used to study the adsorption behaviour of different sulphur compounds rather than just the effect on the total sulphur content.

In this study the GC analysis was conducted using a Varian Saturn 2200 GCMS as shown in Figure 5.31 provided with a Varian VF-5MS capillary column (30 M X 0.25 mm, 0.25 µm) (Parker, 2016). This instrument conditions used for analysis are a 1µm split injection; injector temperature 360 °C; split ratio 13; helium carrier gas flowrate 1mLmin^{-1}; initial oven temperature 60 °C. The machine offers single, dual or triple channel configuration flexibility and automation for maximum productivity. It has full digital pneumatic control of all pneumatic parameters and all inlets can be operated up to 150 psi/10 bar.

Figure 5.31 Gas Chromatography (Wu et al.) setup.

As shown in the block diagram illustrated in Figure 5.32, the carrier gas which was nitrogen passed through the system in a stationary phase which packed into a tubular column. The sample placed at the head of the column to be analysed by passing down the column due to the influence of the moving gas. The detector at the end of the column analysing the presence of the analyte as it elutes in the column. The signal from this detector is amplified and the resulting signal displayed and as a chromatogram (Çalkan, 2007). More detailed description of the method,

software and working principles reference are available in the Operation Manual of Varian Saturn 2200 GCMS in the website.

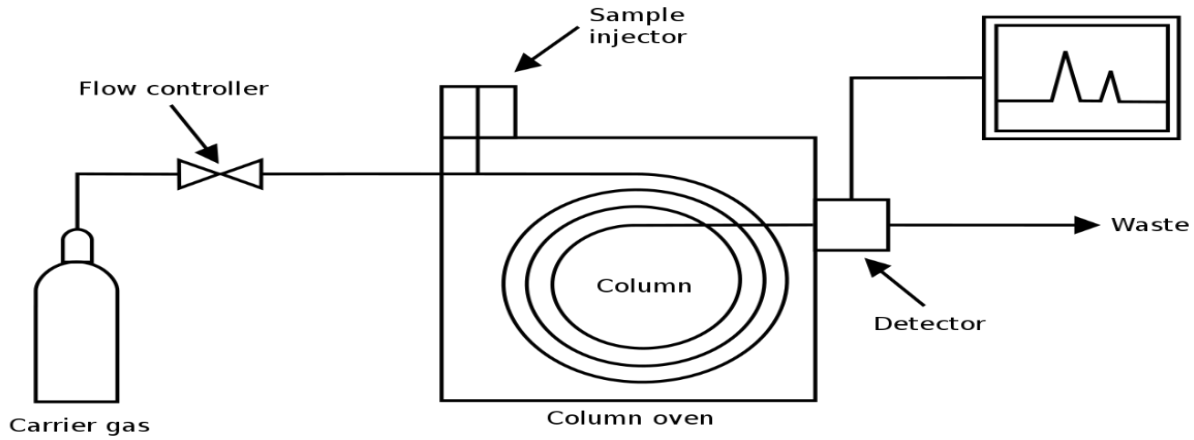

Figure 5.32 Schematic diagram of a gas chromatography (Çalkan, 2007).

The samples were filtered by syringe filter then transferred to special 1 mm vials and closed carefully by using manual seal vial Crimper Penicillin capper as shown in Figure 5.33.

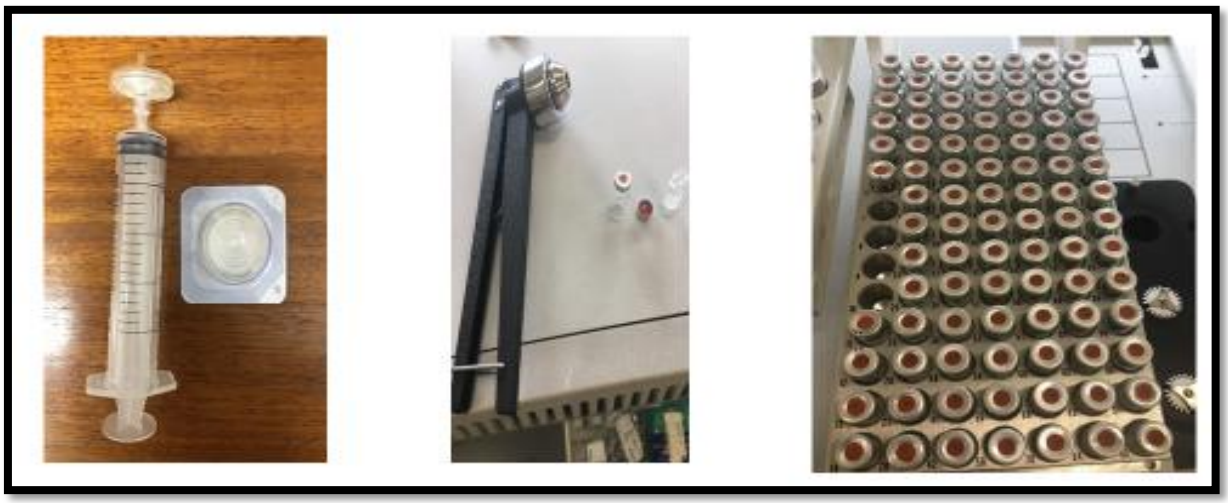

Figure 5.33 Collecting Sulphur samples for GC testing.

Details of the preparation of calibration samples and examples of calibration curves are provided in the fuel oil creation and mixing unit section.

Calibration Curves

A range of different concentrations for each sulphur compound was prepared to analyse the sulphur concentration according to Table 5.3. GC measurements were run on each composition and the area of the peak corresponding to the sulphur compound was used as a measure of concentration. Octane was added to all samples as an internal standard to correct for day to day variability. Figure 5.34 gives example calibration curves produced for the four representatives sulphur compounds.

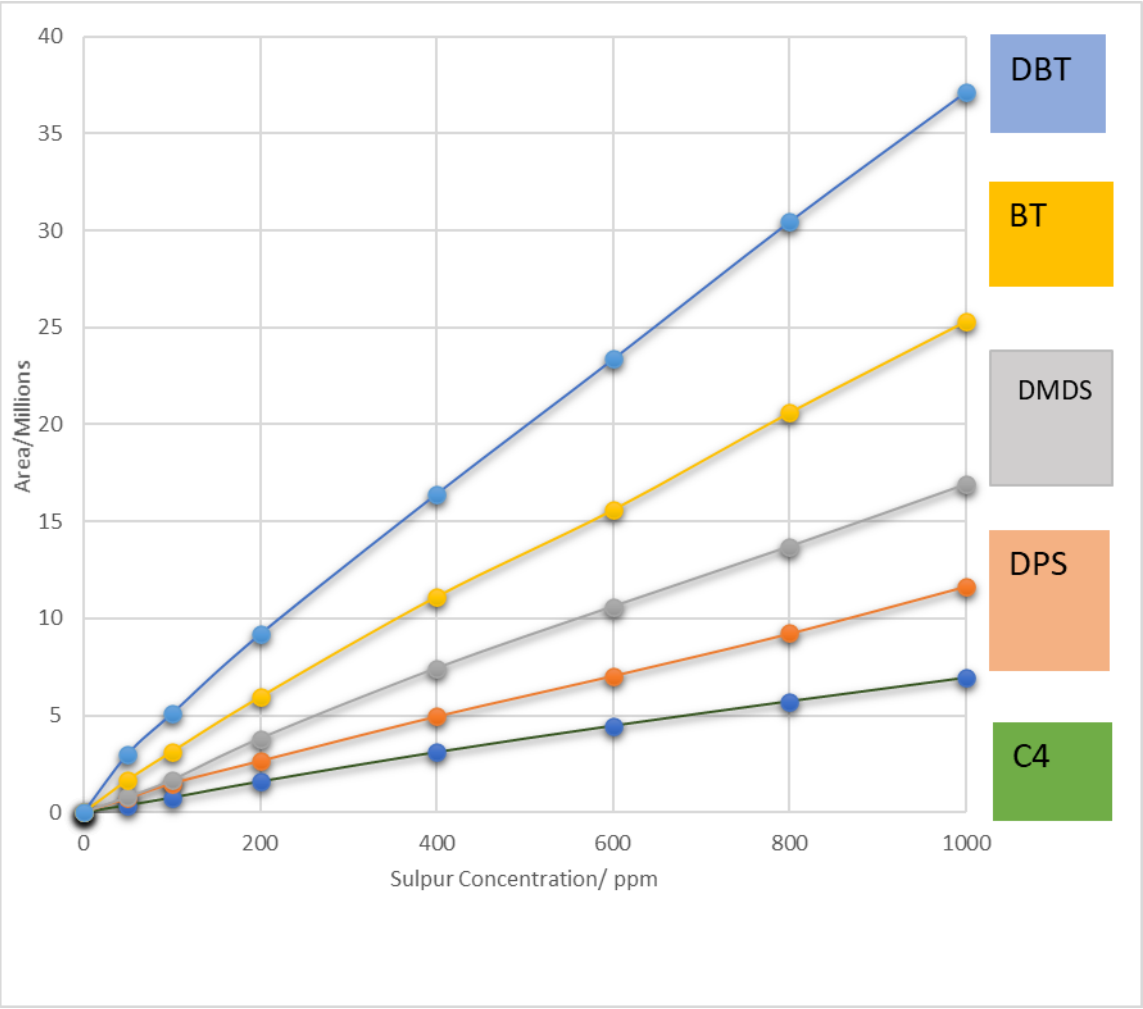

Figure 5.34 Linear calibration curves for model fuel oil .

6 Study Structure, Properties and Adsorptive Desulphurisation Capacity of the PolyHIPEs Produced at Different Mixing Time

6.1 Overview

This chapter discusses the interpretation of the results obtained from the experiments mentioned in the previous chapter. According to the methods described in the schemes of Figures 5.1 and 5.2. The layout of this chapter is presented in the following parts:

1) Section 6.2 covers the preparation and characterization of standard polyHIPEs prepared at different mixing times and a comparison study between them according to this. The morphology, pore size distribution, surface area as well as mechanical properties are obtained by using SEM, BET, FTIR and compression tests.
2) Section 6.3 covers the creation of a model fuel oil, based on the literature survey on crude oil, this model being the feedstock for the adsorption process in this chapter and the next.
3) Section 6.4 covers the adsorptive desulphurisation of the polyHIPEs produced in section 6.2 towards different sulphur groups by using the model created in Section 6.3 as a feedstock for this process. These results determine the adsorption capacity of polyHIPEs and suggest their application.
4) Finally, Section 6.5 summarizes the results of parts 1, 2, and 3 and introduces a comparison between the standard PHPs in term of their pore size distribution morphology, surface area and mechanical properties, and their adsorption capacity and rates.

These fundamental characteristics are essential if using polyHIPE as an adsorbent, as the large and connected porosity is responsible for mass transport. Also, adsorbents should usually possess a high surface area, in parallel, with a large number of active sites to ensure the adsorptive Desulphurisation is successful. At the same time, they should show a high level of chemical stability because of being subjected to different liquids and chemicals. Last but not least, mechanical properties are very important for the polyHIPEs in that for them to be industrially applicable as the adsorbent they should be robust enough to withstand manufacturing, installation and use. The study presented in this chapter is the baseline that will pave the way for subsequent studies in Chapters 7 and 8, and it will also open the way for future studies.

6.2 Analysis of Template PolyHIPEs in standard production at different mixing times

This section covers the characterization of standard polyHIPEs obtained and compares them according to mixing time to identify the optimum template polyHIPE that is most suitable for the adsorptive desulphurisation.

The preparation process is mentioned in Table 6.1 below, including materials, compositions and concentrations based on a study by (Burke et al., 2010). Coding is PHP-ST(X), where ST refers to standard and X to the mixing time/minute from 5-120 minutes.

Type of Polymer	10 % vol Oil phase	90 % Aqueous phase	Function	Target
Standard polyHIPE PHP-ST(X) Where ST refers to standard and X to the Mixing time	Styrene (ST) 78 wt % Divinylbenzene (DVB)8wt % (Span 80) 14 wt.%.	Distilled water 225 ml Potassium persulphate (KPS) 1 wt.%.	Emulsion prepared at different mixing time 5-120 min.	To prepare the best morphology.

Table 6.1 Compostion of oil and aqueous phase of standard PHPs.

6.2.1 Architecture of PolyHIPE Prepared

To investigate the PHP architectural structure SEM images were taken for each sample at different mixing times as shown in Figures 6.1 a-i for standard PHPs. SEM micrograph analysis using IMAGE J software was conducted (as discussed in Section 5.9.1) to determine the diameter of pores, D, minimum and maximum pore size, average interconnect pore size, d, pore wall thickness, Tw, and intersecting vertex thickness, Tv, as illustrated in Table 6-2 and shown in Figure 6.2 a,b. Analytical measurements were taken three times for each independent sample of the same experiment and at a suitable magnification to obtain at least 20 pores to provide better pore size distribution. However, the dimensions measured from the images were underestimates of the actual value as the pores are not generally seen at the equatorial plane (Menner et al., 2008). Besides this, since the fracturing technique was used for sample preparation this generally propagates through the weakest point of the pore and pore structure, which may not be the centre of the sphere, consequently, the results cannot be considered as an absolute reflection of the porosity (Byron, 2000). Nevertheless, this measurement provides an explanation of the phenomena that occur during mixing and the results can be cross-compared with each other as they will all suffer from similar issues, especially if they are compared with other tests such as surface area or mechanical properties or both.

a. PHP-ST5

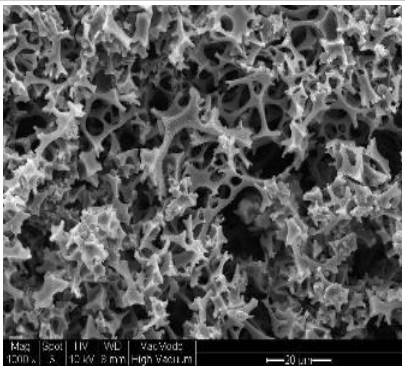

b. PHP-ST10

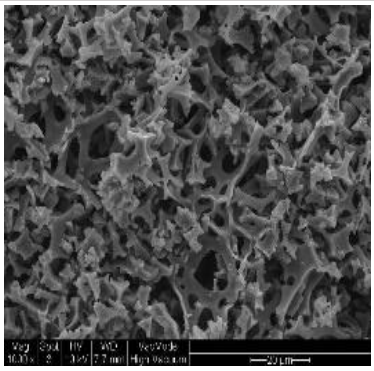

c. PHP-ST15

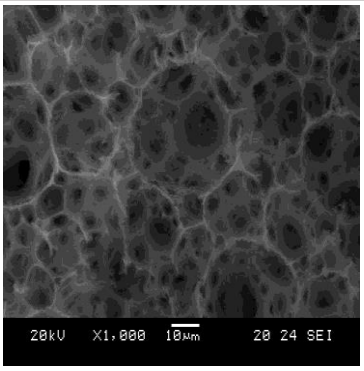

d. PHP-ST20

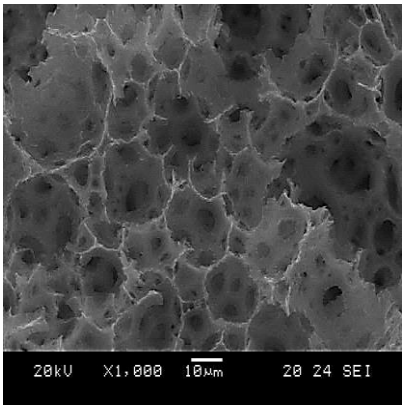

e. PHP-ST25

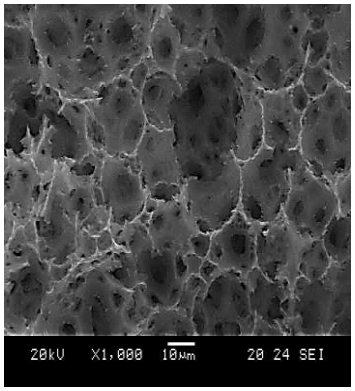

f. PHP-ST30

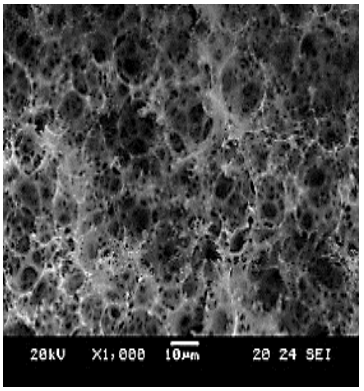

g. PHP-ST60

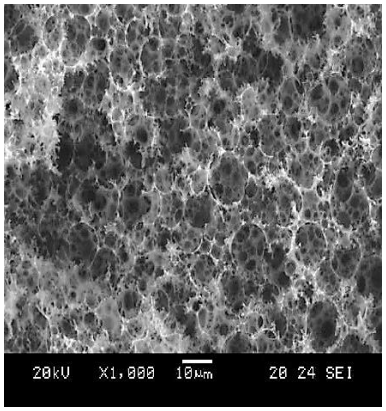

h.PHP-ST90

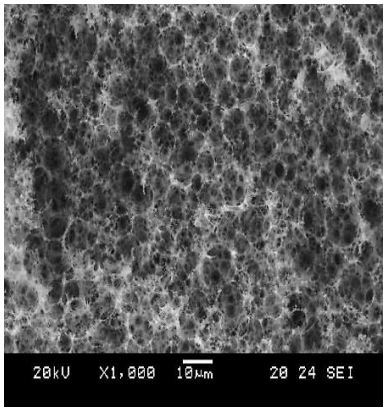

I. PHP-ST120

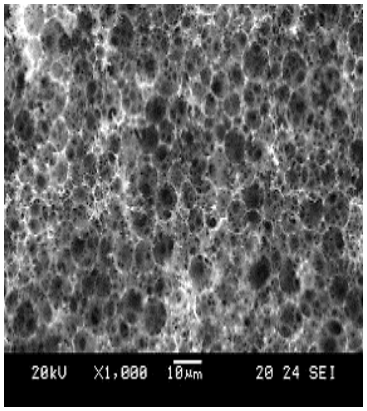

Figure 6.1 SEM images of standard polyHIPEs at different mixing times, x 1000 magnification a) 5 min, b) 10 min, c) 15 min, d) 20 min, e) 25 min, f) 30 min, g) 60 min, h) 90 min and I) 120 min.

The images in Figure 6.1 show that all polyHIPEs exhibited an open structure established after dosing and a short mixing time. The pores and interconnect architecture were well defined and clearly distributed for all nine types of PHPs. The resulting PHPs exhibited a hierarchical pore structure: primary pores that were created from the HIPE droplets and interconnect pores between each primary pore and its neighbors. These three features are important for the adsorption process. Also, the SEM images show the primary pores and network of smaller pores between the main pores and interconnect pore; these are nanopores within the polymer walls which are important for the capacity and selectivity of the adsorbent. Furthermore, it can be observed that pore wall thickness Tw, intersecting vertex thickness Tv and their ratio Tw/Tv, which affects the mechanical properties of the PolyHIPE, are changed by mixing as shown in Figure 6.3.

The pore size D and interconnected pore size d were measured using Image J software as mentioned before. The average size of each sample was determined based on the size results of about 20-50 primary and interconnected pore using the SEM micrographs according to the following equations (Sajad and Moghbeli, 2020)

$D = \sum iNiD/i\sum iNi$ ---------- *equation (6)*

$d = \sum iNidi/\sum iNi$ ---------- *equation (7)*

(a)

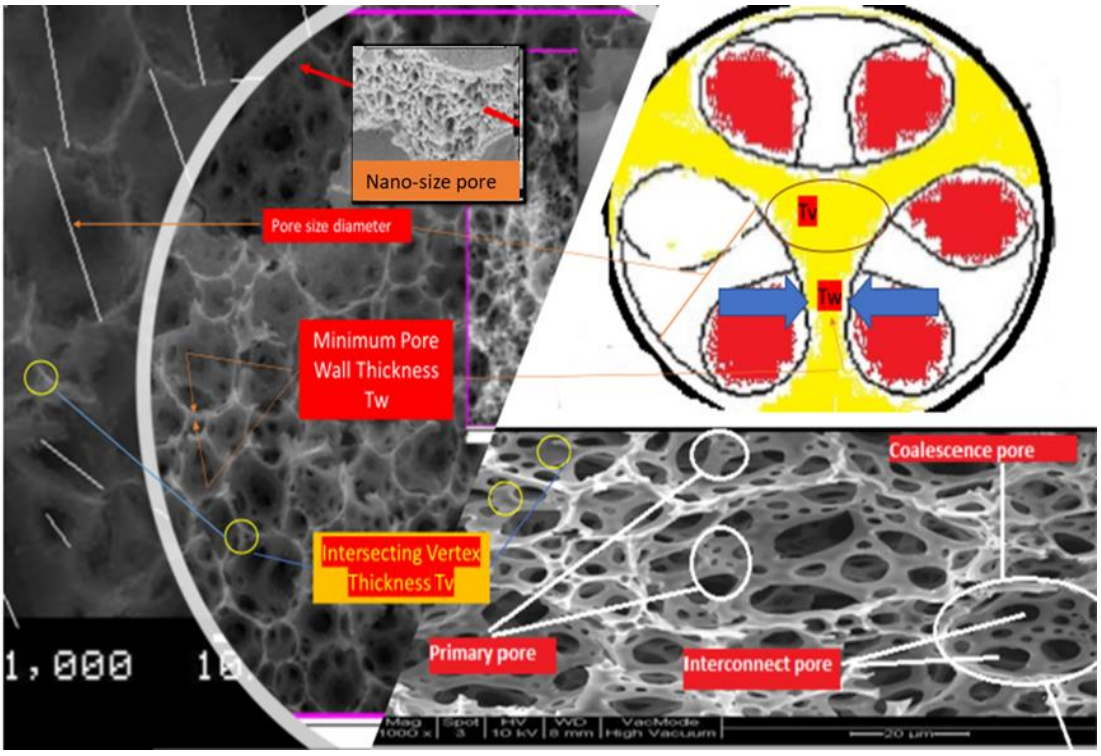

(b)

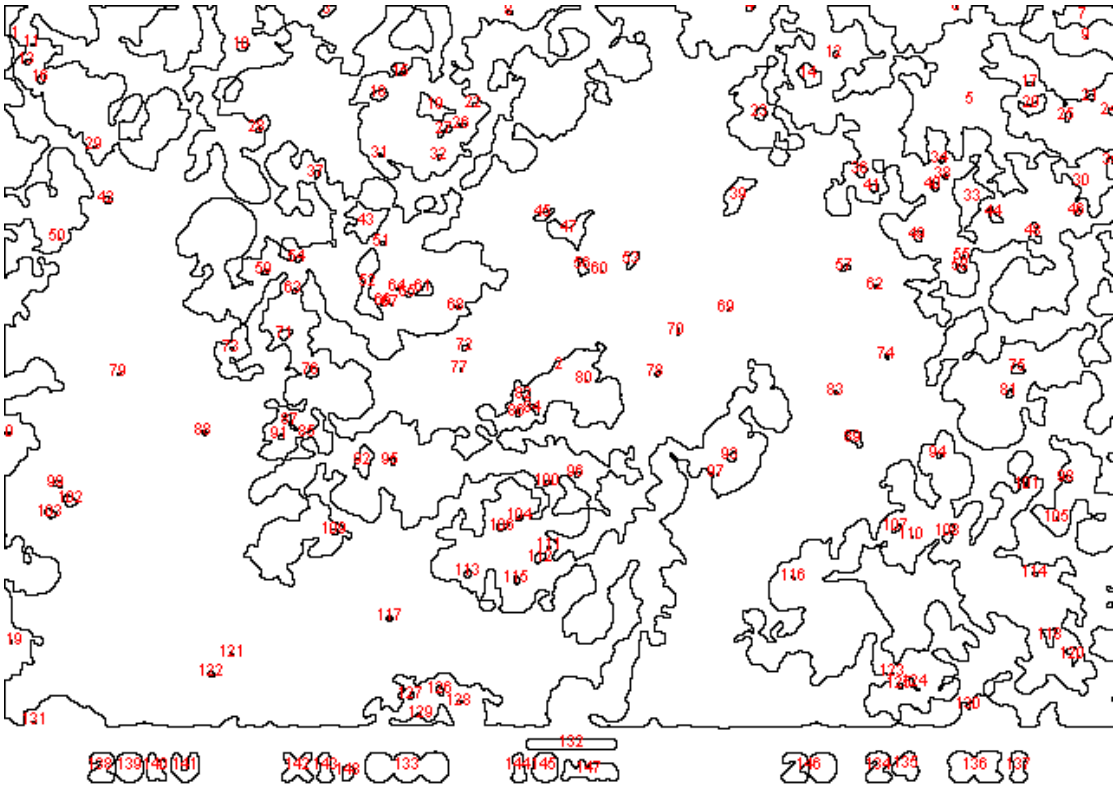

Figure 6.2 a,b Detailed view of primary, interconnecting, coalescence and nano pores also pore size (diameter D) ,intersecting vertex thicknesses Tv and minimum pore wall thickness Tw of standard polyHIPE prepared at mixing time of 30 minutes.

6.2.2 Effects of mixing time on PHP-STs porous structure

Overall results are shown in Table 6.2 with the effects of mixing time on average pore size and interconnect pores size shown in Figure 6.3. The most notable result in Figures 6.3 and Figure 6.4 is the fluctuations in the average size due to the mixing time. The first three times (5,10 and 15 min) were not included in the well-known study of the variation of average pore size (D) with total mixing time (Figure 3-7 Section 3.5.3) reported by Walsh et al. in 1996 (Walsh et al., 1996).

The pore sizes of each polyHIPE of 5, 10 and 15 min are 5.01, 3.85 and 5 µm respectively with random decrease and increase. These fluctuations can be explained as the emulsions at these times are not as stable as this is at the beginning of droplet coalescence resulting from an inhomogeneous structure. This can be seen first by the high range between the minimum and maximum pore size, for instance, PHP-ST5 was 1.8 to 27 µm, and secondly the high d/D

ratio, for instance, in PHP-ST15 at 0.97 while it should be (0 < d/D<0.5.) according to William et al. (1989).

PHP Code	D /µm	Min- Max D /µm	d /µm	Min-Max d /µm	d/D Ratio	Tw /µm	Tv /µm	Tw/Tv Ratio
PHP-ST5	5.01	1.8-27	1.5	1-3	0.3	0.74	1.43	0.5
PHP-ST10	3.85	1.2-7	1.56	1-3	0.4	0.66	1.27	0.5
PHP-ST15	5-16	1.8-40	4.85	1.8-5.6	0.97	0.53	1.05	0.5
PHP-ST20	18.16	7-63	4.76	1.8-5.2	0.3	0.66	1.34	0.5
PHP-ST25	15.30	7-30	3.6	1.6-6.13	0.2	1.6	2.6	0.6
PHP-ST30	12.01	6-17	4	1-7	0.3	1.7	2.8	0.6
PHP-ST60	10.81	6-14	3.6	1-4.5	0.3	0.8	1.7	0.5
PHP-ST90	5.58	4-11	1.9	1.2-2.4	0.3	0.75	1.5	0.5
PHP-ST120	5.29	2-10	2	0.7-3	0.4	0.56	1.3	0.4

Table 6.2 Average pore size D /µm , average interconnecting Size d /µm , d/D ratio, minimum pore wall thickness Tw /µm, intersecting vertex thickness Tv /µm and their ratio Tw/Tv as a function of total mixing time.

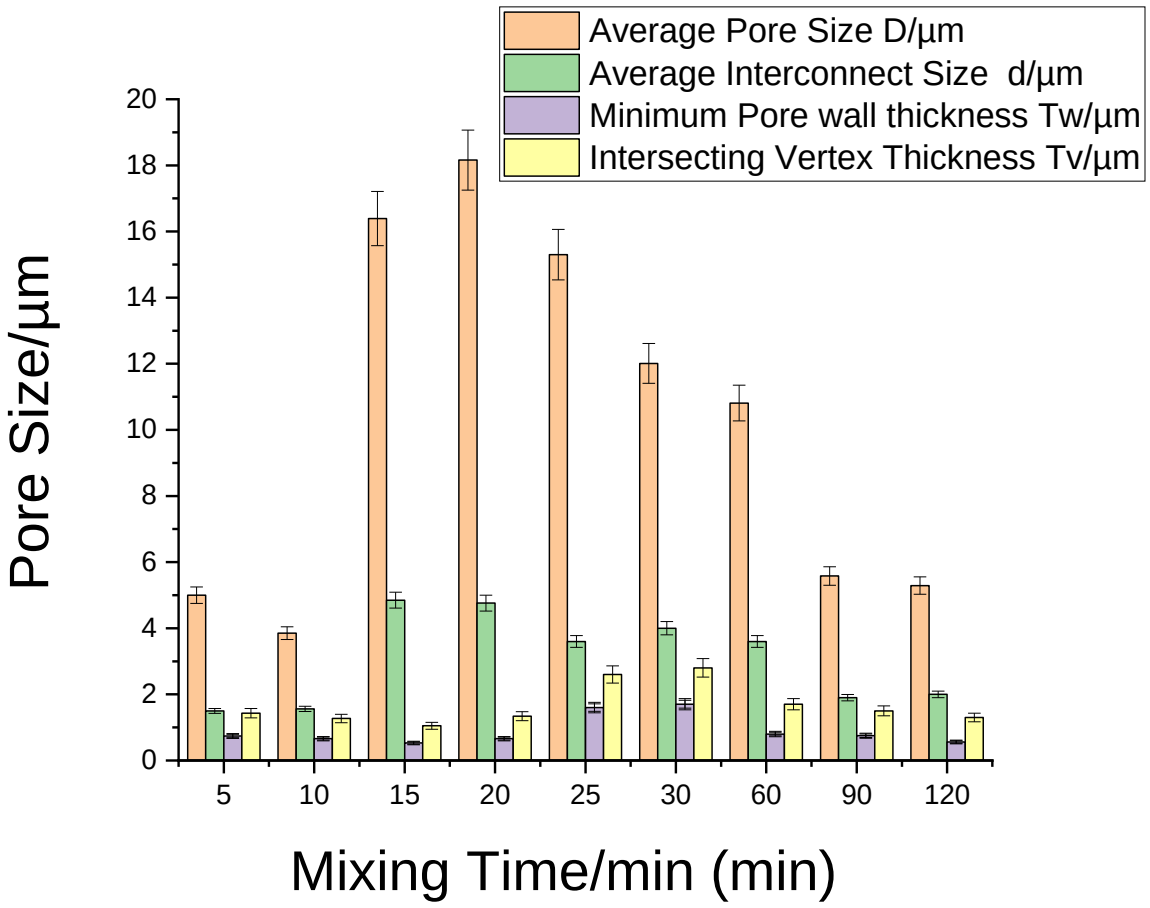

Figure 6.3 Variation of average pore size, D, Average interconnect size, d, minimum pore wall thickness, Tw, and intersecting vertex thickness, Tv, in µm with the total mixing time in minutes.

In these cases, the polyHIPE structures do not have easily definable cells so the expression "pore size" takes on new meaning, it is more like an irregular void or gas volume surrounded by solid mass. These polyHIPE structures result when water is distributed randomly and it is removed during polymerisation from the emulsion solutions without regular pore creation due to the low mixing time (Williams and Wrobleski, 1989, Mohamed, 2011); the microstructure of polyHIPE has a very non- uniform distribution of mass until it is homogeneous after reaching a specific time of about 20 min. (Walsh et al., 1996) .

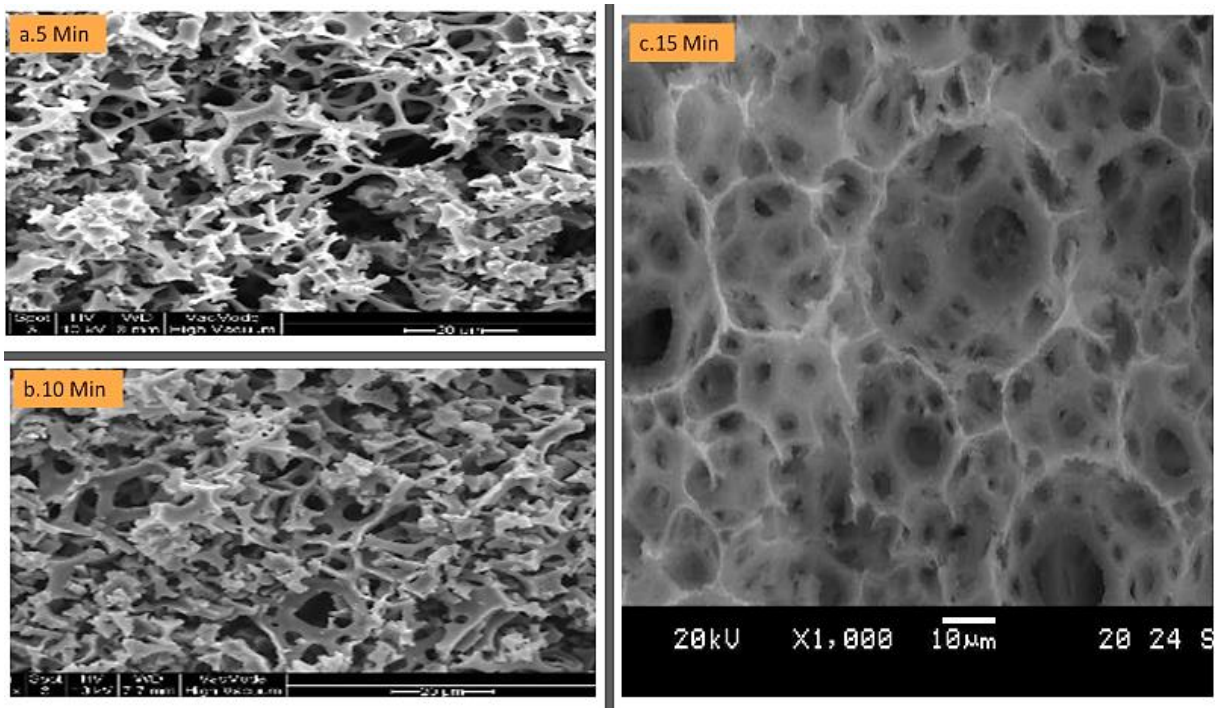

Figure 6.4 Standard polyHIPE prepared at mixing time of a)5, b) 10 and c) 15 minutes.

However, the polyHIPE-ST15 image (average pore size of 5 µm) started to reveal a more uniform structure. This indicates that in the initial phenomena of pore coalescence and homogenisation smaller pores collapse and form the larger pores occurring at the next higher mixing time (PHP-ST20 - average pore size of 18.16 µm) indicating a limit in the stability of the surfactant film that separates the water and oil droplets in the emulsion

Other notable results following an increase of mixing time on the PHP-ST20 to PHP-ST120 series reveal that the average pore size D of each sample decreased steadily as shown in Figure 6.1 d to i and Figure 6.3.

The largest D is that of PHP-ST20 (18.16 µm), followed by PHP-ST25 reducing until PHP-ST120, with 15.3 and 5.29 µm respectively. Their diameter distribution also follows the expected trend, where PHP-ST30 and PHP-ST60 share a very similar interval of (6-17 µm) and (6-14 µm) respectively. At higher mixing times the average pore size shifted towards a lower value and the longest mixed sample, PHP-ST120 is characterised by the smallest D, 5.29 µm. Furthermore, all their distributions are narrower and satisfactorily symmetrical. The uniform reduction in the average pore size results in an approximately constant d/D ratio from 0.3-0.4. Narrowing the overall pore size and increased symmetry also can be seen in an increasing number of windows and the formation of a more micro-size open structure polymer.

It is worth noting that distribution of pore size is more important for adsorption than obtaining specific pore size whether large or small. Consequently, the macro pores are needed for the

mass transfer inside the polymer with the meso –nano pores also being important for the selectivity and capacity of the adsorbent. This will govern the optimisation of the polyHIPE according to the pore size and control of the operating conditions of adsorbent synthesis. The target is to obtain a maximum similarity between the small and large pores. Mixing time as mentioned in Section 3.5.3 is one of the most important factors that could define the activity of the adsorbent. In conclusion, the samples prepared at the mixing time of 25, 30 and 60 minutes are most suitable for this study as they contain an acceptable average pore size and interconnect size. Better characterization can be used in choosing the exact time.

6.2.3 Pore wall thickness Tw and vertex Tv modification with the mixing time

There are other structural/geometrical parameters which could be affected by the mixing time. These effects can be expressed by terms of pore wall thickness Tw, intersecting vertex thickness Tv and their ratio Tw/Tv that occurred for each PHP-STs sample as shown in Table 6.2 and are all plotted for a more effective visual comparison in Figures 6.3 and 6.5.

The importance of these parameters is firstly that they indicate how the solid content is distributed in addition to the pore size and interconnect parameters (Greco, 2014) which further helps in understanding the structure of the adsorbent. Secondly, these parameters are manipulated to reach the highest elastic model, i.e. the highest Young's Moduli of polyHIPE as reported by (Williams and Wrobleski, 1989); at a given density thicker walls provide maximum mechanical properties.

The pore wall thickness can be measured in the centre point of each cells' strut, because the thickness is at its minimum, by SEM images (Mills, 2007). They can be observed at 20,000x magnification (scale bar 1μm) as shown in Figure 6.5.

(a) (b)

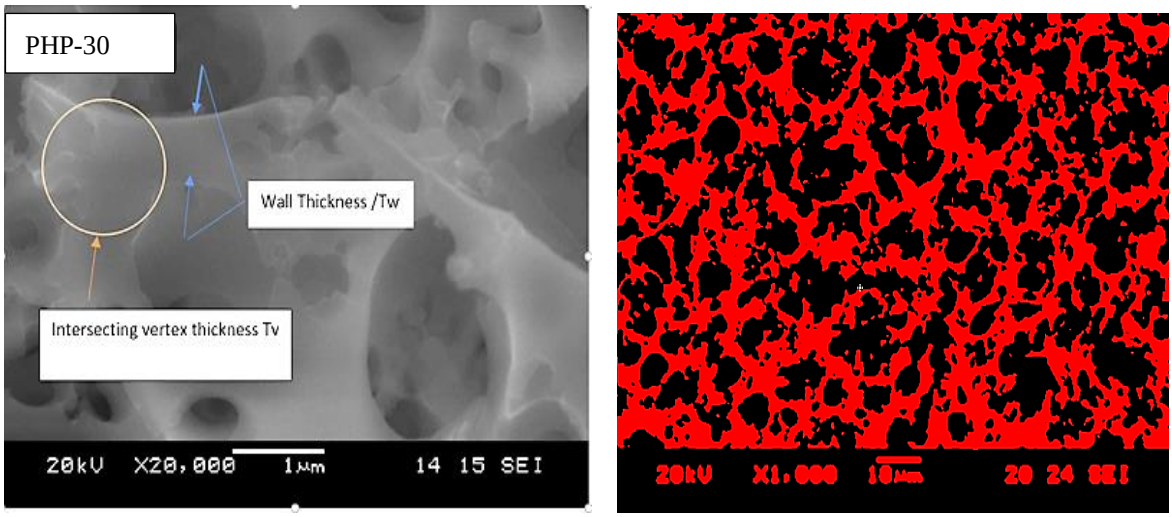

Figure 6.5 a) SEM image, 20,000x magnification, Scale bar 1µm used for the identification of minimum pore wall thickness Tw, intersecting vertex thickness Tv and t/T ratio b) SEM image threshold view revealed the homogeneity of PHP produced at 30 min mixing time.

It can be seen that the range of the minimum pore wall thickness, Tw, for all samples was 0.53 -1.7 µm while the range of intersecting vertex thicknesses Tv was 1.05-2.6 µm with a very similar ratio of 0.4-0.6. Also, any increase/decrease in one of wall parameter is accompanied by an increase/decrease to the other without a direct relationship to the change in other parameters, namely, pores diameter, D, and interconnect size, d.

It is observed that from the mixing times of 5 to 15 min, Tw and Tv are decreased with the increase in mixing time, a decrease in wall thickness is accompanied by a much more pronounced decrease in vertex thickness. This behaviour can be understood as increasing the mixing time leads to the formation of more droplets at a constant oil phase volume; the formation of new pores needing new walls with thinner films. In contrast, the wall and vertex thickness increases with the mixing times of 20, 25 and 30 min from 0.66/1.34 to 1.6/2.6 µm due to greater stability as the small pores tend to coalesce with the others forming larger pores with higher Tw and Tv as the majority of the oil phase tends to accumulate at the walls and vortex. This explanation corresponds to the accompanying noticed changes in pore size where it was observed that in PHP-ST20 for instance, the average pore size increased drastically to 18.16µm. Moreover, it can be noticed that the behaviour of polyHIPEs at mixing time 30 to 120 min show that longer mixing time leads to the production of a higher number of pores with thinner walls due to producing a more stable emulsion of more homogeneous pore size distribution.

The results reported in this section indicate the basic properties of the structure as a function of the effects of mixing time. These results will be used later in understanding the adsorption capacity and adsorbent properties and will pave the way for the manufacture of an effective adsorbent with the required structure and properties. Knowing that although the manipulation of the polyHIPEs morphology and structure have been investigated and discussed recently in many studies and certain interesting results have been achieved, the relationship between actual Process-Manufacturing-Structure and sulphur adsorption has not been investigated. This will be performed in this study.

It has been observed through assessment that the template PHP-STs structure can be modified, particularly, in pore distribution, average pore, and interconnect size in terms of producing smaller and narrower pores. Furthermore, another analysis of the changes that the mixing time produces on the pore wall and intersecting vertexes accords as at stable emulsion longer mixing produces smaller pores at the same time also producing thinner walls and smaller vertexes in the pore structure.

However, higher level details will be provided in the following sections especially concerning descriptions of mechanical properties, surface area, nano pores and pore volume closely related to this section as being based on the of polyHIPE structure. But before these sections, composition and stability of the polyHIPE will be described in term of FTIR results.

6.2.4 FTIR Analysis

It is very important to identify the composition and stability of the polyHIPE for the selection of a suitable polyHIPE that can be used for adsorption. A range of different PHPs according to mixing time have been studied to determine if any changes occur as shown in Figure 6.6. There was no significant difference in the peaks produced with an increase of mixing time. The major peaks are identified according to the numbers denoting each peak in Figure 6.6 which generates the first column in Table 6.3. The spectrum is dictated by the vibrations of the chemical bonds in the sample (Burrows et al., 2017, Stuart, 2000, Silverstein and Bassler, 1962, Fleming and Williams, 1966, Pretsch et al., 2000, Badertscher et al., 2009). For instance, it is observed that the bands at 650 to 759 cm^{-1} (1 and 2 in Figure 6.6) refer to aromatic bonding in styrene, vinyl and benzyl groups. The bands at 837-839 cm^{-1} (3 in Figure 6.6) occurred in only two samples at mixing times of 10 and 15 minutes and refer to C=C bonds in a phenyl ring, however, this bonding was present in all samples (peak number four) for bands at 903-906 cm^{-1}. In general, the details in Figure 6.6 and Table 6.3 show that although the intensity of the peaks may slightly vary among samples, there was no systematic variation in the changes observed and the same structure is always obtained.

This random variation in the readings gives an indication that there is no effect of changing the mixing time on the internal structure of the polymer beyond a small natural variability of the proportions of the resulting functional groups such as vinyl and benzyl groups. This is because of the differences in processing and drying where, for instance, the intensity of the peaks at 3380 cm^{-1} varies with mixing time due to water evapouration and OH bonds in the structure. The essential peak, available in all samples, is the high intensity peak due to C-H bending on the aromatic ring that is characteristic of the styrene monomer.

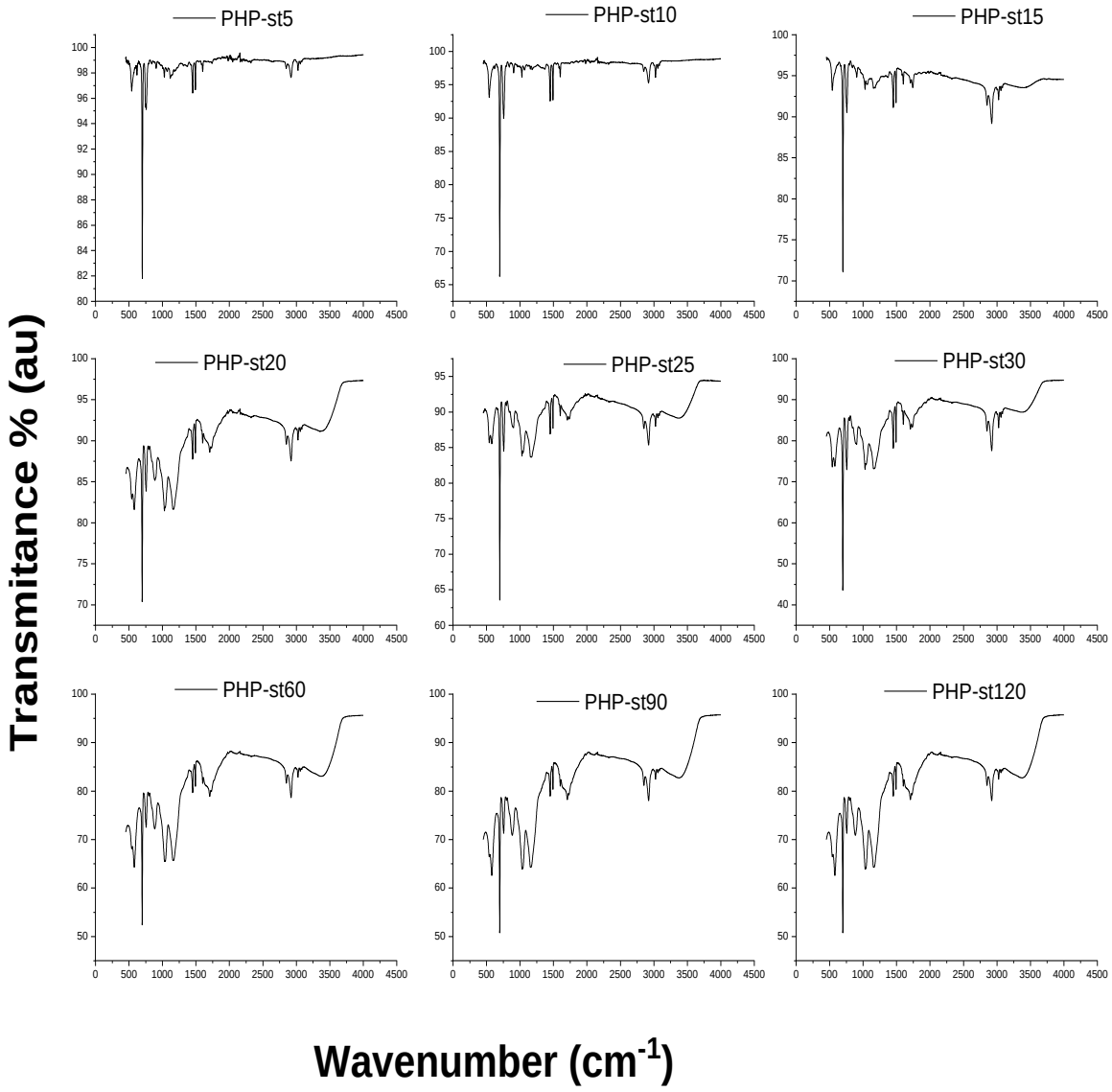

Figure 6.6 FTIR spectrum for different mixing time of standard PHPs, it shows same peaks At different intensities due to the mixing time.

6.2.5 BET Surface Area

Surface area and pore volume are the most important physical features of PHPs because of their importance in providing sufficient sites for adsorption and controlling the mass transfer through the adsorbent. Whereas the SEM can measure large pores and surface topography at the micrometre scale, gas adsorption techniques using the BET approach are needed for assessment at the nanometre scale. The properties of the pore wall surface have therefore been measured from adsorption/desorption isotherms using the BET method described in methodology chapter. The variations of surface area, pore volume, and pore size for the samples as a function of mixing time are shown in Figure 6-7 a, b, and c, respectively.

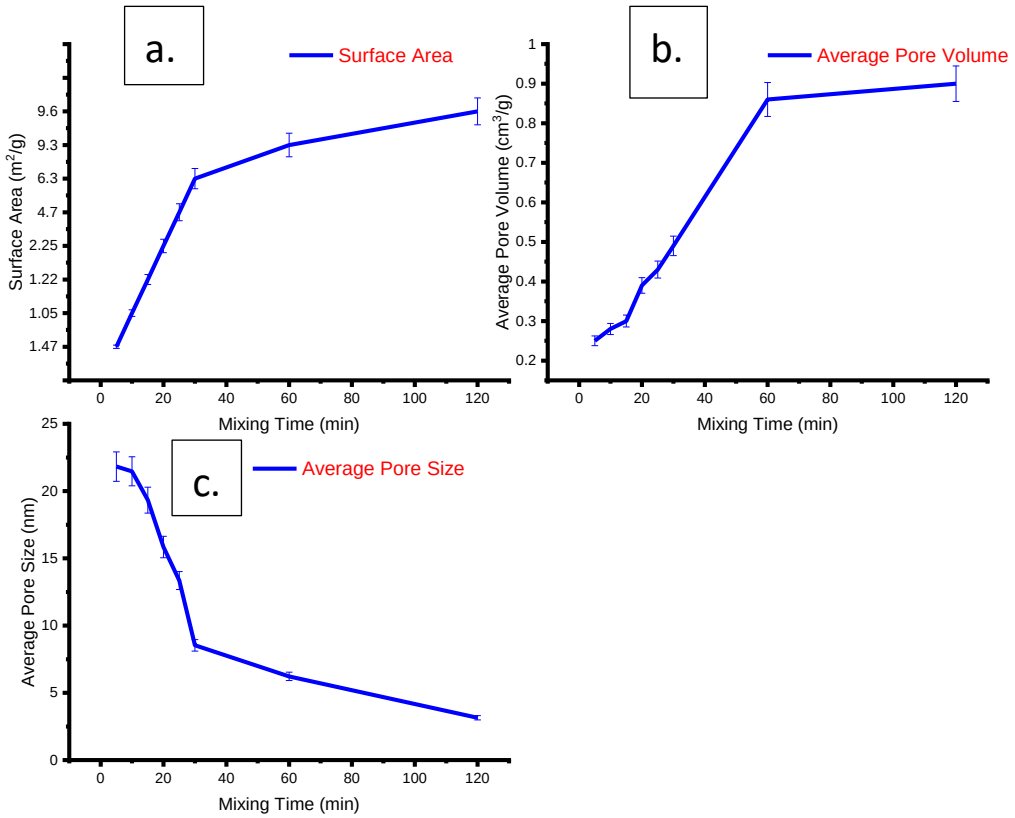

Figure 6.7 The effect of mixing time on a. surface area m2/g, b. average pore volume cm3/g and c. average pore size nm.

It has been observed that the surface area and pore volume are increased from 1.47-9.6 m^2/g and 0.25-0.9 cm^3/g respectively due to the increasing of the mixing time. This variation with mixing time was approximately monotonic except in the case of the sample PHP-ST90 for which the surface area was 4.9±0.31 m^2/g and pore volume 0.27 cm^3/g when stirred for 90 minutes so this finding was excluded. The average pore size which represents the nano pores

in the macro pore walls is decreased from 21.82 nm at 5 minutes mixing time to 3.15 nm at 120 min.

It has been found from the SEM image analysis in Section 6.2.2 that smaller macro-meso pores were produced in the structure with increasing mixing time; similarly, the number of the smaller pores in the nano size range on the walls between two cells, increases equivalently due to the increase of the mechanical energy as a function of input time to the system that leads to a decrease in the total average pore size at nano scale and therefore the surface area being higher.

These values are consistent with the previous studies of typical polyHIPEs as it was found that the modest surface area of standard polyHIPE is between 2-10 m^2/g (Krajnc et al., 2005, Burke et al., 2010, Noor, 2006). Nevertheless, in this study surface area of the adsorbent should be higher than these values, as reported in Section 2.11.3.5 where the higher sulphur adsorption capacity depends on a surface area higher than 300 m^2/g and, pore volume of 0.33-0.93 cm^3/g (Triantafyllidis and Deliyanni, 2014, Bandosz and Ren, 2017, Bandosz, 2006). However, Bandosz (2006) also found that the pore volume effects on adsorption were very small compared with pore size effects. Moreover, in the same section it is mentioned that effective adsorption capacity depends on the numbers of pores with widths of more than 1 nm which was significant towards sulphur compounds since they are similar in size to organosulphur molecules (Bandosz, 2006, Steijns and Mars, 1977). As a result, the PHP-ST produced at mixing time of 30, 60 and 120 min are the most suitable candidate for the sulphur adsorption due to their surface area and pore size results.

6.2.6 Mechanical Properties

In order to produce a commercially attractive adsorbent which could be used in industrial application, it is crucial to have superior strength towards external forces because the adsorbent particles will be exposed to a compression whether they are used in a packed bed column, plate column or molecular sieve in both adsorption and regeneration stages (Speight, 2014). Mechanical Compression Tests (MCT) were performed using the method described in Section 4.9.4 to assess the effects of the PHPs structural changes imparted due to the difference in mixing time. This test was run to obtain Young Modulus, E, the uniaxial elastic modulus, that measures the material stiffness. Together with fracture strength this identified if the material remains stable in service.

The Young's Modulus of the various PHPs sampled is extracted by plotting the stress versus strain curves obtained from the mechanical test machine and determines the tangent slope, represented in the initial region of the curve where proportionality between stress and strain exists. The whole stress versus strain curves are shown in Figure 6.8 for each PHP series to highlight the effects of the mixing time and offer further comparison of Young's Modulus of different PHPs to link the Young's modulus with the structural changes presented earlier.

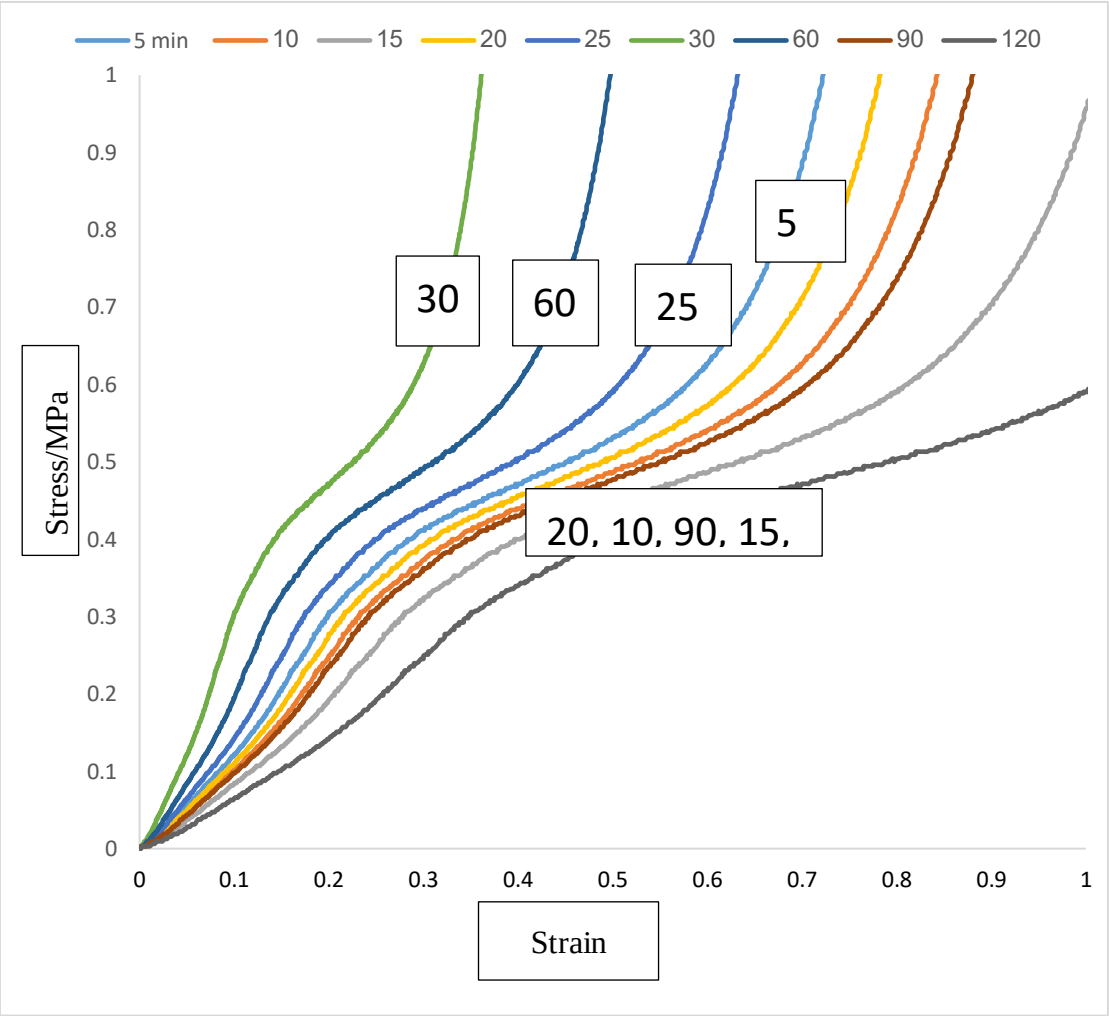

Figure 6.8 Stress vs strain curves at room temperature of different standard PHPs prepared at different mixing time.

The behaviour of all polyHIPEs under compression showed three common regions: elastic or linear stress–strain, a stress plateau, and densification. The elastic region is the most important for the polymers to extract Young's Modulus (Abbasian and Moghbeli, 2010). When the PolyHIPEs are compressed smoothly until the limit of the compression cell was reached no evidence is seen due to fracture in the compression test of cut disc samples. Any deformation produced by loading is completely recoverable within a second of complete unloading; the

sample show some viscoelasticity, but this is a minor effect. The increase of mixing time varies the Young's Modulus from 1.2 to 3 MPa. These low values are not unusual for polyHIPEs - as mentioned before similar Young's Moduli have been measured in other studies as well as other properties such as brittleness, and chalkiness which are some of the reasons that this material has not yet found industrial applications (Haibach et al., 2006). The stiffness is too low to be useful in a packed bed reactor due to excessive particle deformation so improve this property a different composition is probably required, the changing of system parameters by mixing time can be used to optimise a given material. Figure 6.9 shows the variation of Young's Modulus with mixing time. But these changes cannot be interpreted without reviewing the results in Table 6.2.

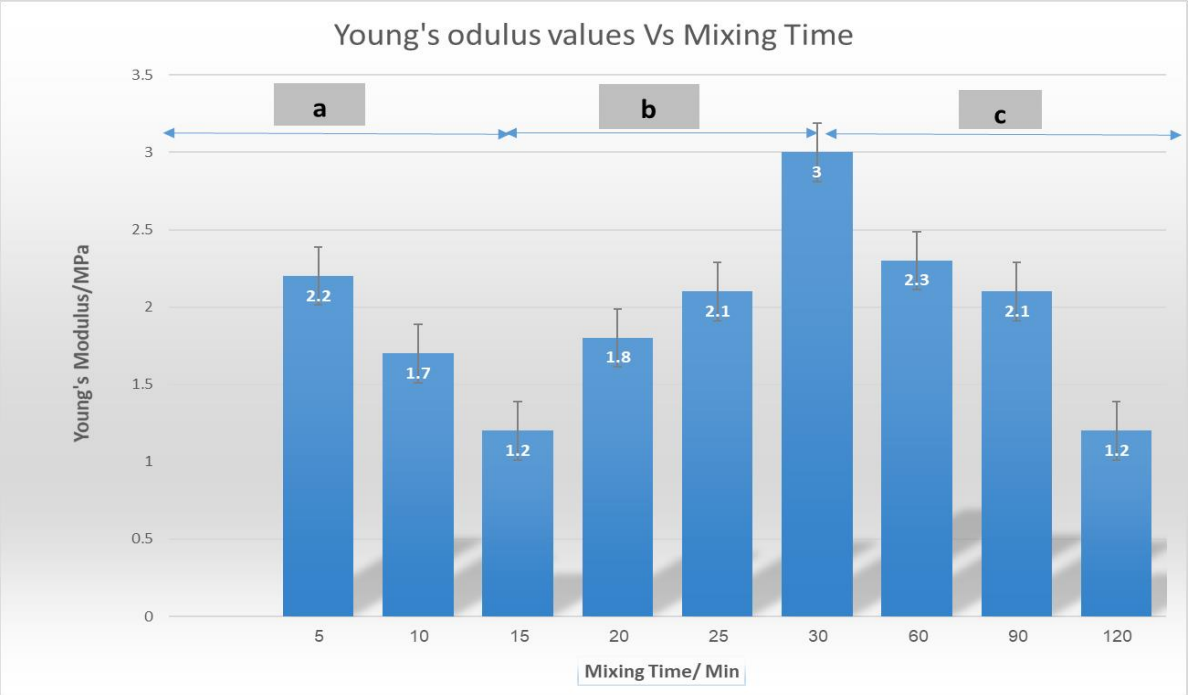

Figure 6.9 Young's Modulus as a function of mixing time, a) represents PHP-ST5, PHP-ST10 and PHP-ST15 series, b) represents PHP-ST15, PHP-ST20, PHP-ST25 and PHP-ST30, c) represents PHP-ST30, PHP-ST60, PHP-ST90 and PHP-ST120.

The three intervals represent different behaviour of the polyHIPEs series towards mixing time. The first mentioned as (a**)** represents PHP-ST5, PHP-ST10 and PHP-ST15, this interval showed a decrease in Young's Modulus from 2.2 -1.2 MPa during the mixing times of 5 to 15 min, respectively. In these time intervals the emulsions are still unstable as at less time, lower homogeneity and coalescence of small pore size into large pores according to the Ostwald Ripening mechanism is occurring, the surfactant and electrolyte (Menner et al., 2008) could not help at this lower time. This leads to formation of larger pores, weakens the structure and reduces the wall thickness and intersecting vertices; this hypothesis is supported by the results of the average, minimum and maximum pore size and the minimum pore wall thickness, and

intersecting vertex thickness illustrated in Table 6.2 and agrees with the study of(Haibach et al., 2006).

The second regime witnessed a different behavior from its predecessor, marked by a noticeable increase of Young's Modulus from 1.2 to 3 MPa during the mixing times of 15 to 30 min, respectively. Greater mixing leads to more homogeneity and more stability as the small pores tend to coalesce with the others forming larger pores with higher Tw and Tv as the majority of the oil phase tends to accumulate at the walls and vertex which is produced has higher elastic properties (Greco, 2014). The last regime, c, is the most important as the samples produced at these times were the most stable due to sufficient mixing time (from 30 to 120 min). However, this interval showed a decrease in Young's Modulus from 3 to 1.8 MPa. Results show that longer mixing time leads to higher number of pores with thinner walls being produced due to the production of more stable emulsions of more homogeneous pore size distribution as shown in Figure 6.4. The Young's modulus is strongly related to the pore size of samples (Table 6.2) but also to the wall thickness and structure. It is revealing that Young's modulus decreases with increasing the pore size (Alikhani and Moghbeli, 2014). It also decreases as the wall thickness is reduced. Another factor is the formation of a larger numbers of nano scale pores in the polyHIPE walls as shown from the BET results (Figure 6.8 c). As a result, the Young's modulus of the sample PHP-ST30 is the optimum result and it will be used as a template in the modification sections in the next chapter.

6.3 Model Fuel Oil Creation

A model fuel oil was created according to the previous specifications by adding different organic sulphur groups available in a typical Iraqi oil to a base fluid. The model oil was prepared by dissolving butanethiol, dipropylsulfide, dimethyl disulphide, benzothiophene and dibenzothiophene in n-octane Table 6.10. The selection of solvent , sulphur group representers and methods of testing and culculations were based on the wide research investigated in many studies illustrated in Table 3.2 about adsorbents, model fuel oils, test methods and adsorbates.

NO	S-group	S-compound	Code	Boiling Point BP / °C	Molecular weight g/mol	Structure Formula
1.	Thiols RSH	Butanethiol	C4	98	90	$C_4H_{10}S$ 
2.	Sulphides RSR	Di n-Propyl sulphide	DPS	142	118	$C_6H_{14}S$ 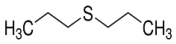
3.	Disulphides RSSR	Dimethyl disulphide	DMDS	109	94	$C_2H_6S_2$ 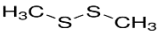
4.	Cyclic S group	Benzothiophene	BT	220	134	C_8H_6S 
5.	Cyclic S group	Dibenzothiophenee	DBT	332	184	$C_{12}H_8S$ 

Figure 6.10 Sulphur-containing compounds in octane to form model fuel oil.

It is worthy of mention that before choosing octane as a basic solvent, different solvents were considered and then changed to find the most suitable solvent. For instance, toluene has a bad effect on the adsorbents in that it changes their mechanical properties. Hexane cannot be used due to its low boiling point and its volatility. Finally, normal octane (boiling point 125°C and molecular weight 114 g/mol) was chosen and supported by the previous literature data. However, before creating the model fuel oil two preliminary tests were conducted in one experiment. Oil uptake tests have been performed to research the behavior of polyHIPE as an adsorbent towards oil by using two solvents separately. The polyHIPE samples were completely immersed in octane and hydraulic liquid for 24h - 48h. Results are shown in Figure 6.11.

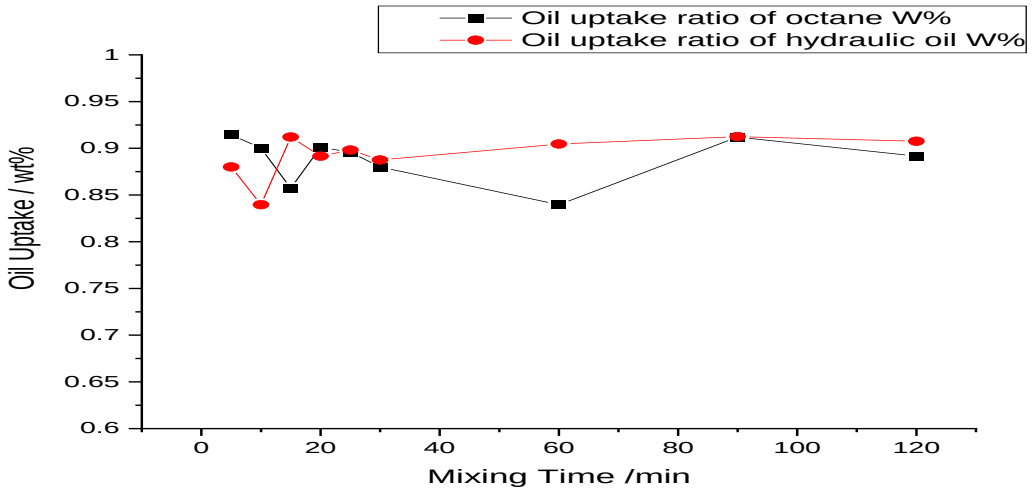

Figure 6.11 Oil uptake ratio of PHP-STs in different mixing time 5-to 120 mins.

Secondly, the research aims to check the composition of octane to determine whether it has been affected by polyHIPE. The results are shown in Figure 6.12 .The weights of the PHP samples before and after immersion were measured and the uptake ratio was extracted by calculating the difference between the initial and final weights divided by the final weight as in Equation 1. The results demonstrate some scatter but with a reasonable range (85%-91%) appropriate to the volume of aqueous phase, with no visible changes or physical, chemical, or mechanical effects on polyHIPEs discs.

The octane used was tested before and after the oil uptake test to look for changes in composition and structure by using FTIR and GC tests. The results showed a consistency between the before and after exposure results and both matched the standard FTIR. Also, it was supported by the GC readings presented below the FTIR spectrum in Figure 6.12.

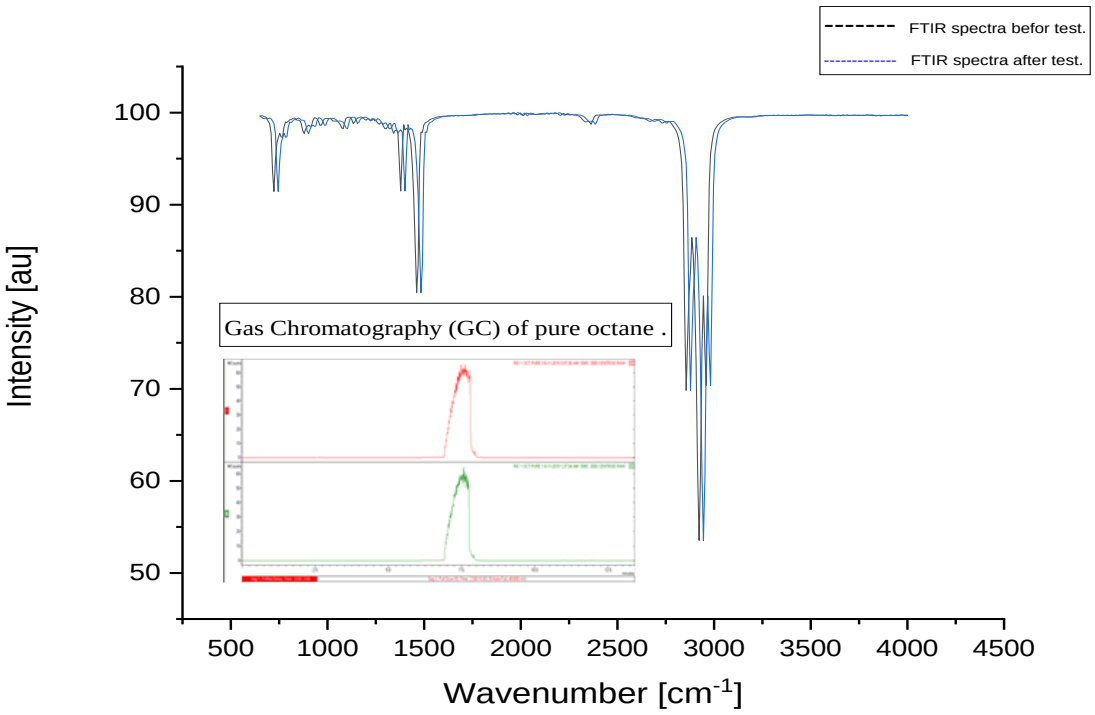

Figure 6.12 FTIR spectrum for pure octane before and after the oil uptake test supported by standard FTIR reading and GC test.

Furthermore, there is no chemical, physical or mechanical effect of octane on the polymer after aging. For instance, the SEM image of PHP-ST30 revealed the same structure and sizes of before and after the tests. The results of FTIR and MC tests are shown in Figure 6.13.

a. SEM Standard polyHIPE prepared at mixing time of 30 min.

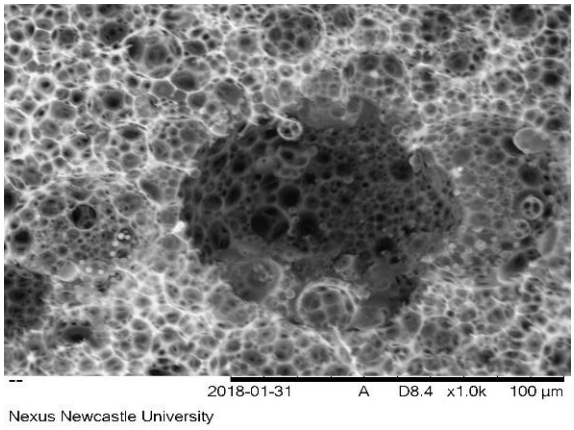

b. FTIR spectrum of PHP-ST30 at mixing time of 30 min.

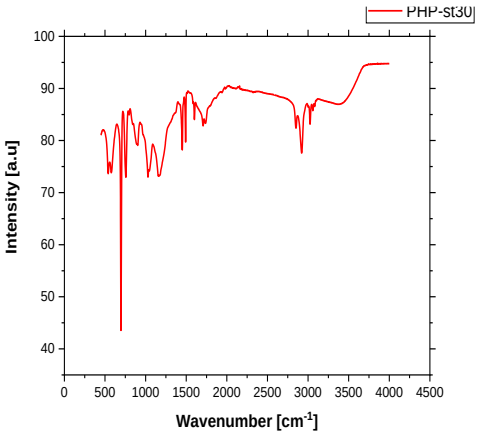

c. Stress vs strain curves of standard PHPs prepared at 30 min mixing time .

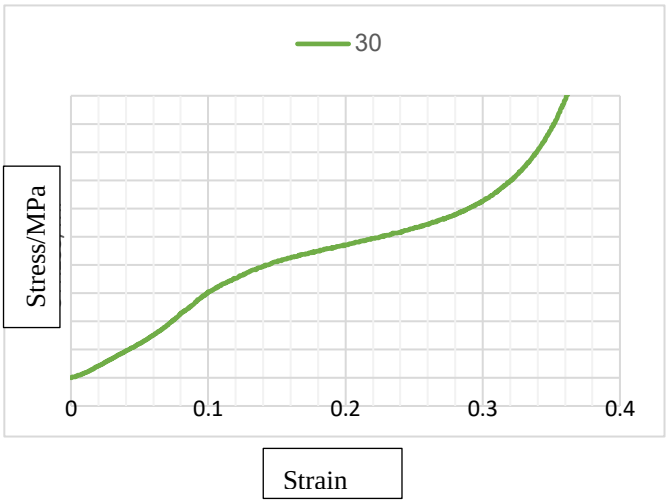

Figure 6.13 Sample of the structure-properties of PHP-ST30 by using a)SEM, B)FTIR, and MCT Prepared at 30 minutes.

Organic sulphur compounds were added to the solvent prepared with a total sulphur concentration ranging from 1000-4000 ppmw for each one by using the mixer described in 5.3.1. The model samples were tested after one hour of mixing and readings were taken each hour for 8 hours to evaluate the stability of its chemical composition using FTIR. The results showed identical peaks which confirmed the stability of the sample as shown in Figure 6.14. A final sample was taken the next day for comparison to recheck the stability of the mixture again using both FTIR and GC. The same results were obtained from the GC test as shown in the chromatogram plots in Figure 6.15.

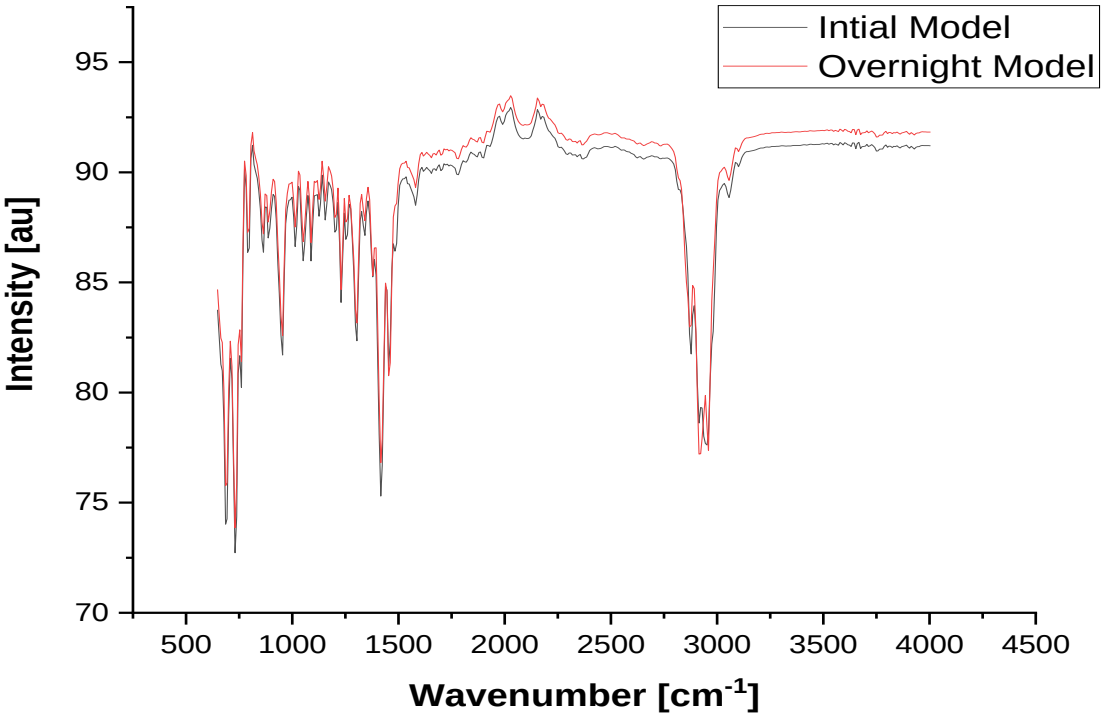

Figure 6.14 FTIR spectrum of the fuel oil (octan-sulphur) mixiture, intial and final readings

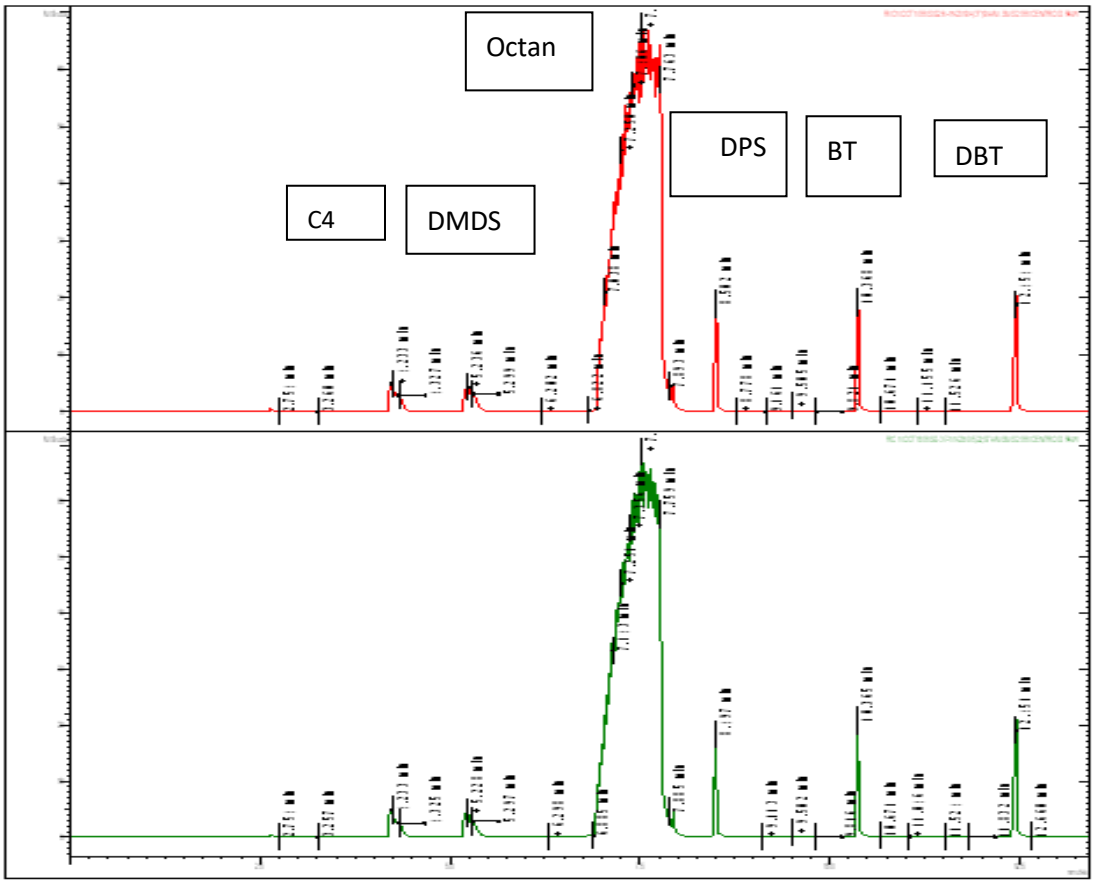

Figure 6.15 Overlaid chromatogram plots of dissolved C4, DMDS, DPS, BT, and DBT in octane forming fuel oil.

The next step was to determine the calibration curves for each sulphur species according to the method described in Section 5.3.2 by diluting the fuel model with octane and then carrying out the test for total sulphur content using GC mass chromatography for each individual sulphur compound. Every single compound had the same concentration range. This range of different concentrations for each sulphur compound was prepared according to Table 4.3. GC measurements were run on each composition and the area of the peak corresponding to the sulphur compound was used as a measure of concentration. Octane was added to all samples as an internal standard to correct for day-to-day variability. Figure 6.16 gives an example of calibration curves produced for all five representative sulphur compounds.

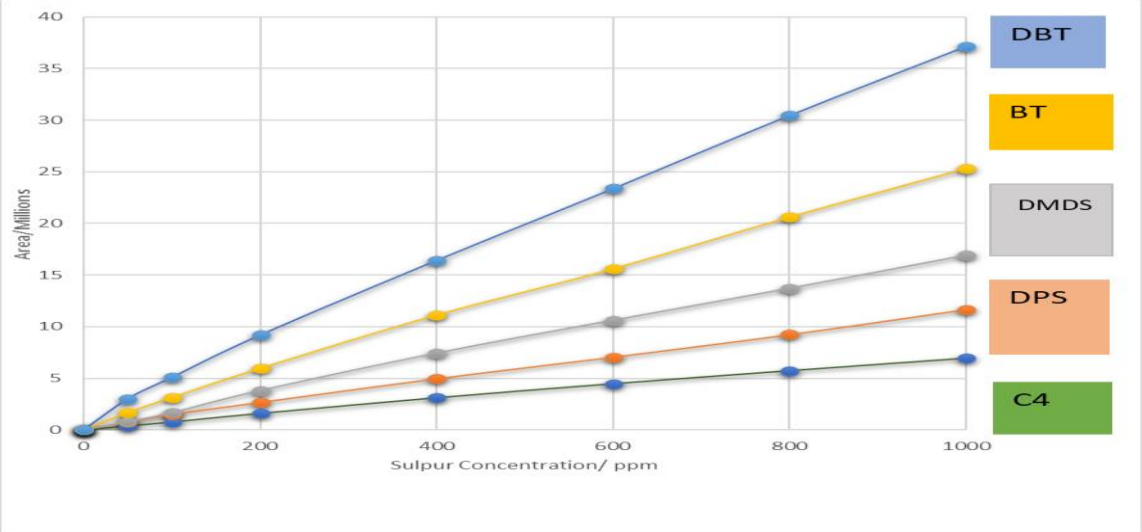

Figure 6.16 Linear calibration curves for five sulphur compounds (DBT, BT, DMDS, DPS, and C4 in the model fuel oil.

6.4 Adsorptive Desulphurisation

Adsorption experiments were performed in a closed, stirred, cylindrical tank 30 cm in height and 10 cm in diameter as shown in schematic in Figure 5.16. and in reality in Figure 5.17. The experiments were performed by adding 10% by weight of the adsorbent to the oil feed (1000 ml). Two kinds of feedstocks were with 1000 ppm and 4000 ppm sulphur similar to the real total sulphur ranges in the oil products (naphtha, kerosene, diesel, vacuum gasoil, and vacuum residue), a sulphur content between 0.02 to 2.9 wt% as illustrated in Table 2.3. The adsorption experiments were performed by adding 10% weight of the adsorbent to 1000 ml of the oil for 1-72 hrs in 12 hour intervals using a reactor flask described in Section 5.6 at a rate of 300 oscillations/min at room temperature. Taking results was actioned every 30 min until 12 hours had passed when the next result was taken after 72 hrs (overnights to ensure a steady state had been reached), each point was measured three times to ensure accuracy and reduce errors. At each point the solution was settled for 2 minutes then filtered using a BD Plastipak 20 ml syringe

filter connected with VWR sterile filter (0.2-µm) Figure 5.18. to separate the solid sediments of the adsorbent (polyHIPE particles) from the solution. The fuel oil was analysed using gas cromatography GC to identify the sulphur content at each point and the adsorption/desulphurisation capacity via equations mentioned in Chapter 5.

The sulphur compounds in the fuel oil expressed different adsorption rates towards the polyHIPE, for example PHP-30 was tested and shown to display different adsorption curves for each sulphur compound group. The initial sulphur content was 4000 ppm in all cases (Figure 6.17).

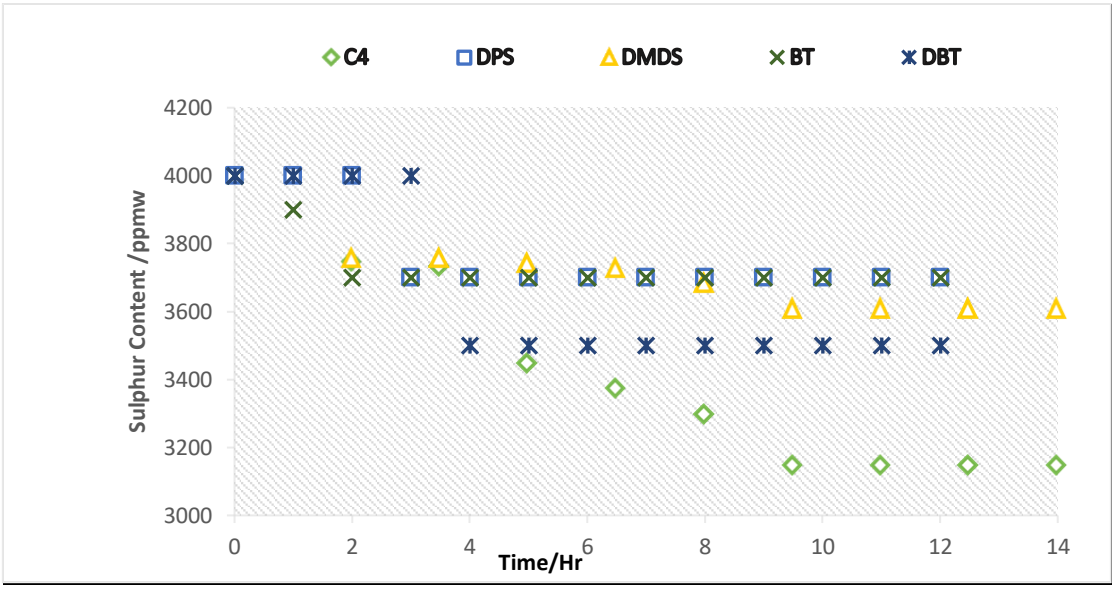

Figure 6.17 The variation of the sulphur content with different adsorption mixing time to evaluate the adsorption capacity of PHP-ST30 to the sulphur compounds C4, DPS, DMDS, BT, and DBT respectively.

It was found that adsorption in this sample varies with each kind of sulphur and started from the first hour for some of them. However, after five hours, sulphur content became constant for all sulphur groups and the average of the final sulphur content for all kinds was 3680 ppm ranging between the minimum value of 3500 ppm of DMDS to 3900 ppm of DBT. The polyHIPE (PHP-30) revealed adsorption affinity to all kinds of sulphur, however, it was a very low adsorption capacity as the rate was 8% with about up to 50% of the sample discs being destroyed and unable to be reused due to poor mechanical properties.

The same method and equation were used for the other PHP-ST to study the adsorption capacity of standard polyHIPEs prepared at different mixing times (Figure 6.18).

The adsorption capacity ranged from 6-10 % and in general it increased with the increasing mixing time due to the greater stability in structure and improving surface area properties.

However, there was a slight decreasing between PHP-90 to PHP-120 but both are higher than the samples prepared at the lowest mixing time. The model fuel oil was prepared with high sulphur content to simulate the products mentioned before and also to study how much sulphur can be reduced among rich solution with sulphur, but the adsorption rate was very low to the sulphur requiring a modification to the structure,

properties and surface chemistry of the standard polyHIPE. After exposure, the sulphur-containing polyHIPE was weighed and it was found that there was more than 50% of the initial weight of the sample lost due to its poor mechanical properties as shown in Figure 6.19.

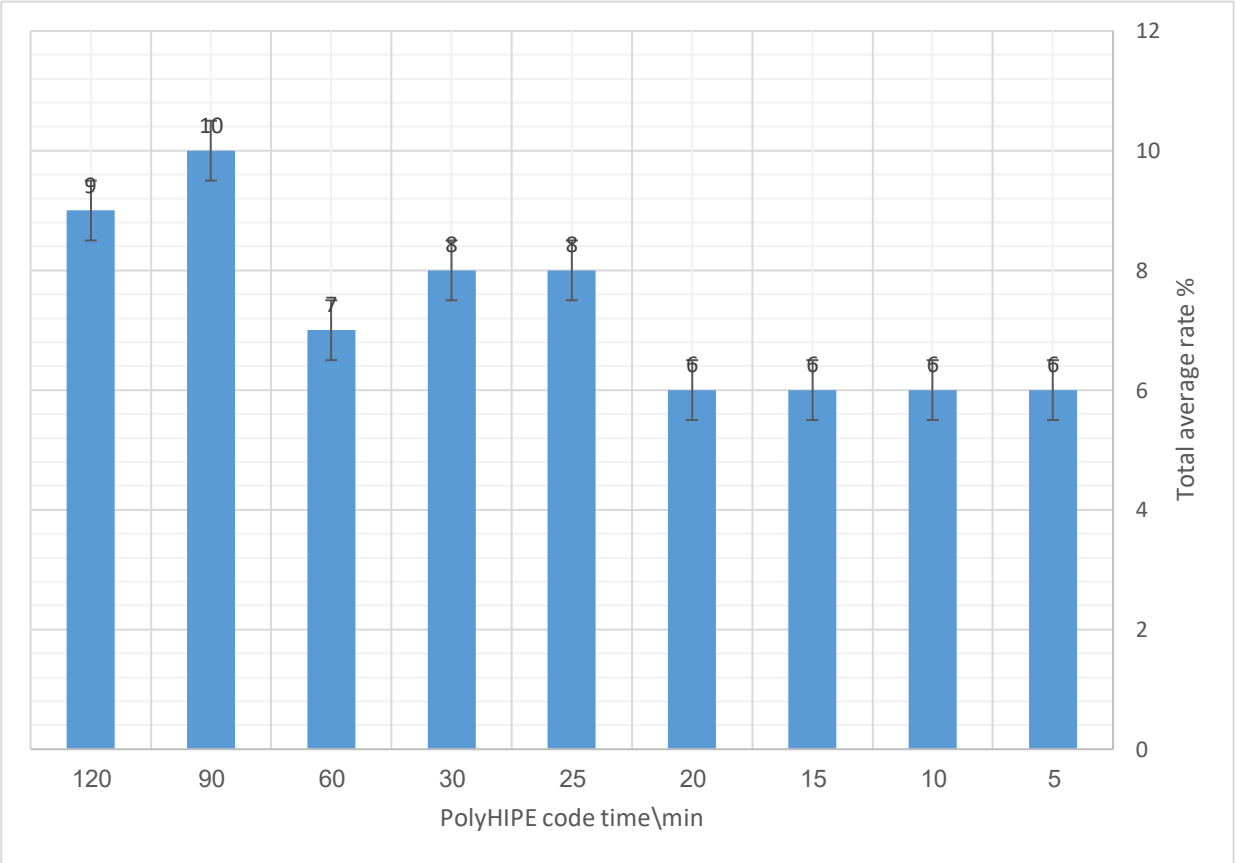

Figure 6.18 Total average adsorption capacity of PHP-ST prepared at different mixing time.

Figure 6.19 PHP-ST before adsorption and the waste PHP after adsorption.

Further Desulphurisation experiments were conducted to estimate the adsorption capacity of the standard polyHIPE to sulphur removal by using fuel oil of 1000 ppm for each sulphur compound with no evidence being found of removing sulphur. The sulphur content remained almost constant with negligible difference as shown in Figure 6.20.

6.5 Summary

This chapter has reported a study which investigated the process-structure-properties relationship of polymerised high internal phase emulsions (PolyHIPE PHP) in order to use it later in a sulphur adsorption process. Different mixing times (5-10-15-20-25-30-60-90 and 120 minutes) were used and samples characterised by using SEM, BET, FTIR, and a comparason test to provide a premilinary study about polyHIPE and create the reasonable media for adsorption. Also, a model fuel oil was created by adding the main organosulphur groups to paraffine solvent (octane); this was chemically stable having no side effects on the polyHIPEs before adsorption. The overall results are shown in the Table 6.3.

PHP Code	D /µm	d /µm	Tw /µm	Tv /µm	Surface Area/ m^2/g	Pore volume cm^3/g	Nanosize particles /nm	Young's Modulus Ma	Adsorption capasity %
PHP-ST5	5.01	1.5	0.74	1.43	1.47	0.25	21.82	2.2	6
PHP-ST10	3.85	1.56	0.66	1.27	1.05	0.28	21.47	1.7	6
PHP-ST15	5	4.85	0.53	1.05	1.22	0.30	19.33	1.2	6
PHP-ST20	18.16	4.76	0.66	1.34	2.25	0.39	15.84	1.8	6
PHP-ST25	15.30	3.6	1.6	2.6	4.7	0.43	13.35	2.1	8
PHP-ST30	12.01	4	1.7	2.8	6.3	0.49	8.53	3.0	8
PHP-ST60	10.81	3.6	0.8	1.7	9.3	0.86	6.22	2.3	7
PHP-ST90	5.58	1.9	0.75	1.5	4.9	0.27	7.79	2.1	10
PHP-ST120	5.29	2	0.56	1.3	9.6	0.90	3.15	1.8	9

Table 6.3 The overall results of average pore size, D (µm), average interconnecting Size, d (µm), minimum pore wall thickness, Tw (µm), intersecting vertex thickness, Tv (µm), BET surface area (m^2/g), pore volume (cm^3/g), Nano size particles (nm), Young's Modulus (MPa) as a function of mixing time and vs adsorption capacity (%).

It has been shown from SEM images that PHPs were successfully produced at different mixing times which exhibited an open structure with many nano and micropores. The pore and interconnect architecture was improved with increasing time and with more homogeneity for these PHPs. It can be observed that the PHPS SEM images revealed a hierarchical pore structure, large pores produced from the HIPE droplets having a size range 3.85-18.16 µm, an average interconnecting widow size of 1.5-4.85 µm, a minimum pore wall thickness Tw of 1.7-0.53 µm with intersecting vertex thickness Tv of 2.8-1.05 µm and nanopores exist within each pore wall with its neighbors ranging from 21.82 to 3.15 nm in diameter.

These ranges are reasonable for the adsorption process and since it improved in general with the time, the best results started after the time of 25-120 minutes. Since the BET surface area increases slightly with the mixing time from (1.05-9.6 m^2/g) due to the formation of more nanopores , the pore volume results show a small increase from 0.25-0.9 cm3/g. These two tests

(SEM and BET) have contributed to reducing the time for searching for the best mixing time to form the best structure-properties as the highest surface area obtained at three times; 30, 90 and 120 minutes. However, surface area should be higher than this value to be an effective adsorbent.

Another factor that is very important for the adsorbent conditions, is mechanical properties; Young's Modulus and fracture strength. The maximum Young's Modulus value was 3 MPa for the higher mixing time sample PHP-ST30. So this mixing time is the optimum which will be used as a template time for preparation and modification of the adsorbent. Specifically, this is when the FTIR results indicate that there was no significant difference in the peaks produced with an increase of mixing time and a stable structure is produced- longer mixing times give limited benefits at the expense of a greater cost of adsorbent manufacture.

The variation in the measured values of structure parameters gives an indication that changing the mixing time can be driven towards improving its properties. Figure 6.20a shows the structure-properties-process data comparison and with adding the adsorption capacity data it provides a full understanding of the adsorbent requirements of the polyHIPE. For instance, it can be seen that the mechanical properties results fluctuated with time, (decreasing-increasing-steady-decreasing) so they only could be improved in a limited period of increasing mixing time (30 and 60 minutes). This variation was explained in the previous sections as it was caused by the preparation factors and formation of thicker walls and vertexes or increases in nanopores. This is essential for producing a PHP for industrial applications.The results of SEM showed that at 30 minutes mixing time polyHIPE revealed the best morophology .

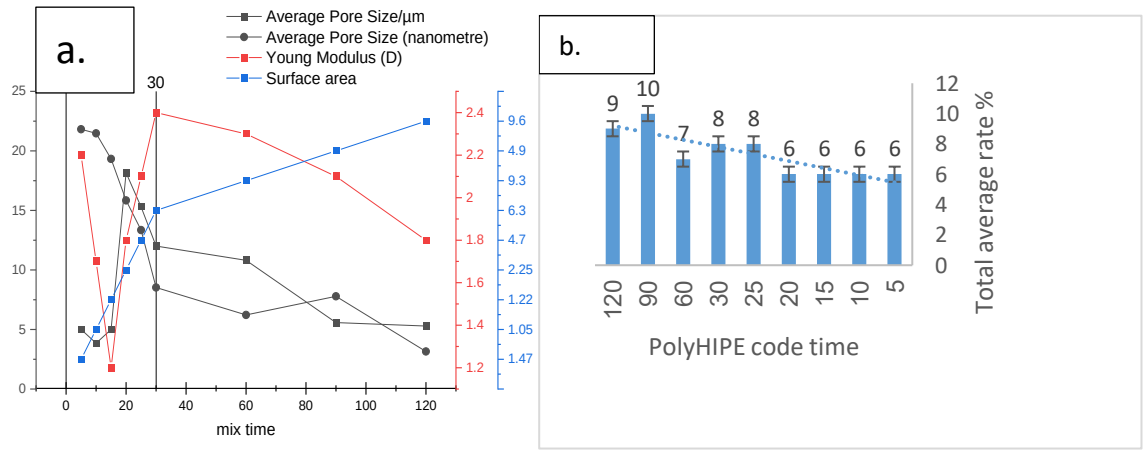

Figure 6.20 a) Structure-properties-process curves showing the relationship of these factors with each other, b) Adsorption capacity as a function of polyHIPE mixing time.

The model fuel oil was prepared with high and low sulphur concentrations (4000 and 1000 ppm of each organosulphur group) and was subjected to further tests to investigate its stability. The aim of the study is to create an adsorbent that handles the deep and ultra-deep Desulphurisation where capacity reaches >98%. The red circle in Figure 6.21 represents this area of work and is called the target adsorption zone. The low concentration sulphur model did not change during the adsorption process as shown in the blue circle which means this adsorbent is not suitable to use for low sulphur concentration feedstock adsorption. While the high concentrations capacity increased with increasing mixing time of polyHIPE preparation for all kinds of sulphur groups as shown in the coloured circle, at 6-10 %, is very low value and still far from the target zone especially when the adsorbent could not be reused due to its poor mechanical properties. Nevertheless, the results are promising since the polyHIPE shows an ability to adsorb the sulphur and a flexibility in modification to improve its structure -properties -processing. In other words, by improving the morphology, activating the surface chemistry-, increasing the surface area and enhancing the mechanical properties the adsorption capacity can be increased to reach the target of removing sulphur to the minimum quantities.

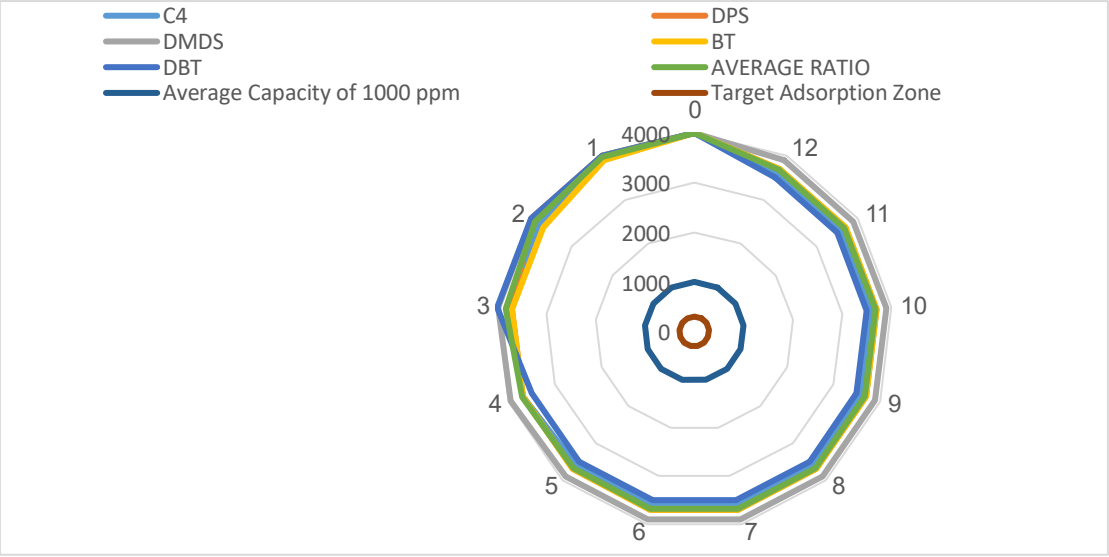

Figure 6.21 The average adsorption capacity of high and low sulphur concentration fuel oil, average ratio and target adsorption ratio

The next chapter reports on the development polyHIPEs surface-modified to produce more effective adsorbents. The sulphonation of surface then tethering of amines to the surface of the functionalised polyHIPE is one such system investigated.

7 Synthesis and characterization of functionalized polyHIPEs for the removal of sulphur compounds

7.1 Overview

This chapter discusses the adsorbent synthesis and the interpretation of the results obtained aaccording to the methods described previously in the schemes in Figures 5.1 and 5.2, the layout of this chapter is presented in the following parts:

1) Section 7.2 covers the first polyHIPE modification, producing functionalized polyHIPE by sulphonation, its characterization, and sulphur adsorption. It also shows the morphology, pore size distribution, surface area as well as mechanical properties estimates by using SEM, BET, FTIR and compression tests of two sulphonation methods, finally connecting the effect of the results on the adsorption capacities.

2) Section 7.3 covers firstly, the characterization and sulphur adsorption of functionalized polyHIPE by amination and, secondly sulphur adsorption of the aminated polyHIPE. These results and discussion are used to estimate the adsorption capacity of each sample and create a novel modification and application for the polyHIPE.

3) As the results of Section 7.2 showed that the mechanical and structural properties of the aminated polyHIPE need to be improved, Section 7.4 demonstrates the preparation, characterization, and adsorption studies of a reinforced polyHIPE using activated carbon. The results cover the activated carbon properties and addition to the polyHIPE to produce 1) reinforced polyHIPE PHP-PAC and 2) reinforced-aminated polyHIPE PHP/MEA/PAC which was finally produced using a combination of the PHP-MEA and PHP-PAC methods. It is an integrated method adding both mono ethanolamine MEA and activated carbon PAC to the optimized PolyHIPE to manufacture the adsorbent PHP-MEA-PAC that has the best structural and mechanical properties and at the same time the best sulphur adsorption capacity.

4) Finally, 7.5 regeneration studies have been conducted including a new molding approach for the adsorbent to enhance the capability of reusing the adsorbent and its regeneration - adsorption cycles, finally studying the regeneration solvent recovery so it can be reused.

Knowing these fundamental characteristics is essential for the use of polyHIPE as an adsorbent, as the large and connected porosity responsible for mass transport must be maintained. Also, adsorbents usually possess a high surface area in parallel with a large number of active sites to ensure the adsorptive Desulphurisation. At the same time, they should extend a high level of chemical stability because of being subjected to different liquids and chemicals. Last but not least, mechanical properties are very important for the polyHIPEs to be industrially

applicable as adsorbents should be robust enough to withstand manufacturing, installing and use. The study presented in this chapter is the cornerstone that will pave the way for subsequent studies in Chapter 8. Photograph showing various states of produced polyHIPEs including in Figure 7.1.

Figure 7.1 Photograph showing various states of polyHIPEs including standard polyHIPE PHP-ST30, thermal sulphonated polyHIPE ATS, microwave sulphonated polyHIPE AMS, Aminated polyHIPE and carbonised polyHIPE PHP-MEA.

7.2 Characterization and sulphur adsorption of polyHIPE functionalized by sulphonation

The first modification in this chapter was conducted via sulphonation methods to improve the structure-properties-processing of the polyHIPE for adsorption efficiency by variation in internal and surface properties of the polyHIPEs such as porosity, surface area, chemical composition, and physical structure. For instance, by increasing the surface area, the contact with the fluid will increase and thus improve the ability of adsorption.

Studying polyHIPE functionalization could not be comprehensive without discussing the starting structure because it is relevant to surface morphology, preparation, electrolyte factors, and structural properties of polyHIPEs such as surface area, mechanical properties, and porosity. Sulphonation is a substitution of sulphur between two media (Barlik and Keskinler, 2014)

similar to adsorptive Desulphurisation which is the removal of sulphur from the adsorbate into the adsorbent (Danmaliki et al., 2017). The highest degree of sulphonation was reached at 60% in the previous studies as mentioned before (Çalkan, 2007, Thumbarathy, 2018, Hasan, 2013). Two sulphonation approaches have been explained in Sections 4.7.1 and 5.4.2. These are thermal sulphonation (Haq, 1985) and microwave sulphonation (Akay et al., 2005). In addition, it was mentioned that the existence of the sulphur in the HIPE emulsion will attract more sulphur molecules to adhere to the polyHIPE. This section discusses the results of these two methods and compares them in two parts: firstly, the characterization of sulphonated polyHIPE including SEM, FTIR, BET and mechanical compression results and secondly the adsorption capacity and sulphur selectivity. In both parts of this section the thermal sulphonation is compared with the microwave sulphonation and both methods were compared to the standard polyHIPE in terms of characterization and adsorption. The preparation mentioned in the third and fourth rows in Table 7.1 in terms of materials, compositions and concentrations, was based on the study reported by Burke et al. in 2010. The coding used for these samples is AMS for those after microwave sulphonation and ATS after thermal sulphonation, knowing that the mixing time selected was 30 minutes as concluded from the previous chapter.

Type of Polymer	10 % vol Oil phase	90 % Aqueous phase	Function	Target
Microwave sulphonated polyHIPE AMS	Styrene (ST) 78 wt % Divinylbenzene (DVB)8wt % (Span 80) 14 wt.%	Distilled water 225 ml Potassium persulphate (KPS) 1 wt.% +5% wt H_2SO_4	Microwave sulphonation 230 v -50 Hz -1305 W	To: Increase the surface activity.
Thermal sulphonated polyHIPE	Styrene (ST) 78 wt % Divinylbenzene (DVB)8wt % (Span 80)14 wt.%	Distilled water 225 ml Potassium persulphate (KPS) 1 wt.%	Traditional thermal sulphonation Set temp. 80 ^{o}C,5 ^{o}C/hr to 100 oC	To: Increase the surface activity

Table 7.1 Composition of oil and aqueous phase of microwave sulphonated polyHIPE AMS, and thermal sulphonated polyHIPE ATS.

7.2.1 Characterization of PolyHIPE prepared by two sulphonation methods

In order to investigate the PHP architecture, SEM images were taken for each sample both before and after sulphonation using the two methods**.** The standard polyHIPE produced with mixing time of 30 minutes PHP-ST30 is shown in Figure 7.2a along with those PHPs produced after thermal and microwave sulphonation 7.2b, c, respectively. In general, it can be observed

all samples exhibited an open structure with a pore and interconnect architecture similar for those of the standard produced as described in the previous chapter and shown in Figure 7.2.

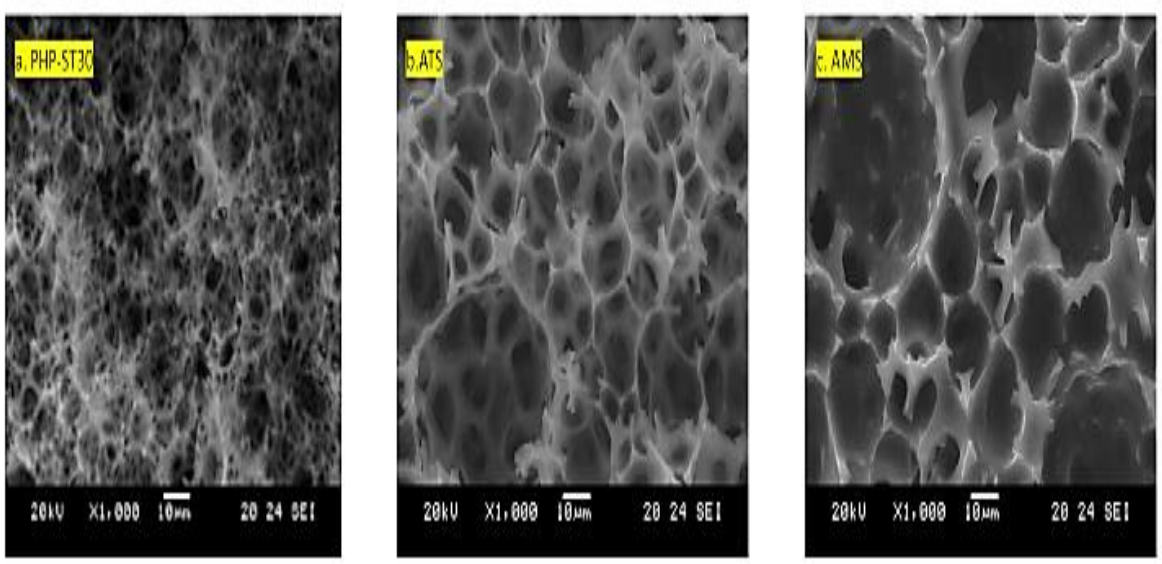

Figure 7.2 SEM images (Magnitude x1000) for a) polyHIPE before sulphonation, b) after thermal sulphonation, and c) after microwave sulphonation.

The PHPs SEM image revealed a hierarchical pore structure, small pores and larger coalescence pores produced from the HIPE droplets, interconnect pores within each large pore wall. The primary pore network is connected through the "window" pores between neighboring large pores. Although samples after sulphonation show that

architectural structure and pore shape were still similar, they revealed some differences as illustrated in Table 7.2.

PHP Code	D /µm	d /µm	Tw /µm	Tv /µm
PHP-ST30	12.01	4	1.7	2.8
ATS	22	7	1.78	4.6
	8-52	4-10	1-4	
AMS	25	9	3.27	8.7
	13-55	3-20	0.74-7.9	

Table 7.2 The results three polyHIPEs ;first row : standard polyHIPE PHP-ST30, second row : thermal sulphonated PHP ; ATS, third row :microwave sulphonated PHP:AMS including : average pore size D (µm) , average interconnecting Size d (µm) minimum pore thickness, Tw (µm), intersecting vertex thickness, Tv (µm).

The main differences between PHPs before and after sulphonation are firstly, the surfaces of the pore walls are cleaner than those samples after both thermal and microwave sulphonation due to the effect of immersion in sulfuric acid. Secondly, there are a few small cracks in the walls which appear after sulphonation due to the thermal cycle the material is put though to drive the sulphonation reaction.

Further comparison in Figure 7.3 shows the difference in surface structure of the pores after sulphonation by the two different methods**.** As a result of the difference in heating technique between microwave and thermal sulphonation there is a remarkable difference in the pore wall structure after sulphonation.

a. Thermal Sulphonation ATS

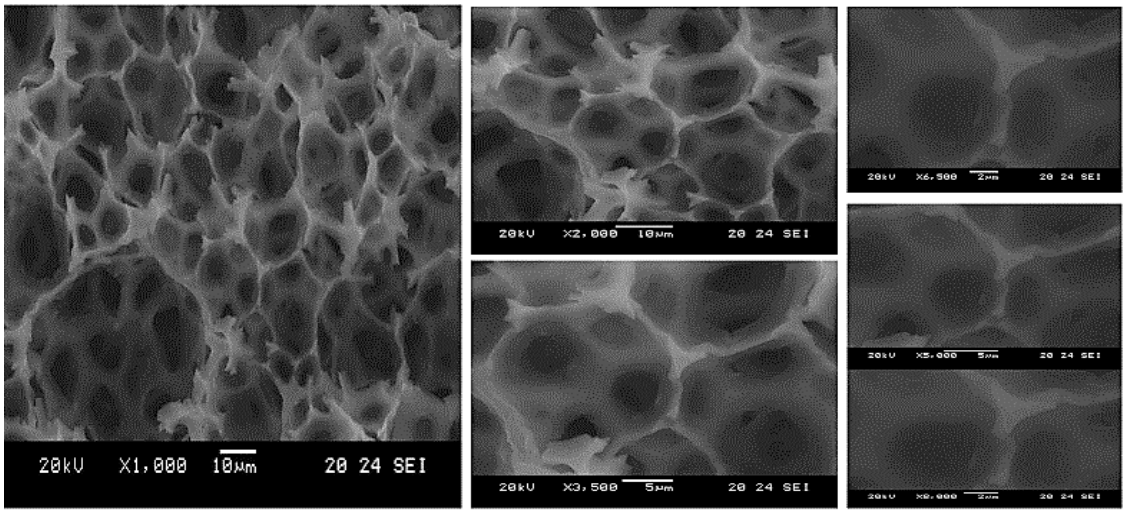

b. Microwave Sulphonation AMS

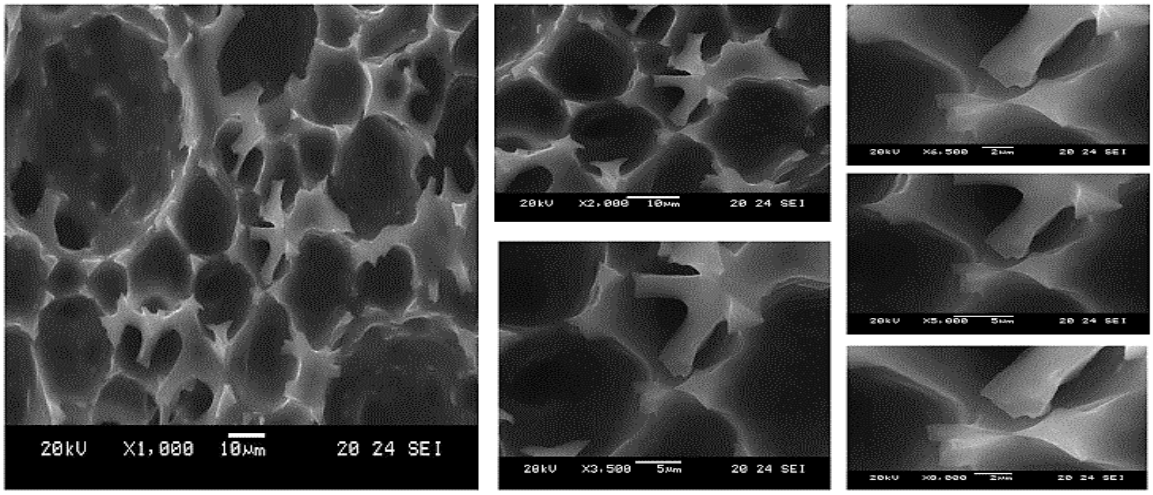

Figure 7.3 The SEM micrograph for a) thermal sulphonation disks (ATS) and (b) the SEM micrograph for microwave sulfonated discs (AMS).

The gradual heating in thermal sulphonation does not allow the sudden evapouration of water inside pores and the subsequent occurrence of blisters (Noor, 2006). Consequently, it can be seen that the thermal method shows a more homogeneous structure and is more similar to the standard polyHIPE PHP-ST30 than AMS. ATS polymers revealed a narrower pore diameter (8-40 μm, on average 22 μm), and interconnecting pore diameter (4-10 μm, on average 7 μm) which is less than those in AMS. This can be explained by the water in any closed pores expanding, bursting the pores and escaping into the acid filled surroundings. Blistering in the pore walls is also a consequence of this but the damage is low due to the slow heating where, for instance, wall thickness of ATS is about 1.78 μm whilst in AMS it is 3.27 μm, higher than in standard polyHIPE PHP-ST30 (1.7 μm). However, during microwave irradiation, closed pores explode suddenly, and form longer cracks as a result of sudden evapouration of water drops. This also affects firstly, their mechanical properties, secondly, their surface area and finally the polyHIPE composition, as reported in Table 7.3.

Surface area and pore size relevant for adsorption is not what is measured by SEM as much smaller surface pores are required. The properties of the pore wall surface have, therefore, been measured from adsorption/desorption isotherms using the BET method explained previously in Section 5.9.3.

PolyHIPE Code	BET Surface Area m^2/g	Pore Volume cm^3/g	Pore Size Nm	Young's Modulus/MPa
PHP-ST30	6.3	0.49	≥8.53	3.0
ATS-30	335	0. 141	1.5-3.84	0.45
AMS-30	355	0.95	0.9-3.16	0.33

Table 7.3 Comparison of BET surface area, pore volume, nano-size pores and Young's Modulus for PHP-ST30, ATS, and AMS prpared at same mixing time of 30 minutes.

The surface area was increased from 6.3 m^2/g for the standard polyHIPE to 335 m^2/g for both ATS and AMS (Table 7.3). This improvement can be attributed to efficient removing of the unreacted monomers and to the drying in the oven that allows complete penetration of the H_2SO_4 during the soaking period. Further changes of the polyHIPE were observed in parallel, such as, darker color and increased diameter with decreases in thickness of the polyHIPE discs along with a transforming to hydrophilicity imparted through sulphonation. The effect of sulphonation and the H_2SO_4 on the internal structure of polyHIPE, surface area and porosity,

whether it is sulphonated traditionally or by using microwave methods were compatible with previous studies in which, for example, Hasan in 2013 and Thumbarathy five years later successfully increased the surface area of the polyHIPE by sulphonation (Hasan, 2013, Thumbarathy, 2018).

The differences in the two methods is that in the traditional method, a high temperature is required due to the thermal treatment, a longer duration for reaction and large amount of sulphuric acid is also needed. In this study the duration is increased due to the need to control the gradual increasing temperature to avoid irregular, uncontrolled pore formation. In microwave sulphonation, the H_2SO_4 is added to the aqueous phase during manufacture increasing the pore diameter as mentioned earlier but in parallel, increasing in the number of the nanopores which leads to decreasing average diameter of the pores in nano-size and increased surface area. These nano size pores have sizes from around 8.53 nm of PHP-ST30, 1.5-3.84 nm AMS and 0.9-3.16 ATS and are formed when the sulphuric acid entrapped in the polyHIPE monolith escapes owing to the heat and elevated temperature (Thumbarathy, 2018). The homogeneous heating in the traditional method (ATS) leads to a more homogenous monolith structure with approximately equal wall thickness (about 1.7 µm) but fewer cracks than in AMS which has higher wall thickness (3.27 µm) but with many cracks (Shakorfow, 2012). This explains the degradation in mechanical properties as shown in Table 7.3 and further the stress strain behaviour in Figure 7.4. Sulphuric acid presence in the liquid phase causes the formation of coalescence pores along with the primary pores. The increase in the rate of coalescence pores is because of the thinning of the liquid film whereby the van der Waals forces are strong due to polarizability (Kizling and Kronberg, 1990).

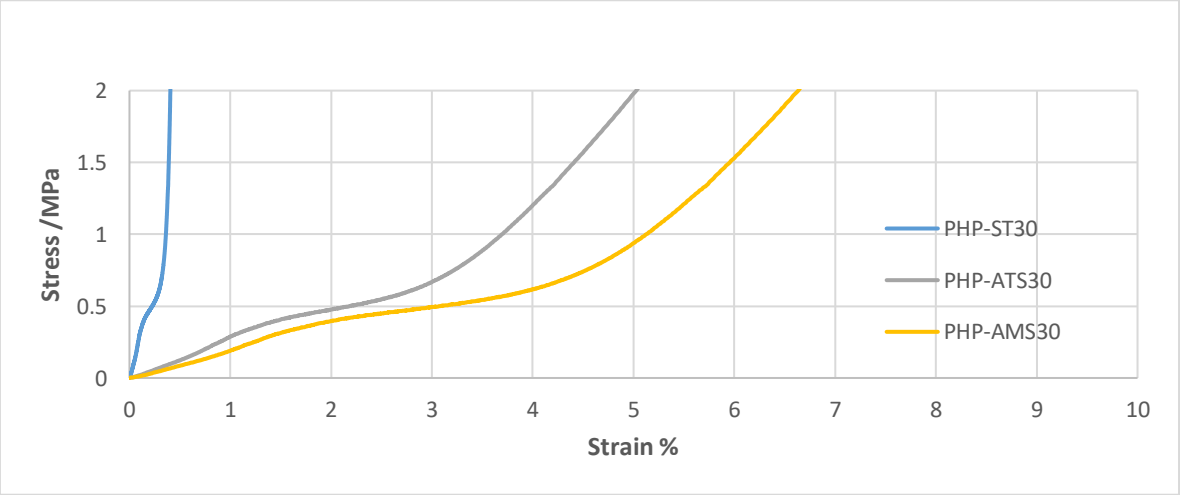

Figure 7.4 Stress-strain curves for sulphonated polyHIPE produced by different approaches.

The method of mechanical compression testing of PHPs has been explained in Section 5.4.5. The effect of sulphonation on the compressive properties of the polyHIPE foams is shown in Figure 7.4 and the Young's Modulus results are presented in Table 7.3. The Young's Modulus for PHP-ST30 varies from 1.2 to 3 MPa, the highest value being at 30 minutes mixing time. Further tests have been done to study the effect of sulphonation on mechanical properties, that with sulphonation the PHPs mechanical properties are reduced for both methods of sulphonation (Young's Modulus for ATS is ~0.45 MPa while for AMS is ~0.33 MPa). This reflects the damage caused by the release of trapped water during the sulphonation process.

Further comparison to identify the changes in composition was conducted by using the FTIR spectrum. The comparison between PHP samples before (PHP-ST30) and after thermal (ATS) and microwave (AMS) sulphonation is shown in Figure 7.5. All samples had the polystyrene standard response with vinyl and benzyl groups and as expected. Because of the $SO_3^-H^+$ groups introduced, there is extra intensity for some of the peaks from 650 to 1300 cm^{-1} due to C–S stretching and S=O stretching peaks which were higher than those in standard polyHIPE (Thumbarathy, 2018). Theses represent the possible sites where sulphur absorbers can be attached to create a sulphur-sorbent.

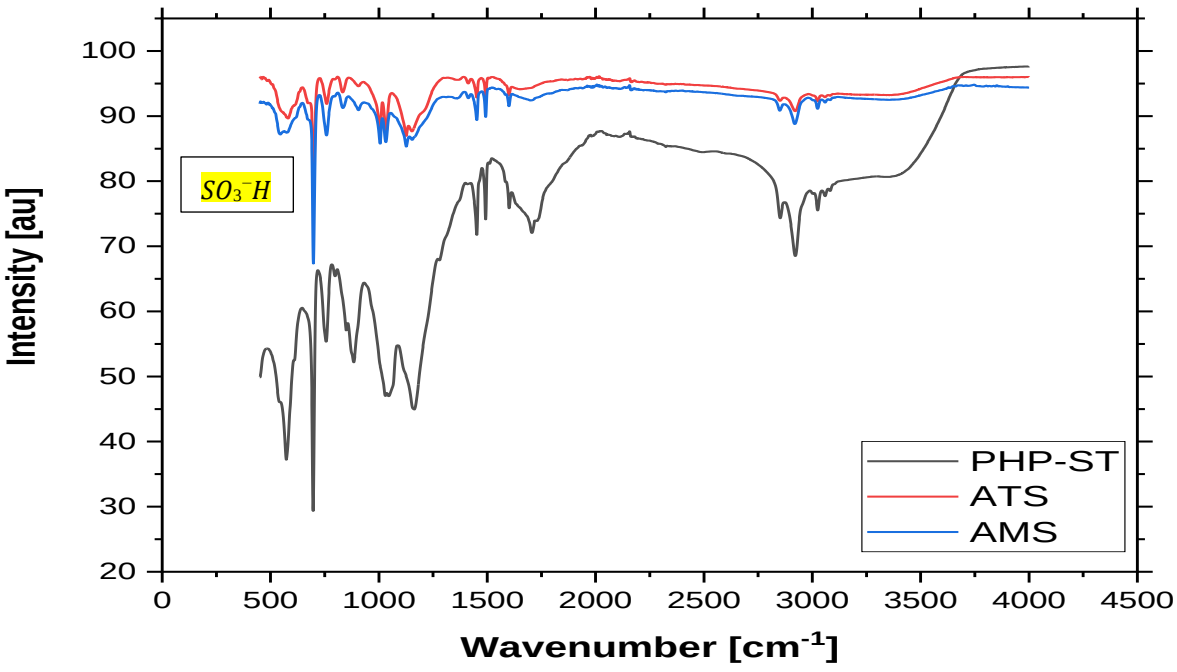

Figure 7.5 Comparison of FTIR spectrum for standard polyHIPE PHP-ST and polyHIPEs after thermal (ATS) and microwave (AMS) sulphonation.

In conclusion, sulphonated polyHIPE was successfully produced with active sites by the two methods. As a result, the chemical, physical and mechanical properties of the ATS and AMS were changed in terms of color, structural characteristics, ion exchange capacity and absorption capability. Despite this the bonds formed within the functionalized polymer are comparable to the standard polymers.

7.2.2 Sulphur adsorption by using the sulphonated polyHIPEs

Adsorption experiments were performed in a closed, stirred, cylindrical as previously shown in the schematic in Figure 5.18. and in reality in Figure 5.19. The experiments were performed by adding 10% by weight of the two sulphonated polyHIPE adsorbents individually to 1000 ml of the oil standard. The model fuel oil was made from octane was mixed with 1000 and 4000 ppm of each organosulphur being the same as used in the previous chapter. There is no sulphur adsorption when 1000 ppm is used for both adsorbents, while adsorption ability occurs for the two adsorbents at the higher concentration. This occurs for all the various organosulphur compounds as breakthrough curves for both ATS and AMS demonstrate in Figures 7.6 a and b.

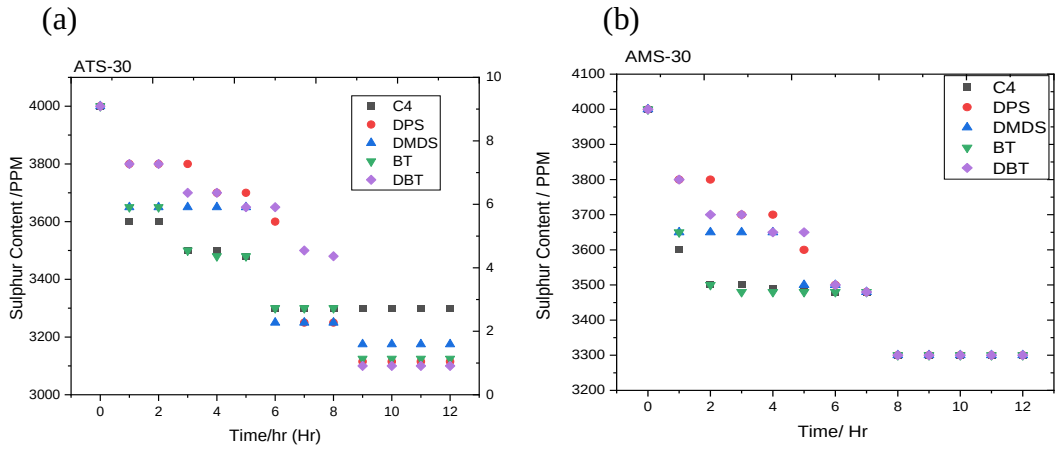

Figure 7.6 Sulphur breakthrough curves for a) ATS-30 and b) AMS-30.

The saturation time is the time in which no more adsorption occurs due to the saturation of the active sites or pores toward the desired substance – Sulphur compounds in this case. This time before the final sulphur concentration representing the best sulphur capacity and selectivity due to the various sulphur compounds. The breakthrough results show that saturation time and final concentration of ATS-30 were 3100 ppm, 8hr for C_4 and in 9 hours were 3115, 3175, 3125, and 3100 ppm for DPS, DMDS, BT, and DBT respectively for the other compounds. While the final adsorption value of AMS was 3300 ppm reached at 8 hr. for all sulphur compounds. Adsorption breakthrough curves for both sulphonated polymers demonstrated a low degree of Desulphurisation (ATS ≤15.8% and AMS ≤12.5 %) and especially have very low reproducibility.

Another comparison is shown in the Figure 7.7 including the adsorption capacity of the standard polyHIPE PHP-ST30 with the sulphonated polyHIPE. It has been observed that adsorption is improved with sulphonation as seen in the figure, rising from 8% using PHP-ST30 to 12.5% and 15.8% using ATS and AMS respectively. This can be explained by the improvement in the surface area which allows a greater number of adsorption sites for sulphur compounds in the fuel oil due to the effect of HSO_3^- entering the chemical structure of the sulphonated polymer according to the reaction in Figure 5.10 .

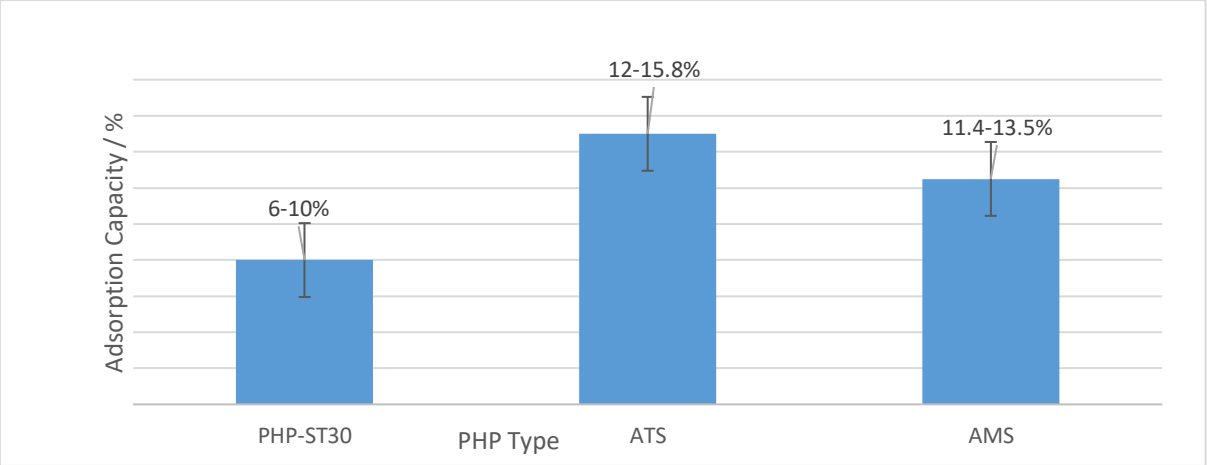

Figure 7.7 Different adsorption capacities of the standard polyHIPE PHP-ST30 versus AMS and ATS.

The sulphonation process has affected some characteristscs in driving the adsorption capacity to be improved. Despite the low sulphur capacity of both polymers, these modified polyHIPEs can be used in some sections of the oil production industry where the mechanical properties and reproducibility are not required and the sulphur content is very high, for instance, filters for pipe lining and dyeing (Sinnott, 2014). In this case, the thermal sulphonation method is more preferred, unlike what was mentioned for other applications (agriculture and bio-process applications or intensified and integrated gasification) in previous studies (Noor, 2006, Çalkan, 2007, Thumbarathy, 2018, Hasan, 2013, Calkan, 2007) which preferred the microwave sulphonation for several reasons. The disadvantages of the traditional method reported in these studies and the production of excessive waste acid, long processing times, production times and problems of scaling up due to the usage of highly concentrated sulphuric acid at high temperature. These faults can be overcome because in Desulphurisation the agent is the same sulphonation agent and, in addition, in oil refineries sulphuric acid is readily available, beside the temperature can be generated by heat transfer in the plant heat exchangers (Speight, 2014, Gary et al., 2007). In addition, the excess amount of waste acid can be regenerated and reused (Xu et al., 2009). The traditional method as shown before produced more homogeneous pore distribution with no burning discs and less cracking than those produced by microwave

sulphonation as shown in Figure 7.8 and reported by (Thumbarathy, 2018) observed in microwave sulphonation .

Figure 7.8 Photograph showing changed samples after sulphonation including cracking after microwave treatment.

Nevertheless, the mechanical properties degradated drastically causing the production of 50% waste polyHIPE that was impossiple to regenerate and reuse. Figure 7.9 displays the actual average adsorption capacity of both samples maintaining their distance from the target adsorption zone shown in red. There is also no effect on the 1000 ppm fuel oil. Another chemical modification is discussed in the next section .

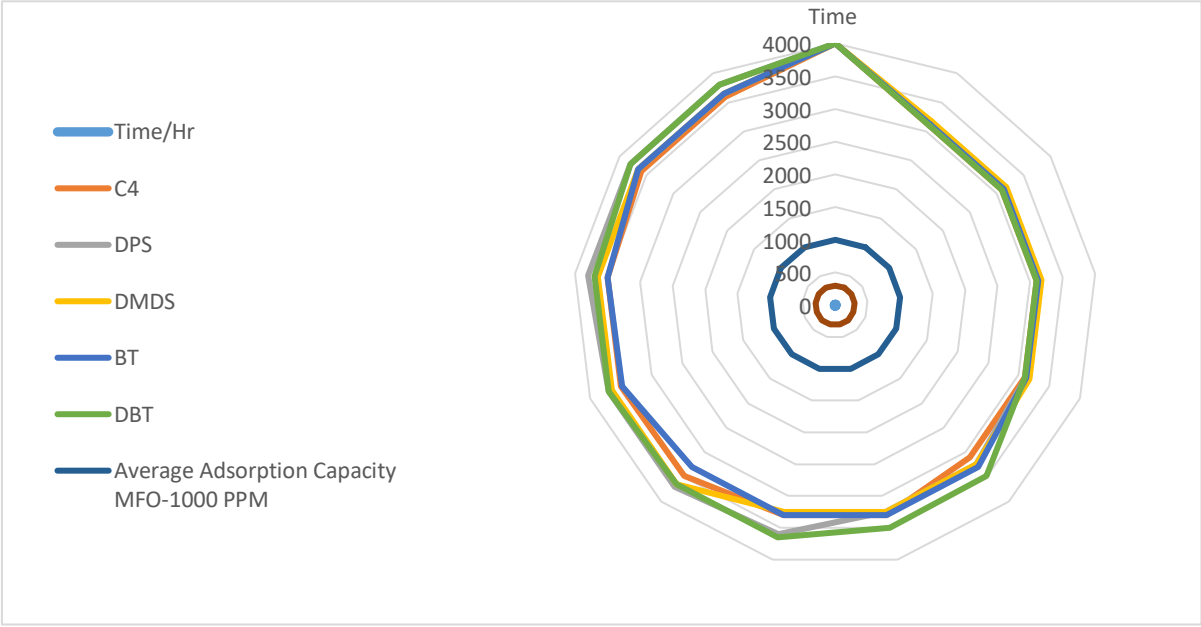

Figure 7.9 The average adsorption capacity of high and low sulphur concentration fuel oil, average ratio, and target adsorption ratio.

7.3 Characterization and sulphur adsorption of functionalized polyHIPE by amination.

PHP/MEA was prepared using the same technique as that of standard polyHIPE in Section 5.4.1, but with the incorporation of MEA (Section 5.4.3) in different trials until the optimum material was achieved. The method created depended on trial and error as well as the study reported by (Alikhani and Moghbeli, 2014). MEA addition was also conducted by adding it to both aqueous and oil phases to improve the surface chemical activity of polyHIPE towards the sulphur compounds and retain its morphology and other features without change. the MEA properties illustrated in Table 7.4.

The tailored properties of polyHIPEs - high porosity and interconnected macropores together with surface chemistry - are very important in both the preparation of PHP-MEA and sulphur-adsorption. MEA and different amines in Table 2.2 have been used in the application of Desulphurisation previously (Abdulrahman et al., 2015, Huertas et al., 2011, Kussainova and Shah, 2020, Speight, 2014).

Olamine	Formula	Derived Name	Molecular Weight	Specific Gravity	Melting point, ℃	Boiling Point, ℃
Ethanolamine	$HOC_2H_4NH_2$	MEA	61.08	1.01	10	170

Table 7. 4 Ethanol amine MEA properties

Preparation involved swelling of the crosslinked polymer discs by acetone (acetone stage) to allow the maximum amount of excess MEA to be absorbed by the solid discs in the ageing step, which can ensure continued access of the reagents to the reactive sites (Cameron et al., 1996). The polyHIPE totally absorbed the MEA and it adhered to the polymer surface allowing adsorption of sulphur. PHP/MEA preparation involved failed procedures as shown in Figure 7.10 before reaching the final method for composition and procedure of preparing amination PHP-MEA as summarized in Table 7.5. Failed steps included, for instance, adding MEA to the aqueous phase alone or to the oil phase alone; this failed as there was no difference in the FTIR results when compared to untreated material. While adding specific amounts of MEA to both oil and aqueous phase, at the same time adding electrolyte to the initiator in the liquid phase and swelling by using acetone leads to produce aminated polyHIPE. Also the electrolyte increased the emulsion stability by inhibiting Ostwald ripening (Alikhani and Moghbeli, 2014) the use of reaction solvents which will swell the crosslinked polymer beads. It should also be

noted that the polymer must remain swollen throughout the entire reaction to ensure continued access of the reagents to the reactive sites.(Cameron et al., 1996)

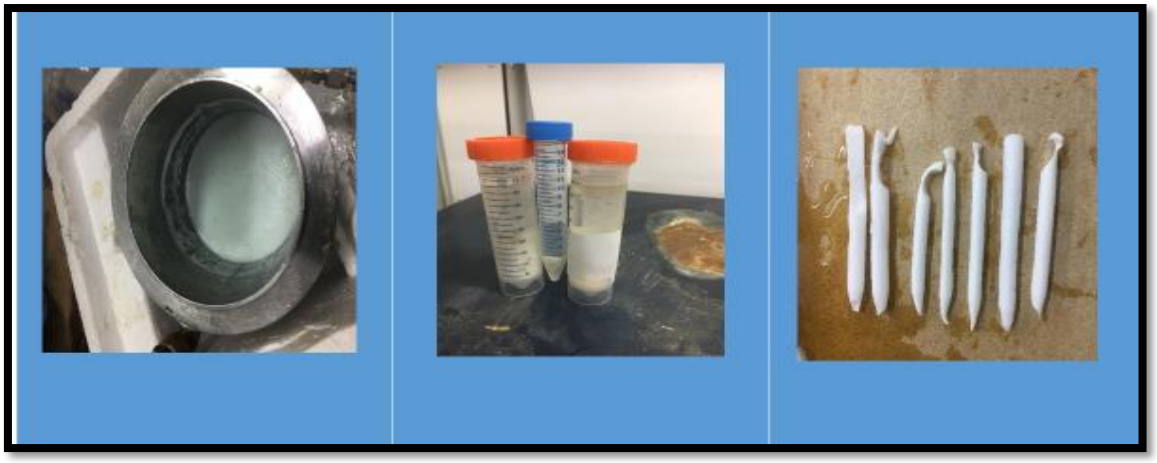

Figure 7.10 Failed samples due to different factors.

The following sections discuss the characterization of the novel polyHIPEs prepared under the code PHP-MEA and then illustrates their adsorption behaviour**.**

Type of Polymer	10 % vol Oil phase	90 % Aqueous phase	Function	Target
Aminated polyHIPE PHP-MEA	Styrene (ST) 78 wt % Divinylbenzene (DVB)8wt % (Span 80)14 wt.% Plus 10 wt.% MEA of the total oil phase weight.	Distilled water 200 ml Potassium persulphate (KPS) and calcium chloride $CaCl_2$ 1 wt.% 10 wt.% MEA of the total liquid phase weight.	Adding MEA to the emulsion. Adding Electrolyte to the liquid phase Acetone stage MEA aging	To: Increase the surface activity To help MEA absorbent PHP Swelling Extra Amination

Table 7.5 Composition of oil and aqueous phase of polyHIPE after amination PHP-MEA.

7.3.1 Characterization of PolyHIPE prepared by the amination method

It was observed that the modified polyHIPE after amination was spongy, swollen, brighter in color, less dense, smaller in volume and more brittle than the standard material (Figure 7.11). Scanning electron microscopy (Dağ et al.), Fourier-transform infrared (FTIR) spectroscopy, BET surface area and compression test MCT were carried out to determine the structural characteristics and mechanical properties of the polyHIPEs.

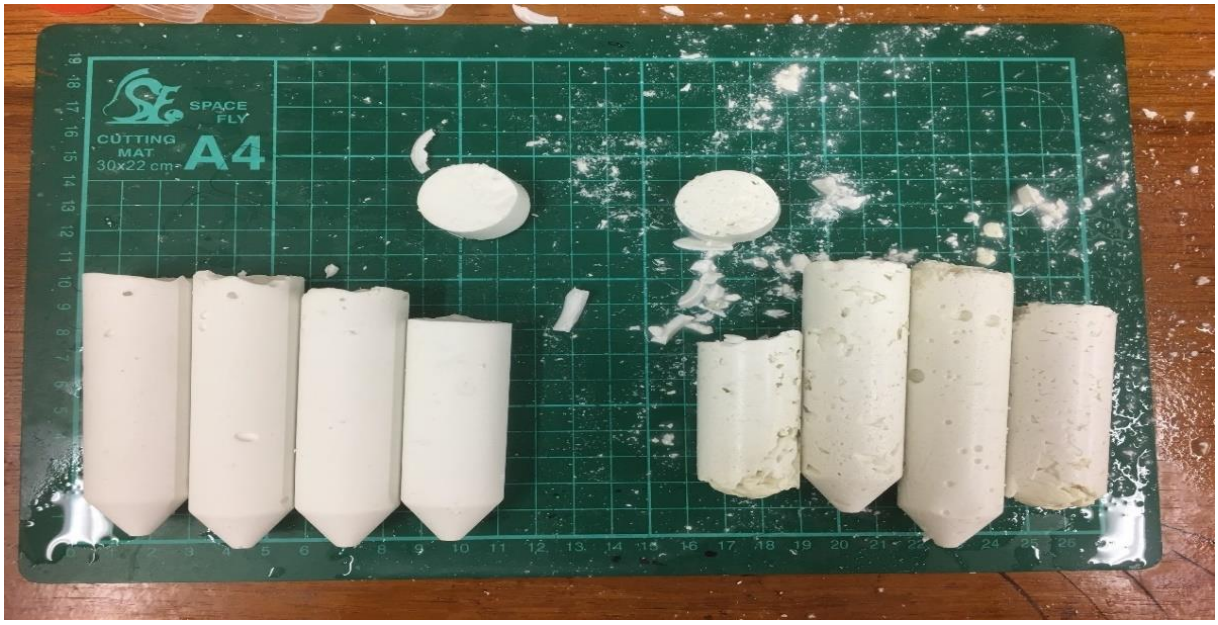

Figure 7.11 Photograph showing the standard polyHIPE PHP-ST30 on the left and the aminated polyHIPE PHP-MEA on the right which has lower mechanical properties and hardness.

The chemical structure of the treated polyHIPE was characterised by Fourier transform infrared (FTIR) spectrometry as shown in Figure 7.12 comparing the standard polyHIPE PHP-ST30, the polyHIPE after amine treatment and the pure amine with several curves of standard polyHIPEs in the inset. The three curves show that the PHP-MEA curve incorporates both the pure MEA curve and standard polyHIPE curve features showing the success of the amination process. The appearance of the band at 1114-1260 cm^{-1} associated with the C-N groups of mono-ethanol amine, and the appearance of new bands at 3421 cm^{-1}, 2914 cm^{-1}, 1481 cm^{-1}, and 1114 cm^{-1}, respectively, corresponding to N=H, (C–H (sp^2), C–H (sp^3)), C = C (aromatic ring), and C–N bonds that confirm a successful surface treatment of the treated polyHIPE by amination (aminated PHP-MEA) has occurred. These results reveal that the amine N-H,C-N groups were successfully added to the chemical structure of the HIPE surface through the amination process (Alikhani and Moghbeli, 2014).

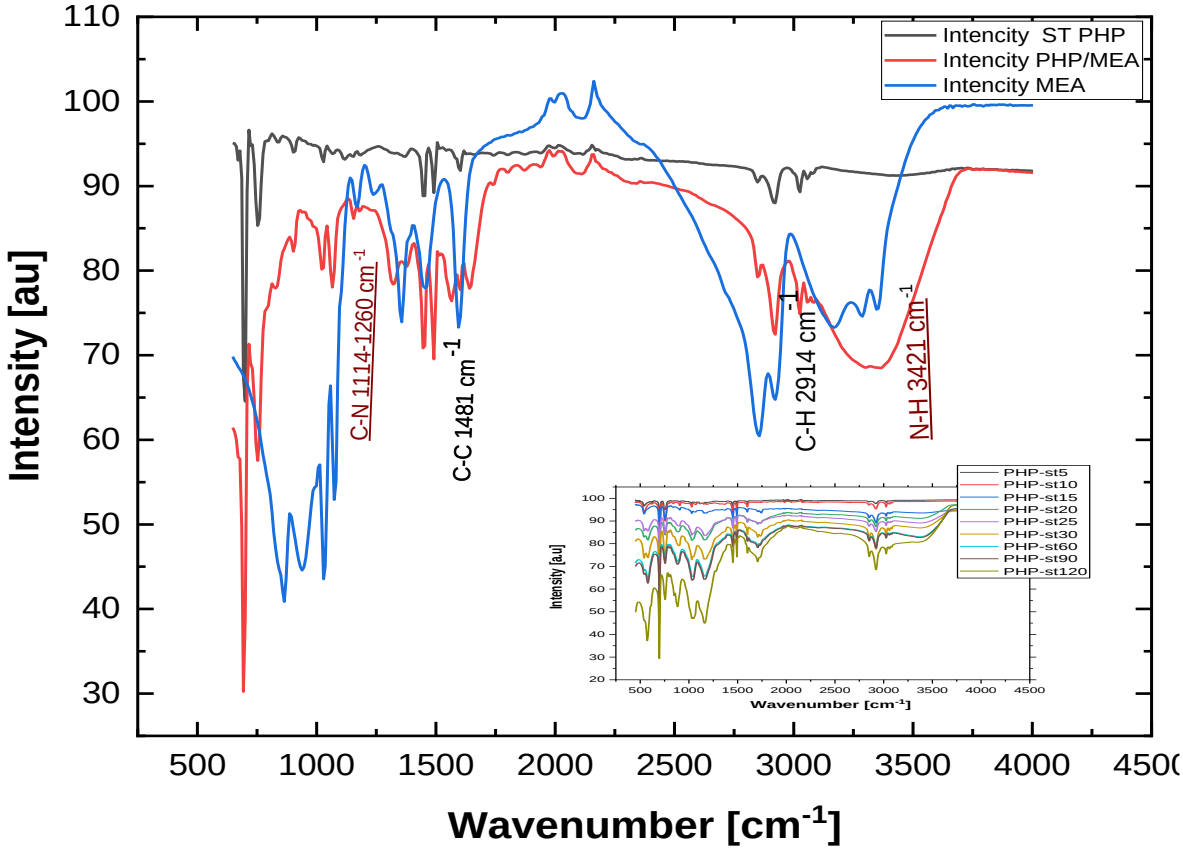

Figure 7.12 FTIR spectra of pure MEA, standard polyHIPE foam before and after the amination treatment.

The SEM images shown in Figure 7.13 were produced when MEA was added directly into both aqueous and oil phases during the emulsification stage. In fact, the incorporation of a higher amount of the amine co-monomer in the emulsion organic phase raised the chances of migration into the aqueous phase which destabilized the prepared HIPE. The addition of MEA to Span80 decreases the interfacial tension between oil and aqueous phases and limits Ostwald ripening in the HIPEs (Sajad and Moghbeli, 2020). The best results were obtained when the polyHIPE discs were saturated with amine through the heating and aging stages. The presence of filler or additives such as acid or amine in the aqueous phase results in destabilization of the emulsion (Thumbarathy, 2018). This destabilization of the HIPE leads to water droplet coalescence, the results of which can be seen in the SEM images in Figure 7.13. Furthermore, it was observed that the morphology of the polyHIPE after amination, such as average pore size, D, interconnectivity, d, minimum wall thickness, Tw and intersection vertex width, Tv and windows, is influenced by the adding of MEA to the HIPE when comparing with standard polyHIPE PHP-ST30 as shown in Table 7.6. Despite the uniform pore distribution its increasing size after amination had negative effects on the structure because of the cracks and breakages in the walls and intersecting vertices as seen in Figure 7.13.

PHP Code	D /µm	Min-Max D /µm	d /µm	Min-Max d /µm	d/D Ratio	Tw /µm	Tv /µm	Tw/Tv Ratio
PHP-ST30	12.01	6-17	4	1-7	0.3	1.7	2.8	0.6
PHP-MEA	16.34	10-28	6	2-11	0.36	2.66	6.27	0.42

Table 7.6 Average pore size D (µm), average interconnecting Size d (µm), d/D ratio, minimum pore wall thickness Tw (µm), intersecting vertex thickness Tv (µm) and their ratio Tw/Tv for standard polyHIPE PHP-ST30 and aminated polyHIPE PHP-MEA

The average pore size D of 16.34 µm, average interconnecting pore size d 6µm, minimum pore wall thickness Tw 2.66 µm and intersecting vertex thickness Tv 6.27 µm were achieved after the amine addition with increasing in sizes of ~25-33 % compared to the standard polyHIPE.

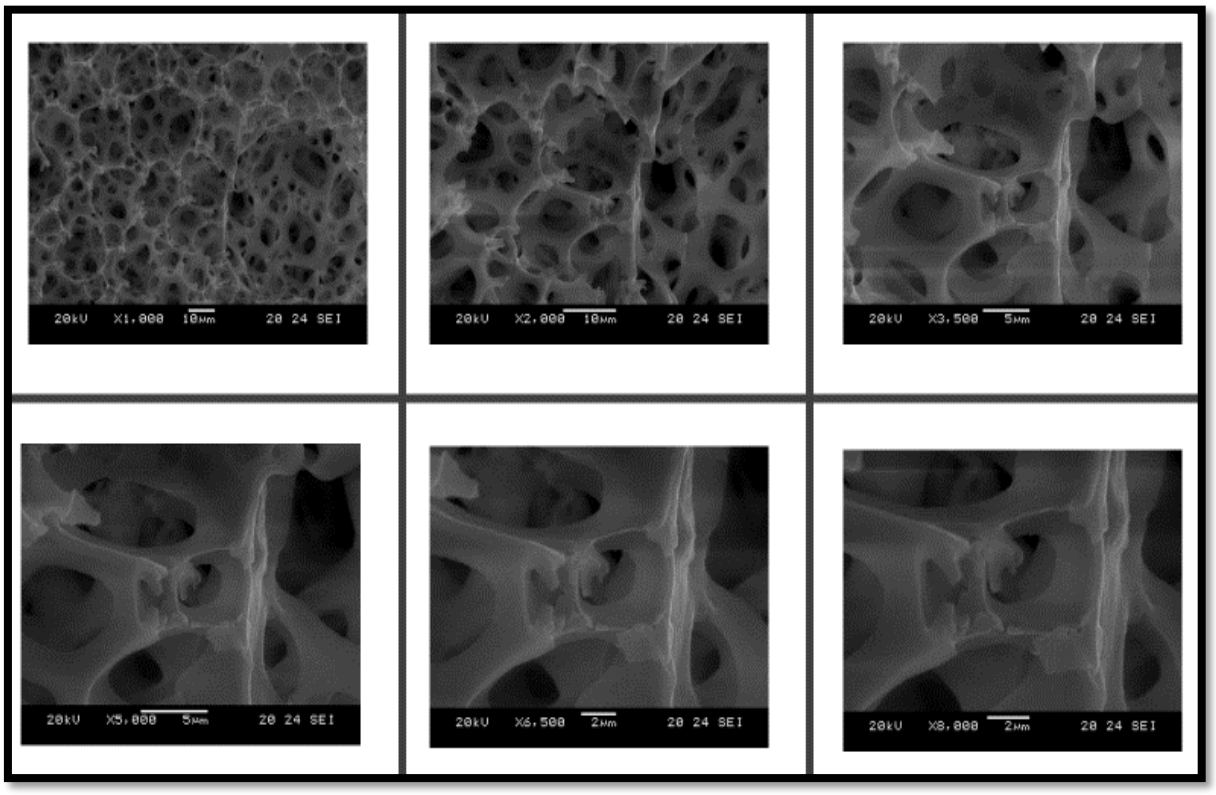

Figure 7.13 SEM images of aminated polyHIPEs PHP-MEA at DIFFERENT magnifications a) x1000, b) x 2000, c) x 3500, d) x 5000 , e) x 6500, and f) x 8000.

An additional feature of the aminated polyHIPEs is the formation of blisters within the structure of the polymer similarly to those for sulphonated polyHIPEs in the previous section as is often observed with fillers or additive reactions (Kizling and Kronberg, 1990). These blisters produced crimped, irregularly structured surfaces and some even appear to form interconnects. Extra amination is carried out immediately after soaking the polyHIPE discs in the amine for the stipulated time and then heating. The trapped amine molecules within the monolith structure, either absorbed or reacted, can escape during the process. This results in the formation of blisters, cracks within the walls and the creation of micro and nano pores as found in the SEM images analysis in Figure 7.13 and BET analysis of the surface area (Table 7.7). Smaller macro-meso pores were produced in the structure with the amination of the polyHIPE in PHP-MEA.

The modification done in the current study was adding the amine in both oil and aqueous phases during HIPE formation, swelling the polyHIPE after polymerisation by acetone, heating with extra excess amine and finally soaking in amine overnight. This aimed to increase the number of the smaller pores in the nano size range on the walls between two cells; an increase in the BET surface area of the PHP-MEA compared to the other polyHIPEs illustrated in Table 7.6. However, when the compression test was performed (resultant stress-strain curves shown in Figure 7.14 a, b), the Young's modulus decreased due to the cracks in the walls and intersecting vertices and the formation of larger pores despite the increased number of nano scale pores.

PolyHIPE Code	BET Surface Area m^2/g	Pore Volume cm^3/g	Pore Size Nm	Young's Modulus/Mpa
PHP-ST30	6.3	0.49	≥8.53	3
ATS-30	335	0. 141	1.5-3.84	0.45
AMS-30	355	0.95	0.9-3.16	0.33
PHP-MEA	369	0.394	0.9-3.6	1.45

Table 7. 7 Comparison of BET surface area, pore volume, nano-size pores and Young's Modulus for PHP-ST30, ATS, AMS and PHP-MEA .

Further comparison of stress-strain curves for PHP-MEA compared with a) standard polyHIPE PHP-ST30 and b) micro and thermal sulphonated polyHIPEs showed that PHP-MEA lies between the standard and sulphonated polyHIPEs. The amination leads to morphological change that can be explain subsequent shrinkage and reduction in mechanical properties.

(a) (b)

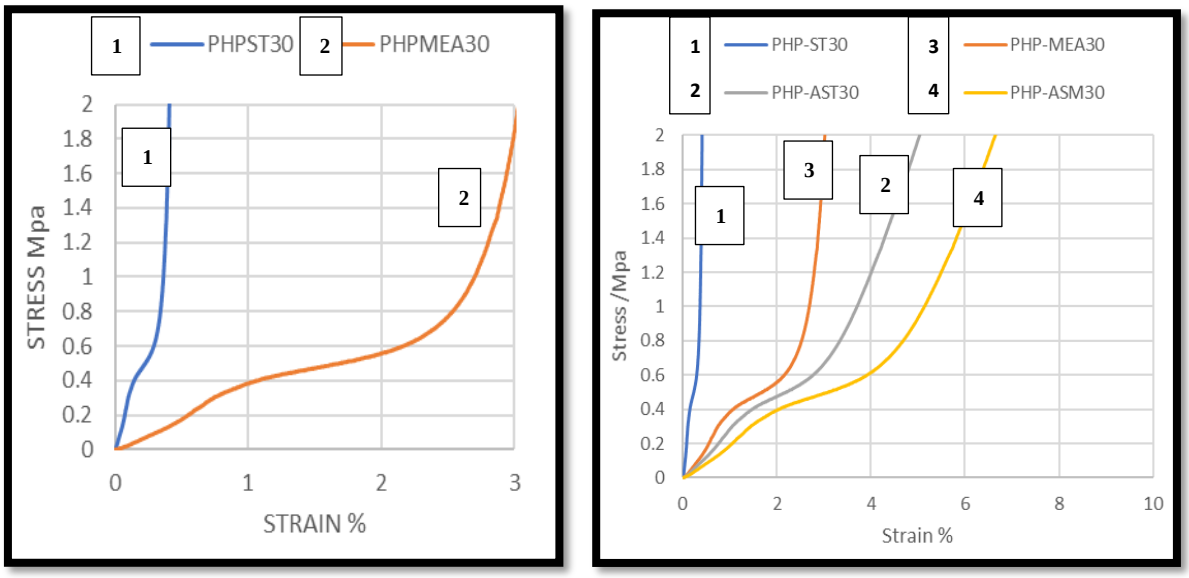

Figure 7.14 Stress versus strain curves for PHP-MEA compared with a) standard polyHIPE PHP-ST30 and b) micro and thermal sulphonated polyHIPE.s

The results presented in this section indicate that PHP-MEA was successfully produced by the novel amination methodology. The morphology showed more effective pore distribution with high levels of improvement in surface area. The composition possesses more active sites represented in amine bonds which could play a fundamental role for sulphur adsorption. However, the mechanical properties could represent a drawback preventing producing a successful adsorbent, which will be shown in the next section.

7.3.2 Sulphur adsorption of the aminated polyHIPE.

The experiments were performed by adding 10% weight of PHP-MEA adsorbent to 1000 ml of the model fuel oil (octane mixed with 1000 and 4000 ppm of each organosulphur compound) which was the same as was used in the previous sections. There is no sulphur adsorption when feedstock of 1000 ppm was tested. As expected, the adsorption capacity increased markedly for the novel adsorbent towards the various organosulphur as shown in the breakthrough curves for PHP-MEA in Figure.7.15.

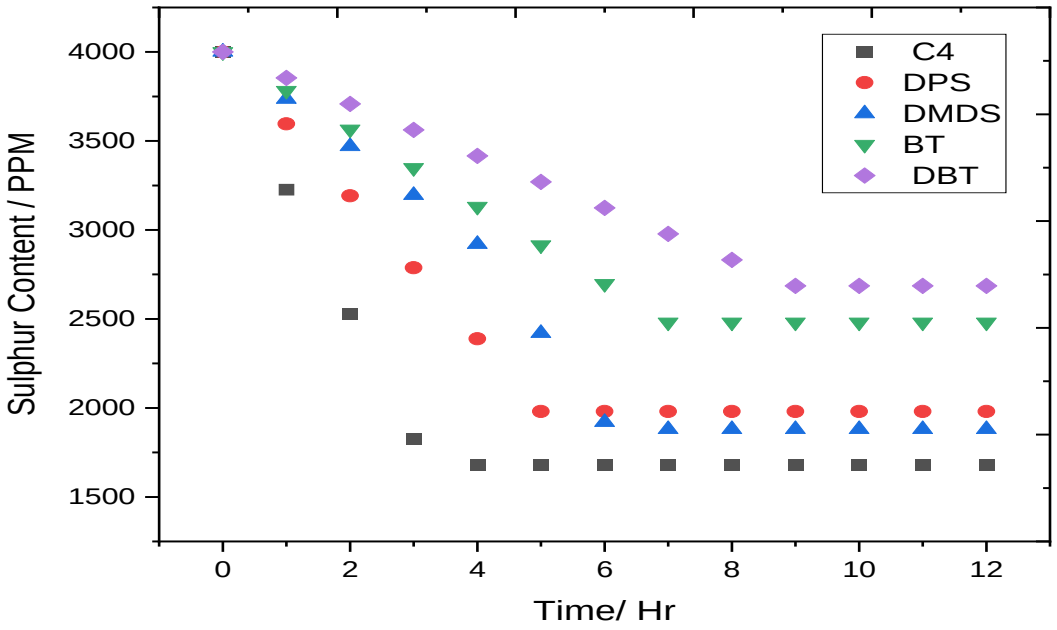

Figure 7.15 Sulphur breakthrough curves for PHP-MEA.

The breakthrough results show that saturation time and final concentration of PHP-MEA were 1680 ppm, 4hr for C4; 1980 ppm, 5 hours for DPS; 1880 ppm, 7 hours for DMDS; 2481 ppm , 7 hours for BT and 2686 ppm, 9 hours for DBT .

The improvement of the PHP-MEA adsorbent can be shown by the comparing the above results with the standard polyHIPE PHP-ST30 and sulphonated polyHIPE. Adsorption breakthrough curves for standard polyHIPEs and both sulphonated polymers demonstrated a low degree of Desulphurisation at about (PHP-ST30 ≤ 8%, ATS ≤15.8% and AMS ≤12.5 %). It has been observed that the adsorption capacity improved by amination as seen in Figure 7.16 a to 33-58 %. This is because of the strong interaction between the amine at the surface and sulphur. However, this modification is still far from the target adsorption zone as shown in Figure 7.17 because of low reproducibility due to the poor mechanical properties.

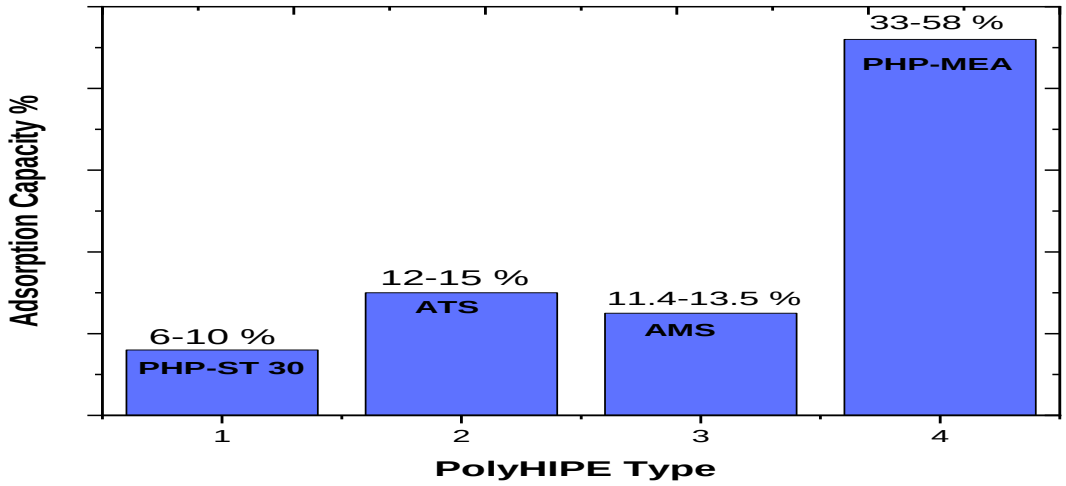

Figure 7.16 Different adsorption capacities of the PHP-MEA versus standard polyHIPE PHP-ST30, AMS and ATS

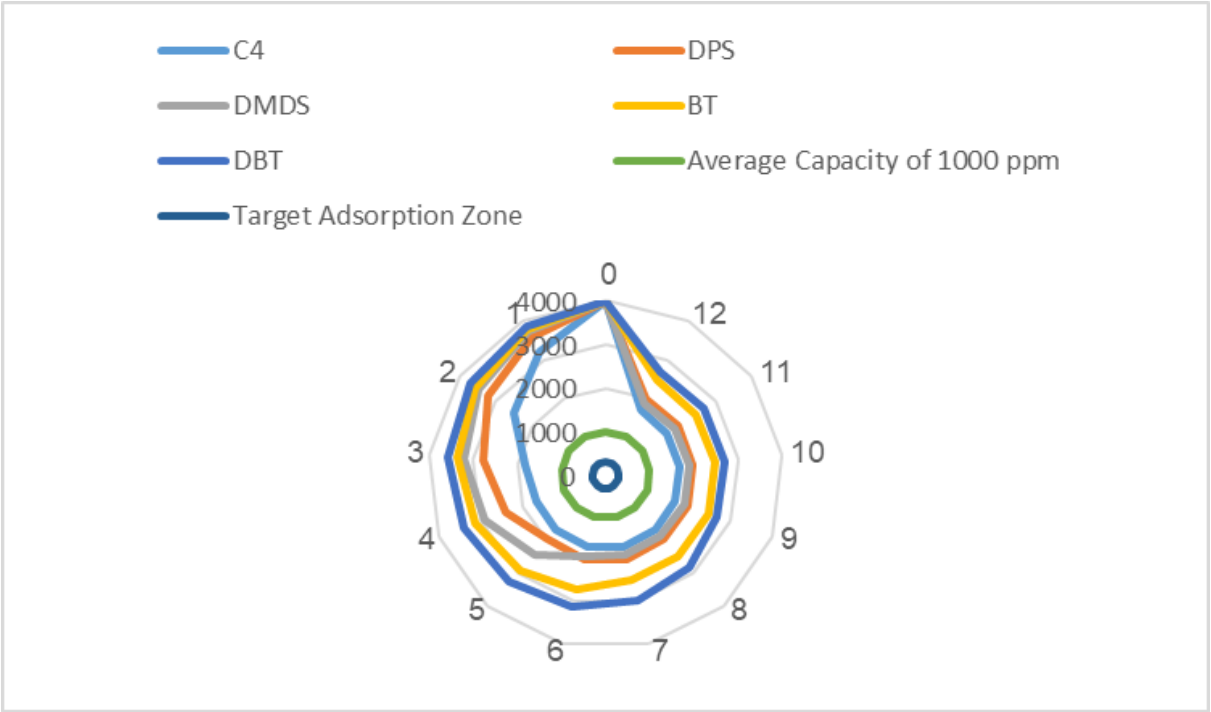

Figure 7.17 The average adsorption capacity of high and low sulphur concentration fuel oil, average ratio and target adsorption ratio.

As a result of poor mechanical properties, the solid discs of the adsorbent converted to cake shape after use, as shown in Figure 7.18.

Figure 7.18 Pictures of the waste PHP-MEA after adsorption trials

The structure is changed due to the effect of the sulphur presence in the walls of the pores as shown in Figure 7.19. It is clear that the porous nature of the adsorbent has diminished completely. Moreover, due to the adhesion of the organosulphur components on the polymer surface due to the MEA presence, some condensed masses appeared on the adsorbent surface. The oil contains bulkier sulphur species that can act as steric blockers on the adsorbent surface and trap other molecules. These results are consistent with the results of a similar study that used real fuel (Shah et al., 2018).

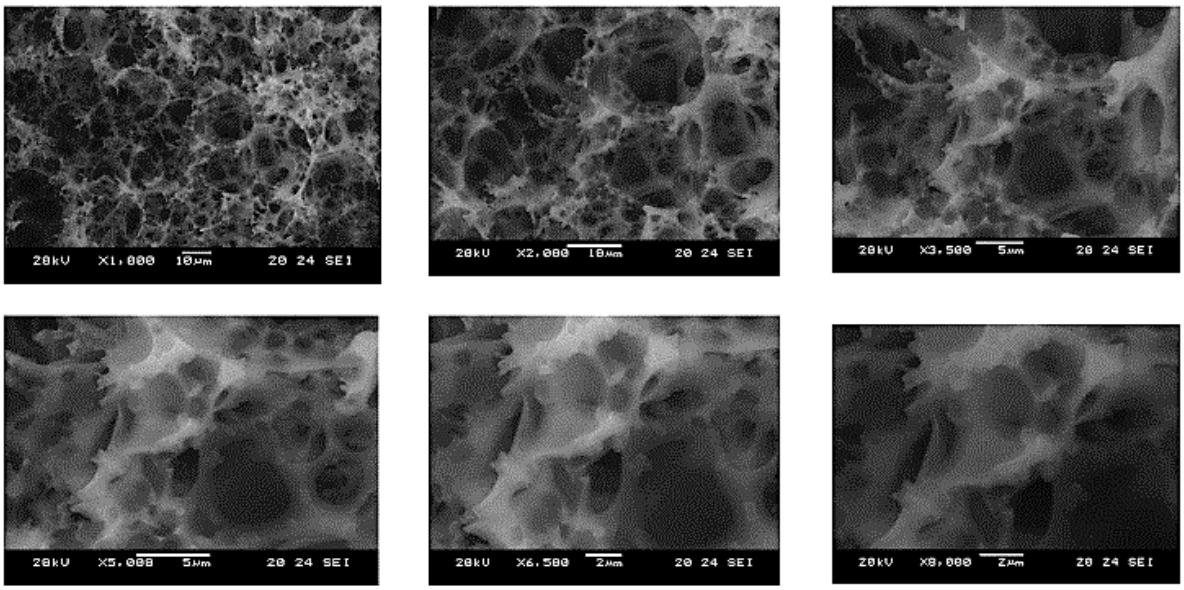

Figure 7.19 SEM images of aminated polyHIPEs PHP-MEA at different magnifications after adsorption trials.

In conclusion the PHP-MEA polyHIPE should be reinforced by using a material that improves its mechanical properties if it is to be a useful adsorbent. This means that a new technique is required, such as, adding other stiffer materials that enable the PolyHIPE to be used as an adsorbent and be regenerated. In the next section the selection of the target reinforcement material and development of the reinforced polyHIPE is introduced.

shown.

7.4 Preparation, characterization, and adsorption study of the reinforced polyHIPE by using activated carbon.

As pyrolytic activated carbon (PAC) possesses excellent physical properties; namely, very high surface area and adsorption capacity, and high mechanical and thermal stability that could improve the overall polyHIPE properties, it was selected as a good candidate to reinforce the polyHIPE while minimally affecting the other properties and potentially adding to its adsorbent capability. In general, PAC is a nano and hybrid material that could be used as directly as adsorbent or indirectly as a filler or additive to polymer composites to enhance the thermal, mechanical, and electrical properties. This is as a result of its low weight, ability to readily spread, whether it is powder or granules and availability in various structural forms and ease of fabrication of these composites through compression moulding..(Abdul Khalil et al., 2013, Haibach et al., 2006, Luo et al., 2012a, Saeidi and Lotfollahi, 2015, Yang et al., 2018).

A challenge was to identify the correct amount and the most appropriate method of adding activated carbon to the PolyHIPE to ensure a uniform distribution of the powder through the HIPE emulsion and avoid clumping, sedimentation or deposits on the bottom of the container. This was reached by mixing the oil phase with PAC overnight then using ultrasound to disperse the activated carbon as was described in the methodology in Section 5.4.4. The manufactured polyHIPE is shown in Figure 7.20; its different color and surface texture due to the changes in composition induced by the reinforcement.

Figure 7.20 Photograph showing reinforced-aminated polyHIPE PHP-MEA-PAC

This adsorbent is manufactured in two steps first adding PAC to the standard polyHIPE producing PHP-PAC and identifying the characterization and adsorption capacity then the second adsorbent is produced by adding both MEA and PAC to the polyHIPE. The compositions are shown in Table 7.8.

Type of Polymer	Oil phase	Aqueous phase	Function	Target
Carbonated polyHIPE	Styrene (ST) 78 wt % Divinylbenzene (DVB)8wt % (Span 80) 14 wt.% 10 wt.% PAC of the total oil phase weight.	Distilled water Potassium persulphate (KPS) 1 wt.%	Adding PAC to the emulsion. Overnight oil phase mixing and sonification	Reinforced Increase surface activity Equal PAC diffusion
Modified Adsorbent	Styrene (ST) 78 wt % Divinylbenzene (DVB)8wt % (Span 80) 14 wt.% Plus 10 wt.% MEA of the total oil phase weight. 10 wt.% PAC of the total oil phase weight.	Distilled water 200 ml Potassium persulphate (KPS) and calcium chloride $CaCl_2$ 1 wt.% 10 wt.% MEA of the total liquid phase weight.	Adding MEA to the emulsion. Adding Electrolyte to the liquid phase Acetone stage MEA aging Adding PAC to the emulsion. Overnights oil phase mixing and sonification	To: Increase the surface activity To help MEA absorbent by PHP emulsion. PHP Swelling Extra Amination Reinforce the adsorbent Increase surface activity Equal PAC diffusion

Table 7.8 Composition of oil and aqueous phase of PHPs.

The activated carbon has been chosen as a reinforcement as explained in Section 3.3.5. It has been recorded that activated carbon, having the largest surface area and highest surface polarity, displayed the highest total capacity for adsorption of sulphur (Saleh et al., 2017). Consequently, activated carbon was treated with H_2SO_4 at 60 ℃ to clean its surface and improve its adsorption ability before being mixed with the oil phase in polyHIPE manufacture(Jiang et al., 2003, Yu et al., 2013).

It was recorded in previous studies how Young's Modulus increases the PolyHIPE density increases (Menner et al., 2006a, Williams et al., 1990, Greco, 2014) as mentioned in Section 4.6.2.1. The mechanical properties of the traditional polyHIPEs were the main obstacle facing this study as they relate to the applicability of the polyHIPE as an adsorbent and its ability to be reused so that it increases the number of adsorption-regeneration cycles run and thereby increases the total adsorption capacity. Adding of a certain amount of PAC to the oil phase increases its density thereafter displaying the ability to improve the mechanical properties of the polyHIPE. However, the biggest challenge was to add activated carbon powder to the oil phase whilst ensuring its stability in the emulsion. Furthermore, the PAC powder should be distributed evenly through the emulsion in all formation stages, for instance, in the oil phase preparation, then in the emulsion stage and lastly in the final polymer product. This was also achieved after several trial experiments and using an ultrasonic bath to homogenize the oil phase, the main trials conducted were as follows:

1) Adding 1-20 % wt to the aqueous phase and continue the same procedures of PHP-ST30. This failed for all concentrations because the peristaltic pump was unable to generate continuous flow and the PAC settled at the bottom of the beaker.
2) Adding 1-20 % wt to the oil phase and continuing the same procedures as with PHP-ST30. This failed due to immiscibility at low concentrations leading to settling and particles leaving the oil phase or emulsion. In addition, the activated carbon separated from the polymer disc during the washing stage. Moreover, the PAC distribution was also poor at high concentrations leading to fracture of cut discs due to non-uniformity.

In the next Section a preliminary assessment of the activated carbon is conducted before mixing with the emulsion to identify its surface properties and adsorption capacity that can be used to improve the characterizations and performance of modified polyHIPE PHP-MEA as an adsorbent.

7.4.1 Activated carbon (PAC) characterization and adsorption capacity test

In this thesis, considerable research has been reported concerning adsorbents and their adsorption capacity, particularly activated carbon, as mentioned in Table 3.1. It was noted that these studies very rarely discussed the reproducibility of the PAC adsorbent used and it was concluded that one of the main reasons that PAC is not widely used, despite having all the properties that qualify it to be an excellent adsorbent, is the lack of the ability to recycle and reuse it. Regeneration may not be economic when it is conducted at a very elevated temperatures of around 400°C (Huertas et al., 2011).

The first group of experiments reported in this study were testing the surface properties and adsorption capacity of the PAC used before being adding to the oil phase in the HIPE. The PAC as received had surface properties as follows: surface area: 1009 m^2/g, pore volume: 0.478 cm^3/g, and average pore size: 2.1 nm, while it was found that PAC after acid treatment had surface area: 821 m^2/g, pore volume: 0.439 cm^3/g, and average pore size: 0.55 nm. The acid treatment cleaned the PAC of ash and other impurities, leading to partial destruction of the pore structure by oxidation and thereby to a significant reduction of the surface area while also improving the adsorption performance as the acid oxidation results in an increase in the acidic oxygen-containing functional groups responsible for many adsorption reactions (Zhou et al., 2009).

Also, In spite of the decrease in surface area to 821 m^2/g, which reduces the number of adsorption sites and limits mass transfer inside the bulk of the adsorbent, there is a reduction in the pore size to 0.55 nm. Ania and Bandosz (2005) found a linear correlation between the adsorption capacity and the volume of small micropores. They proposed that higher uptake during adsorption might be linked to the large volume of small micropores < 0.7 nm in width (Ania and Bandosz, 2005).

The powder was dried and filtered and then 10% by weight was added to the 4000 ppm Sulphur doped model fuel oil as used as in the previous adsorption experiments. The adsorption test results are shown in Figure 7.21.

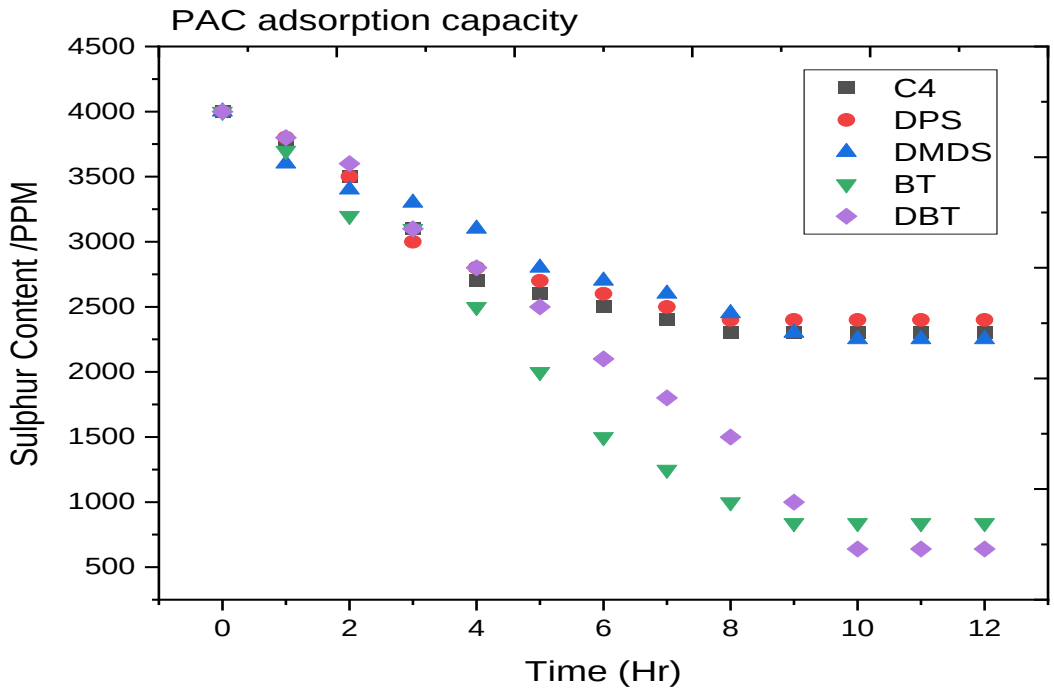

Figure 7.21 Sulphur breakthrough curves for PAC.

The sulphur contents for C4, DPS, DMDS, BT and DBT were decreased from 4000 ppm which was the initial concentration to 2300, 2400, 2250, 840, and 640 ppm representing an adsorption capacity of 42%, 40%, 43%, 79%, and 84% respectively. As seen in Figure 7.20, the adsorption process was rapid within the first 6 hours which depended on the vacant adsorption sites at the initial stage of the adsorption of the sulphur compounds. The maximum equilibrium time was observed to be 10 hours for all sulphur compounds. The observed adsorption capacities were higher than those of the polyHIPEs (PHP-ST30, ATS, AMS, and PHP-MEA) previously investigated. This reflects the extent of the accessible adsorption surface due to the presence of micro-meso porosity, the chemical surface structure, and the high surface area. However, all regeneration attempts to reuse the PAC were unsuccessful due to it clumping within a liquid and the difficulty of separating it from the container in an economical way as seen in Figure 7.22.

Figure 7.22 Pictures of the pure PAC before adsorption and the waste PAC after adsorption and regeneration.

In conclusion, the PAC possess desirable surface structural properties, surface chemistry, selectivity and adsorption capacity which would qualify it to be a very attractive adsorbent towards the sulphur compounds if it had not failed in the regeneration experiments. Mixing PAC with the HIPE could improve the relatively poor mechanical properties of the polyHIPE and produce a combination of properties of both PHP and PAC. In addition, this novel adsorbent could be regenerated unlike the pure PAC**.** However, there are still several technical issues to be resolved. Firstly, the homogeneous and uniform PAC distribution through the polyHIPE particles as mentioned before to be addressed by using an ultrasonic homogenizer bath**.** Secondly it was necessary to find the optimum amount of PAC to add as low amounts could not be effective and higher ones could cause negative effects such as closing the pores**.** In this case, various weight ratios starting from 1 to 20% of the oil phase were investigated. The best polyHIPE was produced by adding PAC to polyHIPE and coded as PHP-PAC. This was subsequently subjected to amination as discussed previously and is coded PHP-MEA-PAC.

7.4.2 Characterization of PHP-PAC and PHP-MEA-PAC.

The surface chemistry of the modified polyHIPEs PHP-PAC and PHP-MEA-PAC samples is an important factor affecting their adsorptive capability of. The compositions of PHP-PAC polyHIPEs with various adding ratios (from 1-20% PAC) and PHP-MEA-PAC were investigated by FT-IR spectroscopy as shown in Figures 7.23 and 7.24, respectively. In the wavenumber region between 300−3600 cm^{-1}, for all the PHP-PAC samples, there are strong peaks centring at 3000 cm^{-1} and 3360 cm^{-1}. These are mainly assigned to O−H stretching vibrations of hydroxyl groups (Table 6.6) and are due to the chemisorbed water and oxygen-containing functional groups on the carbon surface. The intensity of the peak in this region increases with increasing PAC ratio (Figure 7.23). The same occurred with the bands at 2850 cm^{-1} and 2950 cm^{-1} ascribed to the aliphatic C-H stretching vibration of CH, CH_2, and CH_3. On the other hand, the main peak appeared at about 1744 cm^{-1} assigned to C=O vibrations attributed to the carboxyl group and carbonyl group (Wu et al., 2013). These identified functional groups on the surface of PHP-PAC samples have been proved to be significantly useful for the adsorption of recalcitrant sulphur compounds (Zhou et al., 2009, Danmaliki et al., 2017, Saleh et al., 2017).

These results imply that adding PAC to the emulsion increases the amount of oxygen-containing functional groups on the PHP-PAC surface; a high PAC addition ratio is beneficial for the formation of more carboxylic groups until it reaches 10% of PAC. For this reason, 10 % PAC addition was used to produce the PHP-MEA-PAC which has the most important peaks of PAC and MEA (Figure 7.24). For all samples, the FTIR spectra showed that the peak intensity attributed to styrene chemistry is lower than the standard PHP demonstrating the effect of incorporation of PAC in the polyHIPE.

This was confirmed by SEM. The PHP-PAC 10% in the PHP-MEA-PAC shows a homogeneous and strong, open structure having thicker walls and vertices, as shown in Figure 7.25 and Table 7. 8.

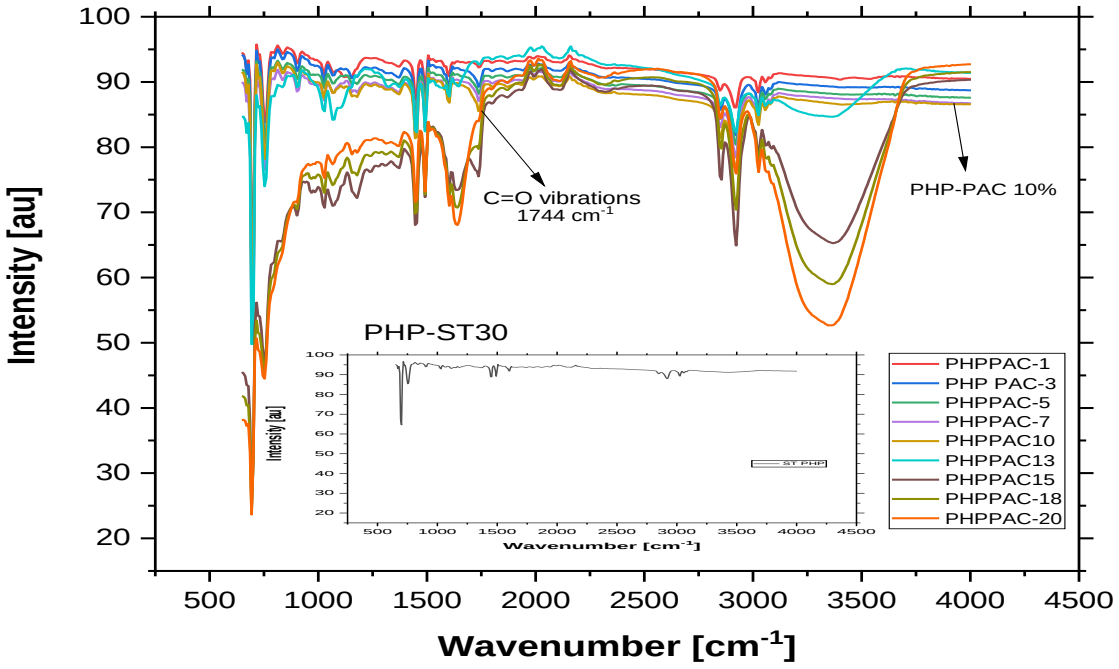

Figure 7.23 FTIR spectra of standard polyHIPE PHP-ST30 and various polyHIPEs mixed with PAC with different adding ratio (1-20%) weight of the oil phase in the emulsion.

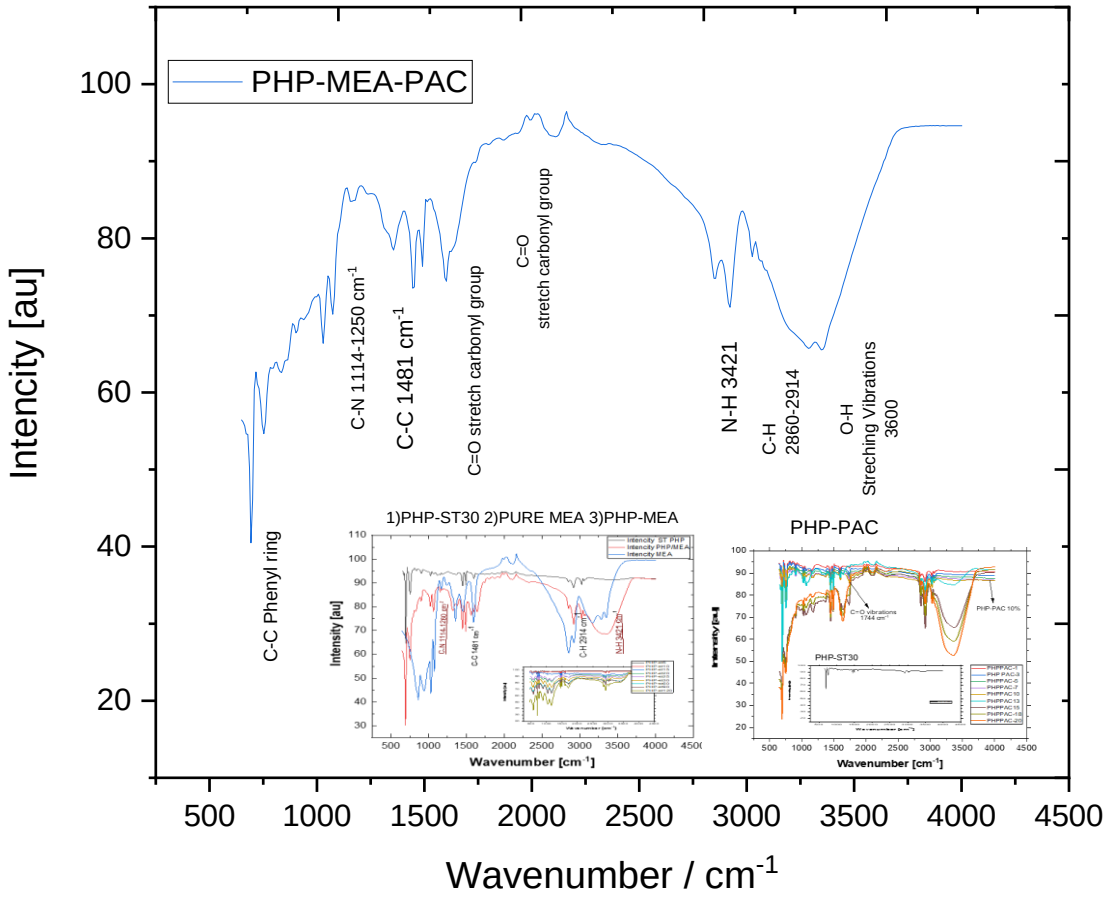

Figure 7.24 FTIR spectra of PHP-MEA-PAC in comparing with PHP-MEA and PHP-PAC.

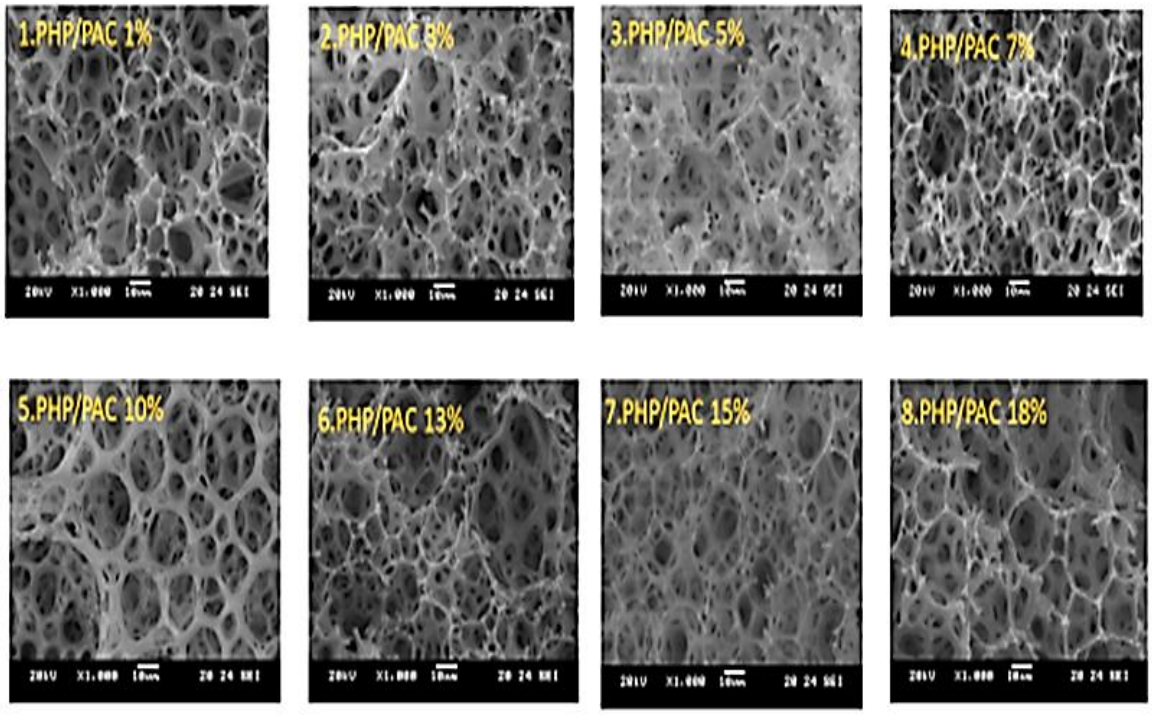

Figure 7.25 SEM micrograph of the PHP-MEA-PAC, modified polyHIPE foams with different PAC ratio: 1) 1%, 2) 3%, 3) 5% 4) 7%, 5) 10% 6) 13%, 7) 15%, 8) 18 wt%. (the magnification of the micrographs is 1000×).

PHP Code	D /µm	d /µm	Tw /µm	Tv /µm
PHP-ST30	12.01	4	1.7	2.8
ATS	22	7	1.78	4.6
AMS	25	9	3.27	8.7
PHP-MEA	16.34	6	2.66	6.27
PHP-MEA-PAC 10%	18.4 12.5	5	4.5	9.2

Table 7.9 Comparison of the average pore size D (µm), average interconnecting pore size d (µm), minimum pore wall thickness Tw (µm), and intersecting vertex thickness Tv (µm) of the standard and modified polyHIPEs versus the reinforced-aminated polyHIPE PHP-MEA-PAC containes 10% PAC.

The structural dimensions of 10% reinforced-aminated polyHIPE comparatively shown in Figure 7.25 (5) and Table 7.9 were also improved by this modification as the pore size D has a bimodal distribution with peaks of of 18.4 and 12.5 µm and average interconnecting size d of 5 µm with narrower differences between the higher and lower values than those in previous adsorbents. Furthermore, there was a significant increase in the minimum pore wall thickness Tw to 4.5 µm, and intersecting vertex thickness Tv of 9.2 µm with a tighter distribution. A significant change was made in morphology, where the network of the pores became more organised, with proportional dimensions close in value. The most important change was the shape of the walls changing into a pyramid shape unlike the film shape in previous polyHIPEs as shown in Figure 7.26. Therefore, this width and shape allow the polyHIPE to have numerous interconnecting pores and nano size pores. At the same time, it does not weaken the strength of the walls and thereby does not affect the mechanical properties whilst increasing the surface area.

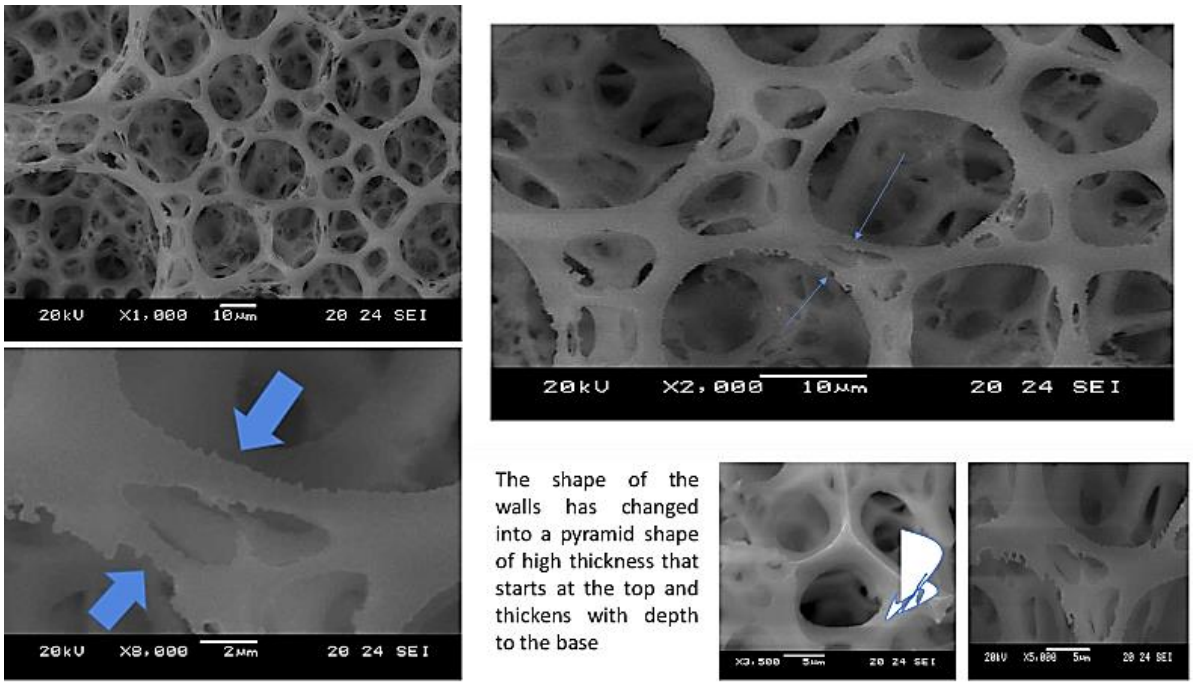

Figure 7.26 SEM image of reinforced aminated polyHIPEs PHP-MEA-PAC at different magnifications before adsorption in which high minimum pore wall thickness Tw, and intersecting vertex thickness Tv.

The mechanical properties improved for all samples of different addition ratios of activated carbon but the losses after washing tended to drive the selection towards the 10% as it has the maximum ratio with the least loss in the PAC content after washing. This addition improved the strain-stress curve and the Young's Modulus to levels about seventy times more than the PHP-MEA. It is worth mentioning that it would never be reached without sonication. The optimum Young's Modulus was 5 MPa obtained at the addition ratio of 10% which, has been

chosen to be the optimum ratio because the SEM image showed the best structure and morphology the highest surface properties, as shown in Figure 7.27and Table 7.10**.**

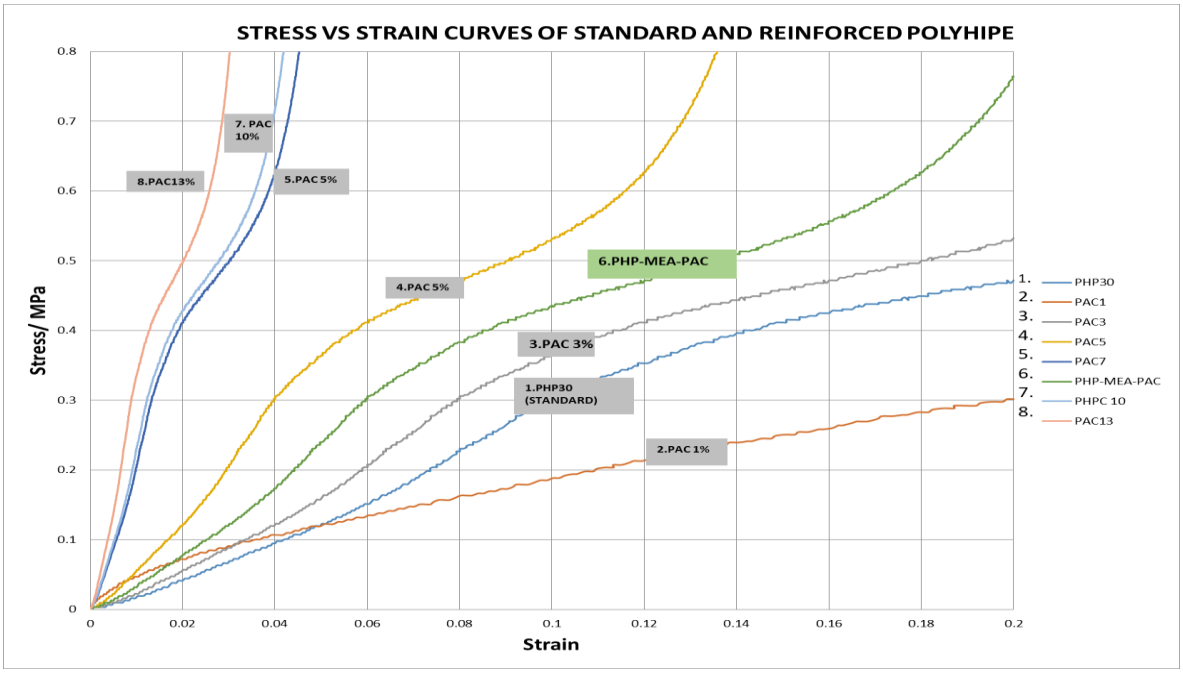

Figure 7. 27 Stress versus strain curves for PHP-MEA-PAC compared with standard polyHIPE PHP-ST30 and PHP-PAC prepared with different addition ratios of PAC to PHP.

PolyHIPE Code	BET Surface Area m^2/g	Pore Volume cm^3/g	Pore Size nm	Young's Modulus/MPa
PHP-ST30	6.3	0.49	≥8.53	3
ATS-30	335	0. 141	1.5-3.84	0.45
AMS-30	355	0.95	0.9-3.16	0.33
PHP-MEA	369.39	0.394	0.9-3.6	1.45
PHP-MEA-PAC	629	0.43	0.5-0.8	5

Table 7.10 Comparison of BET surface area, pore volume, nano-size pores, and Young's Modulus for PHP-ST30, ATS, AMS, PHP-MEA and PHP-PAC (10% weight added to oil phase).

High addition ratios were excluded because they caused the production of closed pores as shown in the Figure 7.28.

The novelty of this work is in increasing both the mechanical properties and the surface area at the same time (surface area of 629 m^2/g and 24 MPa) in addition to the surface structure, colour and physical appearance being improved. Therefore, this modification affected and improved the adsorption capacity, selectivity and regenerability of the adsorbent as will be shown in the next sections.

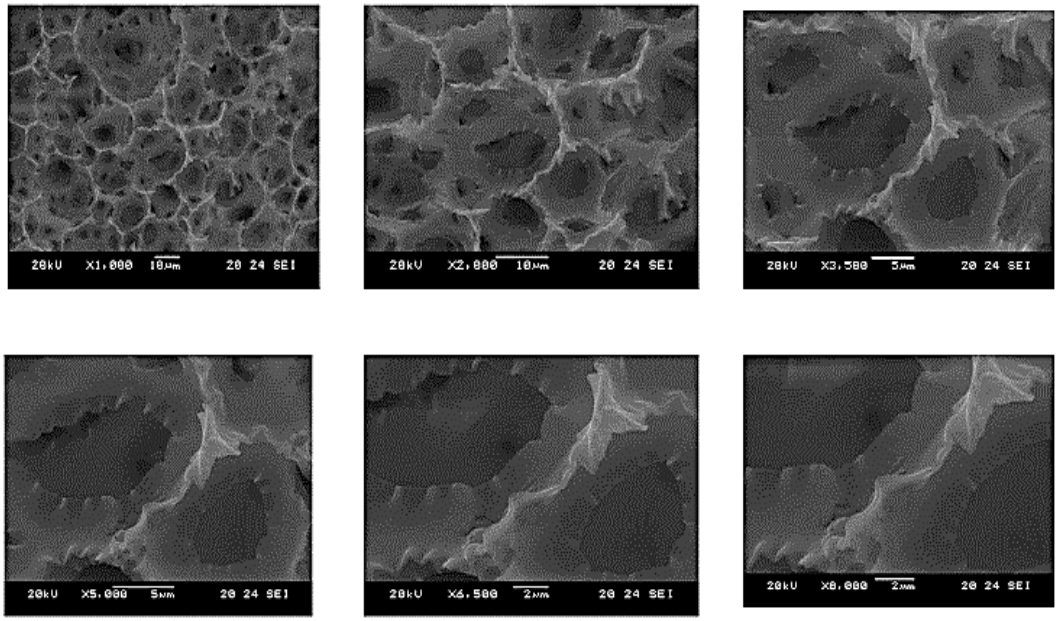

Figure 7. 28 SEM micrographs at different magnifications of the adsorbent PHP-PAC after adding high PAC ratios (higher than 20%) to the HIPE which causes the creation of closed pores.

7.4.3 Sulphur adsorption of the reinforced-aminated polyHIPE PHP-MEA-PAC

Adsorptive Desulphurisation of the model fuel oil by PHP-MEA-PAC is shown in Figure 7.29. The sulphur contents for C4, DPS, DMDS, BT and DBT were decreased from 4000 ppm which was the initial concentration to 1050, 950, 1050, 1025, and 1043 ppm an adsorption capacity of 74%, 76%, 74%, 74%, and 74% respectively. The adsorption process reached plateau after 10 hours for all sulphur compounds.

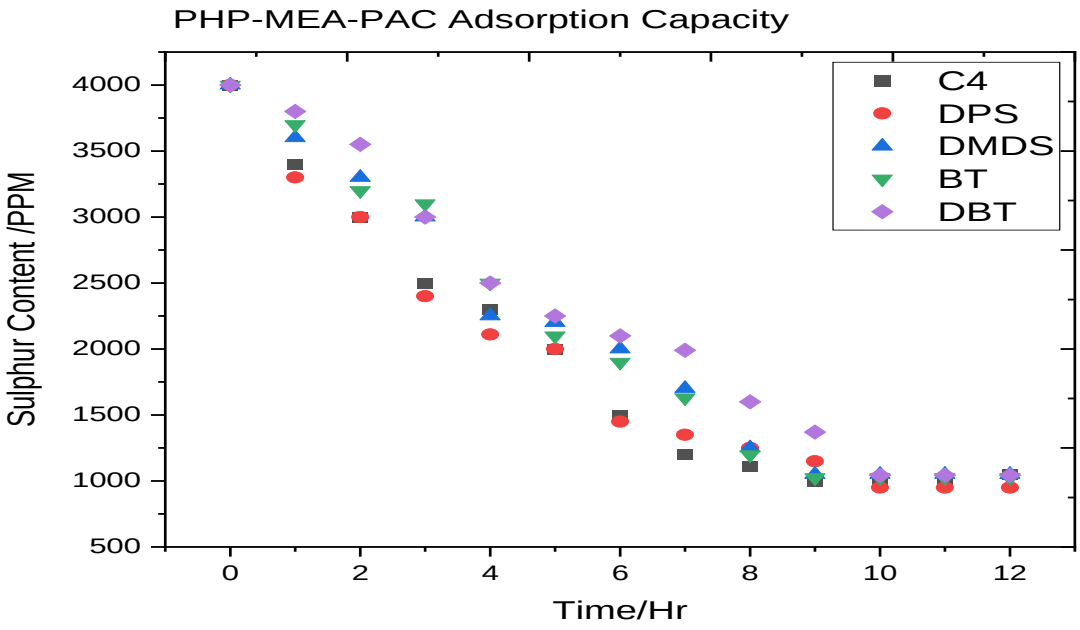

Figure 7. 29 Sulphur breakthrough curves for PHP-MEA-PAC.

The observed adsorption capacities were higher than those of previous polyHIPEs (PHP-ST30, ATS, AMS, and PHP-MEA) including PHP-PAC with the exception of the pure PAC in two results as shown in Figure 7.30. This reflects the extent of accessible adsorption surface due to the additional presence of micro-meso porosity because of the PAC particles trapped in the HIPE, which provides extra possible vacant adsorption sites if they are at the polyHIPE surface. In addition, as a result of HIPE absorption of MEA, the chemical surface of the polyHIPEs are improved because of the active bonds that adhere with sulphur. The high surface area due to both PAC and MEA in the polyHIPE increased the availability of adsorption sites.

Finally, a regeneration process to reuse the PHP-MEA-PAC was successfully developed, which increased the number of useful adsorption cycles, and thus doubled the amount of adsorbed sulphur, thereby giving this adsorbent a comparative advantage, even over activated carbon which had some better initial results, because PAC failed to be regenerated and reused.

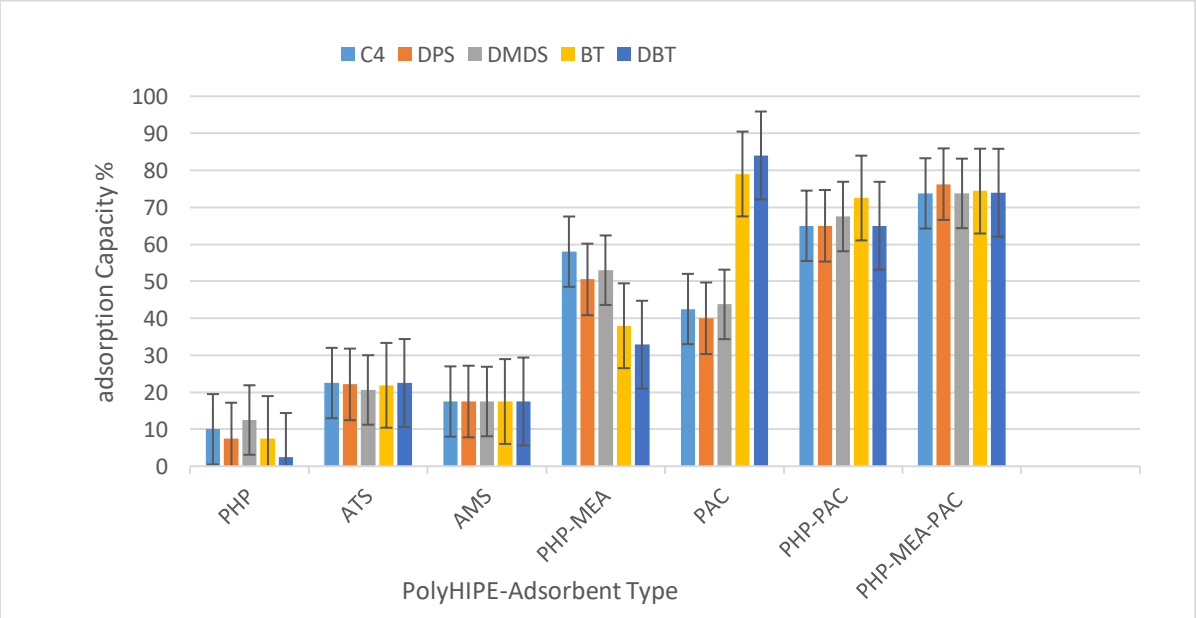

Figure 7.30 Different adsorption capacities of the PHP-ST30, ATS, AMS, PHP-MEA, PAC, PHP-PAC, PHP-MEA-PAC towards the sulphur compounds C4, DPS, DMDS, BT, and DBT.

Preliminary regeneration studies were carried out by filtering the spent adsorbent, removing the waste, followed by isopropanol treatment of the residue in the laboratory atmosphere at 70 °C for 6 hours to remove the adsorbed organosulphur molecules. The starting concentration used was the last concentration reached in the previous adsorption process.

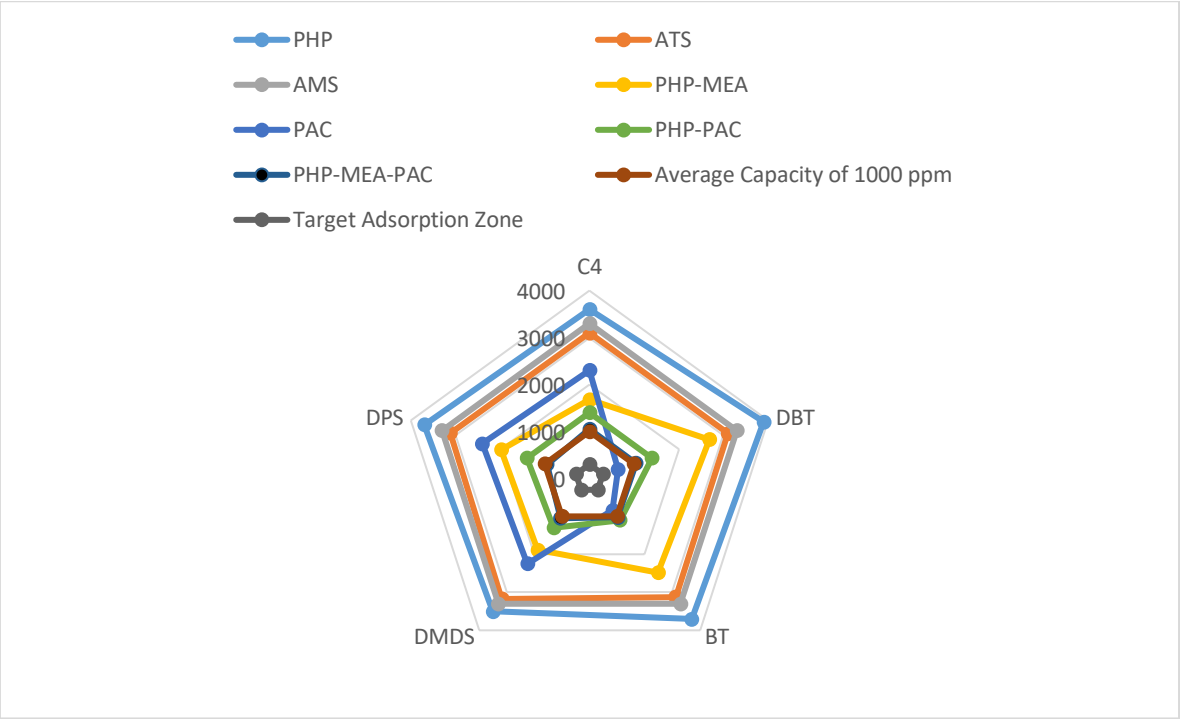

Figure 7.30 Comparison of the average adsorption capacity , average ratio and target adsorption ratio of all produced adsorbents, it shows that PHP-MEA-PAC has reached this value.

Figure 7.30 expressed the actual average adsorption capacity of PHP-MEA-PAC reaching the target adsorption zone in red after several cycles. Regenerable adsorbents, therefore, hold a great promise for an economic factor. Beside the economic factor there are environmental concerns about the disposal of spent adsorbent. Although PHP-MEA-PAC was regenerable, the losses due to fracturing and mechanical damages are still high, as shown in Figure 7.31. Regenerable adsorbents hold great promise for an economically and environmentally friendly adsorbent.

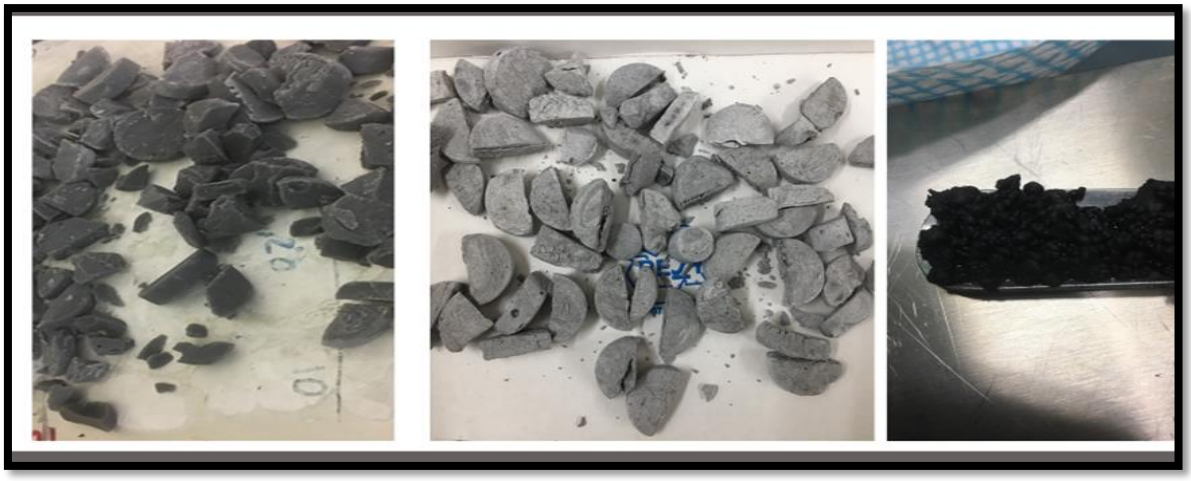

Figure 7.31 Illustration of the losses of waste adsorbent used for the adsorption-regeneration experiments

The spent adsorbent saturated with Sulphur compounds and/or regenerated adsorbent were evaluated after adsorption and regeneration, to assess the amount of wasted adsorbent and determine the efficiency of regeneration and finally to recover the solvent used in regeneration so it could be reused. The results are collected in the next section, which also includes a molding type/regeneration recycling study, together with the regenerated polyHIPE adsorption characterization and solvent recovery studies.

7.5 Regeneration Studies

7.5.1 New Molding type

Losses result because of the physical damage or chemical effects, to avoid these losses and decrease the amount of wasted adsorbent, a new moulding type (Section 4.5.5) has been used, as shown in Figure and has the following advantages and features as shown in Figure 7.32:

1-Less deformation.

2-Reduce Losses.

3-Increased contact surface area. (Barlik and Keskinler, 2014)

4-Uniform particles shape.

5.Identical or approximate characteristics as previous results of large mold since the molding type is made of the same material (Greco, 2014).

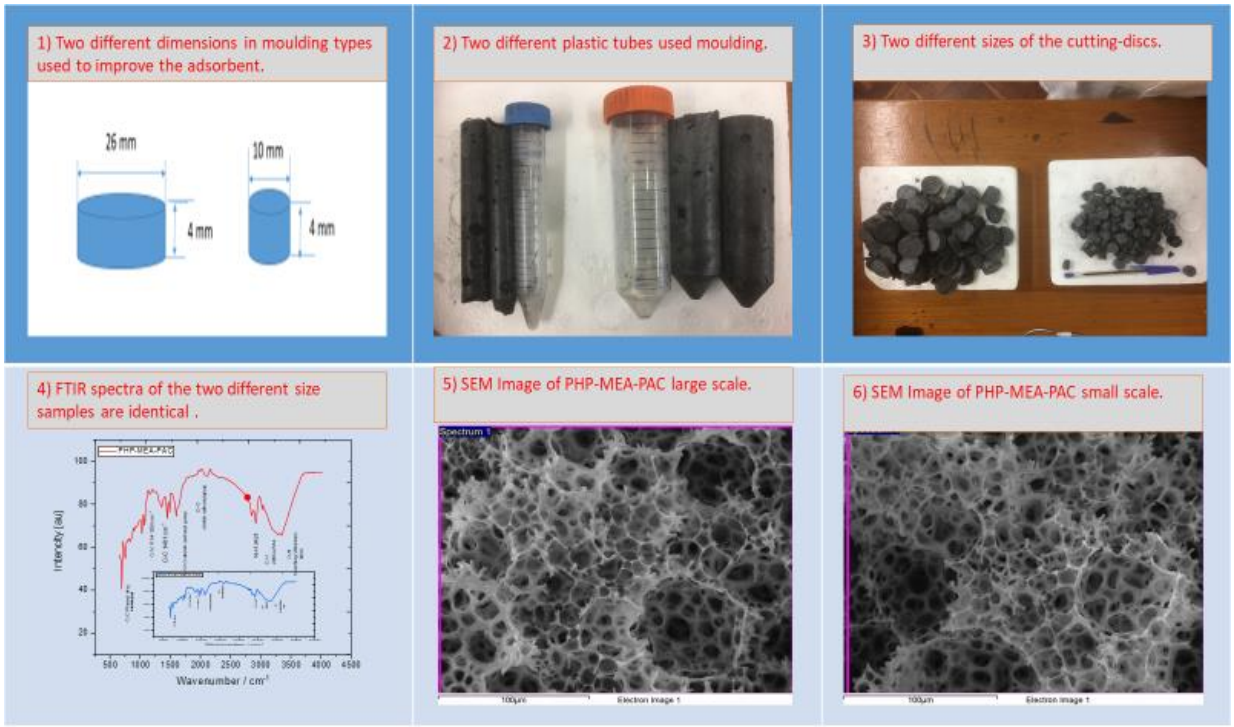

Figure 7.32 Comparison between two PHP-MEA-PAC samples different in size, 1) two different dimensions 2) two different plastic molds 3) different size discs 4) identical FTIR spectra and composition 5,6) SEM revealed same texture and morphology.

7.5.2 Regeneration - adsorption of spent adsorbent

Regeneration of spent adsorbent was carried out using the method explained in Section 5.7 and shown in Figure 5.21 These combined solvent and thermal approaches are similar to previous studies (Shah et al., 2018) but in this study the solvent used was isopropanol to remove the adsorbed sulphur molecules deposited on the surface of the adsorbent. After adsorption using a fixed adsorption time of 10 hours and an initial Sulphur concentration of 4000 ppm, the spent adsorbent was filtered using steel sieves to separate the waste adsorbent and deposited material, followed by drying the remainder of the adsorbent and then determining the weight of the remaining material that can be used followed by isopropanol treatment of the residue in the laboratory atmosphere at 70 °C for 6 hours (two times, 3 hours for each time) to remove the adsorbed organosulphur molecules. Another round of adsorption followed by reusing the regenerated PHP-MEA-PAC – this is called the first regeneration cycle. The overall process was repeated five times for successive adsorption–regeneration cycles. The adsorption breakthrough curves for the regenerated adsorbents are shown in Figure 7.33, where there is marked reduction in the adsorption capacity after the first regeneration then slight differences between successive cycles similar to the results in previous studies (Olajire et al., 2017, Shah et al., 2018, Ma et al., 2003).

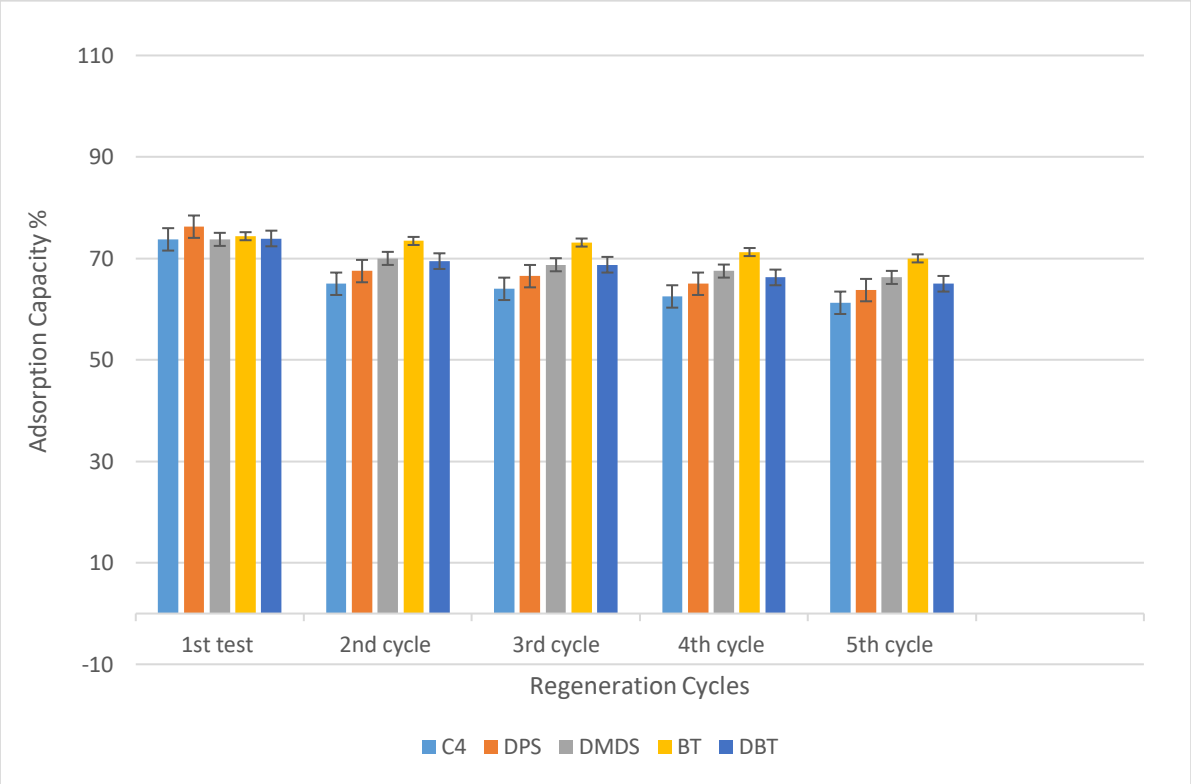

Figure 7.33 The adsorption capacities with error bars after 5 successive adsorbent regeneration cycles for C4, DPS, DMDS, BT and DBT using the PHP-MEA-PAC adsorbent.

In contrast there was a significant reduction in adsorption capacity about 20 % after the five successive regeneration cycles, as shown in Figure 7.33. Despite this, the adsorbent can still be used for at least three regenerative cycles at about 65-73% adsorption capacity for all sulphur compounds.

This result implies that PHP-MEA-PAC is a promising adsorbent for Desulphurisation of the major sulphur compounds existing in liquid hydrocarbon fuels because of its adsorbent capacity, selectivity, and regenerability despite the degradation in the adsorption capacity in use, mainly because the losses approached zero due to the new moulding geometry. Also, there is suitable morphology, surface and mechanical properties that are sufficiently stable for operation.

The sulphur adsorption after the final cycle was tested by FTIR to identify the presence of the five organosulphur groups, the fresh adsorbent and sulphonated adsorbent structure and any changes in the regenerated adsorbents as shown in Figure 7.34. SEM images of the regenerated adsorbent are shown in Figure 7.35. Comparison of the data for the fresh and the regenerated adsorbent, clearly shows that the adsorbent can retain its morphology and composition and thus its mechanical and surface textural properties.

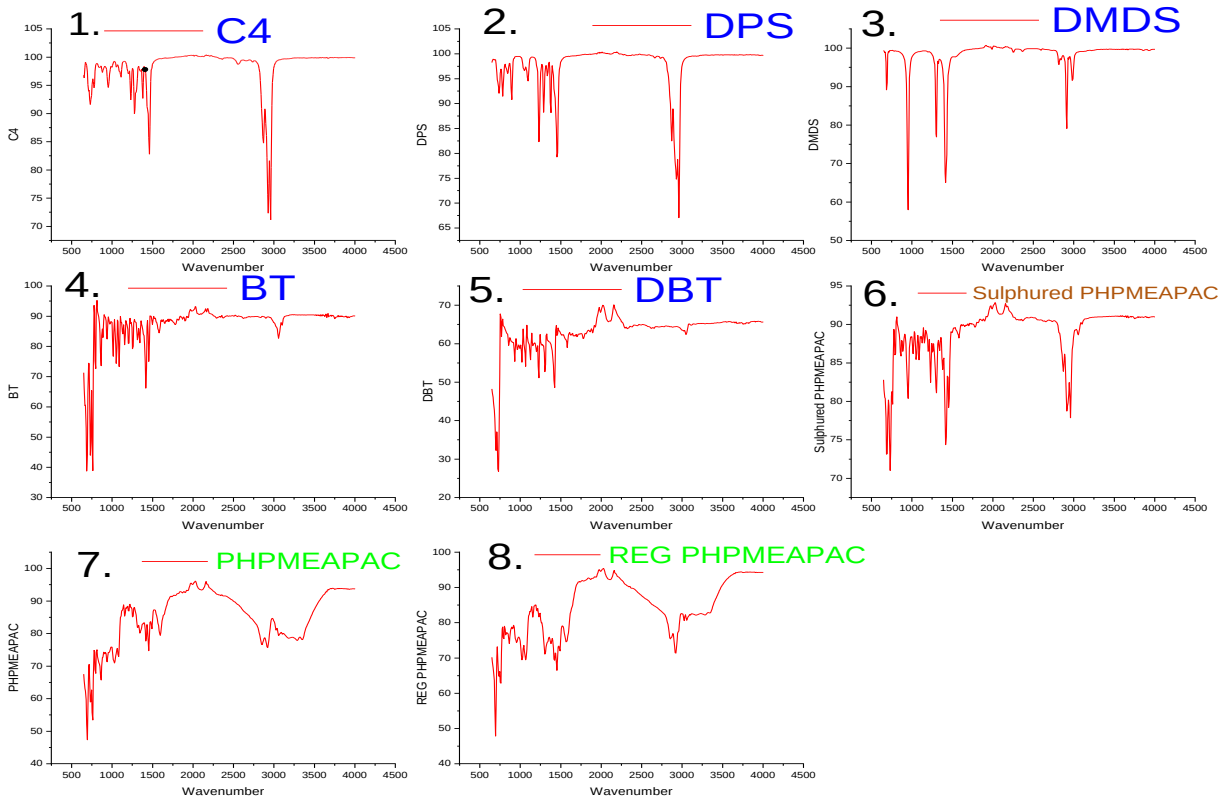

Figure 7. 34 FTIR spectra of organosulphur group 1) C4, 2) DPS, 3) DMDS, 4) BT, and 5) DBT. Also three FTIR spectra of 6) Sulphonated PHP-MEA-PAC affected by the sulphur on its surface, compared with 7) fresh PHP-MEA-PAC and 8) regenerated adsorbent.

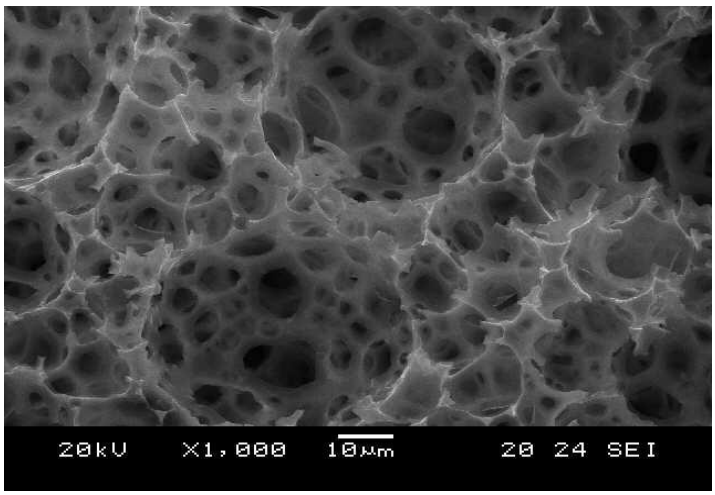

Figure 7. 35 SEM image of regenerated adsorbent PHP-MEA-PAC at magnifications x1000, with same appearance and properties as fresh adsorbent.

It can be seen that the adsorbent behaviour is a result of the synergistic mix of the polyHIPE, MEA, and PAC component behaviours. As explained previously, this is the result of a dual process that includes the absorption of the amine in the HIPE emulsion during preparation as well as the amine in which the polyHIPE discs have been soaked after polymerisation. In addition, PAC was loaded throughout the polymer particles by mixing it carefully in the HIPE. The strength of this adsorbent lies in this combination of polyHIPE, MEA and PAC. Since this product carries the most important characteristics of its components and the highest attraction of sulphur of all samples tested. Moreover, the interaction between the sulphur compounds and the adsorption sites of the three components of the adsorbent allow selective adsorption of a wide range of Sulphur compounds with reasonable, but not excessive, strength. This is important because too strong interaction between them will cause difficulty in the subsequent regeneration operation, while a weak interaction probably leads to low adsorption selectivity and capacity. Thus, any defect of any of the three components will inevitably lead to a less significant failure of the adsorption system because it is based on adsorption of Sulphur by more one component.

This explains the reduction in adsorption capacity after regeneration, there being a reduction in the exposed MEA, or PAC content leading to a reduction in the amount of the adsorbed sulphur. It was found, on the one hand, that some of the sulphur compounds still adhered to the adsorbent surface, as the organosulphur compounds were able to form multilayer stacks on the surface of the modified adsorbent preventing their easy removal from the adsorbent (Danmaliki and Saleh, 2017)**.** This sulphur precipitation eventually causes saturation of the adsorbent**,** which can remain despite re-activation, since it depends on closing of the open pores and reducing the active sites that are responsible for Sulphur adherence, as suggested previously

(Seredych et al., 2009, Ganiyu et al., 2017). This also explains the slight changes in the physical appearance as shown in Figure 7.36.

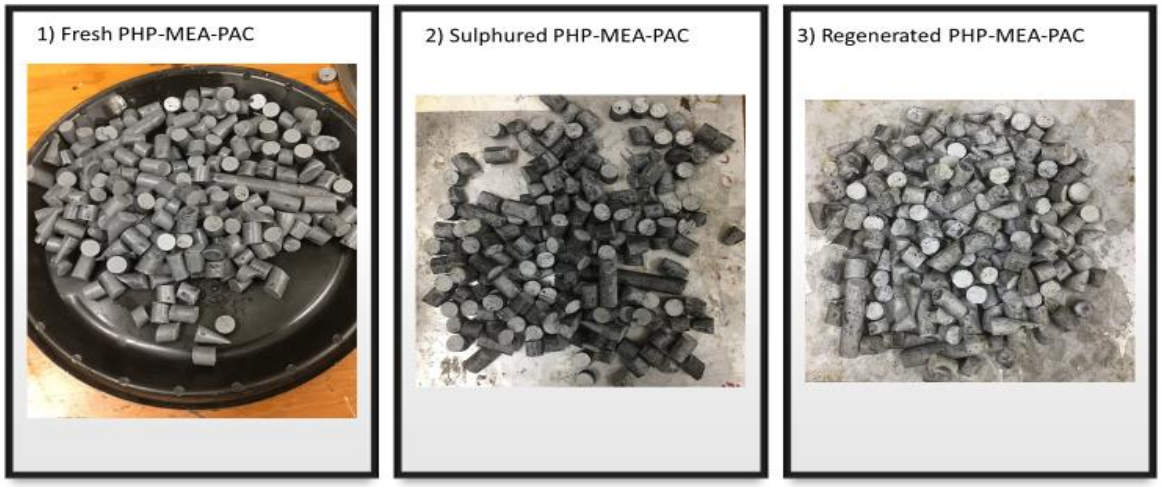

Figure 7. 36 Photograph showing polyHIPE PHP-MEA-PAC, 1) fresh, 2) sulphonated, and 3) regenerated adsorbent.

It was reported in previous studies that the adsorption capacity decreased due to the harsh thermal treatment of the spent adsorbent (Rui et al., 2017), while in this study no harsh treatment in regenerating the spent adsorbent was used as the solvent washing is conducted at 70 ℃ which relatively low temperature. The solvent recovery is an important step in the adsorption-regeneration cycles because it lowers the cost of the process instead of using solvent make-up, the spent solvent can be completely regenerated without losing its quality or quantity as explained in the next section.

7.5.3 Solvent recovery

The final step is to recover the solvent used in the adsorbent regeneration. This experiment was carried out by using the method and distillation column described in Section 5.8. After the condensation of the solvent is conducted, two liquids are produced, these are recovered solvent in the beaker (raffinate or distilled solvent) and high sulphur content waste in the flask (extract or reduced solvent). Desulphurized (regenerated) solvent was used for further FTIR and GC tests to be compared with the standard isopropanol and the same procedure was applied for the high sulphur content solvent as compared to standard solution containg typical model fuel oil dissolved in isopropanol. The GC results and FTIR spectra in Figure 7.37 a and b showed that the recovered isopropanol has identical composition to the standard isopropanol. This promising result implies that the solvent can be re-used as the regenerated solvent has the same results as the pure solvent. This adds an econmic advantage to the method in this study. The

high sulphur residual solvent has some differences in the FTIR peaks because it contain some waste from water, chemicals or impurities in the adsorbents discs.

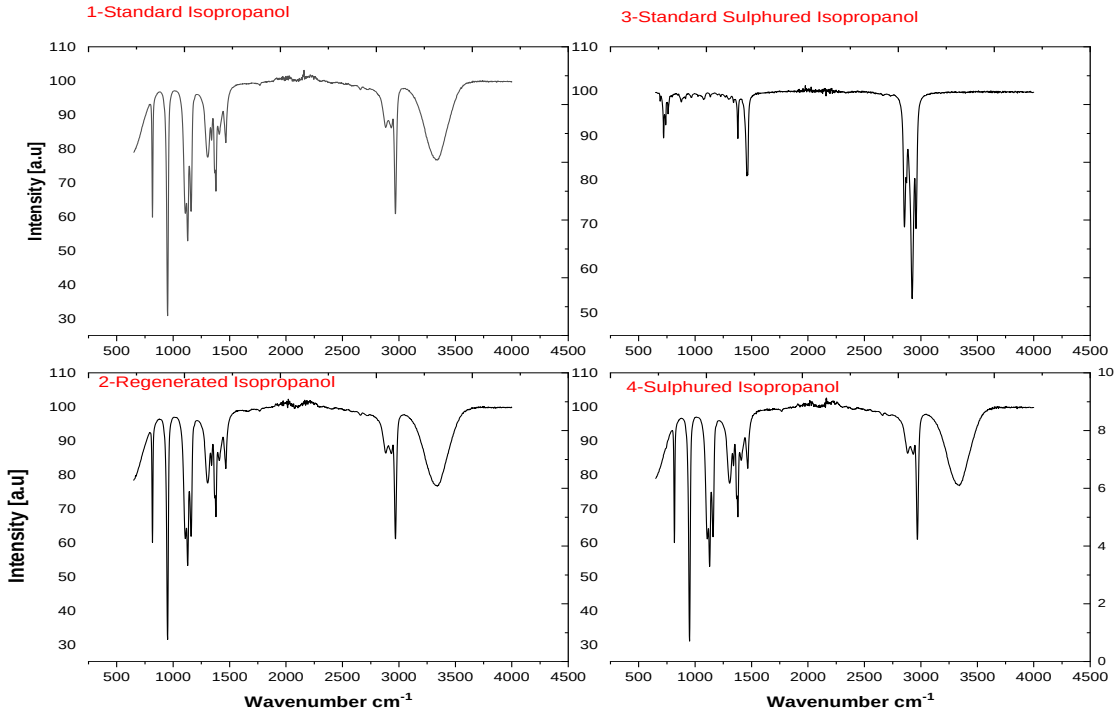

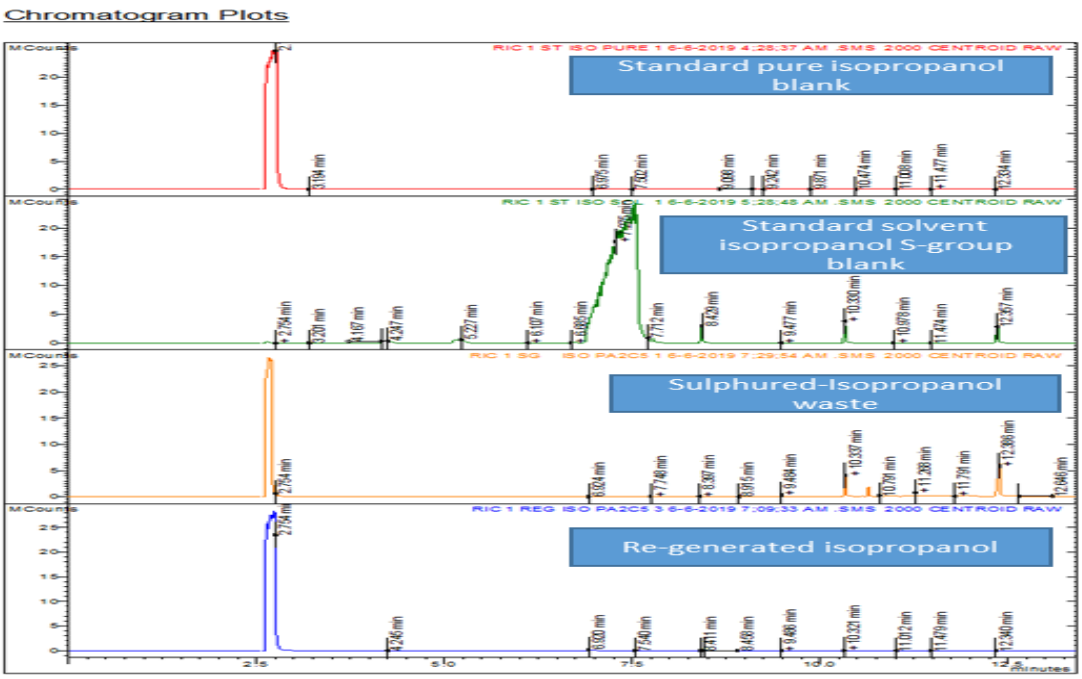

Figure 7. 37 FTIR spectra and (b) gas chromatogram plots showing identical results between pure and regenerated isopropanol.

The residue of the solvent, which contains sulphur deposits, cab be treated (preferably) by known methods such as burning or sulphuric acid production, and this will complete the production cycle mentioned in the methodology chapter.

7.6 Summary and Preliminary Conclusion

This chapter has described a novel Desulphurisation process for model fuel oil containing various kinds of sulphur compounds, based on a new synthesis technique for an adsorbent using a series of modified polyHIPEs optimised for for sulphur removal and mechanical strength.

The first polyHIPE modification produced functionalized polyHIPE by sulphonation. The results showed that ATS and AMS slightly improved adsorption capacity in comparing with those of standard polyHIPE PHP-ST30 produced in the previous chapter but with a reduction in mechanical properties, characterization results giving a priority to the thermal sulphonation method rather than the microwave method.

The next modification was by adding MEA to the HIPE. The polyHIPE was modified as the MEA spread through minute pores or spaces between its molecules in complete absorption. Amine modification (amination) showed an increased adsorption capacity due to the enhancement in its porosity and the appearance of several different active sites that adsorbed sulphur. However, this adsorbent failed to be applicable due to its poor mechanical properties and incapability for regeneration and reuse. Then, to improve the mechanical and physical properties of the previous adsorbent, the polyHIPE was reinforced by adding a specific amount of PAC. Some of experiments conducted characterised the raw materials both PAC and PHP-PAC before producing the best version of the adsorbent PHP-MEA-PAC.

PHP-MEA-PAC is a promising adsorbent for desulphurisation of all types of organosulphur in liquid fuels. The presence of MEA and PAC on the surface of the polyHIPE was confirmed by surface characterizations.

The adsorbent was successfully optimized and produced to fit the adsorbent requirement conditions which are adsorption capacity, selectivity, and regenerability.

These promising results encouraged the study to go further to examine the adsorbent with real fuel oil produced from Iraqi oil refineries and suggest a position and layout for the proposed sulphur treatment operation unit in a typical refinery.

8 Iraqi oils: Desulphurisation of naphtha, kerosene, and gas oil

8.1 Country analysis in brief: Iraq oil consumption and refining

Iraq a leading oil-producing county and a founding member of OPEC. It represents the second-largest crude oil producer and possesses the fifth largest proved crude oil reserves in the world. Iraq's economy is heavily dependent on oil revenues, for instance, in 2014, revenue from crude oil exports accounted for 93% of economic exports, according to the International Monetary Fund (IMF) (Administration, 2016).

Iraqi crude oil production has achieved increased growth over the last twenty years. For example, between 2011 and 2015, it achieved growth of about 1.5 million bbl/d (barrels per day), as it increased from 2.6 million bbl/d in 2011 to 4.1 million bbl/d in the year 2015 (Hadi, 2017, Donovan et al., 2013), then to 4.5 bbl./d for March 2020 (Energy Information Administration, 2020).

In Iraq, the domestic crude oil consumption is 770,000 bbl/d of produced crude oil and other liquids. Most of Iraq's petroleum consumption is produced in oil refineries, which are supplied by domestically produced oil. However, Iraq typically imports approximately 100,000 b/d of petroleum products such as gas oil and jet fuel. This is for several reasons, the first of which is a decrease in production due to a shortage in the number of production units as a result of war and equipment deterioration over time, offset by an increase in the population and the actual need to maximize production, as well as a lack of important operational units such as hydrogenation, isomerization, alkylation, and sulphur treatment.

Today, the total design refinery capacity is more than 1.0 million b/d as shown in Table 8.1., while the effective capacity which is actually available to use has decreased to lower than the design capacity at many refineries, for instance, the Baiji refinery which has the largest capacity is not operational, reducing total effective capacity to below 600,000 b/d.

Refinery	Design Capacity `000 b/d	Notes
North Refineries Company Effective capacity was 230,000 b/d prior to the June 2014 attack on the refinery by ISIL. Total North	412	
Baiji	310	Baiji is not operating and is severely damaged.
Kirkuk	30	
Sininya	30	
Hadeetha	16	
Qayyarah	16	
Kasak	10	
Midland Refineries Company Total Midland	270	
Daura	210	Effective capacity is 140,000 b/d
Najaf	30	3 package units of 10,000 b/d
Samawah	30	3 package units of 10,000 b/d
Diwania	30	3 package units of 10,000 b/d
Karbalaa	---	Under project design capacity is 140,000 b/d
South Refineries Company Total south	270	
Basrah	210	effective capacity is 135,000 b/d
Missan	30	3 package units of 10,000 b/d
Nassiriya	30	3 package units of 10,000 b/d
(Iraq Kurdistan)		
KAR Group	80	
Qaiwan Group	34	

Table 8.1 Existing oil refineries; the yellow background refers to small refineries of 10,000 b/d capacity.

Iraqi refineries can be classified into small and medium capacity 210 to 310 bbl./d. In Table 8.1 Baiji, Daura and Basrah are medium production capacity, each with the highest capacities and different sulphur treatments units such as hydrodesulphurisation. While the yellow highlighted

capacity in the table refers to the small refineries; these are a mix of small distillation units of 10,000 bbl/d without sulphur treatment or other advanced units. They produce more heavy fuel oil than is needed domestically and insufficient other refined products, such as gasoline, because of the lack of sulphur treatment necessary for sale to the final consumer. Therefore, light distillation products are sometimes transferred to other medium capacity refineries as seen in the map drawn in Figure 8.1 to reduce their sulphur content adding extra transportation costs. There are plans to build new Desulphurisation units in these refineries, but many obstacles are anticipated because the hydrodesulphurisation units need high capacities to be economically viable. This encourages studies to find other solutions or new technologies.

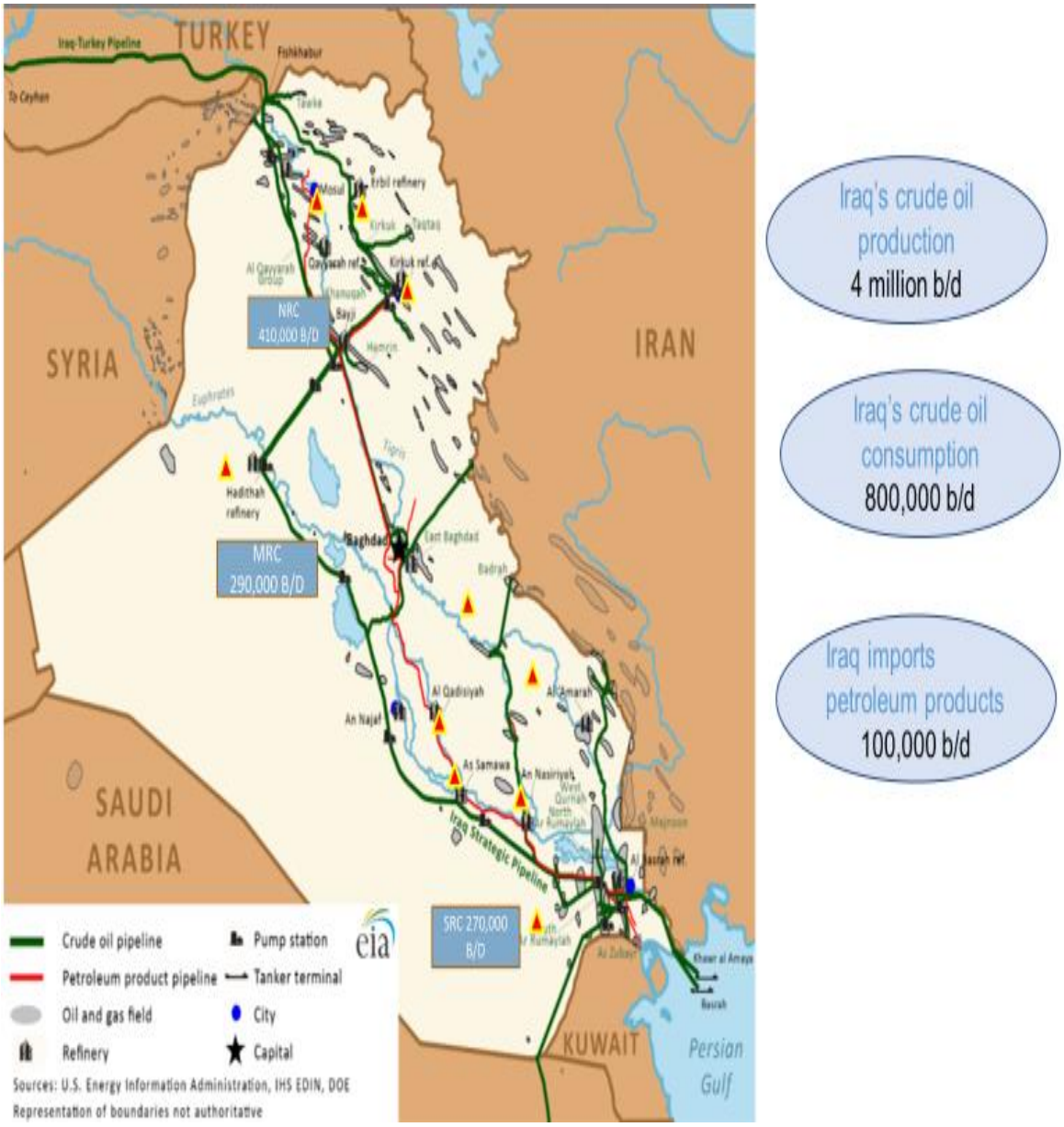

Figure 8.1 Iraq's oil and natural gas infrastructure; three main refineries are named with the red triangles indicating to the small refineries.

Among the different technologies for sulphur treatment, adsorption offers better solution, performance and fewer problems compared with other advanced processes as shown in previous chapters. It is also an economical solution by developing adsorbent at much lower cost and is potentially suitable for the smaller refineries. However, it needs to be demonstrated that it works with Iraqi crude at sufficient scale to be practicable.

8.2 Fixed bed adsorption experiments using PHP-MEA-PAC as adsorbent

In this study, a fixed bed adsorption experiment was conducted to evaluate the adsorption capacity at ambient temperature and pressure of the synthesized adsorbent PHP-MEA-PAC for a real crude oil product. The use of continuous adsorption was chosen in terms of fixed bed adsorption as in the photo in Figure 5.3 and the scheme in Figure 8.2 to mimic the continuous adsorptive Desulphurisation treatment of larger volumes that are used industrially, removing or reducing sulphur content from the main derivatives. The feedstock of the process are the light oil products; naphtha, kerosene, and gas oil produced in the Midland Refineries Company in Iraq. These are analysed in the laboratories of the refinery, for more details, results are shown in the Appendices 4,6 and 8.

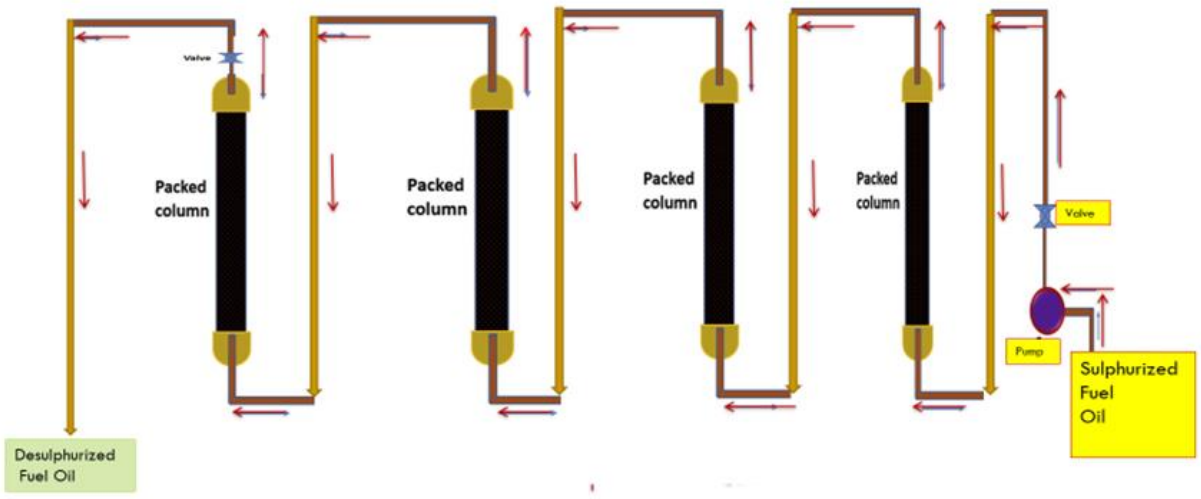

Figure 8.2 Illustration of the fixed bed reactor used for the breakthrough experiments.

A preliminary survey and experimental studies were conducted in the refineries to identify the general characterizations and specifications of both crude oil and the three light products before preparing them for adsorption. These are detailed in Appendices 4 and 6 in addition to a brief explanation of their methodology in Appendix 5. It worthy of mention that this adsorbent was not suitable for unprocessed crude oil and reduced crude vacuum residue and fuel since they

have high a viscosity and density and cannot penetrate through the individual adsorbent discs and flow through the column.

In addition, this work aims to develop the novel technology of removing sulphur from commercial products by using the adsorbent PHP-MEA-PAC to overcome the challenges of expanding capacity in some of the existing refineries, to ease the shortage of transportation fuel and eventually export refined products which will add an economic viability to both medium and small refineries**.** The main goal of this process is therefore to assess the PHP-MEA-PAC as a nano-adsorbent, evaluate its adsorption capacity to the sulphur content and suggest where this process can be located in the process flow in the refinery.

8.3 Desulphurisation curves of naphtha, kerosene, and gas oil

Figure 8.3.1,2 and 3 represent continious adsorptive desulphurisation curves of naphtha, kerosene, and gas oil respectively using the adsorbent PHP-MEA-PAC. The experiment and analysis have been conducted in the Midland Refinires Company (MRC) in Iraq under the agreement of the outstanding study in Appendix 7. Also Appendix 5 explained the test methods used. ASTM D5453 - which is used as a standard test method for determination of total sulphur in light hydrocarbons, specifically naphtha and kerosene. While secondly ASTM 4294 was the standard test method for determination of total sulphur in petroleum and petroleum product namely as gas oil by X-ray fluorescence spectrometry.

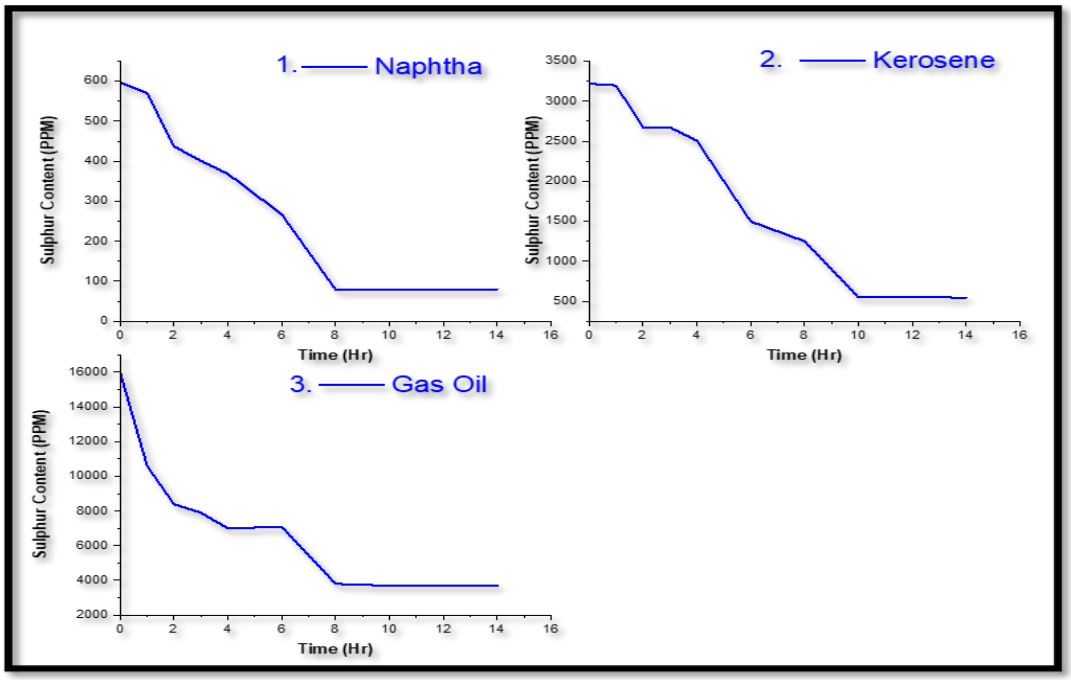

Figure 8.3 Sulphur breakthrough curve using PHP-MEA-PAC at room temperature and 14 hr. 1. Naphtha 2. Kerosene and 3.Gas oil.

Naphtha (explained in both Sections 2.6, 2.7 and 2.8) is an intermediate hydrocarbon liquid stream derived from the refining of crude oil entered in the main distillation column C-101. Naphtha should be treated and have a sulphur content of 1.2 ppm before transferring it to the catalytic reforming to produce the final product, which is gasoline (as shown in Figure 2.8). The initial sulphur content was between (597-789) ppm. Although the adsorbent showed high sulphur capacity and removed about 87%, it did not reach thesulphur content of 1.2 ppm previously mentione and was between 30-80 ppm as shown in Figure 8.3-1. However, the adsorbent showed good regeneration ability with insignificant losses in the total mass.

Kerosene was desulphurised to reach the target sulphur content of 11 ppm from the initial sulphur content of 3200 ppm. The first adsorption cycle reached constant sulphur content of 550 ppm in 14 hours as shown in Figure 8.3-2. The adsorbent reveals promising results in terms of the high adsorption capacity, which is about 82% and the ability for regeneration as no physical changes in the discs appearnce, the losses in the adsorbent discs approched to zero as no fragment or broken discs.This makes it an effective adsorbent despite it not reaching the industrial target.

Similarly, the Desulphurisation of gas oil with PHP-MEA-PAC as adsorbent was carried out under the same operating conditions. The produced gas oil from the distillation tower has an initial sulpur content of 16000 ppm. The adsorbent showed a high capacity of 77% after the first adsorptive Desulphurisation cycle as the sulphur content obtained was 3700 ppm and then the adsorption-regeneration cycles reach 545 ppm which is still far away from the target of 11 ppm (Figure 8.3-3). However, the result reveals that the PHP-MEA-PAC possesses promising adsorption capacity and regenerabilty as the final capacity was 96 % and no changes in the discs appearnce, the losses in the adsorbent discs approched to zero as no fragment or broken discs.

8.4 Suggesting the addition of adsorptive desulphorization units in light of the marketing specifications of the Iraqi petroleum products

According to the marketing specifications guide of Iraqi petroleum products 2013 (Appendix 9, pages 29 naphtha, 31 kerosene and 32 gas oil) the local marketing sulphur content illustrated that 2000 ppm for naphtha and kerosene and 10000 ppm for gas oil is produced from the oil refineries. So the proposition to construct an adsorption unit will definitely improve the specifications of the fuel and reduce its environmental impact. In addition for small refineries, the adsorption unit will improve the sulphur content and other relevant specifications (Al

Zubaidy et al., 2013, Al Zubaidi et al., 2015). The nominated places where Desulphurisation units should be installed and their exact configuration are determined by refinery capacity and the nature of stream to be desulphurized, its sulphur content, and the desired product specifications. A modified flow scheme of an oil refinery (previously shown in Figure 2.8) is shown in Figure 8.4 with the possible locations for Desulphurisation units. For the small Iraqi refineries in Table 8.1, the package units of 10,000 b/d refer to the blue blocks after the main distillation tower. This will reduce transportation costs from small refineries to medium capacity refineries (for Desulphurisation) and save production costs and others, not to mention that it will maximize final products, and thus save the import of these fuels from neighbouring countries. From an engineering point of view the yellow blocks in the scheme refer to the proposed roles that unit could play, ranging in importance from being an alternative unit of hydroDesulphurisation units or playing a supporting role to protect the catalyst (guard) or a complementary role to obtain complete removal of sulphur.

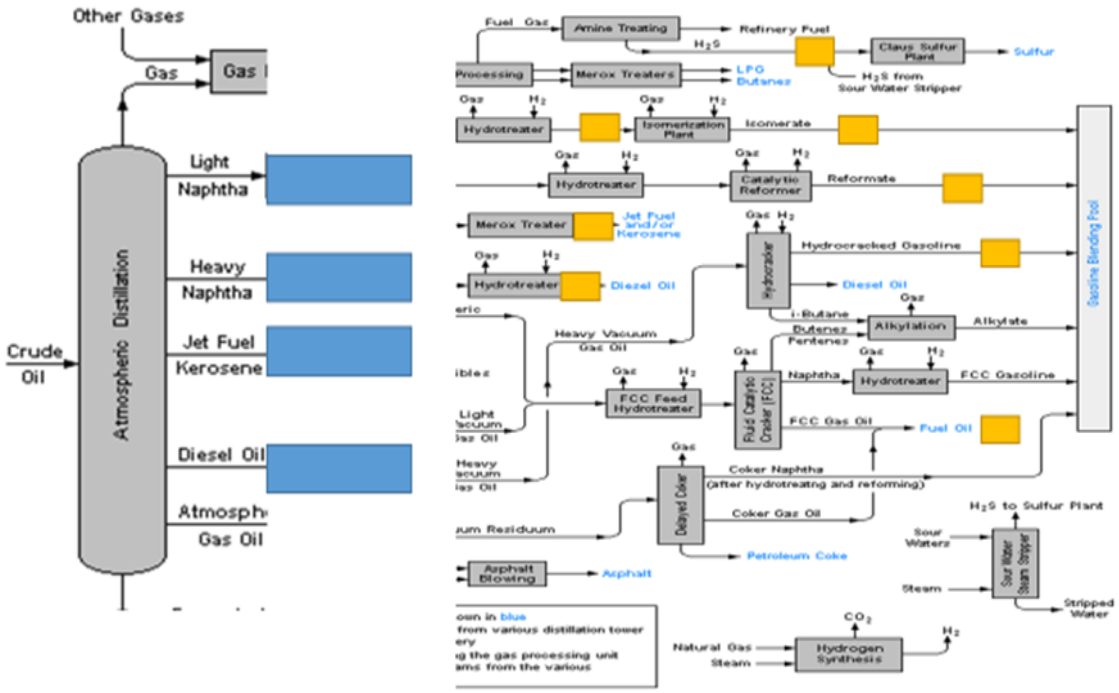

Figure 8.4 Modifying Figure 2. 3 by adding a simplified flow scheme of an oil refinery with possible locations of sulphur treating units; the blue block shows small refineries while the yellow is for the medium capacity refineries.

In conclusion, the adsorbent showed a unique property of selectively adsorbing molecules based on their size, configuration, polarity, and other physical characteristics, namely a sufficient stiffness to withstand the real light petroleum products flow rate and sufficient strength to not break during the adsorptive Desulphurisation process. For all main and real light products the raw materials for the transportation fuels were products such as gasoline, diesel, and jet fuel.

9 Conclusions and Future work

This chapter presents the conclusions that can be drawn in the light of the experimental and analytical findings on the three parts of work

9.1 Overview of the findings

The aim of this thesis was to develop a technology based on adsorptive desulphurisation using a nanostructured polyHIPE material due to high surface area can adsorb many times its own weight in sulphur compounds whilst rejecting hydrocarbons. To achieve this challenging task, three main steps have been conducted. Firstly, in Chapter six, the study investigated producing a standard polyHIPE using methodologies based on past research in order to determine the relationship between the standard PHP morphology and the sulphur adsorption capacity from a pre-prepared model fuel oil created by adding the main organosulphur compounds to octane. The aim was to find the optimum process-structure-property combination for best adsorption capacity of the adsorbent since this depends on its surface properties, including surface area and porosity and the best regenerability which depends on the mechanical properties as well. This provided the baseline for more in-depth research in Chapter 7, which dealt with modification of PHP to increase its chances to be used as effective adsorbent. This requited more detailed adsorptive desulphurisation studies. This chapter examined the adsorbent synthesis by modifying the adsorbent to improve its features. The adsorbent was evaluated at each modification stage to test the adsorbents sulphur removal capability and the adsorbent reusability. Meanwhile regeneration, solvent recovery and structural investigations after adsorption have been conducted to ensure that the adsorbent can be applicable and economic industry.

Finally, the best performing and most cost-effective hierarchical porous polymer-adsorbent PHP-MEA-PAC was successfully produced in larger amounts and applied as an absorbent for the removal of organosulphur species of real transportation fuel oil which was produced in Iraqi oil refineries. This will be used to assess the future work that is necessary to take the current developments to commercial scale.

The present study showed that PHP-MEA-PAC nanoparticles-modified polyHIPE pellets is a promising adsorbent for desulphurisation of transportation fuel with high sulphur capacity.

The following conclusions can be drawn from the current study: -

- In chapter six, it has been shown standard polyHIPE (PHP-ST) were successfully produced at different mixing times (5-10-15-20-25-30-60-90 and 120 minutes) which exhibited an open structure with many nano- and micro-pores. PHP-ST SEM images revealed a hierarchical pore structure, large pores produced from the HIPE droplets having a range 3.85-18.16 µm, average interconnecting size of 1.5-4.85 µm, minimum pore wall thickness Tw /µm of 1.7-0.53 µm with intersecting vertex thickness Tv of 2.8-1.05 µm. Oil uptake tests indicate hierarchical porosity required for adsorbent particles is present in polyHIPE materials.

- It can be observed from the FTIR results that there was no significant difference in the material produced with an increase of mixing time which means there is no effect of mixing time on the chemical composition of the standard polyHIPEs. BET surface area increases slightly with the mixing time from (1.05-9.6 m^2/g) due to formation of more nanopores, the pore volume results show a small increase from 0.25-0.9 cm^3/g and nanopores within each pore wall with its neighbors ranging from 21.82 to 3.15 nm. These ranges are reasonable for the adsorption process and improved in general as the mixing time increased; the best results occurred after the time of 25-120 minutes and since the BET surface area increases only slightly with the mixing time from 1.05-9.6 m^2/g in this range due to formation of more nanopores. In the same conditions the pore volume results show a small increase from 0.25-0.9 cm^3/g. The Young's Modulus results indicate that the mechanical properties are not really suitable for adsorbent particles as too high deformation would be produced in use, the maximum Young's Modulus value was only 3MPa for the higher mixing time sample PHP-ST30. These results have been used to set the best mixing time to give the best structure-property relationship for the materials; the highest surface area and Young's Modulus was obtained at 30 minutes mixing time for sample PHP-ST30.

- A model fuel oil was created by adding the different organic sulphur compounds available in a typical Iraqi oil to a base fluid. The model oil was prepared by dissolving butanethiol, methyl n-propylsulfide, dipropyldisulfide, benzothiophene and dibenzothiophene in n-octane. The GC and FTIR tests indicated that the model oil was stable and does not affect the material of the adsorbent and vice versa.

- Finally, the adsorption capacity for all adsorbents (standard polyHIPEs of different mixing time) was measured and ranged between 6-10 %: this is a very low value and still far from the target zone 98 % especially when the adsorbent could not be reused due to its poor mechanical properties.

- From the previous findings, it can be concluded that a promising adsorbent has been produced since the polyHIPE shows an ability to adsorb the sulphur and a flexibility in modification to improve its structure, properties, and processing. However, its adsorption capacity and regenerability should be improved and its surface area should be increased to be an effective adsorbent. This requires improving the morphology, activating the surface chemistry, increasing the surface area and enhancing the mechanical properties of the standard material produced at mixing time of 30 minutes. There suits of this activity form the basis for Chapter 7.

- The first polyHIPE modification was to produce a functionalized polyHIPE by sulphonation. The results showed that improvement in surface area leads to slight improvement in adsorption capacity when compared to the standard polyHIPE PHP-ST30; it has been observed that adsorption improved with sulphonation, from 6-8% using PHP-ST30 to 12.5% and 15.8% using ATS and AMS respectively but with a reduction in mechanical properties. Structural characterization results give a slight advantage to the thermal sulphonation method rather than the microwave method. The traditional thermal method as shown before produced more homogeneous pore distribution with no local burning of discs and less cracking than in microwave sulphonation.

- PHP/MEA was prepared using the same technique as that of standard polyHIPE but with the incorporation of MEA. The results indicate that PHP-MEA was successfully produced by the novel amination methodology. SEM images and BET tests revealed a sucessful morphology, relatively high surface area and improved surface textural properties, - a more effective pore distribution. The composition possesses more active sites represented by amine bonds which played a fundamental role for sulphur adsorption up to 33-58% . However, the mechanical properties, physical appearance and

other properties represent a drawback that make it hard to rgenerate and reuse which prevents producing a successful adsorbent

- PHP-PAC was prepared to reinforce polyHIPE by using activated carbon to improve the mechanical and physical properties of the previous adsorbent. It was found that adding 10 % PAC to the emulsion improved the mechanical properties and increased the surface area. SEM images of the morphology of PHP-PAC 10% also revealed a homogeneous and strong / open structure, having thicker walls and vertices. This encouraged the study to produce the final modified version of the adsorbent as PHP-MEA-PAC.

The novelty of this work is in increasing both the mechanical properties and the surface area at the same time (surface area of 629 m^2/g and Young's Modulus 5 MPa) in addition to the texture, colour and physical appearance being improved. This modification improved the adsorption capacity, selectivity and regenerability of the adsorbent as shown in the Table 9.1.

PolyHIPE Code	BET Surface Area m^2/g	Pore Volume cm^3/g	Pore Size Nm	Young's Modulus/MPa	Adsorption Capacity%
PHP-ST30	6.3	0.49	≥8.53	3	6-8
ATS-30	335	0. 141	1.5-3.84	0.45	12-15
AMS-30	355	0.95	0.9-3.16	0.33	11-13.5
PHP-MEA	369	0.394	0.9-3.6	1.45	33-58
PHP-MEA-PAC	629	0.43	0.5-0.8	5	74-76

Table 9.1 Comparison of BET surface area, pore volume, nano-size pores and Young's Modulus for PHP-ST30, ATS, AMS and PHP-MEA and their adsorption capacity.

In conclusion a novel combination of polyHIPE, MEA and activated carbon has been successfully used to create a cost-effective adsorbent with synergistic propertiesbased on a hierarchical porous polymer-adsorbent. PHP-MEA-PAC showed a high Sulphur capacity of more than 74%. FTIR measurements confirmed the formation of PHP-MEA-PAC bonding with Sulphur compounds. The composite showed a high capacity even in low sulphur concentrations.

The optimum adsorption desulfurization capacity of the adsorbent varies from PHP-MEA-PAC > PHP-PAC > PHP-MEA > ATS > AMS > PHP-ST. Among them, the PHP-MEA-PAC adsorbent showed good adsorption capacities for all sulphur compounds.

A cost-effective hierarchical porous polymer PHP-MEA-PAC was produced in larger quantities for tests on real oils. This has a large surface area as well as the proper mesoporosity to ensure it to be a good substrate for sulphur species provide the oil is not too viscous to penetrate the adsorbent particle. This a system has all the major requirements for a successful adsorbent. These are adsorption capacity, thermal and mechanical stability, and the ability to be regenerated (regenerability).

In chapter eight, the adsorbent showed sufficient properties to withstand real light petroleum product flow rates and sufficient strength to not break during the adsorptive Desulphurisation process. This was true for all main real light oil products which are the raw materials for transportation fuels such as gasoline, diesel, and jet fuel.

9.2 Significance of the study

1. The study introduced novel preparation and modification methods that improved the process-structure-property relationship of the polyHIPE for use as an adsorbent.
2. The study paves the way for a new application of polyHIPE as a selective adsorbent depending on the new additive surface chemistry.
3. Results both in terms of adsorption capacity and surface modification indicate that the modified adsorbent could find useful applications in petroleum industry because of its simplicity, eco-friendliness, and high efficiency.

9.3 Future work

Despite significant insights into adsorbent manufacture and desorption desulfurization developed in this study, a number of points remain unanswered. These defined the follow-on work needed to produce a commercial adsorbent based on the technology developed. Future work needed includes:

- The material cannot be used for the Desulphurisation of all oil fractions. If the material can be developed for operation with crude oil, heavy oils and natural gas, and will remove sulphur and other impurities from these, it would have more widespread use. The study stated that it was not possible to use PHP-MEA-PAC with crude oil or heavy oils due to its viscosity and high density but in the future, it is worth trying to mix crude oil with diluent materials like naphtha or kerosene and then use it.
- The losses of the main additives MEA and PAC was the essential reason behind the decreasing of the adsorption capacity after regeneration. This can be solved by strengthening the bond between the MEA and the monomer through chemical reaction rather than the current physical absorption process with keeping the Sulphur adsorption process the same, so it is easy to separate by isopropanol wash. This probably will need to use different monomers.
- In Chapter 8 the adsorbent used with real products and it kept its appearance, shape and physical and mechanical properties. However, analysing the adsorbents after regeneration-adsorption cycles especially when they conducted the remove sulphur from real transportation oil needs to be done in the future.
- The adsorption conditions have not been optimized. It will be necessary to study the effect of adsorbent dosage on adsorptive desulfurization activity and the effect of operation temperature on adsorptive desulfurization performance.
- This is not yet a commercial process. It will be necessary to configure and scale-up the process with the adsorbent material. This will involve sizing the adsorbent columns based on the total adsorption capacity, adsorption kinetics, fluid residence time and regeneration and solvent recovery rates. A simplified possible process scheme is shown in Figure 9.1

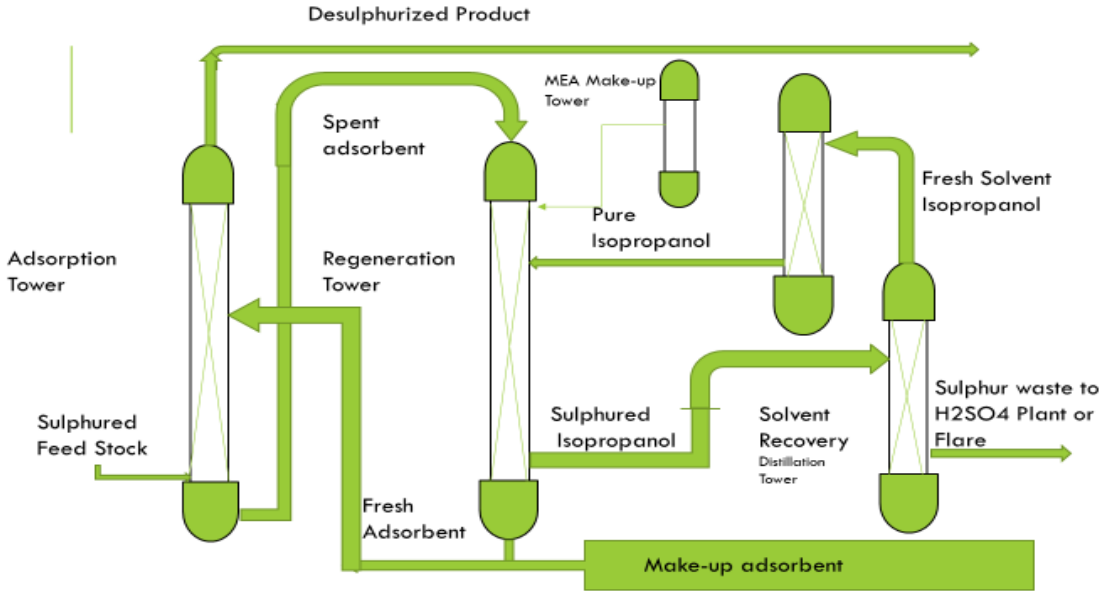

Figure 9.1 Simplified assumed adsorptive Desulphurisation process flow.

The process assumes a moving bed technology and a solid adsorbent disc, which is counter-currently brought into contact with a sulphur-rich feedstock. The desulphurised hydrocarbon stream is produced at the top of the adsorption tower whereas the spent adsorbent is withdrawn at the bottom. The spent adsorbent is circulated into the regenerator to treat it with isopropanol where organosulphur compounds and some adsorbed hydrocarbons are desorbed from the adsorbent surface. The regenerated adsorbent is recirculated back to the adsorption tower. The polluted solvent is fed from the bottom of the regeneration tower to the distillation tower to remove the sulphur compounds providing the fresh solvent feed to the isopropanol tower. It preferred to add the amine after solvent wash and regeneration depending on the sulphur adsorption capacity of each cycle. Finally, the wasted sulphur sends to H_2SO_4 plant or flare to avoid sulphur containment and create a process that friendly environment.

Considerable work is needed to make a commercial technology from the results presented here. This study has shown the potential but a more detailed project on absorber design is required to take things further.

References

.

ABBASIAN, Z. & MOGHBELI, M. 2010. Open porous emulsion-templated monoliths: Effect of the emulsion preparation conditions on the foam microstructure and properties. *Journal of applied polymer science,* 116**,** 986-994.

ABBASIAN, Z. & MOGHBELI, M. 2011. Preparation of highly open porous styrene/acrylonitrile and styrene/acrylonitrile/organoclay polymerized high internal phase emulsion (PolyHIPE) foams via emulsion templating. *Journal of Applied Polymer Science,* 119**,** 3728-3738.

ABDUL KHALIL, H., JAWAID, M., FIROOZIAN, P., ZAINUDIN, E. & PARIDAH, M. 2013. Dynamic mechanical properties of activated carbon–filled epoxy nanocomposites. *International Journal of Polymer Analysis and Characterization,* 18**,** 247-256.

ABDULRAHMAN, R., KAMAL, I. & ALI, J. 2015. Natural Gas Desulfurization Process By MEA Amine: The preferable Engineering Design Procedure. *International Journal of Engineering Trendsand Technology,* 28**,** 241-248.

ABEDI, A., CHITANDA, J., DALAI, A. K. & ADJAYE, J. 2015. Synthesis and application of functionalized polymers for the removal of nitrogen and sulfur species from gas oil. *Fuel processing technology,* 131**,** 473-482.

ABID, M. F. 2015. Desulfurization of gas oil using a solar photocatalytic microreactor. *Energy Procedia,* 74**,** 663-678.

ABID, M. F., AHMED, S. M., ABUHAMID, W. H. & ALI, S. M. 2019. Study on novel scheme for hydrodesulfurization of middle distillates using different types of catalyst. *Journal of King Saud University-Engineering Sciences,* 31**,** 144-151.

ADMINISTRATION, U. E. I. 2016. Country analysis brief: Iraq. EIA Beta Independent and Statistic USA.

AHMAD, W. 2016. Sulfur in petroleum: petroleum desulfurization techniques. *Applying Nanotechnology to the Desulfurization Process in Petroleum Engineering.* IGI Global.

AHMAD, W., AHMAD, I., ISHAQ, M. & IHSAN, K. 2017. Adsorptive desulfurization of kerosene and diesel oil by Zn impregnated montmorollonite clay. *Arabian Journal of Chemistry,* 10**,** S3263-S3269.

AKAY, G. 1995. Flow induced phase inversion in powder structuring by polymers. *Polymer Powder Technology***,** 542-587.

AKAY, G., BHUMGARA, Z. & WAKEMAN, R. 1995. Self-supported porous channel filtration modules-preparation, properties and performance. *Chemical engineering research & design,* 73**,** 782-797.

AKAY, G., BIRCH, M. & BOKHARI, M. 2004. Microcellular polyHIPE polymer supports osteoblast growth and bone formation in vitro. *Biomaterials,* 25**,** 3991-4000.

AKAY, G. & CALKAN, B. 2015. Preparation of nanostructured microporous metal foams through flow induced electroless deposition. *Journal of Nanomaterials,* 2015.

AKAY, G., DOGRU, M., CALKAN, B. & CALKAN, O. 2005. Flow-induced phase inversion phenomenon in process intensification and microreactor technology: Preparation and applications of nanostructured microporous polymers and metals. ACS Publications.

AKAY, G., DOWNES, S. & PRICE, V. 2002. Microcellular polymers as cell growth media and novel polymers. *European patent EP,* 1183328**,** A2.

AL ZUBAIDI, I., DARWISH, N. N., EL SAYED, Y., SHAREEFDEEN, Z. & SARA, Z. 2015. Adsorptive desulfurization of commercial diesel oil using granular activated charcoal. *Int. J. Adv. Chem. Eng. Biol. Sci,* 2**,** 15-18.

AL ZUBAIDY, I. A. H., TARSH, F. B., DARWISH, N. N., MAJEED, B., AL SHARAFI, A. & CHACRA, L. A. 2013. Adsorption process of sulfur removal from diesel oil using sorbent materials. *Journal of Clean Energy Technologies,* 1**,** 66-68.

ALI, H. & KHAN, E. 2017. Environmental chemistry in the twenty-first century. *Environmental Chemistry Letters,* 15**,** 329-346.

ALIKHANI, M. & MOGHBELI, M. R. 2014. Ion-exchange polyHIPE type membrane for removing nitrate ions: Preparation, characterization, kinetics and adsorption studies. *Chemical Engineering Journal,* 239**,** 93-104.

ANIA, C. O. & BANDOSZ, T. J. 2005. Importance of structural and chemical heterogeneity of activated carbon surfaces for adsorption of dibenzothiophene. *Langmuir,* 21**,** 7752-7759.

ANISUZZAMAN, S., ABANG, S., KRISHNAIAH, D. & RAZLAN, M. 2017. Adsorptive desulfurization of model fuel by activated oil palm shell.

ANTOS, G. J. & AITANI, A. M. 2004. *Catalytic naphtha reforming, revised and expanded*, CRC Press.

ARONSON, M. P. & PETKO, M. F. 1993. Highly concentrated water-in-oil emulsions: Influence of electrolyte on their properties and stability. *Journal of colloid and interface science,* 159**,** 134-149.

AWADH, S. M. & AL-MIMAR, H. 2015. Statistical analysis of the relations between API, specific gravity and sulfur content in the universal crude oil. *International Journal of Science and Research,* 4**,** 1279-1284.

BABICH, I. & MOULIJN, J. 2003. Science and technology of novel processes for deep desulfurization of oil refinery streams: a review☆. *Fuel,* 82**,** 607-631.

BADERTSCHER, M., BÜHLMANN, P. & PRETSCH, E. 2009. *Structure Determination of Organic Compounds: Tables of Spectral Data,* Springer.

BAEZA, P., AGUILA, G., VARGAS, G., OJEDA, J. & ARAYA, P. 2012. Adsorption of thiophene and dibenzothiophene on highly dispersed Cu/ZrO2 adsorbents. *Applied Catalysis B: Environmental,* 111**,** 133-140.

BANDOSZ, T. 2006. Desulfurization on activated carbons. *Interface Science and Technology.* Elsevier.

BANDOSZ, T. J. & REN, T.-Z. 2017. Porous carbon modified with sulfur in energy related applications. *Carbon,* 118**,** 561-577.

BARBETTA, A. & CAMERON, N. R. 2004. Morphology and surface area of emulsion-derived (PolyHIPE) solid foams prepared with oil-phase soluble porogenic solvents: Span 80 as surfactant. *Macromolecules,* 37**,** 3188-3201.

BARBETTA, A., CAMERON, N. R. & COOPER, S. J. 2000. High internal phase emulsions (HIPEs) containing divinylbenzene and 4-vinylbenzyl chloride and the morphology of the resulting PolyHIPE materials. *Chemical Communications***,** 221-222.

BARBY, D. & HAQ, Z. 1985. Low density porous cross-linked polymeric materials and their preparation and use as carriers for included liquids. Google Patents.

BARLIK, N. & KESKINLER, B. 2014. Sulfonation of crosslinked styrene/divinyl benzene copolymer beads formed from porous foam and ion adsorption of copper by them: column adsorption modeling. *Water science and technology,* 69**,** 286-292.

BASHKOVA, S., BAGREEV, A. & BANDOSZ, T. J. 2002. Adsorption of methyl mercaptan on activated carbons. *Environmental science & technology,* 36**,** 2777-2782.

BASHKOVA, S., BAGREEV, A., LOCKE, D. C. & BANDOSZ, T. J. 2001. Adsorption of SO2 on sewage sludge-derived materials. *Environmental science & technology,* 35**,** 3263-3269.

BEILER, B., VINCZE, Á., SVEC, F. & SÁFRÁNY, Á. 2007. Poly (2-hydroxyethyl acrylate-co-ethyleneglycol dimethacrylate) monoliths synthesized by radiation polymerisation in a mold. *Polymer,* 48**,** 3033-3040.

BEN, T. & QIU, S. 2013. Porous aromatic frameworks: Synthesis, structure and functions. *CrystEngComm,* 15**,** 17-26.

BETTERMANN, I. & STAUDT, C. 2009. Desulphurization of kerosene: Pervaporation of benzothiophene/n-dodecane mixtures. *Journal of Membrane Science,* 343**,** 119-127.

BOKHARI, M. 2003. *Bone tissue engineering using novel microcellular polymers.* University of Newcastle upon Tyne.

BOKHARI, M. A., AKAY, G., ZHANG, S. & BIRCH, M. A. 2005. The enhancement of osteoblast growth and differentiation in vitro on a peptide hydrogel—polyHIPE polymer hybrid material. *Biomaterials,* 26**,** 5198-5208.

BRAGINSKII, O. B. 2009. Crude oil prices: history, forecast, and impact on economy. *Russian Journal of General Chemistry,* 79**,** 2486-2498.

BREYSSE, M., HÉDOIRE, C. E., LOUIS, C. & PÉROT, G. 2003. 17 Deep hydrodesulfurization: Reactions and catalysts. *Studies in Surface Science and Catalysis.* Elsevier.

BRUNAUER, S., EMMETT, P. H. & TELLER, E. 1938. Adsorption of gases in multimolecular layers. *Journal of the American chemical society,* 60**,** 309-319.

BRUNET, S., MEY, D., PÉROT, G., BOUCHY, C. & DIEHL, F. 2005. On the hydrodesulfurization of FCC gasoline: a review. *Applied Catalysis A: General,* 278**,** 143-172.

BURKE, D. R., AKAY, G. & BILSBORROW, P. E. 2010. Development of novel polymeric materials for agroprocess intensification. *Journal of applied polymer science,* 118**,** 3292-3299.

BURROWS, A., HOLMAN, J., PARSONS, A., PILLING, G. & PRICE, G. 2017. *Chemistry3: Introducing inorganic, organic and physical chemistry,* Oxford University Press.

BUSBY, W., CAMERON, N. R. & JAHODA, C. A. 2001. Emulsion-derived foams (PolyHIPEs) containing poly (ε-caprolactone) as matrixes for tissue engineering. *Biomacromolecules,* 2**,** 154-164.

BYRON, V. J. 2000. *The development of microcellular polymers as a support for tissue engineering.* University of Newcastle.

CALKAN, B. 2007. *Preparation of novel nano-structured macro-and meso-porous metal foams for process intensification and miniaturization.* University of Newcastle Upon Tyne.

ÇALKAN, O. M. F. 2007. *Intensified, integrated gasification system development.* University of Newcastle Upon Tyne.

CAMERON, N. R. 2005. High internal phase emulsion templating as a route to well-defined porous polymers. *Polymer,* 46**,** 1439-1449.

CAMERON, N. R. & BARBETTA, A. 2000. The influence of porogen type on the porosity, surface area and morphology of poly (divinylbenzene) PolyHIPE foams. *Journal of Materials Chemistry,* 10**,** 2466-2471.

CAMERON, N. R. & SHERRINGTON, D. C. 1997. Synthesis and Characterization of Poly (aryl ether sulfone) PolyHIPE Materials. *Macromolecules,* 30**,** 5860-5869.

CAMERON, N. R., SHERRINGTON, D. C., ANDO, I. & KUROSU, H. 1996. Chemical modification of monolithic poly (styrene–divinylbenzene) polyHIPE® materials. *Journal of Materials Chemistry,* 6**,** 719-726.

CATALAN, L. J., LIANG, V. & JIA, C. Q. 2006. Comparison of various detection limit estimates for volatile sulphur compounds by gas chromatography with pulsed flame photometric detection. *Journal of Chromatography A,* 1136**,** 89-98.

CHIANG, H.-L., HUANG, C., CHIANG, P. & YOU, J. 1999. Effect of metal additives on the physico-chemical characteristics of activated carbon exemplified by benzene and acetic acid adsorption. *Carbon,* 37**,** 1919-1928.

CHIANG, H.-L., TSAI, J.-H., TSAI, C.-L. & HSU, Y.-C. 2000. Adsorption characteristics of alkaline activated carbon exemplified by water vapor, H2S, and CH3SH gas. *Separation science and technology,* 35**,** 903-918.

CHITANDA, J. M., AZAR, R., ABEDI, A., DALAI, A. K. & ADJAYE, J. D. 2016. π-Acceptor-functionalized particles: Synthesis, characterization and effect of cross-linking agents on adsorptive removal of nitrogen-and sulfur-compounds from light gas oil. *Journal of Industrial and Engineering Chemistry,* 44**,** 43-51.

COOPER, A. I. 2009. Conjugated microporous polymers. *Advanced Materials,* 21**,** 1291-1295.

COTE, A. P., BENIN, A. I., OCKWIG, N. W., O'KEEFFE, M., MATZGER, A. J. & YAGHI, O. M. 2005. Porous, crystalline, covalent organic frameworks. *science,* 310**,** 1166-1170.

CYCHOSZ, K. A., WONG-FOY, A. G. & MATZGER, A. J. 2009. Enabling cleaner fuels: desulfurization by adsorption to microporous coordination polymers. *Journal of the American Chemical Society,* 131**,** 14538-14543.

DAĞ, M., AKTUĞ, S. S. & ALı, Z. S. A. 2019. Evaluation of Relationship between Oil Revenues and Government Budget in Iraq: 2006-2016 Period. *EMAJ: Emerging Markets Journal,* 9**,** 49-53.

DALAI, A., TOLLEFSON, E., YANG, A. & SASAOKA, E. 1997. Oxidation of methyl mercaptan over an activated carbon in a fixed-bed reactor. *Industrial & engineering chemistry research,* 36**,** 4726-4733.

DANMALIKI, G. I. & SALEH, T. A. 2017. Effects of bimetallic Ce/Fe nanoparticles on the desulfurization of thiophenes using activated carbon. *Chemical Engineering Journal,* 307**,** 914-927.

DANMALIKI, G. I., SALEH, T. A. & SHAMSUDDEEN, A. A. 2017. Response surface methodology optimisation of adsorptive desulfurization on nickel/activated carbon. *Chemical Engineering Journal,* 313**,** 993-1003.

DANTAS, T. N. C., NETO, A. A. D., MOURA, M., NETO, E. L. B. & DUARTE, K. R. F. 2014. Study of new alternatives for removal of sulfur from diesel. *Brazilian Journal of Petroleum and Gas,* 8.

DE FILIPPIS, P. & SCARSELLA, M. 2008. Functionalized hexagonal mesoporous silica as an oxidizing agent for the oxidative desulfurization of organosulfur compounds. *Industrial & engineering chemistry research,* 47**,** 973-975.

DEHGHAN, R. & ANBIA, M. 2017. Zeolites for adsorptive desulfurization from fuels: A review. *Fuel Processing Technology,* 167**,** 99-116.

DEMIRBAS, A., ALIDRISI, H. & BALUBAID, M. 2015. API gravity, sulfur content, and desulfurization of crude oil. *Petroleum Science and Technology,* 33**,** 93-101.

DENG, L., LU, B., LI, J., LV, G., DU, S., SHI, J. & YANG, Y. 2017. Effect of pore structure and oxygen-containing groups on adsorption of dibenzothiophene over activated carbon. *Fuel,* 200**,** 54-61.

DHAGE, P., SAMOKHVALOV, A., REPALA, D., DUIN, E. C. & TATARCHUK, B. J. 2011. Regenerable Fe–Mn–ZnO/SiO 2 sorbents for room temperature removal of H 2 S from fuel reformates: performance, active sites, Operando studies. *Physical Chemistry Chemical Physics,* 13**,** 2179-2187.

DICKS, A. L., ENSELL, R. L., PHILLIPS, T. R., SZCZEPURA, A. K., THORLEY, M., WILLIAMS, A. & WRAGG, R. D. 1981. A study of relationships between pore size distribution, hydrogen chemisorption, and activity of hydrodesulphurisation catalysts. *Journal of Catalysis,* 72**,** 266-273.

DING, S.-Y. & WANG, W. 2013. Covalent organic frameworks (COFs): from design to applications. *Chemical Society Reviews,* 42**,** 548-568.

DONOVAN, T., ABDUL-RAHMAN, S., SKIBIAK, N. & FONO, A. 2013. Iraq's Petroleum Industry: Unsettled Issues. *Middle East institute.*

ERGENEKON, P., GÜRBULAK, E. & KESKINLER, B. 2011. A novel method for sulfonation of microporous polystyrene divinyl benzene copolymer using gaseous SO2 in the waste air streams. *Chemical Engineering and Processing: Process Intensification,* 50**,** 16-21.

FALLAH, R. N., AZIZIAN, S., REGGERS, G., CARLEER, R., SCHREURS, S., AHENACH, J., MEYNEN, V. & YPERMAN, J. 2014. Effect of aromatics on the adsorption of thiophenic sulfur compounds from model diesel fuel by activated carbon cloth. *Fuel processing technology,* 119**,** 278-285.

FARSHI, A. & SHIRALIZADEH, P. 2015. SULFUR REDUCTION OF HEAVY FUEL OIL BY OXIDATIVE DESULFURIZATION (ODS) METHOD. *Petroleum & Coal,* 57.

FLEMING, I. & WILLIAMS, D. H. 1966. *Spectroscopic methods in organic chemistry,* McGraw-Hill New York.

FORTE, P. 1996. Process for the removal of sulfur from petroleum fractions. Google Patents.

FUKUNAGA, T., KATSUNO, H., MATSUMOTO, H., TAKAHASHI, O. & AKAI, Y. 2003. Development of kerosene fuel processing system for PEFC. *Catalysis Today,* 84**,** 197-200.

FUNAKOSHI, I. & AIDA, T. 1998. Process for recovering organic sulfur compounds from fuel oil. Google Patents.

FURMAN, K. C., EL-BAKRY, A. S. & SONG, J.-H. 2017. Optimisation in the oil and gas industry. Springer.

GANIYU, S. A., AJUMOBI, O. O., LATEEF, S. A., SULAIMAN, K. O., BAKARE, I. A., QAMARUDDIN, M. & ALHOOSHANI, K. 2017. Boron-doped activated carbon as efficient and selective adsorbent for ultra-deep desulfurization of 4, 6-dimethyldibenzothiophene. *Chemical Engineering Journal,* 321**,** 651-661.

GANIYU, S. A., ALHOOSHANI, K., SULAIMAN, K. O., QAMARUDDIN, M., BAKARE, I. A., TANIMU, A. & SALEH, T. A. 2016. Influence of aluminium impregnation on activated carbon for enhanced desulfurization of DBT at ambient temperature: role of surface acidity and textural properties. *Chemical Engineering Journal,* 303**,** 489-500.

GARY, J. H., HANDWERK, G. E. & KAISER, M. J. 2007. *Petroleum refining: technology and economics,* CRC press.

GATES, B. & TOPSØE, H. 1997. Reactivities in deep catalytic hydrodesulfurization: challenges, opportunities, and the importance of 4-methyldibenzothiophene and 4, 6-dimethyldibenzothiophene. *Polyhedron,* 16**,** 3213-3217.

GERBER, M. A., FRYE, J. G., BOWMAN, L. E., FULTON, J. L., SILVA, L. J. & WAI, C. M. 1999. Regeneration of hydrotreating and FCC catalysts. Pacific Northwest National Lab.(PNNL), Richland, WA (United States).

GLASBY, G. P. 2006. Abiogenic origin of hydrocarbons: An historical overview. *Resource Geology,* 56**,** 83-96.

GOUGH, T. & SIMPSON, C. 1970. Variation of performance of porous polymer bead columns in gas chromatography. *Journal of Chromatography A,* 51**,** 129-137.

GOYAL, S. 2006. Silanes: Chemistry and applications. *The journal of Indian Prosthodontic Society,* 6**,** 14.

GRAY, P. 1993. A fundamental study on the removal of air pollutants (sulfur dioxide, nitrogen dioxide and carbon dioxide) by adsorption on activated carbon. *Gas separation & purification,* 7**,** 213-224.

GRECO, P. P. 2014. *Development of novel polymeric and composite Nano-Structured Micro-Porous Materials for impact resistance applications.* Newcastle University.

GUPTA, R. P. & TURK, B. S. 2007. Process for desulfurizing hydrocarbon fuels and fuel components. Google Patents.

HADI, H. 2017. *Regulating the Oil and Gas Sector in Iraq.* Thesis or dissertation.

HAIBACH, K., MENNER, A., POWELL, R. & BISMARCK, A. 2006. Tailoring mechanical properties of highly porous polymer foams: Silica particle reinforced polymer foams via emulsion templating. *Polymer,* 47**,** 4513-4519.

HAINEY, P., HUXHAM, I., ROWATT, B., SHERRINGTON, D. & TETLEY, L. 1991. Synthesis and ultrastructural studies of styrene-divinylbenzene polyhipe polymers. *Macromolecules,* 24**,** 117-121.

HAJI, S. & ERKEY, C. 2003. Removal of dibenzothiophene from model diesel by adsorption on carbon aerogels for fuel cell applications. *Industrial & engineering chemistry research,* 42**,** 6933-6937.

HAQ, Z. 1985. Porous cross-linked absorbent polymeric materials. Google Patents.

HART, M., FULLER, G., BROWN, D., DALE, J. & PLANT, S. 2002. Sulfonated poly (styrene-co-divinylbenzene) ion-exchange resins: acidities and catalytic activities in aqueous reactions. *Journal of molecular catalysis A: chemical,* 182**,** 439-445.

HASAN, H. 2013. *Preparation of novel composite polyHIPE polymers and their applications in intensified removal of tars from syngas.* Newcastle University.

HAUTHAL, H. 1990. Myers, D.: Surfactant science and technology. 331 S., 78 Abb., 44 Tab., 16× 24 cm. Weinheim, Basel, Cambridge, New York: VCH Verlagsgesellschaft 1988. Kart., 58,–DM. *Journal für Praktische Chemie,* 332**,** 587-588.

HERNÁNDEZ-MALDONADO, A. J. & YANG, R. T. 2004. Desulfurization of diesel fuels by adsorption via π-complexation with vapor-phase exchanged Cu (I)− Y zeolites. *Journal of the American Chemical Society,* 126**,** 992-993.

HERNÁNDEZ-MALDONADO, A. J. & YANG, R. T. 2004. New sorbents for desulfurization of diesel fuels via π-complexation. *AIChE Journal,* 50**,** 791-801.

HERNANDEZ, S., FINO, D. & RUSSO, N. 2010. High performance sorbents for diesel oil desulfurization. *Chemical Engineering Science,* 65**,** 603-609.

HOSSEINI, H. 2012. Novel methods for desulfurization of fuel oils. *International Journal of Chemical, Molecular, Nuclear, Materials and Metallurgical Engineering,* 6**,** 1072-1074.

HUA, R., LI, Y., LIU, W., ZHENG, J., WEI, H., WANG, J., LU, X., KONG, H. & XU, G. 2003. Determination of sulfur-containing compounds in diesel oils by comprehensive two-dimensional gas chromatography with a sulfur chemiluminescence detector. *Journal of Chromatography A,* 1019**,** 101-109.

HUERTAS, J. I., GIRALDO, N. & IZQUIERDO, S. 2011. Removal of H2S and CO2 from Biogas by Amine Absorption. *Mass Transfer in Chemical Engineering Processes***,** 133-150.

IKEM, V. O., MENNER, A. & BISMARCK, A. 2008. High internal phase emulsions stabilized solely by functionalized silica particles. *Angewandte Chemie International Edition,* 47**,** 8277-8279.

IM, S. H., JEONG, U. & XIA, Y. 2005. Polymer hollow particles with controllable holes in their surfaces. *Nature materials,* 4**,** 671-675.

IRVINE, R. L. 1998. Process for desulfurizing gasoline and hydrocarbon feedstocks. Google Patents.

JAVADLI, R. & DE KLERK, A. 2012. Desulfurization of heavy oil. *Applied Petrochemical Research,* 1**,** 3-19.

JAYNE, D., ZHANG, Y., HAJI, S. & ERKEY, C. 2005. Dynamics of removal of organosulfur compounds from diesel by adsorption on carbon aerogels for fuel cell applications. *International Journal of Hydrogen Energy,* 30**,** 1287-1293.

JEEVANANDAM, P., KLABUNDE, K. & TETZLER, S. 2005. Adsorption of thiophenes out of hydrocarbons using metal impregnated nanocrystalline aluminum oxide. *Microporous and Mesoporous Materials,* 79**,** 101-110.

JIANG, J.-X., SU, F., TREWIN, A., WOOD, C. D., NIU, H., JONES, J. T., KHIMYAK, Y. Z. & COOPER, A. I. 2008. Synthetic control of the pore dimension and surface area in conjugated microporous polymer and copolymer networks. *Journal of the American Chemical Society,* 130**,** 7710-7720.

JIANG, J.-X., TREWIN, A., SU, F., WOOD, C. D., NIU, H., JONES, J. T., KHIMYAK, Y. Z. & COOPER, A. I. 2009. Microporous poly (tri (4-ethynylphenyl) amine) networks: synthesis, properties, and atomistic simulation. *Macromolecules,* 42**,** 2658-2666.

JIANG, J. X., SU, F., TREWIN, A., WOOD, C. D., CAMPBELL, N. L., NIU, H., DICKINSON, C., GANIN, A. Y., ROSSEINSKY, M. J. & KHIMYAK, Y. Z. 2007. Conjugated microporous poly (aryleneethynylene) networks. *Angewandte Chemie International Edition,* 46**,** 8574-8578.

JIANG, Z., LIU, Y., SUN, X., TIAN, F., SUN, F., LIANG, C., YOU, W., HAN, C. & LI, C. 2003. Activated carbons chemically modified by concentrated H2SO4 for the adsorption of the pollutants from wastewater and the dibenzothiophene from fuel oils. *Langmuir,* 19**,** 731-736.

JIMAT, D. N. 2011. *Bioprocess intensification: production of a-amylase by immobilised Bacillus subtilis in porous polymeric polyHIPE.* Newcastle University.

KADHIM, M. S. 2017. *Characterisation of a nanoporous polymers for water treatment.* Newcastle University.

KHAN, N. A., HASAN, Z., MIN, K. S., PAEK, S.-M. & JHUNG, S. H. 2013. Facile introduction of Cu+ on activated carbon at ambient conditions and adsorption of benzothiophene over Cu+/activated carbon. *Fuel processing technology,* 116**,** 265-270.

KIM, H., PARK, D. W., WOO, H. C. & CHUNG, J. S. 1998. Reduction of SO2 by CO to elemental sulfur over Co3O4–TiO2 catalysts. *Applied Catalysis B: Environmental,* 19**,** 233-243.

KIM, J. H., MA, X., ZHOU, A. & SONG, C. 2006. Ultra-deep desulfurization and denitrogenation of diesel fuel by selective adsorption over three different adsorbents: a study on adsorptive selectivity and mechanism. *Catalysis Today,* 111**,** 74-83.

KIZLING, J. & KRONBERG, B. 1990. On the formation and stability of concentrated water-in-oil emuslions, aphrons. *Colloids and surfaces,* 50**,** 131-140.

KOPARKAR, Y. P. & GAIKAR, V. G. 2011. Diesel Desulfurization Using Reactive Adsorption on Metal Impregnated Functionalized Polymer. *Separation Science and Technology,* 46**,** 1647-1655.

KRAJNC, P., ŠTEFANEC, D., BROWN, J. F. & CAMERON, N. R. 2005. Aryl acrylate based high-internal-phase emulsions as precursors for reactive monolithic polymer supports. *Journal of Polymer Science Part A: Polymer Chemistry,* 43**,** 296-303.

KUČERA, F. & JANČÁŘ, J. 1998. Homogeneous and heterogeneous sulfonation of polymers: a review. *Polymer Engineering & Science,* 38**,** 783-792.

KUMAR, S., SRIVASTAVA, V. C. & BADONI, R. 2011. Studies on adsorptive desulfurization by zirconia based adsorbents. *Fuel,* 90**,** 3209-3216.

KUMAR, S., SRIVASTAVA, V. C. & NANOTI, S. M. 2017. Extractive desulfurization of gas oils: A perspective review for use in petroleum refineries. *Separation & Purification Reviews,* 46**,** 319-347.

KUNIEDA, H., YANO, N. & SOLANS, C. 1989. The stability of gel—emulsions in a water/nonionic surfactant/oil system. *Colloids and surfaces,* 36**,** 313-322.

KUSSAINOVA, D. & SHAH, D. 2020. Monoethanolamine based DESs for CO2 absorption: Insights from molecular dynamics simulations. *Separation and Purification Technology,* 231**,** 115931.

LANGMUIR, I. 1918. The adsorption of gases on plane surfaces of glass, mica and platinum. *Journal of the American Chemical society,* 40**,** 1361-1403.

LEBODA, R., SKUBISZEWSKA-ZIĘBA, J., TOMASZEWSKI, W. & GUN'KO, V. 2003. Structural and adsorptive properties of activated carbons prepared by carbonization and activation of resins. *Journal of colloid and interface science,* 263**,** 533-541.

LEPRINCE, P. 2001. *Petroleum refining. Vol. 3 conversion processes,* Editions Technip.

LI, Z., JIN, S., ZHANG, R., SHAO, X., ZHANG, S., JIANG, N., JIN, M., MENG, T. & MU, Y. 2016. Adsorption of thiophene, dibenzothiophene, and 4, 6-dimethyl dibenzothiophene on activated carbons. *Adsorption Science & Technology,* 34**,** 227-243.

LIM, C. & LEE, J. 2020. An analysis of the efficiency of the oil refining industry in the OECD countries. *Energy Policy,* 142**,** 111491.

LINDBERG, R., SUNDHOLM, G., ØYE, G. & SJÖBLOM, J. 1998. A new method for following the kinetics of the hydrolysis and condensation of silanes. *Colloids and Surfaces A: Physicochemical and Engineering Aspects,* 135**,** 53-58.

LIU, B., LI, H., MA, X., CHEN, R., WANG, S. & LI, L. 2018. The synergistic effect of oxygen-containing functional groups on CO 2 adsorption by the glucose–potassium citrate-derived activated carbon. *RSC advances,* 8**,** 38965-38973.

LIU, Z.-W., LI, W.-X., MA, W.-H., YIN, Z.-L. & WU, G.-B. 2015. Comparison of deep desulfurization methods in alumina production process. *Journal of Central South University,* 22**,** 3745-3750.

LUCCHESI, C., PASCUAL, S., DUJARDIN, G. & FONTAINE, L. 2008. New functionalized polyHIPE materials used as amine scavengers in batch and flow-through processes. *Reactive and Functional Polymers,* 68**,** 97-102.

LUDWIG, E. E. 1997. *Applied process design for chemical and petrochemical plants,* Gulf Professional Publishing.

LUO, Y., LI, B., WANG, W., WU, K. & TAN, B. 2012a. Hypercrosslinked aromatic heterocyclic microporous polymers: a new class of highly selective CO2 capturing materials. *Advanced Materials,* 24**,** 5703-5707.

LUO, Y., WANG, A.-N. & GAO, X. 2012b. Miniemulsion template polymerisation to prepare a sub-micrometer porous polymeric monolith with an inter-connected structure and very high mechanical strength. *Soft Matter,* 8**,** 7547-7551.

MA, X., SAKANISHI, K., ISODA, T. & MOCHIDA, I. 1995. Hydrodesulfurization reactivities of narrow-cut fractions in a gas oil. *Industrial & engineering chemistry research,* 34**,** 748-754.

MA, X., SAKANISHI, K. & MOCHIDA, I. 1996. Hydrodesulfurization Reactivities of Various Sulfur Compounds in Vacuum Gas Oil. *Industrial & Engineering Chemistry Research,* 35**,** 2487-2494.

MA, X., SUN, L. & SONG, C. 2002. A new approach to deep desulfurization of gasoline, diesel fuel and jet fuel by selective adsorption for ultra-clean fuels and for fuel cell applications. *Catalysis today,* 77**,** 107-116.

MA, X., SUN, L. & SONG, C. 2003. Adsorptive desulfurization of diesel fuel over a metal sulfide-based adsorbent. *Prepr. Pap.-Am. Chem. Soc., Div. Fuel Chem,* 48**,** 522.

MA, X., VELU, S., KIM, J. H. & SONG, C. 2005. Deep desulfurization of gasoline by selective adsorption over solid adsorbents and impact of analytical methods on ppm-level sulfur quantification for fuel cell applications. *Applied Catalysis B: Environmental,* 56**,** 137-147.

MA, X., ZHOU, A. & SONG, C. 2007. A novel method for oxidative desulfurization of liquid hydrocarbon fuels based on catalytic oxidation using molecular oxygen coupled with selective adsorption. *Catalysis Today,* 123**,** 276-284.

MAHADIK, D., LEE, K.-Y., GHORPADE, R. & PARK, H.-H. 2018. Superhydrophobic and compressible silica-polyHIPE covalently bonded porous networks via emulsion templating for oil spill cleanup and recovery. *Scientific reports,* 8**,** 1-9.

MANTELL, A. 1951. TP156. A35M3.

MARTIN, R. L. & GRANT, J. A. 1965. Determination of sulfur-compound distributions in petroleum samples by gas chromatography with a coulometric detector. *Analytical Chemistry,* 37**,** 644-649.

MATAJI, M. & KHOSHANDAM, B. 2014. Benzene adsorption on activated carbon from walnut shell. *Chemical Engineering Communications,* 201**,** 1294-1313.

MCKEOWN, N. B. & BUDD, P. M. 2006. Polymers of intrinsic microporosity (PIMs): organic materials for membrane separations, heterogeneous catalysis and hydrogen storage. *Chemical Society Reviews,* 35**,** 675-683.

MENNER, A., HAIBACH, K., POWELL, R. & BISMARCK, A. 2006a. Tough reinforced open porous polymer foams via concentrated emulsion templating. *Polymer,* 47**,** 7628-7635.

MENNER, A., POWELL, R. & BISMARCK, A. 2006b. A new route to carbon black filled polyHIPEs. *Soft Matter,* 2**,** 337-342.

MENNER, A., SALGUEIRO, M., SHAFFER, M. S. P. & BISMARCK, A. 2008. Nanocomposite foams obtained by polymerisation of high internal phase emulsions. *Journal of Polymer Science Part A: Polymer Chemistry,* 46**,** 5708-5714.

MERCIER, A., DELEUZE, H. & MONDAIN-MONVAL, O. 2001. Thiol Addition to the Pendant Vinylbenzene Groups of (Vinyl) polystyrene PolyHIPE Via a Batch and a Cross-Flow Method. *Macromolecular Chemistry and Physics,* 202**,** 2672-2680.

MESROGHLI, S., YPERMAN, J., REGGERS, G., JORJANI, E. & CARLEER, R. 2016. Impacts of sonication and post-desulfurization on organic sulfur species by reductive pyrolysis. *Fuel,* 183**,** 278-291.

MEYER, B. 2013. *Sulfur, energy, and environment,* Elsevier.

MIAO, G., YE, F., WU, L., REN, X., XIAO, J., LI, Z. & WANG, H. 2015. Selective adsorption of thiophenic compounds from fuel over TiO2/SiO2 under UV-irradiation. *Journal of hazardous materials,* 300**,** 426-432.

MIHAELA, P. 2008. BRIEF PRESENTATION OF THE WORLD FOSSIL ENERGY MARKET. *Europe,* 13**,** 103.536.

MILLS, N. 2007. *Polymer foams handbook: engineering and biomechanics applications and design guide,* Elsevier.

MISRA, P., BADOGA, S., CHENNA, A., DALAI, A. K. & ADJAYE, J. 2017. Denitrogenation and desulfurization of model diesel fuel using functionalized polymer: charge transfer complex formation and adsorption isotherm study. *Chemical Engineering Journal,* 325**,** 176-187.

MOGHBELI, M., KHAJEH, A. & ALIKHANI, M. 2017. Nanosilica reinforced ion-exchange polyHIPE type membrane for removal of nickel ions: Preparation, characterization and adsorption studies. *Chemical Engineering Journal,* 309**,** 552-562.

MOHAMED, R. 2011. *Preparation of nano-structured macro-porous materials.* Newcastle University.

MURAOKA, Y., RICH, M. J. & DRZAL, L. T. 2002. Sulfonation of UHMW-PE fibers for adhesion promotion in epoxy polymers. *Journal of adhesion science and technology,* 16**,** 1669-1685.

NELSON, W. L. 2018. *Petroleum refinery engineering,* McGraw-Hill.

NEUBAUER, R., HUSMANN, M., WEINLAENDER, C., KIENZL, N., LEITNER, E. & HOCHENAUER, C. 2017. Acid base interaction and its influence on the adsorption kinetics and selectivity order of aromatic sulfur heterocycles adsorbing on Ag-Al2O3. *Chemical engineering journal,* 309**,** 840-849.

NOOR, Z. Z. 2006. *Intensification of separation processes using functionalised polyhipe polymers.* University of Newcastle upon Tyne.

NORMATOV, J. & SILVERSTEIN, M. S. 2007. Porous interpenetrating network hybrids synthesized within high internal phase emulsions. *Polymer,* 48**,** 6648-6655.

OLAJIRE, A. A., ABIDEMI, J. J., LATEEF, A. & BENSON, N. U. 2017. Adsorptive desulphurization of model oil by Ag nanoparticles-modified activated carbon prepared from brewer's spent grains. *Journal of environmental chemical engineering,* 5**,** 147-159.

OLSON, D. A., CHEN, L. & HILLMYER, M. A. 2008. Templating nanoporous polymers with ordered block copolymers. *Chemistry of Materials,* 20**,** 869-890.

ORDOMSKY, V., SCHOUTEN, J., VAN DER SCHAAF, J. & NIJHUIS, T. 2012. Foam supported sulfonated polystyrene as a new acidic material for catalytic reactions. *Chemical engineering journal,* 207**,** 218-225.

PAKEYANGKOON, P., MAGARAPHAN, R., MALAKUL, P. & NITHITANAKUL, M. Effect of soxhlet extraction and surfactant system on morphology and properties of poly (DVB) polyHIPE. Macromolecular symposia, 2008. Wiley Online Library, 149-156.

PAKEYANGKOON, P., MAGARAPHAN, R., MALAKUL, P. & NITHITANAKUL, M. 2009. Polymeric foam via polymerized high internal phase emulsion filled with organo-modified bentonite. *Journal of applied polymer science,* 114**,** 3041-3048.

PALOMINO, J. M., TRAN, D. T., HAUSER, J. L., DONG, H. & OLIVER, S. R. 2014. Mesoporous silica nanoparticles for high capacity adsorptive desulfurization. *Journal of Materials Chemistry A,* 2**,** 14890-14895.

PARKER, J. 2016. *A study of the phenylacetylene oxidative carbonylation reaction in oscillatory and non-oscillatory modes.* Newcastle University.

PERALTA, D., CHAPLAIS, G., SIMON-MASSERON, A., BARTHELET, K. & PIRNGRUBER, G. D. 2012. Metal–organic framework materials for desulfurization by adsorption. *Energy & fuels,* 26**,** 4953-4960.

PERRY, R. H. 1954. Chemical engineers' handbook.

PIETRZAK, R. & BANDOSZ, T. J. 2007. Activated carbons modified with sewage sludge derived phase and their application in the process of NO2 removal. *Carbon,* 45**,** 2537-2546.

PLUEDDEMANN, E. P. 1983. Silane adhesion promoters in coatings. *Progress in organic coatings,* 11**,** 297-308.

PRAJAPATI, Y. N. & VERMA, N. 2017. Adsorptive desulfurization of diesel oil using nickel nanoparticle-doped activated carbon beads with/without carbon nanofibers: Effects of adsorbate size and adsorbent texture. *Fuel,* 189**,** 186-194.

PRETSCH, E., BÜHLMANN, P., AFFOLTER, C., PRETSCH, E., BHUHLMANN, P. & AFFOLTER, C. 2000. *Structure determination of organic compounds,* Springer.

REN, S., BOJDYS, M. J., DAWSON, R., LAYBOURN, A., KHIMYAK, Y. Z., ADAMS, D. J. & COOPER, A. I. 2012. Porous, fluorescent, covalent triazine-based frameworks via room-temperature and microwave-assisted synthesis. *Advanced Materials,* 24**,** 2357-2361.

RODRIGUES, A. K. O., RAMOS, J. E. T., CAVALCANTE JR, C. L., RODRÍGUEZ-CASTELLÓN, E. & AZEVEDO, D. C. 2014. Pd-loaded mesoporous silica as a robust adsorbent in adsorption/desorption desulfurization cycles. *Fuel,* 126**,** 96-103.

ROSEN, M. J. 1972. The relationship of structure to properties in surfactants. *Journal of the American Oil Chemists' Society,* 49**,** 293-297.

RUI, J., LIU, F., WANG, R., LU, Y. & YANG, X. 2017. Adsorptive desulfurization of model gasoline by using different Zn sources exchanged NaY zeolites. *Molecules,* 22**,** 305.

RUTHVEN, D. M. 1984. *Principles of adsorption and adsorption processes,* John Wiley & Sons.

SAEIDI, N. & LOTFOLLAHI, M. N. 2015. Effects of powder activated carbon particle size on adsorption capacity and mechanical properties of the semi activated carbon fiber. *Fibers and Polymers,* 16**,** 543-549.

SAJAD, S. & MOGHBELI, M. 2020. Allyl-3-methylimidazolium bromide (AmIB) functionalized PolyHIPE to surface immobilize H3PW12O40 catalyst: Chemical oxidation of dibenzothiophene. *Reactive and Functional Polymers,* 146**,** 104406.

SALEH, T. A. 2015. *Applying nanotechnology to the desulfurization process in petroleum engineering,* IGI global.

SALEH, T. A., AL-HAMMADI, S. A., TANIMU, A. & ALHOOSHANI, K. 2018. Ultra-deep adsorptive desulfurization of fuels on cobalt and molybdenum nanoparticles loaded on activated carbon derived from waste rubber. *Journal of colloid and interface science,* 513**,** 779-787.

SALEH, T. A. & DANMALIKI, G. I. 2016. Influence of acidic and basic treatments of activated carbon derived from waste rubber tires on adsorptive desulfurization of thiophenes. *Journal of the Taiwan Institute of Chemical Engineers,* 60**,** 460-468.

SALEH, T. A., SULAIMAN, K. O., AL-HAMMADI, S. A., DAFALLA, H. & DANMALIKI, G. I. 2017. Adsorptive desulfurization of thiophene, benzothiophene and dibenzothiophene over activated carbon manganese oxide nanocomposite: with column system evaluation. *Journal of cleaner production,* 154**,** 401-412.

SALEM, A. B. S. H. 1994. Naphtha desulfurization by adsorption. *Industrial & engineering chemistry research,* 33**,** 336-340.

SAMADI, M. & ZARENEZHAD, B. 2016. Extension of gas adsorption models to liquid diesel fuel desulfurization: Validity and predictability. *Petroleum Science and Technology,* 34**,** 1826-1832.

SAMOKHVALOV, A. & TATARCHUK, B. J. 2010. Review of experimental characterization of active sites and determination of molecular mechanisms of adsorption, desorption and regeneration of the deep and ultradeep desulfurization sorbents for liquid fuels. *Catalysis Reviews,* 52**,** 381-410.

SCHURING, D. 2004. Diffusion in zeolites: Towards a microscopic understanding.

SENTORUN-SHALABY, C., SAHA, S. K., MA, X. & SONG, C. 2011. Mesoporous-molecular-sieve-supported nickel sorbents for adsorptive desulfurization of commercial ultra-low-sulfur diesel fuel. *Applied Catalysis B: Environmental,* 101**,** 718-726.

SEREDYCH, M., LISON, J., JANS, U. & BANDOSZ, T. J. 2009. Textural and chemical factors affecting adsorption capacity of activated carbon in highly efficient desulfurization of diesel fuel. *Carbon,* 47**,** 2491-2500.

SHAFI, R. & HUTCHINGS, G. J. 2000. Hydrodesulfurization of hindered dibenzothiophenes: an overview. *Catalysis Today,* 59**,** 423-442.

SHAFIEE, S. & TOPAL, E. 2008. An econometrics view of worldwide fossil fuel consumption and the role of US. *Energy policy,* 36**,** 775-786.

SHAH, S. S., AHMAD, I., AHMAD, W., ISHAQ, M., GUL, K., KHAN, R. & KHAN, H. 2018. Study on adsorptive capability of acid activated charcoal for desulphurization of model and commercial fuel oil samples. *Journal of environmental chemical engineering,* 6**,** 4037-4043.

SHAHBAZ, M., SARWAR, S., CHEN, W. & MALIK, M. N. 2017. Dynamics of electricity consumption, oil price and economic growth: Global perspective. *Energy Policy,* 108**,** 256-270.

SHAKIRULLAH, M., AHMAD, I., AHMAD, W. & ISHAQ, M. 2010. Desulphurization study of petroleum products through extraction with aqueous ionic liquids. *Journal of the Chilean Chemical Society,* 55**,** 179-183.

SHAKORFOW, A. M. 2012. *Process intensification in the demulsification of water-in-crude oil emulsions via crossflow microfiltration through a hydrophilic polyHIPE polymer (PHP).* Newcastle Universtity.

SHANG, H., DU, W., LIU, Z. & ZHANG, H. 2013. Development of microwave induced hydrodesulfurization of petroleum streams: A review. *Journal of Industrial and Engineering Chemistry,* 19**,** 1061-1068.

SHEN, F., LIU, J., ZHANG, Z., DONG, Y. & GU, C. 2018. Density functional study of hydrogen sulfide adsorption mechanism on activated carbon. *Fuel Processing Technology,* 171**,** 258-264.

SHEN, Y., LI, P., XU, X. & LIU, H. 2012. Selective adsorption for removing sulfur: a potential ultra-deep desulfurization approach of jet fuels. *RSC advances,* 2**,** 1700-1711.

SILVERSTEIN, R. M. & BASSLER, G. C. 1962. Spectrometric identification of organic compounds. *Journal of Chemical Education,* 39**,** 546.

SINNOTT, R. 2014. *Chemical engineering design,* Elsevier.

SONG, C. 2003. An overview of new approaches to deep desulfurization for ultra-clean gasoline, diesel fuel and jet fuel. *Catalysis today,* 86**,** 211-263.

SONG, C. & MA, X. 2003. New design approaches to ultra-clean diesel fuels by deep desulfurization and deep dearomatization. *Applied Catalysis B: Environmental,* 41**,** 207-238.

SONG, C. & MA, X. 2004. Ultra-deep desulfurization of liquid hydrocarbon fuels: Chemistry and process. *International Journal of Green Energy,* 1**,** 167-191.

SOTELO, J., UGUINA, M. & ÁGUEDA, V. 2007. Fixed bed adsorption of benzothiophene over zeolites with faujasite structure. *Adsorption,* 13**,** 331-339.

SPEIGHT, J. G. 2014. *The chemistry and technology of petroleum,* CRC press.

SRIVASTAV, A. & SRIVASTAVA, V. C. 2009. Adsorptive desulfurization by activated alumina. *Journal of hazardous materials,* 170**,** 1133-1140.

STEIJNS, M. & MARS, P. 1977. Catalytic oxidation of hydrogen sulfide. Influence of pore structure and chemical composition of various porous substances. *Industrial & Engineering Chemistry Product Research and Development,* 16**,** 35-41.

STUART, B. 2000. Infrared spectroscopy. *Kirk-Othmer Encyclopedia of Chemical Technology*.

SUZUKI, M. 1990. *Adsorption engineering,* Kodansha.

TAI, H., SERGIENKO, A. & SILVERSTEIN, M. 2001. Organic–inorganic networks in foams from high internal phase emulsion polymerisations. *Polymer,* 42**,** 4473-4482.

TAKAHASHI, A., YANG, R. T., MUNSON, C. L. & CHINN, D. 2001. Cu (I)− Y-zeolite as a superior adsorbent for diene/olefin separation. *Langmuir,* 17**,** 8405-8413.

TAN, L. & TAN, B. 2017. Hypercrosslinked porous polymer materials: design, synthesis, and applications. *Chemical Society Reviews,* 46**,** 3322-3356.

TANG, K., SONG, L.-J., DUAN, L.-H., LI, X.-Q., GUI, J.-Z. & SUN, Z.-L. 2008. Deep desulfurization by selective adsorption on a heteroatoms zeolite prepared by secondary synthesis. *Fuel processing technology,* 89**,** 1-6.

TEBBOTH, M., MENNER, A., KOGELBAUER, A. & BISMARCK, A. 2014. Polymerised high internal phase emulsions for fluid separation applications. *Current Opinion in Chemical Engineering,* 4**,** 114-120.

THUMBARATHY, D. 2018. *a Preparation of functional polyHIPE polymers for agro-process and bio-process applications.* Newcast; e University.

TRIANTAFYLLIDIS, K. S. & DELIYANNI, E. A. 2014. Desulfurization of diesel fuels: adsorption of 4, 6-DMDBT on different origin and surface chemistry nanoporous activated carbons. *Chemical Engineering Journal,* 236**,** 406-414.

TURK, B. & GUPTA, R. RTI's trend process for deepdesulfurization of naphtha. abstracts of papers of the American Chemical Society, 2001. AMER CHEMICAL SOC 1155 16TH ST, NW, WASHINGTON, DC 20036 USA, U462-U462.

VELU, S., MA, X. & SONG, C. 2002. Zeolite-based adsorbents for desulfurization of jet fuel by selective adsorption. *Fuel Chemistry Division Preprints,* 47**,** 447-448.

WAKEMAN, R., BHUMGARA, Z. & AKAY, G. 1998. Ion exchange modules formed from polyhipe foam precursors. *Chemical Engineering Journal,* 70**,** 133-141.

WALSH, D., STENHOUSE, J., KINGSBURY, L. & WEBSTER, E. 1996. Polymipe foams: Production, characterisation and performance as aerosol filtration materials. *Journal of Aerosol Science,* 27**,** S629-S630.

WANG, B., ZHU, J. & MA, H. 2009. Desulfurization from thiophene by SO42−/ZrO2 catalytic oxidation at room temperature and atmospheric pressure. *Journal of hazardous materials,* 164**,** 256-264.

WANG, X., WAN, H., HAN, M., GAO, L. & GUAN, G. 2012. Removal of thiophene and its derivatives from model gasoline using polymer-supported metal chlorides ionic liquid moieties. *Industrial & Engineering Chemistry Research,* 51**,** 3418-3424.

WANG, X., WANG, A., LI, N., WANG, X., LIU, Z. & ZHANG, T. 2006. Catalytic reduction of SO2 with CO over supported iron catalysts. *Industrial & engineering chemistry research,* 45**,** 4582-4588.

WEBER, J., SU, Q., ANTONIETTI, M. & THOMAS, A. 2007. Exploring polymers of intrinsic microporosity–microporous, soluble polyamide and polyimide. *Macromolecular Rapid Communications,* 28**,** 1871-1876.

WILLIAMS, J. M. 1988. Toroidal microstructures from water-in-oil emulsions. *Langmuir,* 4**,** 44-49.

WILLIAMS, J. M. 1991. High internal phase water-in-oil emulsions: influence of surfactants and cosurfactants on emulsion stability and foam quality. *Langmuir,* 7**,** 1370-1377.

WILLIAMS, J. M., GRAY, A. J. & WILKERSON, M. H. 1990. Emulsion stability and rigid foams from styrene or divinylbenzene water-in-oil emulsions. *Langmuir,* 6**,** 437-444.

WILLIAMS, J. M. & WROBLESKI, D. A. 1988. Spatial distribution of the phases in water-in-oil emulsions. Open and closed microcellular foams from cross-linked polystyrene. *Langmuir,* 4**,** 656-662.

WILLIAMS, J. M. & WROBLESKI, D. A. 1989. Microstructures and properties of some microcellular foams. *Journal of materials science,* 24**,** 4062-4067.

WITUCKI, G. L. 1993. A silane primer: chemistry and applications of alkoxy silanes. *Journal of coatings technology,* 65**,** 57-57.

WOODWARD, R. T., JOBBE-DUVAL, A., MARCHESINI, S., ANTHONY, D. B., PETIT, C. & BISMARCK, A. 2017. Hypercrosslinked polyHIPEs as precursors to designable, hierarchically porous carbon foams. *Polymer,* 115**,** 146-153.

WU, D., XU, F., SUN, B., FU, R., HE, H. & MATYJASZEWSKI, K. 2012. Design and preparation of porous polymers. *Chemical reviews,* 112**,** 3959-4015.

WU, R., MENNER, A. & BISMARCK, A. 2010. Tough interconnected polymerized medium and high internal phase emulsions reinforced by silica particles. *Journal of Polymer Science Part A: Polymer Chemistry,* 48**,** 1979-1989.

WU, X., HONG, X., LUO, Z., HUI, K. S., CHEN, H., WU, J., HUI, K., LI, L., NAN, J. & ZHANG, Q. 2013. The effects of surface modification on the supercapacitive behaviors of novel mesoporous carbon derived from rod-like hydroxyapatite template. *Electrochimica Acta,* 89**,** 400-406.

XIA, Y., LI, Y., GU, Y., JIN, T., YANG, Q., HU, J., LIU, H. & WANG, H. 2016. Adsorption desulfurization by hierarchical porous organic polymer of poly-methylbenzene with metal impregnation. *Fuel,* 170**,** 100-106.

XIAO, J., LI, Z., LIU, B., XIA, Q. & YU, M. 2008. Adsorption of benzothiophene and dibenzothiophene on ion-impregnated activated carbons and ion-exchanged Y zeolites. *Energy & Fuels,* 22**,** 3858-3863.

XING, R., LIU, Y., WANG, Y., CHEN, L., WU, H., JIANG, Y., HE, M. & WU, P. 2007. Active solid acid catalysts prepared by sulfonation of carbonization-controlled mesoporous carbon materials. *Microporous and Mesoporous Materials,* 105**,** 41-48.

XU, J., FU, D. & LU, S. 2009. The recovery of sulphuric acid from the waste anodic aluminum oxidation solution by diffusion dialysis. *Separation and Purification Technology,* 69**,** 168-173.

XU, S., LUO, Y. & TAN, B. 2013. Recent development of hypercrosslinked microporous organic polymers. *Macromolecular rapid communications,* 34**,** 471-484.

YANG, C.-M. & KANEKO, K. 2002. Adsorption properties of iodine-doped activated carbon fiber. *Journal of colloid and interface science,* 246**,** 34-39.

YANG, P.-Y., JU, S.-P. & HUANG, S.-M. 2018. Predicted structural and mechanical properties of activated carbon by molecular simulation. *Computational Materials Science,* 143**,** 43-54.

YANG, X., ERICKSON, L. E., HOHN, K. L., JEEVANANDAM, P. & KLABUNDE, K. J. 2006. Sol− Gel Cu− Al2O3 adsorbents for selective adsorption of thiophene out of hydrocarbon. *Industrial & engineering chemistry research,* 45**,** 6169-6174.

YIN, C. & XIA, D. 2004. A study of the distribution of sulfur compounds in gasoline produced in China. Part 3. Identification of individual sulfides and thiophenes. *Fuel,* 83**,** 433-441.

YU, C., FAN, X., YU, L., BANDOSZ, T. J., ZHAO, Z. & QIU, J. 2013. Adsorptive removal of thiophenic compounds from oils by activated carbon modified with concentrated nitric acid. *Energy & fuels,* 27**,** 1499-1505.

YUAN, Z.-Y. & SU, B.-L. 2006. Insights into hierarchically meso–macroporous structured materials. *Journal of Materials Chemistry,* 16**,** 663-677.

ZAKI, T., MOHAMED, N. H., NESSIM, M. I. & EL SALAM, H. A. 2013. Characterization and application of nano-alumina sorbents for desulfurization and dearomatization of Suez crude petrolatum. *Fuel processing technology,* 106**,** 625-630.

ZHENG, X., ZHANG, Y., WANG, H. & DU, Q. 2014. Interconnected macroporous polymers synthesized from silica particle stabilized high internal phase emulsions. *Macromolecules,* 47**,** 6847-6855.

ZHOU, A., MA, X. & SONG, C. 2009. Effects of oxidative modification of carbon surface on the adsorption of sulfur compounds in diesel fuel. *Applied Catalysis B: Environmental,* 87**,** 190-199.

ZHOU, W.-Q., GU, T.-Y., SU, Z.-G. & MA, G.-H. 2007. Synthesis of macroporous poly (styrene-divinyl benzene) microspheres by surfactant reverse micelles swelling method. *Polymer,* 48**,** 1981-1988.

ZHOU, W., APKARIAN, R., WANG, Z. L. & JOY, D. 2006. Fundamentals of scanning electron microscopy (SEM). *Scanning microscopy for nanotechnology.* Springer.

Appendices

Appendix- 1 Hydrocarbon Characteristics

Hydrocarbon Characteristics

		Paraffin		Naphthenics	Aromatics	Olefins
		Normal	Iso			
Characteristics						
Specific Gravity		Low	Low	Medium	High	Low
COMBUSTION	Octane n° (RON)	Very low	High	Medium	Very high	High
	Sensitivity RON/MON	Very low	Very low	Low	High	Very high
	Cetane n°	High	Low	Medium	Very low	Low
	C/H Race	Low	Low	Medium	High	Medium
	Specific Gravity Kj/Kg	High	High	Medium	Low	Medium
Cold properties		Very weak	Good	Good	Good	Good
Chemical Stability		Good	Good	Good	Good	Very weak

Appendix- 2a. Physical Constants of the main sulphur Compounds and b. Chemical formulas of organosulfur contents.

	Chemical formula	Structural formula	Molecular weight	Normal boiling point °C	Sp gr_4^{15} (liquid)
Hydrogen sulfide	H_2S	H–S–H	34,1	-60.3	
MERCAPTANS					
Methylmercaptan	CH_3SH	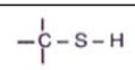	48,1	6,0	0,873
Ethylmercaptan	C_2H_5SH	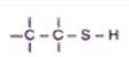	62,1	35,0	0,845
n-Propylmercaptan	C_3H_7SH	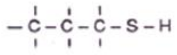	76,2	67,6	0,847
n-Butylmercaptan	C_4H_9SH	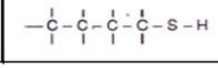	90,2	98,5	0,847
SULFIDES					
Dimethylsulfide	C_2H_6S	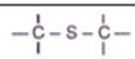	62,1	37,3	0,854
Ethylmethylsulfide	C_3H_8S	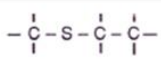	76,2	66,6	0,848
Diethylsulfide	$C_4H_{10}S$	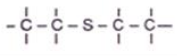	90,2	92,1	0,841
Methyl n-Propylsulfide	$C_4H_{10}S$	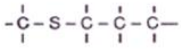	90,2	95,5	0,847
DISULFIDES					
Dimethylsulfide	C_2H_6S	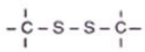	94,2	109,6	1,069
Diethylsulfide	$C_4H_{10}S_2$		122,2	152,6	0,998
Dipropyldisulfide	$C_6H_{14}S_2$	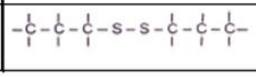	150,3	126.5 at 100 mm of Hg	0,964
THIOPHENIC COMPOUNDS					
Thiofene	C_4H_4S	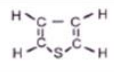	84,1	84	1,070
Methylthiophene	$CH_3C_4H_3S$	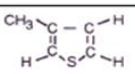	98,2	119	1,069
Benzothiophene	C_8H_6S	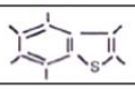	134,2	220	1,165

Appendix 2/b

Hydrogen sulfid

H_2S bp = – 60°C

- Gaseous
- corrosive
- Very toxic (deadly)

Mercaptans

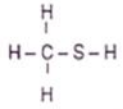

Methylmercaptan CH_3SH bp = + 6°C

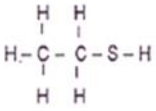

Ethylmercaptan C_2H_5SH bp = 35°C

- acidic
- Very bad smell

Sulfids and Disulfids

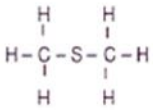

Dimethyldisulfid C_2H_6S bp = 37°C

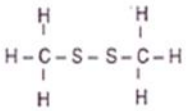

Dimethyldisulfid $C_2H_6S_2$ bp = 109.6°C

- Non acidic
- No bad smell
- Decompose into mercaptans unter heating

Cyclic Sulfur

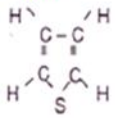

Thiophene C_4H_4S bp = 84°C

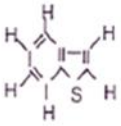

Benzothiophene C_8H_6S bp = 220°C

- Not corrosive
- stable

Appendix- 3Reactivity of various organic sulphur compounds in HDS versus their ring sizes and alkyl postion. (Song 2003).

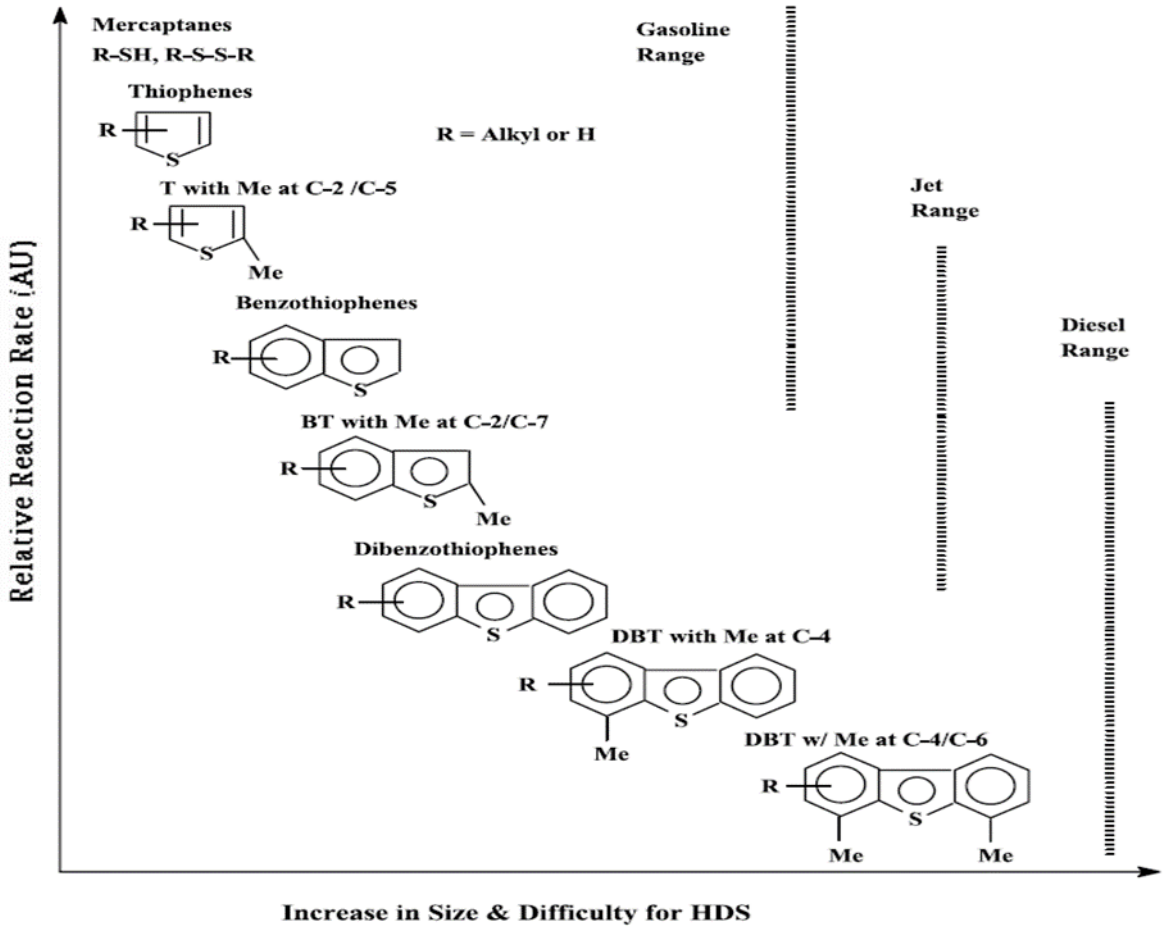

Appendix- 4 Typical Refinery analysis log sheet (Aldaura refinery –Iraq)

Crude Oil Sample		Duara Heavy				API			36.0		No CA-34	
Producing Country		IQ				s wt%			3.5			
Sample Origin		N/C MUTANABBI 30/12/86				K Factor			11.4	Crude	Assay	N°
							Crude Oil Peculiarities				Yields	on
Density @ 15/4 °C		0.844	Distillation		(Barbetta		Chromatograp				Wt%	vol%
Viscosity @	cS	7.00										
Viscosity @	cS	4.32	P.I.	°C		40	C2 +	wt%	0.01	GPL	1.67	2.49
	w	1.9	@ 50	°C	vol%	1				(C1-		
Pour Point	°C	<-20	@ 75	°C	vol%	5	C3 +	wt%	0.16	V.Na	21.35	25.24
Reid Vap.P.@	Ps	5.80	@	°C	vol%	10				C5-		
	Kg/	0.41	@	°C	vol%	15	i C4 +	wt%	0.31	Gasoi	36.59	37.16
Asphaltenes	w	2.10	@	°C	vol%	21				170-		
Carb. Residue	w	4.80	@	°C	vol%	27	n C4	wt%	0.70	Gasoi	5.03	4.76
Ashes	w		@	°C	vol%	33				370-		
Nickel	p	11	@	°C	vol%	37	i C5 +	wt%	1.19	Resid	35.36	30.35
Vanadium	p	26	@	°C	vol%	42				400 +		
Water for distillation	w	0.02	@	°C	vol%	47	n C5	wt%	1.25			
Salts as NaCl	m	<5	@	°C	vol%	52						
Water and sediments	w	0.02										

Yields and Properties of the products

Products		Virgin Naphthas			Kero		Gas Oils		VGO	Residues		
°C		C5-80	80-	80-	170-	250-	250-	250-	400-	350 +	370 +	525 +
Crude Yields	w	6.05	12.44	15.30	14.31	13.05	18.22	22.28	16.16	44.45	40.39	19.20
	vo	7.85	14.28	17.39	15.11	13.14	18.17	22.04	14.67	38.99	35.11	15.68
Density @ 15/4 °C		0.647	0.732	0.739	0.797	0.835	0.843	0.850	0.922	0.957	0.965	1.029
	w	0.021	0.071	0.089	0.25	0.87	0.95	1.02	2.5	3.91	4.02	5.56
Viscosity @	cS				1.72							
Viscosity @	cS				1.31	3.09	3.71	4.34				
Viscosity @	cS					2.44	2.86	3.26	49	253	478	
n-Paraffins tot	w	44.18	27.03	28.26	23.73							
i-Paraffins tot	w	47.62	35.98	38.08								
Naphtens tot	w	8.00	28.41	23.63								
Aromatics tot	w	0.20	8.58	10.03								
Aniline Point	°C				61.80	72.20	73.40	74.10				
Diesel Index					65.60	61.10	59.20	57.60				
Smoke Point	m				26							
Freezing Point	°C				-52							
Cloud Point	°C					-16	-10	-6				
Pour Point	°C					-16	-12	-10	38	22	24	38
CFPP	°C											
Molecular Weight		77.3	108.5	109.6					370			
C/H		5.12	5.74	5.80	6.27	6.59	6.67	6.73	7.40	7.76	7.84	8.55
BMCI		0.18	14.39	15.56	23.34	28.12	30.19	31.24				
K Factor (UOP)		12.87	12.10	12.06	11.86	11.86	11.86	11.82				
Asphaltanes	w											11.30
Conradson Res.	w											25.00
Nickel	p											54
Vanadium	p											110

Midland Refineries Company (MRC)

Research & Quality Control Department

Sample: Evaluation of Basra Crude Oil (BSH) In April / 2017

TEST	RESULT	METHOD
API Gravity @15.6 C^{o}	30.6	ASTM-D1298
SP. Gravity @ 15.6 C^{o}/ 15.6 C^{o}	0.8729	ASTM-IP
Density @ 15 C^{o}	0.8725	----------
Sulfur Content wt.%	3.11	ASTM-4294
Kinetic Viscosity Cst.		ASTM-D445
@10 C^{o}	28.00	----------
@21.1 C^{o}	16.9	----------
@37.8 C^{o}	9.7	----------
@50.0 C^{o}	6.5	----------
Pour Point C^{o}	Below -30	ASTM-D97
R.V.P Kg/cm^{2}	0.56	ASTM-D323
water and sediment Vol.%	0.2	IP-75
Salt Content wt.%	0.0072	IP-77 & ASTM-D3230
Ram. Carbon Residue wt.%	5.4	ASTM-D524
Asphaltenes Content wt.%	2.03	JPI-55-45-95
Ash Content Wt.%	0.0140	ASTM-D482
Vanadium PPM	62.19	ASTM-D6728
Nickel PPM	19.69	ASTM-D6728
KUOP Characterization Factor	11.9	UOP Method 375
Water Content Vol.%	0.15	IP-74
Distillation		IP-24
IBP C^{o}	46	
Rec. @50.0 C^{o}	0.5	
@75.0	3.5	
@100.0	7.0	
@125.0	11.0	
@150.0 C^{o}	16.00	
@175.0 C^{o}	20.0	
@200.0 C^{o}	25.0	
@225.0 C^{o}	30.0	
@250.0 C^{o}	34.0	
@275.0 C^{o}	39.0	
@300.0 C^{o}	44.0	
Total Distil.Vol. %	45.0	

AYAD AHMED MOHAMED

Manager of Research & Quality Control Department

Midland Refineries Company (MRC)

Research & Quality Control Department

Sample: Evaluation of Midland Refineries Company (MRC) - April / 2017

TEST	RESULT	METHOD
API Gravity @15.6 C^{O}	30.8	ASTM-D1298
SP. Gravity @ 15.6 C^{O}/ 15.6 C^{O}	0.8718	ASTM-IP
Density @ 15 C^{O}	0.8714	----------
Sulfur Content wt.%	3.09	ASTM-4294
Kinetic Viscosity Cst.		ASTM-D445
@10 C^{O}	26.5	----------
@21.1 C^{O}	15.3	----------
@37.8 C^{O}	8.1	----------
@50.0 C^{O}	5.4	----------
Pour Point C^{O}	Below -30	ASTM-D97
R.V.P Kg/cm^{2}	0.54	ASTM-D323
water and sediment Vol.%	0.1	IP-75
Salt Content wt.%	0.0015	IP-77 & ASTM-D3230
Ram. Carbon Residue wt.%	5.1	ASTM-D524
Asphaltenes Content wt.%	1.87	JPI-55-45-95
Ash Content Wt.%	0.0110	ASTM-D482
Vanadium PPM	57.85	ASTM-D6728
Nickel PPM	18.31	ASTM-D6728
KUOP Characterization Factor	11.9	UOP Method 375
Water Content Vol.%	0.05	IP-74
Distillation		IP-24
IBP C^{O}	44	
Rec. @50.0 C^{O}	1.0	
@75.0	5.0	
@100.0	9.0	
@125.0	14.0	
@150.0 C^{O}	18.0	
@175.0 C^{O}	23.0	
@200.0 C^{O}	27.0	
@225.0 C^{O}	31.0	
@250.0 C^{O}	35.0	
@275.0 C^{O}	40.0	
@300.0 C^{O}	45.0	
Total Distl.Vol.%	47.0	

AYAD AHMED MOHAMED

Manager of Research & Quality Control Department

Midland Refineries Company (MRC)

Research & Quality Control Department

Sample: Evaluation of Different Iraqi Crude Oil samples - March / 2017

TEST	Rumaila South crude oil. (RSC)	Ashamia degassing station. (ADSH)	Almarkazia degassing station. (AKDS)	Mushraf qurainat degassing station (MQDS)	Mushraf shamia gas station. (MSGS)	Qurainat gas station. (QGS)	METHOD
API Gravity @15.6 Co	33.9	33.5	33.5	26.8	28	32.9	ASTM-D1298
SP. Gravity @ 15.6 Co/15.6 Co	0.8555	0.8576	0.8576	0.8939	08871	0.8607	ASTM-IP
Density @ 15 Co	0.8551	0.8571	0.8571	0.8934	0.8867	0.8603	----------
Sulfur Content wt.%	2.11	2.14	2.01	3.832	3.71	2.16	ASTM-4294
Kinetic Viscosity Cst.							ASTM-D445
@10 Co	23.20	26.8	24.9	49.3	43.5	28.8	----------
@21.1 Co	15.07	17.05	16.01	31.56	27.4	16.55	----------
@37.8 Co	6.90	7.8	7.6	17.6	15.7	8.8	----------
@50.0 Co	5.3	6.0	6.1	12.5	10.7	6.2	----------
Pour Point Co	Below -24	Below -24	Below -24	Below -30	Below -30	Below-30	ASTM-D97
R.V.P Kg/cm2	0.33	0.2	0.2	0.59	0.700	0.55	ASTM-D323
water and sediment Vol.%	0.05	0.3	0.1	0.05	0.2	0.1	IP-75
Salt Content wt.%	0.0138	0.1230	0.0209	0.0015	0.0024	0.0150	IP-77 & ASTM-D3230
Ram. Carbon Residue wt.%	3.5	4.1	4.0	7.5	6.5	4.3	ASTM-D524
Asphaltenes Content wt.%	1.40	2.08	1.70	3.02	2.57	2.4	JPI-5S-45-95
Ash Content Wt.%	0.05	0.5	0.05	traces	0.2	0.05	ASTM-D482
Vanadium PPM	34.33	42.02	34.30	98.26	84.84	53.90	ASTM-D6728
Nickel PPM	9.29	13.43	10.11	28.47	24.92	17.09	ASTM-D6728
KUOP Characterization Factor	11.9	11.9	11.9	11.6	11.7	11.9	UOP Method 375
Water Content Vol.%	0.0208	--	0.0250	0.0321	0.0290	0.0200	IP-74
Distillation							IP-24
IBP Co	34	37	36	34	34	30	
Rec. @50.0 Co	2.0	1.0	2.5	2.0	1.5	3.5	
@75.0	5.0	5.0	5.5	5.0	4.0	7.0	
@100.0	9.0	9.0	10.0	9.0	7.5	11.0	
@125.0	14.0	14.0	15.0	12.5	9.5	15.5	
@150.0 Co	19.0	19.0	20.0	16.5	14.0	20.5	
@175.0 Co	24.5	25.0	25.5	21.0	18.0	26.0	
@200.0 Co	30.0	30.0	30.5	25.0	22.0	31.0	
@225.0 Co	34.0	34.5	35.0	29.0	26.0	35.0	
@250.0 Co	39.0	38.5	39.0	32.5	29.0	40.0	
@275.0 Co	42.0	43.0	44.0	36.0	33.0	43.0	
@300.0 Co	47.5	48.0	48.0	40.5	37.0	48.0	
Total Distil.Vol. %	49.0	49.0	50.0	42.5	39.0	50.0	

AYAD AHMED MOHAMED

Manager of Research & Quality Control Department

Midland Refineries Company (MRC)

Research & Quality Control Department

Sample: Evaluation of Kirkuk Crude Oil (KKO) April / 2017

TEST	RESULT	METHOD
API Gravity @15.6 C^{o}	34.3	ASTM-D1298
SP. Gravity @ 15.6 C^{o}/ 15.6 C^{o}	0.8534	ASTM-IP
Density @ 15 C^{o}	0.8530	----------
Sulfur Content wt.%	2.53	ASTM-4294
Kinetic Viscosity Cst.		ASTM-D445
@10 C^{o}	13.7	----------
@21.1 C^{o}	8.98	----------
@37.8 C^{o}	6.12	----------
@50.0 C^{o}	4.83	----------
Pour Point C^{o}	Below -30	ASTM-D97
R.V.P Kg/cm^{2}	0.53	ASTM-D323
water and sediment Vol.%	0.1	IP-75
Salt Content wt.%	0.0012	IP-77 & ASTM-D3230
Ram. Carbon Residue wt.%	4.5	ASTM-D524
Asphaltenes Content wt.%	1.75	JPI-55-45-95
Ash Content Wt.%	0.0110	ASTM-D482
Vanadium PPM	31.2	ASTM-D6728
Nickel PPM	11.15	ASTM-D6728
KUOP Characterization Factor	12.0	UOP Method 375
Water Content Vol.%	0.05	IP-74
Distillation		IP-24
IBP C^{o}	34	
Rec. @50.0 C^{o}	2.0	
@75.0	9.0	
@100.0	14.0	
@125.0	19.0	
@150.0 C^{o}	25.0	
@175.0 C^{o}	31.0	
@200.0 C^{o}	36.0	
@225.0 C^{o}	40.0	
@250.0 C^{o}	45.0	
@275.0 C^{o}	51.0	
@300.0 C^{o}	55.0	
Total Distil.Vol. %	57.0	

AYAD AHMED MOHAMED

Manager of Research & Quality Control Department

Appendix 5 ASTM & API Standard Tests Methods

1-API Gravity @15.6 Co ASTM-D1298

Standard Test Method for Density, Relative Density, or API Gravity of Crude Petroleum and Liquid Petroleum Products by Hydrometer Method

1.1 This test method covers the laboratory determination using a glass hydrometer in conjunction with a series of calculations, of the density, relative density, or API gravity of crude petroleum, petroleum products, or mixtures of petroleum and nonpetroleum products normally handled as liquids, and having a Reid vapor pressure of 101.325 kPa (14.696 psi) or less. Values are determined at existing temperatures and corrected to 15 °C or 60 °F by means of a series of calculations and international standard tables.

1.2 The initial hydrometer readings obtained are uncorrected hydrometer readings and not density measurements. Readings are measured on a hydrometer at either the reference temperature or at another convenient temperature, and readings are corrected for the meniscus effect, the thermal glass expansion effect, alternative calibration temperature effects and to the reference temperature by means of the Petroleum Measurement Tables; values obtained at other than the reference temperature being hydrometer readings and not density measurements.

1.3 Readings determined as density, relative density, or API gravity can be converted to equivalent values in the other units or alternative reference temperatures by means of Interconversion Procedures (API *MPMS* Chapter 11.5), or Adjunct to D1250Guide for Petroleum Measurement Tables (API *MPMS* Chapter 11.1), or both, or tables, as applicable.

1.4 The initial hydrometer readings determined in the laboratory shall be recorded before performing any calculations. The calculations required in Section 10 shall be applied to the initial hydrometer reading with observations and results reported as required by Section 11 prior to use in a subsequent calculation procedure (ticket calculation, meter factor calculation, or base prover volume determination).

1.5 Annex A1 contains a procedure for verifying or certifying the equipment for this test method.

1.6 The values stated in SI units are to be regarded as standard.

1.7 *This standard does not purport to address all of the safety concerns, if any, associated with its use. It is the responsibility of the user of this standard to establish appropriate safety and health practices and determine the applicability of regulatory limitations prior to use.*

1.8 *This international standard was developed in accordance with internationally recognized principles on standardization established in the Decision on Principles for the Development of International Standards, Guides and Recommendations issued by the World Trade Organization Technical Barriers to Trade (TBT) Committee.*

2-SP. Gravity @ 15.6 Co/ Co ASTM-IP

Product group(s): Density & Gravity User group(s): Airports & Aviation, Batteries, Beverages, Biofuel, Bitumen, Crude Petroleum, Density, Gravity, Mastics, Paint, Varnish Scope: The Hydrometer Method is suitable for determining the density of cutback asphalts which are liquid at room temperature by using a glass hydrometer. For materials that are solid or semi-solid at room temperature, use Hubbard Pycnometer Method ASTM D 70. The sample is brought to the testing temperature and transferred to a cylinder at approximately the same temperature. The cylinder and its contents are placed in a constant temperature bath to avoid excessive temperature variation during the test. The appropriate hydrometer is lowered into the sample and allowed to settle. After temperature equilibrium, the hydrometer is read and the temperature of the sample is noted. The hydrometer reading is converted to the density at +15°C using standard tables.

3.1 Sulphur Content wt.% ASTM-4294

Measuring the sulfur in fuel oil via XRF (ASTM D4294)

Standard Test Method for Sulfur in Petroleum and Petroleum Products by Energy Dispersive X-ray Fluorescence Spectrometry1

This test method covers the determination of total sulfur in petroleum and petroleum products that are single-phase and either liquid at ambient conditions, liquefiable with moderate heat, or soluble in hydrocarbon solvents. These materials can include diesel fuel, jet fuel, kerosine, other distillate oil, naphtha, residual oil, lubricating base oil, hydraulic oil, crude oil, unleaded gasoline

5. Pour Point Co ASTM-D97

Standard Test Method for Pour Point of Petroleum Products

1.1 This test method covers and is intended for use on any petroleum product.2 A procedure suitable for black specimens, cylinder stock, and nondistillate fuel oil is described in 8.8. The cloud point procedure formerly part of this test method now appears as Test Method D2500.1.2 Currently there is no ASTM test method for automated Test Method D97 pour point measurements.1.3 Several ASTM test methods offering alternative procedures for determining pour points using automatic apparatus are available. None of them share the same designation number as Test Method D97. When an automatic instrument is used, the ASTM test method designation number specific to the technique shall be reported with the results. A procedure for testing the pour point of crude oils is described in Test Method D5853.1.4 The values stated in SI units are to be regarded as standard. No other units of measurement are included in this standard.

6. R.V.P Kg/cm2 ASTM-D323

Standard Test Method for Vapor Pressure of Petroleum Products (Reid Method)1.1 This test method covers procedures for the determination of vapor pressure (see Note 1) of gasoline, volatile crude oil, and other volatile petroleum products.1.2 Procedure A is applicable to gasoline and other petroleum products with a vapor pressure of less than 180 kPa (26 psi).1.3 Procedure B may also be applicable to these other materials, but only gasoline was included in the interlaboratory test program to determine the precision of this test method.1.4 Procedure C is for materials with a vapor pressure of greater than 180 kPa (26 psi).1.5 Procedure D for aviation gasoline with a vapor pressure of approximately 50 kPa (7 psi).1.6 This test method is not applicable to liquefied petroleum gases or fuels containing oxygenated compounds other than methyl t-butyl ether (MTBE). For determination of the vapor pressure of liquefied petroleum gases, refer to Test Method D1267 or Test Method D6897. For determination of the vapor pressure of gasoline-oxygenate blends, refer to Test Method D4953. The precision for crude oil has not been determined since the early 1950s (see Note 3). Test Method D6377 has been approved as a method for determination of vapor pressure of crude oil. IP 481 is a test method for determination of the air-saturated vapor pressure of crude oil.

7. water and sediment Vol.% IP-75 Standard

Test Method for Water and Sediment in Fuel Oils by the Centrifuge Method

This standard is issued under the fixed designation D 1796; the number immediately following the designation indicates the year of original adoption or, in the case of revision, the year of last revision. A number in parentheses indicates the year of last reapproval. A superscript epsilon (e) indicates an editorial change since the last revision or reapproval.This standard has been approved for use by agencies of the Department of Defense.

1.1 This test method covers the laboratory test for determination of water and sediment in fuel oils by using the centrifuge method in the range from 0 to 30 % volume. This chapter, along with API MPMS Chapter 10.3 (Test Method D 4007, IP 359), supersedes the previous edition of Test

Method D 1796 (API Standard D 2548, IP 75).NOTE 1—With some types of fuel oils such as residual fuel oils or distillate fuel oils containing residual components, it is difficult to obtain

water or sediment contents with this test method. When this situation is encountered, Method D 95 (API MPMS Chapter 10.5) or Test Method D 473 (API MPMS Chapter 10.1) may be used. 1.2 Annex A2 contains a procedure for saturating toluene with water. 1.3 The values stated in SI units are to be regarded as the standard. The values in parentheses are for information only.1.4 This standard does not purport to address all of thesafety concerns, if any, associated with its use. It is the responsibility of the user of this standard to establish appropriate safety and health practices and determine the applicability of regulatory limitations prior to use. For a specific precautionary statement .

8. Salt Content wt.% IP-77 & ASTM-D3230

The Seta Salt-in-Crude Analyser is a robust and portable instrument for determining the chloride (salt) content of crude oils in full conformity to ASTM D3230, IP 77 and equivalent test methods.The Seta Salt-in-Crude Analyser is pre-calibrated and automatically displays salt concentration measurements in g/m3 or lbs/1000bbl (pounds per thousand barrels), this avoids the need to mix salt calibration standards and makes testing a simple and fast procedure.

9. Ram. Carbon Residue wt.% ASTM-D524

This test method covers the determination of the amount of carbon residue (Note 1) left after evaporation and pyrolysis of an oil, and it is intended to provide some indication of relative coke-forming propensity. This test method is generally applicable to relatively nonvolatile petroleum products which partially decompose on distillation at atmospheric pressure. This test method also covers the determination of carbon residue on 10 % (V/V) distillation residues (see Section 10). Petroleum products containing ash-forming constituents as determined by Test Method D482, will have an erroneously high carbon residue, depending upon the amount of ash formed (Notes 2 and 3). NOTE 1-The term carbon residue is used throughout this test method to designate the carbonaceous residue formed during evaporation and pyrolysis of a petroleum product. The residue is not composed entirely of carbon, but is a coke which can be further changed by pyrolysis. The term carbon residue is continued in this test method only in deference to its wide common usage. NOTE 2-Values obtained by this test method are not numerically the same as those obtained by Test Method D189, or Test Method D4530. Approximate correlations have been derived (see Fig. X2.1) but need not apply to all materials which can be tested because the carbon residue test is applicable to a wide variety of petroleum products. The Ramsbottom Carbon Residue test method is limited to those samples that are mobile below 90 °C. NOTE 3-In diesel fuel, the presence of alkyl nitrates such as amyl nitrate, hexyl nitrate, or octyl nitrate, causes a higher carbon residue value than observed in untreated fuel, which can lead to erroneous conclusions as to the coke-forming propensity of the fuel. The presence of alkyl nitrate in the fuel can be detected by Test Method D4046. NOTE 4-The test procedure in Section 10 is being modified to allow the use of a 100 mL volume automated distillation apparatus. No precision data is available for the procedure at this time, but a round robin is being planned to develop precision data. The 250 mL volume bulb distillation method described in Section 10 for determining carbon residue on a 10 % distillation residue is considered the referee test. The values stated in SI units are to be regarded as standard. No other units of measurement are included in this standard.

10. Asphaltenes Content wt.% JPI-5S-45-95

There Asphaltene the in) 143 IP to equivalent (D6560 Both. oil petroleum and oil crude for Methods Testing solvent ed specifi the using process ltration fi in niquetech gravimetric manual by conducted are methods take will It. concentration Asphaltene calculate to with, analysis this make to day one full a to day a half .vary widely will data measured as disadvantage such is measurement, Analyzer Asphaltene this Using sample for time the except, minute one about in done measured of variation less much with, pretreatment .now until companies oil Japanese many to ducedintro been have analyzer this of sets many so, data wavelength dual this, background said the From 1995 in formalized was method spectrophotometric of method authorized the as analysis Asphaltene for .(JPI (Institute Petroleum Japan the by'' 95-45-5S-JPI'' the as calculated automatically are values mentmeasure the, Analzyer Asphaltene this using When data less has which, method D3279 ASTM of values D6560 ASTM of values the with compared variation .(143 IP or(formalized was method analysis Asphaltene this When of values measurement the on study careful, JPI the by ,done was) 143 IP or (D6560 ASTM and D3279 ASTM good quite was there that result a as proved was it and both the of values measurement the on correlation .methods correlation a set optionally can analyzer this of user A＊ of values the obtain automatically to even formula conventional the to addition in) 143 IP or (D6560 ASTM correlation c specifi own s'User. values measurement .

11. Ash Content Wt.% ASTM-D482

Standard Test Method for Ash from Petroleum Product

1.1 This test method covers the determination of ash in the range 0.001–0.180 mass %, from distillate and residual fuels, gas turbine fuels, crude oils, lubricating oils, waxes, and other petroleum products, in which any ash-forming materials present are normally considered to be undesirable impurities or contaminants (Note 1). The test method is limited to petroleum products which are free from added ash-forming additives, including certain phosphorus compounds (Note 2).Note 1—In certain types of samples, all of the ash-forming metals are not retained quantitatively in the ash. This is particularly true of distillate oils, which require a special ash procedure in order to retain metals quantitatively.Note 2—This test method is not intended for the analysis of unused lubricating oils containing additives; for such samples use Test Method D874. Neither is it intended for the analysis of lubricating oils containing lead nor for used engine crankcase oils.1.2 The values stated in SI units are to be regarded as the standard. The values given in parentheses are for information only. The preferred expression of the property is mass %.

1.3 *This standard does not purport to address all of the safety concerns, if any, associated with its use. It is the responsibility of the user of this standard to establish appropriate safety and health practices and determine the applicability of regulatory limitations prior to use.*

12. Vanadium PPM, Nickel PPM ASTM-D6728

Standard Test Method for Determination of Contaminants in Gas Turbine and Diesel Engine Fuel by Rotating Disc Electrode Atomic Emission Spectrometry1.1 This test method covers the determination of contaminants and materials as a result of corrosion in gas turbine or diesel engine fuels by rotating disc electrode atomic emission spectroscopy (RDE-AES).1.1.1 The test method is applicable to ASTM Grades 0-GT, 1-GT, 2-GT, 3-GT, and 4-GT gas turbine fuels and Grades Low Sulfur No. 1-D, Low Sulfur No. 2-D, No. 1-D, No. 2-D, and No. 4-D diesel fuel oils.1.1.1.1 Trace metal limits of fuel entering turbine combustor(s) are given as 0.5 mg/kg each for vanadium, sodium + potassium, calcium, and lead in Specification D2880 for all GT grades.1.1.2 This test method provides a rapid at-site determination of contamination and corrosive elements ranging from fractions of mg/kg to hundreds of mg/kg in gas turbine and diesel engine fuels so the fuel quality and level of required treatment can be determined.1.1.3 This test method uses oil-soluble metals for calibration and does not purport to quantitatively determine or detect insoluble particles.1.2 The values stated in SI units are to be regarded as standard. No other units of measurement are included in this standard. The preferred units are mg/kg (ppm by mass).1.3 This standard does not purport to address all of the safety concerns, if any, associated with its use. It is the responsibility of the user of this standard to establish appropriate safety and health practices and determine the applicability of regulatory limitations prior to use.

This apparatus usually measures the sulfur amount between ranges 100ppm-3 %wt. The XRF apparatus type 1100 measures only one sample and XRF apparatus type 1800 measures more than one sample (8 samples) simultaneously. Calibration and standardization of the apparatus was done via 4 standard samples of petroleum and oil cuts. In this method the existing total sulfur in fuel oil that in room temperature would become liquid or liquid able with the thermal medium or would dissolve in hydrocarbon solvents, would be measured. These materials could be as diesel fuel, jet fuel, kerosene or the other petroleum compounds that are produced from distillation like naphtha, residual oil, fuel oil and gasoline. Samples like gasoline (with high vapor pressure or light hydrocarbons) could not measure accurately with this method, because they waste during the analysis. Testing method of ASTM D 2622 and 4294 has high working capacity, less stages for preparation of the sample, more ability and accuracy in measuring sulfur in heavy fuel. The outfits of this method are more expensive than the other methods.

3.2 Sulphur Content wt.% ASTM D 5453

Standard Test Method for Determination of Total Sulfur in Light Hydrocarbons, Spark Ignition Engine Fuel, Diesel Engine Fuel, and Engine Oil by Ultraviolet Fluorescence. This test method covers the determination of total sulfur in liquid hydrocarbons, boiling in the range from approximately 25 to 400°C, with viscosities between approximately 0.2 and 20 cSt (mm2/S) at room temperature. 1.2 Three separate interlaboratory studies (ILS) on precision, and three other investigations that resulted in an ASTM research report, have determined that this test method is applicable to naphthas, distillates, engine oil, ethanol, Fatty Acid Methyl Ester (FAME), and engine fuel such as gasoline, oxygen enriched gasoline (ethanol blends, E-85, M-85, RFG), diesel, biodiesel, diesel/biodiesel blends, and jet fuel. Samples containing 1.0 to 8000 mg/kg total sulfur can be analyzed

4. Kinetic Viscosity Cst. ASTM-D445

This test method specifies a procedure for the determination of the kinematic viscosity, v, of liquid petroleum products, both transparent and opaque, by measuring the time for a volume of liquid to flow under gravity through a calibrated glass capillary viscometer. The dynamic viscosity, η, can be obtained by multiplying the kinematic viscosity, v, by the density, ρ, of the liquid

NOTE 1—For the measurement of the kinematic viscosity and viscosity of bitumens, see also Test Methods D2170 and D2171

NOTE 2—ISO 3104 corresponds to Test Method D445 – 03 The result obtained from this test method is dependent upon the behavior of the sample and is intended for application to liquids for which primarily the shear stress and shear rates are proportional (Newtonian flow behavior). If, however, the viscosity varies significantly with the rate of shear, different results may be obtained from viscometers of different capillary diameters. The procedure and precision values for residual fuel oils, which under some conditions exhibit non-Newtonian behavior, have been included The range of kinematic viscosities covered by this test method is from 0.2 mm2/s to 300 000 mm2/s (see Table A1.1) at all temperatures (see 6.3 and 6.4). The precision has only been determined for those materials, kinematic viscosity ranges and temperatures as shown in the footnotes to the precision section .The values stated in SI units are to be regarded as standard. The SI unit used in this test method for kinematic viscosity is mm2/s, and the SI unit used in this test method for dynamic viscosity is mPa·s. For user reference, 1 mm2/s = 10-6 m2/s = 1 cSt and 1 mPa·s = 1 cP = 0.001 Pa·s

Appendix 6. Feed stock analysis

MIDLAND REFINERIES COPMANY

Midland Refineries Company

Research & quality control Department

Daura Refinery

Light Naphtha

Heavy Naphtha

Test	L.N	H.N
RVP@ 37.8 C°	68-70	---
API .gravity @ 15.6 C°	80-81	60-60.5
Doctor test	PS	PS
Octane no.	--	--
Sulfur /PPM	789	597
R.V.P		--
Distillation :- IBP	35-36	88-86
10%	42-44	100
20%	46-48	106-105
30%	50-54	112-110
40%	54-58	118-115
50%	60-64	124-120
60%	65-68	130-128
70%	70-74	136-135
80%	78-80	142-140
90%	88-86	148-145
E.P. C°	118-120	178-176
T.D	96	98
Res	0.6	0.8

Product	Test	Results
Naphtha mix	Sp.gravity @ 15.6 C°	0.71 – 0.69
	API .gravity @ 15.6 C°	66 -72
	Doctor test	Post
	Octane no.	40 -56
	Sulfur wt%	0.02 - 0.078
	R.V.P	0.70 - 0.74
	Distillation :- IBP	30 - 40
	10%	61
	20%	74
	30%	85
	40%	94
	50%	100
	60%	112
	70%	120
	80%	128
	90%	140
	E.P. C°	162 - 187
	Rec. @100 C°	44 - 50 ml
	Rec. @145 C°	91 - 93 ml

Kerosene	Flash point (pm) C°		44 - 48
	API gravity @ 15.6 C°		49 – 52
	Density KG/M^3 @ 15.6 C°		775 -785
	I.B.P C°		155 - 160
	E.B.P C°		225 - 250
	Colour NO.		+28
	Sulfur Wt%		0.32
	Doctor test	H_2S	Negative
		R-SH	Positive

G.O	Flash point (pm) C°	60 - 80
	API gravity @ 15.6 C°	41 - 49
	Density KG/M^3 @ 15.6 C°	812 - 832
	I.B.P C°	170 - 190
	E.B.P C°	330 - 360
	Colour NO.	0.5>
	Cetane NO.	52 - 56
	Diesel index	55 - 65
	Sulfur Wt%	0.850 - 1.6

AYAD AHMED MOHAMED — **AHMED GHAFIL ALIBRAHEEMI**

MANAGER OF RESEARCH & QUALITY CONTROL DEPARTMENT — **RESEARCHER**

Appendix 7. Approval of outstanding study

جمهورية العراق
وزارة النفـــط
شـــركة مصـــافي الوســـط / شـــركة عامـــة
بغـــداد

العـدد : 16323
التاريخ :
الموافق : 8/8/2019

REPUBLIC OF IRAQ
MINISTRY OF OIL
MIDLAND REFINERIES COMPANY
(GENERAL COMPANY) MRC
BAGHDAD

REF : 2382
DATE: 2019/8/8

To Whom It May Concern

Subject : Approval For Laboratory Calibration

Dear, Sir/Madam

With reference to the submitted request by Mr. Ahmed Ghafil Alibraheemi, a PhD student in (Newcastle University / Chemical Engineering and Advanced Material) has expressed his interest to visit our laboratories in Iraq - Baghdad, Oil refineries complex.

The purpose of this visit will be focusing on doing a survey of the laboratory tests and analysis to the Iraqi crude oil and products.

This letter is to confirm our approval up on his request.

Kindest Regards

MINISTRY OF OIL DAURA REFINERY BAGHDAD - IRAQ MIDLAND REFINERIES CO.

08.08.2019
General Manager
ZAID K.SHARIF

MINSTRY OF OIL DIVISION FAX & E-MAIL MIDLAND REFINERIES CO.

Daura fax@mrc.oil.gov.iq
Purchase@mrc.oil.gov.iq
Info@mrc.oil.gov.iq
العناوين الالكترونية لشركة مصافي الوسط

P.O Box 2075 Baghdad
Cable: Daura Baghdad
Tel: 7765471
Fax: 7765482 / 7751096

العنوان البرقي : دورة – بغداد– ص .ب ٢٠٧٥
بغداد – دورة
هاتف البدالة : ٧٧٦٥٤٧١ ب ٩ خط
فاكس : ٧٧٦٥٤٨٢ / ٧٧٥١٠٩٦

Appendix 8.1 Naphtha Results

MIDLAND REFINERIES COPMANY

Midland Refineries Company

Research & quality control Department

Sample: Naphtha.

Naphtha is an intermediate hydrocarbon liquid stream derived from the refining of crude oil entered the distillation column C-101. It has been desulfurized by using continuous adsorptive desulphurization. This process will prepare the product for the catalytic reforming to produce the final product, which is gasoline.

Test Method: ASTM D5453

Standard test method for determination of total sulphur in light hydrocarbons, spark ignition engine fuel, diesel engine fuel and engine oil by ultraviolet florescence.

Sampling: Each two hours using filter syringe.

SEQ.	SAMPLE NAME	RESULT /SULPHUR PPM
1	FEED ONE NF1	789
2	FEED TWO NF2	597
3	N 1HR	570
4	N 2HR	437
5	N 4HR	368
6	N 6HR	267
7	N 8HR	79
8	N 10HR	78
9	N 12HR	80
10	TARGET	1.2
11	AFTER REGENERATION / RE-DESULPHORIZATION/CIRCULATION NR1-5	30-34

AYAD AHMED MOHAMED — MANAGER OF RESEARCH & QUALITY CONTROL DEPARTMENT

AHMED GHAFIL ALIBRAHEEMI — RESEARCHER

Appendix 8.2 Kerosene Results

MIDLAND REFINERIES COPMANY

Midland Refineries Company

Research & quality control Department

Sample: Kerosene.

Kerosene is an intermediate hydrocarbon liquid stream derived from the refining of crude oil entered the distillation column C-101. It has been desulfurized by using continuous adsorptive desulphurization to reach the target sulphur content of 11 ppm. This process will prepare the product for final use as a lamps ,lighting and heating fuel . This also used in aviation, jet engine of aircraft and some rocket engines.

Test Method: ASTM D5453

Standard test method for determination of total sulphur in light hydrocarbons, spark ignition engine fuel, diesel engine fuel and engine oil by ultraviolet florescence.

Sampling: Each two hours using filter syringe.

SEQ.	SAMPLE NAME	RESULT /SULPHUR PPM
1	Raw Kerosene RK	3218.130
2	RK 1HR	3195.759
3	RK 2HR	2677.466
4	RK 3HR	2673.527
	RK 4HR	2506.079
5	RK 6HR	1497.366
6	RK 8HR	1250.445
7	RK 10HR	551.995
8	RK 12HR	551.214
9	RK 14HR	546.07
10	TARGET	11
11	AFTER REGENERATION / RE-DESULPHORIZATION/CIRCULATION RK1-5	545-550

AYAD AHMED MOHAMED — **MANAGER OF RESEARCH & QUALITY CONTROL DEPARTMENT**

AHMED GHAFIL ALIBRAHEEMI — **RESEARCHER**

Appendix 8.3 Gas Oil Results

MIDLAND REFINERIES COPMANY

Midland Refineries Company

Research & quality control Department

Sample: Gasoil .

Gasoil is an intermediate hydrocarbon liquid stream derived from the refining of crude oil entered the distillation column C-101. It has been desulfurized by using continuous adsorptive desulphurization to reach the target sulphur content of 11 ppm. This process will prepare the product for final use as diesel fuel.

Test Method: ASTM 4294

Standard test method for determination of total sulphur in petroleum and petroleum product by energy X-ray fluorescence spectrometry.

Sampling: Each two hours using filter syringe. Then sampling after regeneration / re-desulphurization/circulation .

RK1-5

SEQ.	SAMPLE NAME	RESULT /SULPHUR PPM
1	Raw Gas Oil RG	16000
2	GO 1HR	10600
3	GO 2HR	8400
4	GO 3HR	7900
	GO 4HR	7000
5	GO 6HR	7100
6	GO 8HR	3800
7	GO 10HR	3700
8	GO 12HR	3700
9	GO 14HR	3700
10	TARGET	11
11	AFTER REGENERATION / RE-DESULPHORIZATION/CIRCULATION RK1-5	2500-545

AYAD AHMED MOHAMED — MANAGER OF RESEARCH & QUALITY CONTROL DEPARTMENT

AHMED GHAFIL ALIBRAHEEMI — RESEARCHER

Appendix 9 Marketing specifications guide of Iraqi petroleum products 2013

9.1 Naphtha

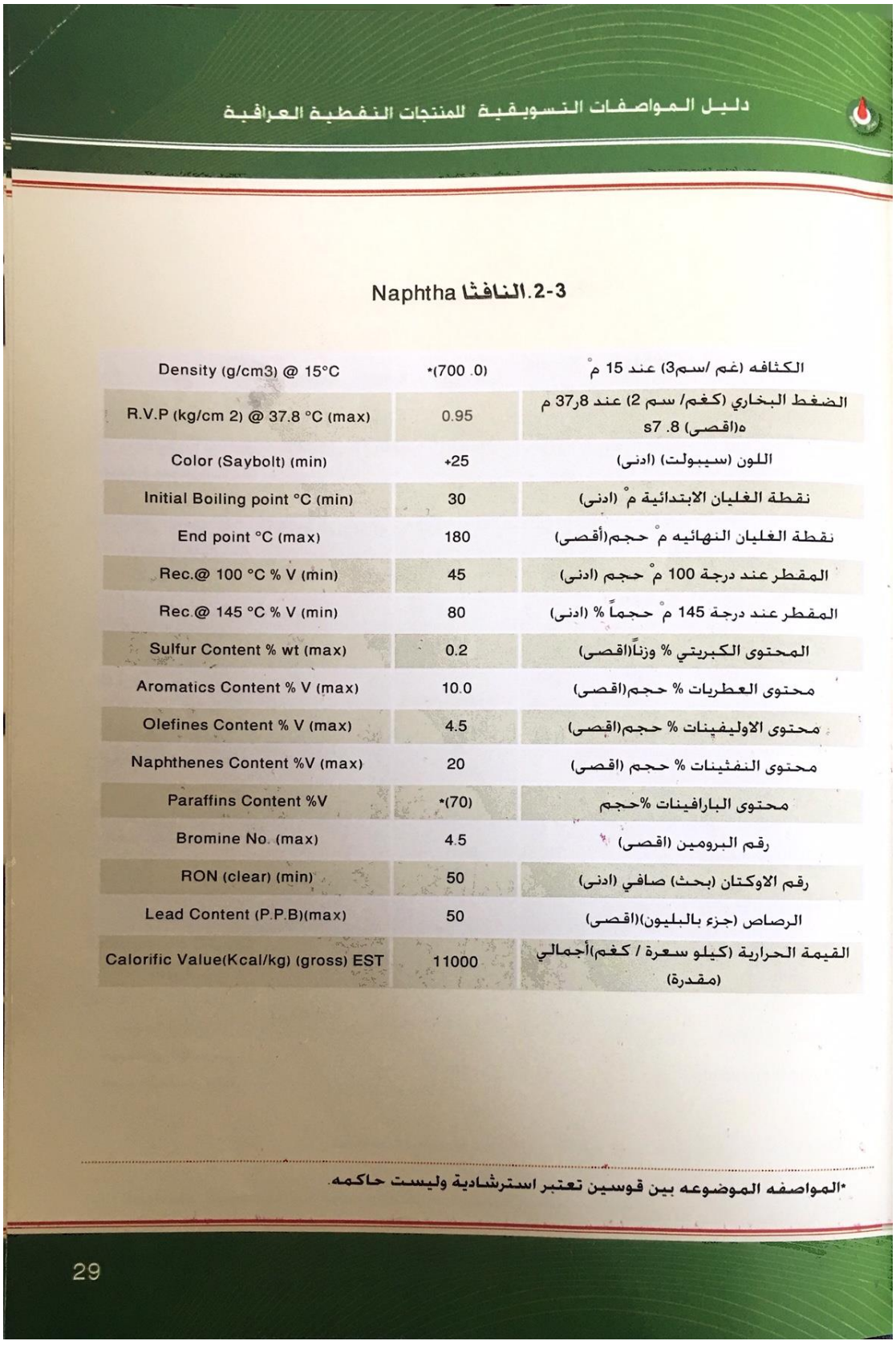

دليل المواصفات التسويقية للمنتجات النفطية العراقية

3-2.النافثا Naphtha

Density (g/cm3) @ 15°C	*(700 .0)	الكثافه (غم /سم3) عند 15 مْ
R.V.P (kg/cm 2) @ 37.8 °C (max)	0.95	الضغط البخاري (كغم/ سم 2) عند 37ر8 م ه(اقصى) 8. s7
Color (Saybolt) (min)	+25	اللون (سيبولت) (ادنى)
Initial Boiling point °C (min)	30	نقطة الغليان الابتدائية مْ (ادنى)
End point °C (max)	180	نقطة الغليان النهائيه مْ حجم(أقصى)
Rec.@ 100 °C % V (min)	45	المقطر عند درجة 100 مْ حجم (ادنى)
Rec.@ 145 °C % V (min)	80	المقطر عند درجة 145 مْ حجماً % (ادنى)
Sulfur Content % wt (max)	0.2	المحتوى الكبريتي % وزناً(اقصى)
Aromatics Content % V (max)	10.0	محتوى العطريات % حجم(اقصى)
Olefines Content % V (max)	4.5	محتوى الاوليفينات % حجم(اقصى)
Naphthenes Content %V (max)	20	محتوى النفثينات % حجم (اقصى)
Paraffins Content %V	*(70)	محتوى البارافينات %حجم
Bromine No. (max)	4.5	رقم البرومين (اقصى)
RON (clear) (min)	50	رقم الاوكتان (بحث) صافي (ادنى)
Lead Content (P.P.B)(max)	50	الرصاص (جزء بالبليون)(اقصى)
Calorific Value(Kcal/kg) (gross) EST	11000	القيمة الحرارية (كيلو سعرة / كغم)أجمالي (مقدرة)

*المواصفه الموضوعه بين قوسين تعتبر استرشادية وليست حاكمه.

29

9.2 Kerosene

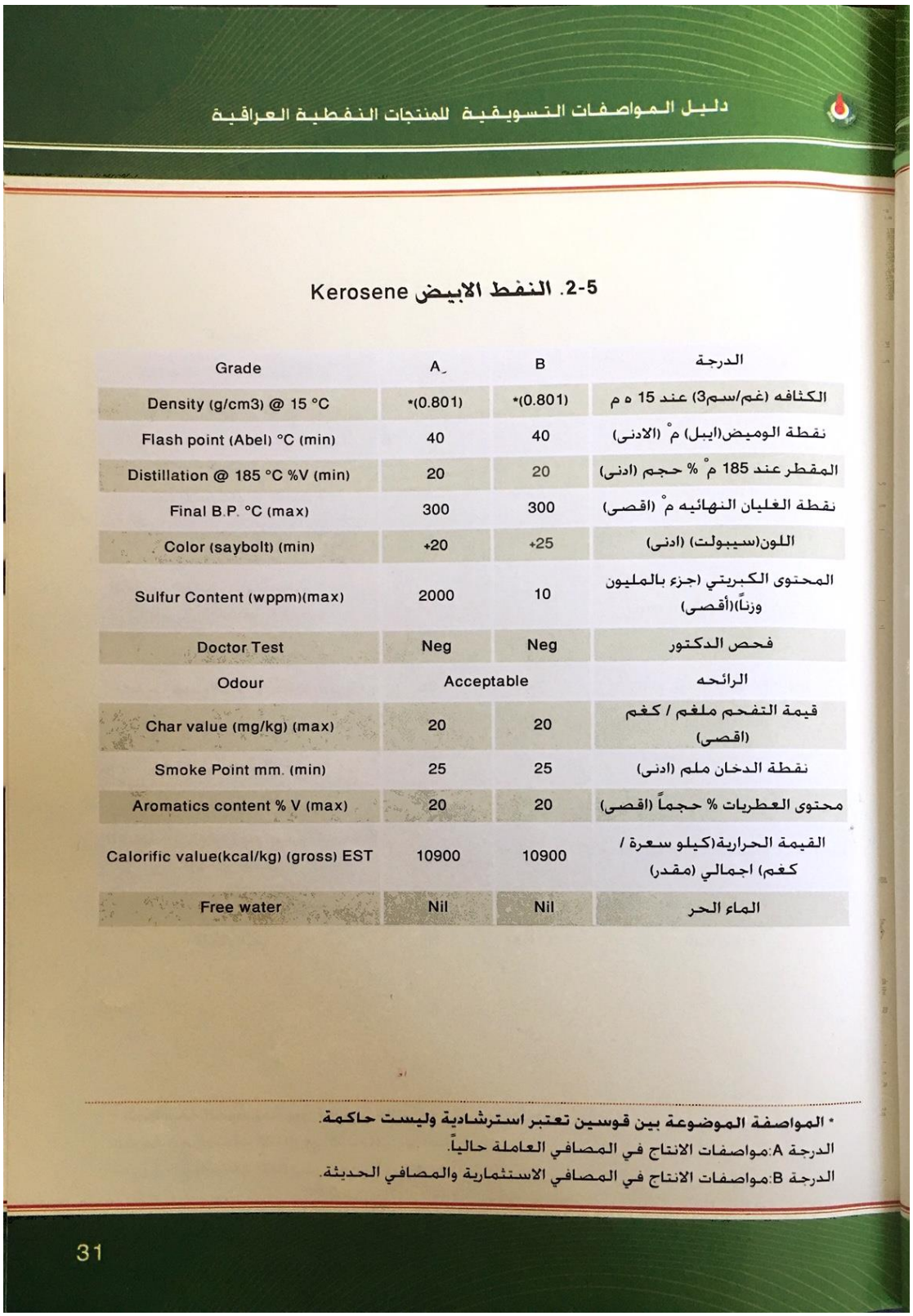

2-5. النفط الابيض Kerosene

Grade	A	B	الدرجة
Density (g/cm3) @ 15 °C	*(0.801)	*(0.801)	الكثافه (غم/سم3) عند 15 ° م
Flash point (Abel) °C (min)	40	40	نقطة الوميض(ابل) م° (الادنى)
Distillation @ 185 °C %V (min)	20	20	المقطر عند 185 م° % حجم (ادنى)
Final B.P. °C (max)	300	300	نقطة الغليان النهائيه م° (اقصى)
Color (saybolt) (min)	+20	+25	اللون(سيبولت) (ادنى)
Sulfur Content (wppm)(max)	2000	10	المحتوى الكبريتي (جزء بالمليون وزناً)(أقصى)
Doctor Test	Neg	Neg	فحص الدكتور
Odour	Acceptable		الرائحه
Char value (mg/kg) (max)	20	20	قيمة التفحم ملغم / كغم (اقصى)
Smoke Point mm. (min)	25	25	نقطة الدخان ملم (ادنى)
Aromatics content % V (max)	20	20	محتوى العطريات % حجماً (اقصى)
Calorific value(kcal/kg) (gross) EST	10900	10900	القيمة الحرارية(كيلو سعرة / كغم) اجمالي (مقدر)
Free water	Nil	Nil	الماء الحر

* **المواصفة الموضوعة بين قوسين تعتبر استرشادية وليست حاكمة.**

الدرجة A:مواصفات الانتاج في المصافي العاملة حالياً.

الدرجة B:مواصفات الانتاج في المصافي الاستثمارية والمصافي الحديثة.

9.3 Gas Oil

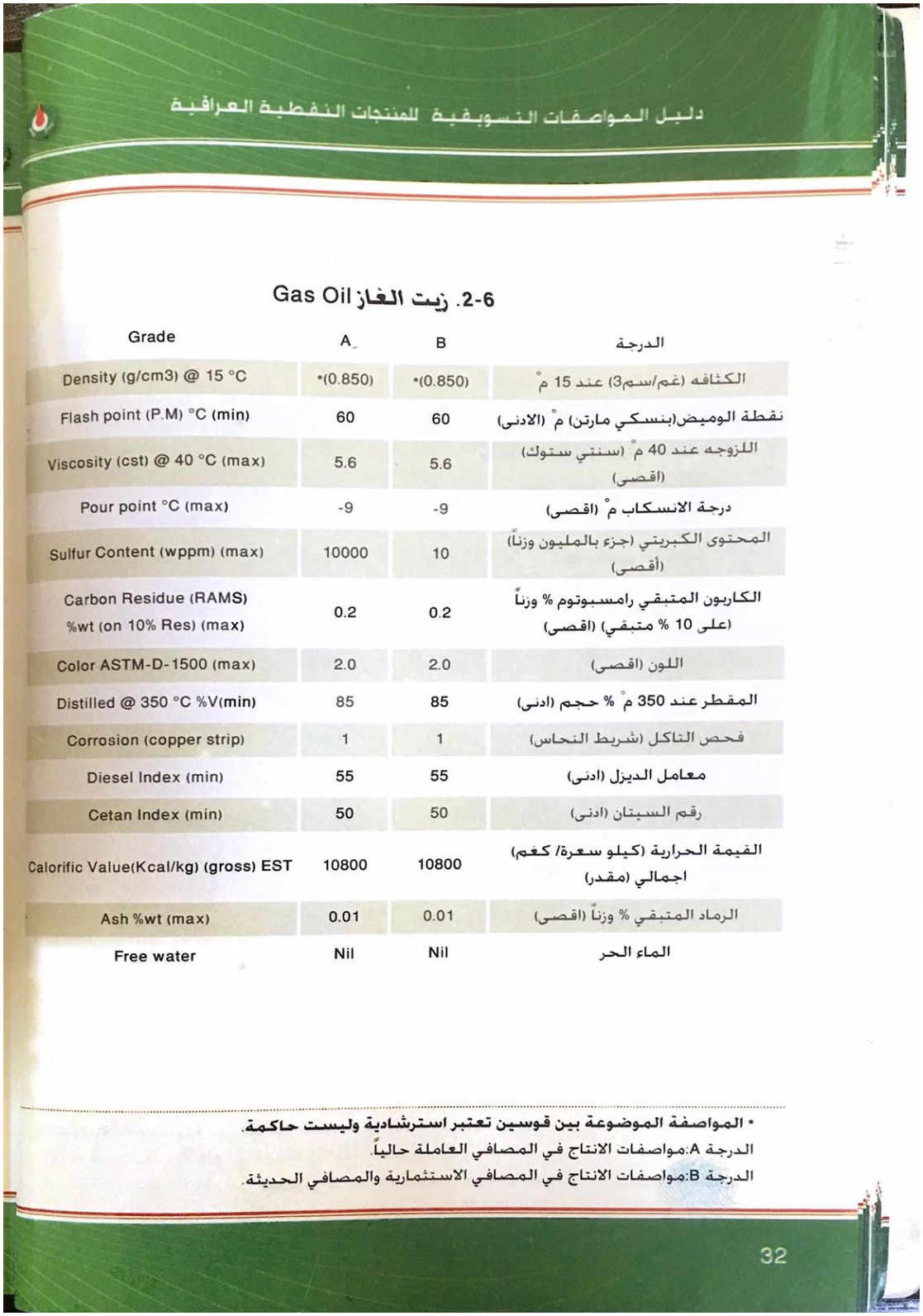

2-6. زيت الغاز Gas Oil

Grade	A	B	الدرجة
Density (g/cm3) @ 15 °C	*(0.850)	*(0.850)	الكثافه (غم/سم3) عند 15 مْ
Flash point (P.M) °C (min)	60	60	نقطة الوميض(بنسكي مارتن) مْ (الادنى)
Viscosity (cst) @ 40 °C (max)	5.6	5.6	اللزوجه عند 40 مْ (سنتي ستوك) (اقصى)
Pour point °C (max)	-9	-9	درجة الانسكاب مْ (اقصى)
Sulfur Content (wppm) (max)	10000	10	المحتوى الكبريتي (جزء بالمليون وزناً) (أقصى)
Carbon Residue (RAMS) %wt (on 10% Res) (max)	0.2	0.2	الكاربون المتبقي رامسبوتوم % وزناً (على 10 % متبقي) (اقصى)
Color ASTM-D-1500 (max)	2.0	2.0	اللون (اقصى)
Distilled @ 350 °C %V(min)	85	85	المقطر عند 350 مْ % حجم (ادنى)
Corrosion (copper strip)	1	1	فحص التاكل (شريط النحاس)
Diesel Index (min)	55	55	معامل الديزل (ادنى)
Cetan Index (min)	50	50	رقم السيتان (ادنى)
Calorific Value(Kcal/kg) (gross) EST	10800	10800	القيمة الحرارية (كيلو سعرة/ كغم) اجمالي (مقدر)
Ash %wt (max)	0.01	0.01	الرماد المتبقي % وزناً (اقصى)
Free water	Nil	Nil	الماء الحر

* المواصفة الموضوعة بين قوسين تعتبر استرشادية وليست حاكمة.

الدرجة A:مواصفات الانتاج في المصافي العاملة حالياً.

الدرجة B:مواصفات الانتاج في المصافي الاستثمارية والمصافي الحديثة.